CRANFIELD UNIVERSITY

EMMANUEL MATAS

THE GLUTAMATE POST-SYNAPTIC DENSITY IN SCHIZOPHRENIA

CRANFIELD HEALTH

Doctor of Philosophy

Academic Year: 2013

Supervisor: Dr Carla Toro

November 2012

CRANFIELD UNIVERSITY

CRANFIELD HEALTH

Doctor of Philosophy

Academic Year 2013

EMMANUEL MATAS

The glutamate post-synaptic density in schizophrenia

Supervisor: Dr Carla Toro
November 2012

This thesis is submitted in partial fulfilment of the requirements for the degree of PhD

Abstract

Non-competitive antagonists of the glutamate *N*-methyl-D-aspartate receptor (NMDAR) induce a broad range of schizophrenia-like symptoms in humans. Consequently hypothesis has emerged suggesting that glutamate or NMDAR hypofunction may occur in schizophrenia. The NMDAR is localised at dendritic spines of neurons and is embedded in a multi-protein complex called the post-synaptic density (PSD). The biochemical composition of the postsynaptic membrane and the structure of dendritic spines are continuously modulated by glutamatergic synaptic activity. The activity-dependent interaction between glutamate receptors and proteins of the PSD stimulate intracellular signalling pathways underlying learning and memory processes. These may be disturbed in schizophrenia.

In the present study we hypothesised that molecules of the PSD may be disturbed in expression in the premotor cortex of patients with schizophrenia. Postmortem premotor cortex from patients with schizophrenia, major depressive disorder, bipolar disorder and healthy controls were processed for PSD extraction and purification. Protein expression of the PSD fraction was assessed using co-immunoprecipitation (co-IP) and Western blotting (WB) methods. The expression of NMDAR subunit NR2A, PSD-95, Ca^{2+}/calmodulin-dependent protein kinase II subunit β (CaMKIIβ) and truncated isoform of the tropomyosin receptor kinase type B (TrkB-T1) were significantly reduced in schizophrenia. A significant decrease in the expression of NR2A was also observed in patients with major depressive disorder relative to controls.

A decrease in the abundance of key PSD proteins in schizophrenia provides strong evidence that PSD function and possibly synaptic plasticity may be disturbed in the premotor cortex in the disease. There may also be more subtle disturbances in PSD function in major depressive disorder.

Keywords: premotor cortex, synaptic plasticity, protein-protein interactions

For Brigitte

Acknowledgements

I am deeply grateful to Dr. Carla Toro for her guidance, advice, patience and support, which made these past years an incredible learning experience.

I am also grateful to Dr Pierre Olivier Lang, Dr Wayne Mitchel and Dr Sheila Govind for their friendship and camaraderie. They were a source of contagious optimism, positive energy and motivation.

I also thank Dr. Jeremy Skepper for his help and his participation to this project.

I am indebted to my family and friends for all their patience and encouragement.

I dedicate this thesis to my parents Brigitte Dumté and Pierre Matas and my sister Chanterelle Matas.

Table of contents

List of figures

List of tables

List of abbreviations

2D LC-MS/MS	Two dimensional gel electrophoresis followed by liquid chromatography coupled with tandem mass spectrometry
5-HT_{2A}	5-hydroxytryptamine
Abp1	Actin binding protein 1
AKAP79/150	A-kinase anchoring protein 79/150
AMPAR	α-amino-3-hydroxy-5-methyl-4-isoxazole propionic acid receptor
ANK	*N*-terminal ankyrin
APS	Ammonium persulfate
BDNF	Brain derived neurotrophic factor
BRET	Bioluminescence resonance energy transfer
BSA	Bovine serum albumin
$CaCl_2$	Calcium chloride
CAMs	Cell adhesion molecules
CC	Coiled-coil
CNS	Central nervous system
DAO	D-amino acid oxydase
DISC1	Disrupted in schizophrenia 1
DLPFC	Dorsolateral prefrontal cortex
DSM-IV-TR	Diagnostic and statistical manual of mental disorders, fourth edition, text revision
DTNBP1	Dysbindin
DTT	Dithiothreitol
ErbB4	V-erb-a erythroblastic leukemia viral oncogene homolog 4
EVH1	Ena/VASP Homology 1
fMRI	Functional magnetic resonance imaging
G72	D-amino acid oxydase activator DAOA
GFAP	Glial fibrillary acidic protein
GK	Guanylate kinase
GluR3	Metabotropic glutamate receptor 3
Glutamate	L-glutamic acid

GRM3	G-coupled receptor mGluR3
GSK-3β	Glycogen synthase kinase 3β
Hepes	Hydroxyethyl piperazineethanesulfonic acid
IP3	Inositol 1,4,5-trisphosphate
KCl	Potassium chloride
LAR	Leukocyte common antigen-related
LSD	Lyserge saüre diäthylamid
LTP	Long term potentiation
MAGUK	Membranes associated guanylate kinases
MASC	Membranes associated guanylate kinases (MAGUK)-associated signalling complex
MATRICS	Measurement and treatment research to improve cognition in schizophrenia
$MgCl_2$	Magnesium chloride
mGluRs	Metabotropic glutamate receptors
MRI	Magnetic resonance imaging
mRNA	Messenger ribonucleic acid
N/A	Not appropriate
$NaHCO_3$	Sodium bicarbonate
NG	Netrin-G
NGF	Neurotrophins nerve growth factor
NGL	Netrin-G ligand
NMDAR	*N*-methyl-D-aspartate receptor
NRG1	Neuregulin1
NRG	Neuregulins
NSF	*N*-ethylmaleimide sensitive factor
NT-3	Neurotrophin-3
PDZ	PSD-95/Discs-large/Zona occludens-1
PET	Positron emission tomography
PCP	Phencyclidine
PFC	Prefrontal cortex

ppI	Cortactin binding domain
PRC	Proline-rich clusters
PSD	Post-synaptic density
PSP	Pro-SAP/Shank platform
PVDF	Polyvinylidene difluoride
RGS4	Regulator G protein signaling 4
rpm	Rotations per minute
RTKs	Receptor tyrosine kinases
SAM	Sterile alpha motif
SAP	Synapse-associated proteins
SDS	Sodium dodecyl sulfate
SEM	Standard error of the mean
SER	Smooth endoplasmic reticulum
SH3	src-homology 3
SMRI	Stanley medical research institute
SNc	Substantia nigra pars compacta
SVZ	Subventricular zone
synCAMs	Synaptic cell adhesion molecules
TEM	Transmission electron microscopy
Tris HCl	Tris-buffered saline hydrochloric acid
TrkA/B/C	Tropomyosin receptor kinase type A/B/C
TURNS	Treatment units for research on neurocognition and schizophrenia
VTA	Ventral tegmental area

1 Literature review

1.1 Schizophrenia

Schizophrenia is a grave psychiatric disorder of thought and sense of self, which generally appears soon after adolescence. Because of its early onset, schizophrenia poses a great burden on emotional, social and economic aspects within a society. Furthermore, deficiencies in sociability during the illness lead to earlier death by natural causes (poor diet, little exercise, obesity, and smoking) or by suicide (van Os and Kapur, 2009). The prevalence of this illness is approximately one percent of the world population and its incidence is higher in men (McGrath, 2006). This disease of the brain is known to affect emotional behaviours to a higher degree than mood disorders. Furthermore, although cognitive functions such as memory, language and attention are affected to a lesser degree than in dementia, they are still severely disabling in affected individuals.

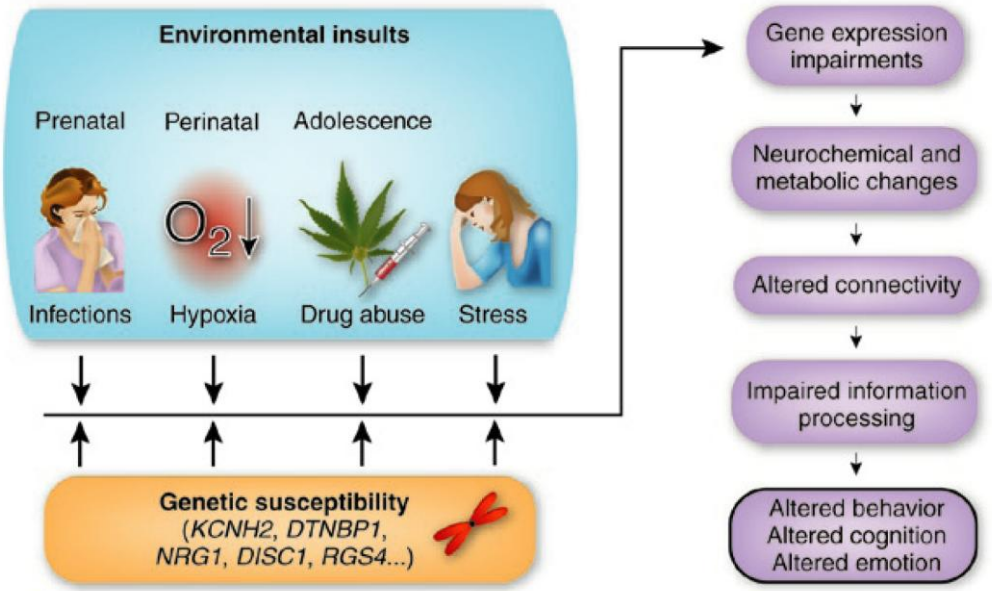

Figure 1-1: Environmental factors and associated genes risk hypothesis for the aetiology of schizophrenia. Taken from (Horváth and Mirnics, 2009).

In contrast to neurodegenerative diseases such as Alzheimer's disease, Parkinson's disease or Huntington's disease, characteristic pathological hallmarks for schizophrenia have not been established. Multiple factors seem to be at the origin of this complex illness. The most probable hypothesis is that individuals carrying a genetic vulnerability develop schizophrenia according to environmental factors (see Figure 1-1).

Schizophrenia has a significant genetic component since the heritability of schizophrenia reaches up to 80% among monozygotic twins (Sullivan et al., 2003). The environmental factors implicated in the aetiology of schizophrenia include abuse of drugs such as amphetamine, LSD (*lyserge saüre diäthylamid)* or cannabinoids, which can induce similar symptoms as those found in schizophrenia and constitute to risk (Demily and Thibaut, 2008). Furthermore, numerous studies have shown that more schizophrenic patients are born during the winter-spring months (Torrey et al., 1997), which may be due to infection or nutritional deficiencies. Other retrospective studies have found a link between obstetric complications such as bleeding, congenital malformation, or asphyxia and the development of schizophrenia in offspring (Cannon and Clarke, 2005).

1.1.1 Symptoms

The term schizophrenia (schizo: "to split"; phrenia: "though") was introduced by Eugen Bleuler in the article entitled "Dementia praecox or the group of schizophrenias" in Aschaffenburg's Handbook of Psychiatry of 1911 (Stotz-Ingenlath, 2000). For Bleuler, Kraepelin's "dementia praecox" designation was not appropriate for patients showing split personality as a first symptom (Tandon et al., 2009). However, Bleuler did not consider delusions and hallucinations which are now currently admitted as principal features of the disease. Although this appellation continues to be used to date, progress in diagnosis and description of the illness seem to lead to a new definition of schizophrenia. In Japan schizophrenia has already be renamed "integration-dysregulation syndrome" (van Os and Kapur, 2009).

Currently the diagnosis of schizophrenia is carried out by psychiatrists using either ICD-10 or DSM-IV-TR criteria (Diagnostic and Statistical Manual of Mental Disorders, Fourth Edition, Text Revision). Diagnosis is based on the concomitant occurrence of at least two of the following symptoms each one representing a significant position of time within a six month period: delusions, hallucinations, disorganized speech, excessively disorganized behaviour, and the negative symptoms (American psychiatric Association, 2000). Symptoms can be broadly separated into three categories: positive, negative and cognitive symptoms (see Table 1-1). Positive symptoms, also called psychotic symptoms, include delusions, hallucinations, disorganized speech and disorganized behaviour. The deficit symptoms currently defined as negative symptoms include blunted emotion, anergia, alogia, poor sociability and anhedonia. The cognitive symptoms in schizophrenia are in particular related to disorders of abstraction, attention, working memory, language and executive functions (Frankle et al., 2003).

Table 1-1: Symptoms of schizophrenia are categorized into three broad subgroups: positive, negative, and cognitive symptoms.

Positive symptoms	**Negative symptoms**	**Cognitive symptoms**
Hallucinations	Alogia	Disturbances in:
Delusions	Anhedonia	Abstraction
Disorganised speech	Poor sociability	Memory
Disorganised behaviour	Psychomotor poverty	Attention
	Blunted emotions	Language
		Executive functions

The loss of contact with reality is characteristic of the positive symptoms. These implicate high brain functions and manifest as abnormalities in perception (auditory hallucinations), inferential thinking (delusions), language (disorganised speech) and behavioural monitoring and control (disorganised behaviour), in which normal brain functions are disturbed or exacerbated (Andreasen, 2000). Functional magnetic resonance imaging (fMRI) studies have shown that frontal cortex areas such as inferior frontal gyri, including the Broca's language region, are activated during hallucinations in schizophrenic patients. Furthermore, other cortical structures such as ventral striatum, the auditory cortex, the right posterior temporal lobe, and the cingulate cortex are also implicated (Raij et al., 2009).

In contrast to the episodic feature of positive symptoms, longitudinal stability characterises negative symptoms of schizophrenia which are present during as well as between episodes of positive symptom exacerbation. The definition of these symptoms is the absence or diminution of normal behaviours and functions which lead to alogia (literally "without speech"), anhedonia (literally "without pleasure"), poor sociability, psychomotor poverty and blunted emotions (Buchanan, 2007). Functional imaging studies have led to the identification of particular cerebral regions implicated in negative symptoms. These studies showed a decrease in activity of the prefrontal cortex and parietal cortex while activity was increased in the caudate nuclei bilaterally characterising psychomotor poverty (Liddle, 1996).

Contrary to positive and negative symptoms, cognitive disturbances are not incuded as part of the criteria to establish schizophrenia diagnosis. However, these symptoms are integrally part of the illness and are found in 94% of schizophrenic patients (Waldo et al., 1994). Neuropsychological studies of cognitive symptoms highlighted dysfunction in capacity of abstraction, memory, attention, language and executive functions (Kurachi, 2003). Frontal lobe dysfunction and deficits in cognitive function are evaluated using neuropsychological test such as Wisconsin Card Sorting Test which assesses executive functions and the Stroop test which measure attention during tasks with distraction interferences (Goldberg and Bougakov, 2005). Furthermore, a

quantitative meta-analysis of functional imaging studies showed a correlation between decreased activation of the dorsolateral/ventrolateral prefrontal cortex and impairments in episodic memory tasks in affected individuals (Ragland et al., 2009).

1.1.2 Treatments

At the beginning of the 20th century, the use of barbiturates, coma by insulin injection, electro-convulsive therapy and frontal leucotomy were used as treatments for schizophrenia. In the mid fifties, a synthesized compound, chlorpromazine, initially utilised for anaesthesia and surgery was identified as a dopamine receptor antagonist and gave rise to the pharmaceutical management of schizophrenia (Stip, 2002). Since that time, numerous types of antipsychotics have been developed. Chlorpromazine and haloperidol are classed as “typical” antipsychotics, while clozapine and quetiapine, the second generation of antipsychotic, are termed “atypical” by contrast to “typical” antipsychotics which induce movement disorder side-effects. The use of animals treated with Phencyclidine (PCP) or Ketamine as a model of schizophrenia have led to a better understanding of mechanisms of action and side effects of these compounds.

Chlorpromazine, the first compound qualified as antipsychotic, was used to treat schizophrenia in the late 1970s. Its introduction led to deinstitutionalization of psychiatric patients and their social reinsertion, reducing at the same time the stigma associated with schizophrenia (López-Muñoz et al., 2005). In addition, during the same period another compound named haloperidol was synthesized. Used to treat schizophrenia, this compound showed a great effect on positive symptoms of the disease, particularly on hallucinations and delusions (Granger and Albu, 2005). However, from the first clinical trials, it was obvious that both chlorpromazine and haloperidol induced extrapyramidal side effects, characterized by tardive dyskinesia, parkinsonism, dystonias and akathisia (Shen, 1999). These side effects have been attributed as result of D2 dopamine receptor blockade in the basal ganglia (Kuperberg et al., 2002).

The second generation of antipsychotics termed “atypical” are represented by clozapine. This compound showed a decreased effect on the dopamine D2 compared to older antipsychotics, and instead affected other neuroreceptors, such as dopamine D1, histamine H1, serotonin 5-HT2 and muscarinic M1 receptors. Studies demonstrated a better efficacy of clozapine and a diminution of extrapyramidal side effects relative to chlorpromazine and haloperidol treatment. Furthermore, clinical trials highlighted that some negative symptoms were ameliorated in schizophrenic patients treated with clozapine (Kapur and Mamo, 2003). However, in spite of the beneficial effects of these compounds on positive and negative symptoms of schizophrenia, their exact mechanisms of action remain speculative. A newer second generation of “atypical” antipsychotics is represented by drugs such as olanzapine, quetiapine, risperidone and amisulpride. These compounds have equal or better efficacy than clozapine on acute schizophrenia, on positive and negative symptoms and induce less motor side-effects. For instance, olanzapine enhance benefit for psychosis and negative symptoms with very few extrapyramidal side effects. However, this compound induces other side effects such as weight gain and, in some patients, hyperlipidaemia, hyperglycaemia and diabetes (Lambert and Castle, 2003). Nevertheless, the second generation of “atypical” antipsychotics is now widely used to treat schizophrenia. Moreover, studies have shown that these new drugs reduce suicide attempts among patients affected by schizophrenia compared to haloperidol-treated patients (Meltzer and Okayli, 1995; Glazer and Dickson, 1998).

Mood stabilisers and antidepressants drugs are often added to the treatment regime for schizophrenia patients to prevent affective syndromes, such as mania, characterised by period excitement and agitation, and depression which occur commonly during the course of illness. Studies have demonstrated that the co-administration of antidepressants and mood stabilisers such as imipramine and lithium respectively lead to improvements of depressive symptoms (Escamilla, 2001). Mood stabilizers and antidepressants such as sodium valproate and benzodiazepines are usually used to treat schizophrenic patients with anxiety and sleep disturbance.

However, the fact that mood symptoms appear generally after typical and atypical antipsychotic drugs treatment and not in all patients suggest that optimisation of antipsychotic treatment should be attempted instead of multiple drugs treatment (Levinson et al., 1999).

"Typical" antipsychotics are effective only for positive symptoms, whilst "atypical" antipsychotics show efficacy for both positive and negative symptoms. Both types of antipsychotic have various side effects and can lead to secondary symptoms such as depression. Also, these drugs do not have efficacy for treating cognitive symptoms of schizophrenia. New strategies of treatment are needed to treat all symptoms of the disease and avoid drugs side effects. Two projects, the Measurement and Treatment Research to Improve Cognition in Schizophrenia (MATRICS) and the Treatment Units for Research on Neurocognition and Schizophrenia (TURNS), were setup respectively for the discovery and validity of new therapeutic targets. The MATRICS project, involved in the research of new targets highlighted cholinergic, dopaminergic, and glutamatergic systems as potentially effective to treat cognitive symptoms of schizophrenia. These findings led to the development of cholinergic, dopaminergic, and glutamatergic drugs which are currently in early stages of pharmacological and pharmaceutical testing (Buchanan et al., 2007).

1.2 Pathophysiology of schizophrenia

1.2.1 Genes involved in schizophrenia

Evidence for the genetic aetiological component of schizophrenia comes from results of numerous family, twin, and adoption studies. These studies showed that disease risk is dramatically increased among the relatives of schizophrenic patients. More recent studies have demonstrated that the heritability of schizophrenia reaches 41 to 65% in monozygotic twins, and 0 to 28% in dizygotic twins. Although these results highlight a high heritability of the illness in twins, environmental factors remain implicated due to

a broadly heritability (85%) inferior to 100% (Cardno and Gottesman, 2000). Association studies implicate several loci in schizophrenia, such as 6p24–22, 1q21–22, 13q32–34, 8p21–22, 6q16–25, 22q11–12, 5q21–q33, 10p15–p11, and 1q42, including neuregulin (NRG1), dysbindin (DTNBP1), disrupted in schizophrenia (DISC1), D-amino acid oxydase activator DAOA (G72), D-amino acid oxydase (DAO), metabotropic Glutamate Receptor 3 (GluR3) and regulator G protein signaling 4 (RGS4) genes (Craddock et al., 2005). Most of these genes encode proteins acting at the glutamatergic synapse (see Figure 1-2).

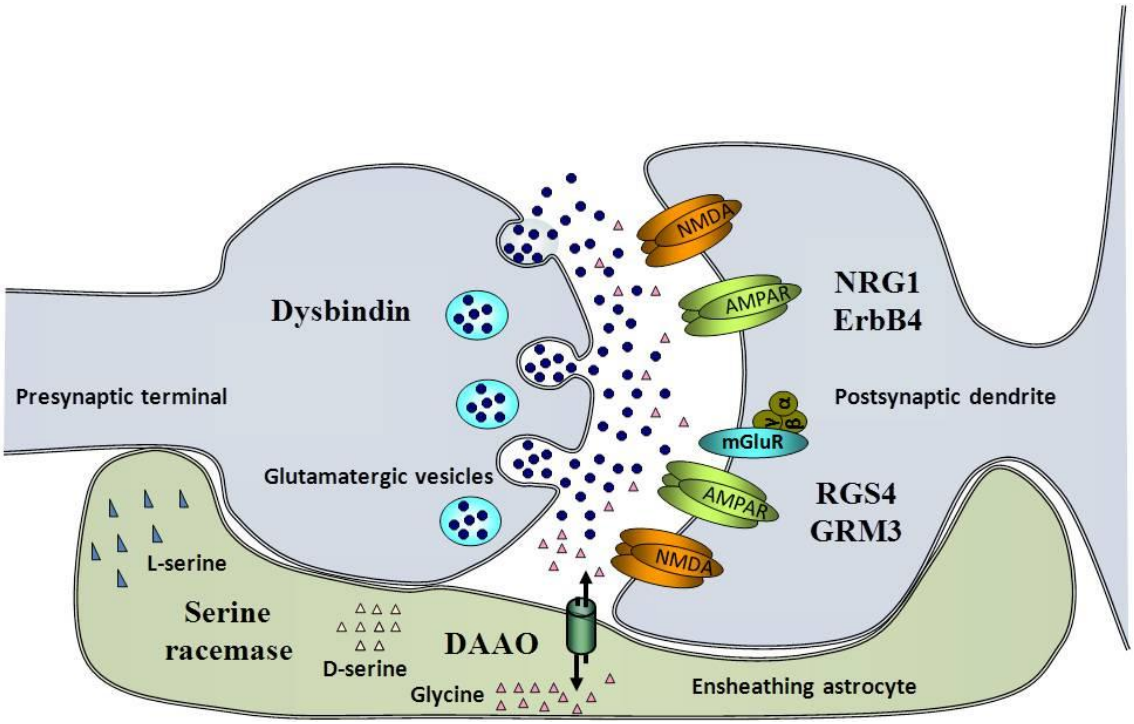

Figure 1-2: The glutamate synapse and associated susceptibility genes in schizophrenia.

Evidence for a disturbance in the genes coding for subunits of the NMDA receptor in schizophrenia is equivocal (Kristiansen et al., 2007a). However, evidence is stronger for dysbindin which is present at the synaptic bouton of glutamate synapses and modulates vesicular glutamate release (Numakawa et al., 2004). This protein is widely

expressed in the human brain and seems to play an important part in cognitive function and memory (Owen et al., 2004). Postmortem studies suggest that dysbindin concentrations are reduced in schizophrenic patient brains (Weickert et al., 2004), in particular in the prefrontal cortex and the hippocampus (Talbot et al., 2004). Straub *et al.* 2002 showed, using a family-based association analysis, that SNPs within the DTNBP1 gene (locus 6p22.3) were strongly implicated in schizophrenia (Straub et al., 2002). Another genetic study demonstrated that haplotype variation of DTNBP1 was associated with negative symptoms of schizophrenia, this finding led the authors to suggest that dysbindin was implicated in mechanisms that give rise to negative symptoms via a glutamate receptor activity (DeRosse et al., 2006).

Other proteins present at the glutamate synapse such as NRG1 and its receptor V-erb-a erythroblastic leukemia viral oncogene homolog 4 (ErbB4) have also been shown to be associated with schizophrenia in many studies (Petryshen et al., 2005). Genetic studies have shown that several haplotypes of NRG1 are associated with schizophrenia particularly on glutamatergic synapses (Stefansson et al., 2002). Concerning the ERBB4 gene, a study identified 3 SNPs in exon 3 associated with schizophrenia, and using RT-PCR, showed that ERBB4 isoforms were increased in patients affected by the illness.

At the post-synaptic level of glutamatergic synapse, activation of the G-coupled receptor mGluR3 (GRM3) is known to result in decreased glutamate release into the synapse and was identified as a potential genetic risk factor for schizophrenia (Fujii et al., 2003). Also, the RGS4 protein which negatively controls the Gi/o subunits and Gq of the G-coupled receptor was implied in genetic studies as a likely candidate gene in schizophrenia (Ding and Hegde, 2009). Association and linkage studies showed that 4 SNPs within RGS4 gene were linked to schizophrenia (Morris et al., 2004).

Glycine and D-serine released from unsheathing astrocytes, are NMDA receptor activators via the co-agonist binding site. D-serine is synthesised from L-serine in local astrocytes via the action of serine racemase. Another enzyme, DAOA, which degrade D-serine has been associated with the risk of schizophrenia in several studies (Corvin et

al., 2007). Moreover, serine racemase, has also been implicated in schizophrenia (Morita et al., 2007). Meta-analysis studies have demonstrated that two loci 13q32-q33 and 22q11 were associated with schizophrenia (Badner and Gershon, 2002), and in postmortem dorsolateral prefrontal cortex samples DAOA was found over-expressed in patients with schizophrenia (Korostishevsky et al., 2006).

1.2.2 Brain regions involved in schizophrenia

Evidence from neuropsychological, post-mortem and neuroimaging studies suggest that symptoms of schizophrenia arise from neuro-physiological disturbances in all major brain areas and neuronal circuits. These observations are in concordance with multiple different forms and symptoms of schizophrenia. Concerning structural brain changes, the most consistent findings from post-mortem and imaging studies are an enlargement of lateral ventricular size, a loss of grey matter and a reduction in brain volume, all potentially leading to a cortical surface mis-folding. Considering circuit abnormalities, studies implicate and involvement of circuits between the prefrontal cortex, basal ganglia, thalamus, hippocampus and medial temporal lobe in patients with schizophrenia (Fallon et al., 2003). Although many different cerebral structures are involved in the pathology of schizophrenia, the prefrontal cortex (PFC) and the temporal lobe seem to be particularly implicated in the disease (Kawada et al., 2009).

The prefrontal cortex play a critical role in complex functions of the brain, such as planning, attention, language, working memory and emotion. It can be divided into dorsal, dorsolateral, lateral, orbital and parietal prefrontal cortices, which are all connected with sub-cortical areas. The dorsolateral prefrontal (DLPFC) cortex has been widely studied. This part of the PFC is known to be associated with working memory, which is disturbed in patients with schizophrenia. Recently, a study showed, using cognitive tests and magnetic resonance imaging (MRI), a correlation between reduced DLPFC volume and executive functions impairment in patients with schizophrenia (Kawada et al., 2009). Furthermore, the importance of PFC function during memory

tasks was demonstrated in a study using the Wisconsin Card Sorting Test and positron emission tomography (PET) in schizophrenic patients (Bertolino et al., 2000).

The hippocampus, situated in the temporal lobe, is part of the limbic system and is involved in memory and learning. Evidence for the involvement of the hippocampus in schizophrenia stems from multiple research disciplines. In vivo studies showed that hippocampus volume is reduced in brain of schizophrenic patients, even in early onset of the illness, which means that reduced volume isn't due to the disease or medication (Velakoulis et al., 2006). In addition, PET and fMRI studies have reported respectively abnormalities in neuronal metabolism and decreased *N*-acetyl aspartate in hippocampus of affected individuals (Harrison, 2004). Moreover, post-mortem studies highlighted dysfunction of numerous neuroreceptors, such as glutamate receptors, GABA receptors, nicotinic receptors and serotonin receptors in patients with schizophrenia (Harrison, 2004).

Although these findings implicate the PFC and hippocampus in the pathology of schizophrenia, an involvement of other structures such as cerebellum, cingulate cortex and thalamus was also reported. It is well known that all these regions of the brain are interconnected via neuronal circuitry and this connectivity has been suggested to be disturbed in schizophrenia (Bertolino et al., 2000).

1.2.3 Dysconnection in schizophrenia

The idea that schizophrenia could be due to dysconnection between regions of the brain was introduced by Wernicke and Bleuler at the early beginning of the twentieth century. They proposed that schizophrenia was not only a disease involving several regions of the brain, but also a disease of the connection of these regions. The hypothesis is that disturbances within neural network of brain regions and dysfunctional connectivity between these regions give rise to symptoms of schizophrenia, such as auditory hallucination and cognitive impairment (Stephan et al., 2006). The use of techniques such as PET and fMRI during the last three decades have

led to a better understanding of disturbed activity and functional connectivity of brain regions implied in schizophrenia (Liang et al., 2006). A recent study showed using fMRI showed that connectivity between insula, temporal lobe, prefrontal cortex and basal ganglia was disturbed in patients with schizophrenia (Stephan et al., 2006; Liang et al., 2006). Another fMRI study showed disconnection between DLPFC and hippocampus in subjects with schizophrenia during working memory activation (Meyer-Lindenberg et al., 2005). In addition a PET study demonstrated that cooperative activity between PFC and temporal lobe was disrupted in schizophrenia (Meyer-Lindenberg et al., 2001).

Despite evidence of dysconnection in schizophrenia the mechanisms that underlie its occurrence are still unclear. Two possible explanations may explain dysconnectivity, one is based on disturbances of neurodevelopment, the other on impairments in neuroplasticity, or even perhaps both occur. To consolidate the first hypothesis, a study showed that loss of neuronal connections in DLPFC which occur in normal teenagers is increased in patients with early onset of schizophrenia (Glantz and Lewis, 2000). The second theory is supported by the involvement of NMDAR and its neuro-modulators, such as dopamine, serotonin, or acethylcholine in learning processes such as long term potentiation (LTP). Long term potentiation plays a critical role in the survival of dendritic synapses and disturbed LTP may explain abnormal connectivity in patients with schizophrenia. Studies of post-mortem brains have highlighted a decreased dendritic field size and dendritic spines in patients affected by schizophrenia (Garey et al., 1998), suggesting a reduction in afferent connections.

1.3 Developmental theories of schizophrenia

1.3.1 Neurodevelopment

The idea that schizophrenia may be a disease of neurodevelopment arises from numerous studies of environmental factors affecting foetal or postnatal brain development as a risk to develop schizophrenia. Environmental factors such as

asphyxia or virus infection can interfere in the functioning of critical neurodevelopment processes such as proliferation, migration, differentiation, synaptogenesis, myelination or apoptosis and lead to disturbed brain functions. A study demonstrated that, during the 1957 type A2 influenza pandemic, the risk of developing schizophrenia in later life was significantly increased when foetuses were exposed to the virus during the second trimester of development compared to non-affected subjects (Mednick et al., 1988). In addition, seasonal birth studies have shown 5 to 8% excess of schizophrenia births in the winter-spring months (Torrey et al., 1997). The period of gestation for winter-spring birth is the most vulnerable period for virus infections, and migration of embryonic neurons during human neurodevelopment occurs in the second trimester of pregnancy. It is well known that neuronal migration via radial glia during neurodevelopment forms the cytoarchitecture of the cortex. Several studies have detected cytoarchitectural alterations in particular in the medial temporal cortex and hippocampal formation in patients with schizophrenia (Harrison, 1999).

After birth and during adolescence, the human brain continues its development and maturation in processes such as axonal elimination and synaptic pruning (Gogtay et al., 2004). Studies showed that in early onset schizophrenia the brain undergoes excessive synaptic elimination which may lead to the illness (Innocenti et al., 2003) (see Figure 1-3). In addition, another study demonstrated that mRNA levels of the synaptic protein synaptophysin, which plays an important role in the establishment of new synapses, was down-expressed in the medial temporal lobe in patients with schizophrenia (Eastwood and Harrison, 1995).

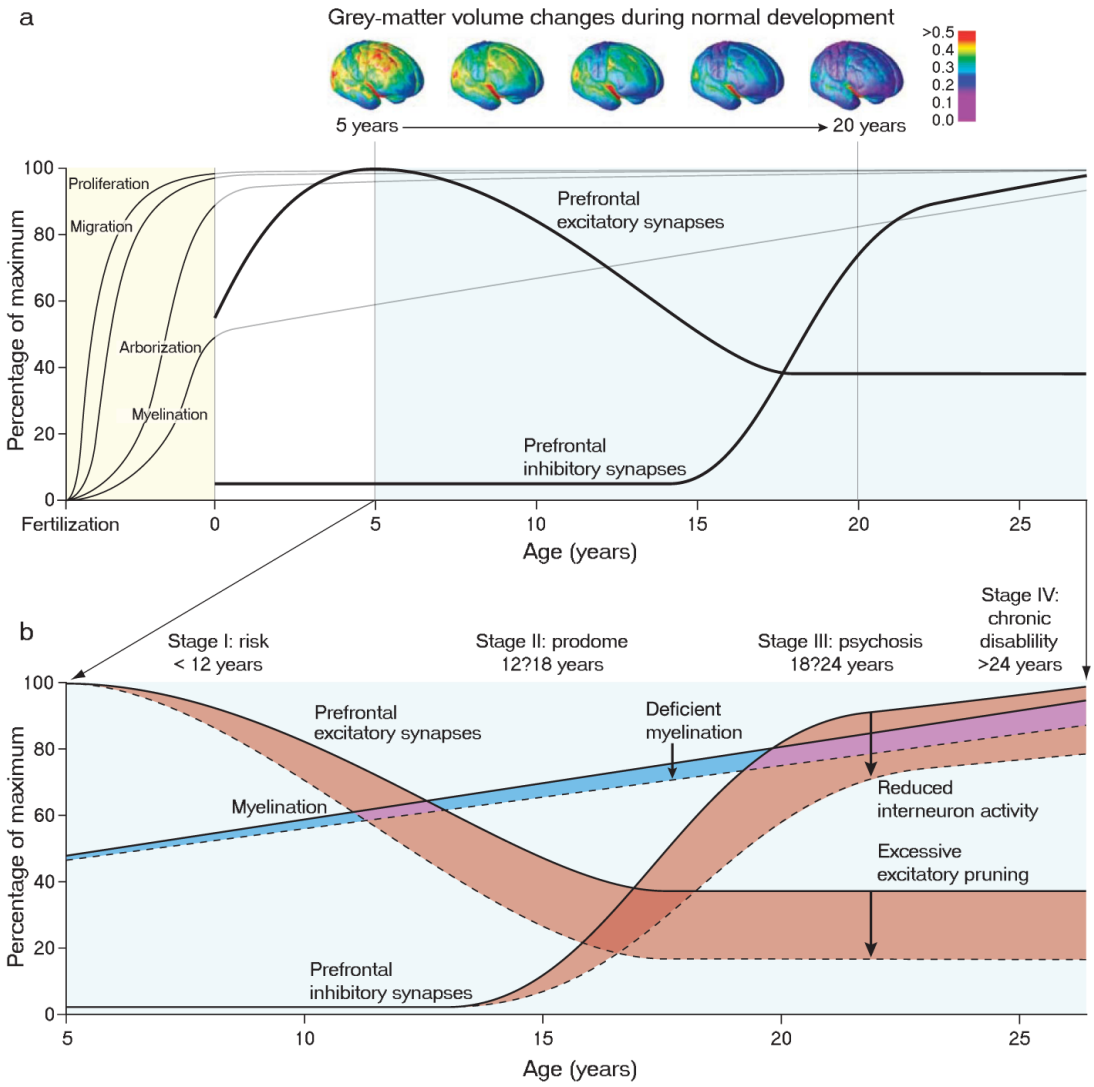

Figure 1-3: Neurodevelopmental model of schizophrenia.

(a) Diagram of proliferation, migration, arborisation and myelination in prefrontal and changes in brain grey matter volume in healthy subjects. (b) Comparison of brain neurodevelopment between healthy subjects and schizophrenic patients. Patient with schizophrenia show excessive excitatory pruning, reduced interneuron activity and deficient myelination during neurodevelopment. Taken from (Insel, 2010).

All these findings suggest neurodevelopmental alterations in the pathology of schizophrenia. However, after adolescence, the adult brain still undergoes neurogenesis and neuroplasticity to produce new neurons and new neuronal connections. These mechanisms may also be implicated in schizophrenia.

1.3.2 Neurogenesis

There are several evidences that early onset of schizophrenia is associated with reduction of the hippocampus and an increase of ventricles volume (McDonald et al., 2002; Pantelis et al., 2003). The hippocampus, the subventricular zone (SVZ) and the olfactory bulb are well known to house adult neurogenesis (Kornack and Rakic, 2001). Adulthood neurogenesis is known to be implicated in learning processes in the hippocampus and in olfactory tissue regeneration. Although disturbance of adult neurogenesis has not yet been demonstrated, several clues suggest that it may be involved in schizophrenia. Olfactory impairments have been reported in patients with schizophrenia (Rupp et al., 2005). Furthermore, cultured olfactory cells from schizophrenic patients showed differential expression of cell surface molecules regulating cell proliferation, differentiation and death compared to healthy individuals (Féron et al., 1999). During development of the central nervous system the Wnt-dependent signaling pathway regulates cell adhesion, proliferation and differentiation (Dale, 1998). Briefly, Wnt interacts with 'frizzled' receptors which activate disheveled and lead to the degradation of β-catenin via glycogen synthase kinase 3β (GSK-3β). This signaling pathway might be implicated in neurogenesis mechanisms and disturbed in schizophrenia. A post-mortem study demonstrated that GSK-3β mRNA was significantly decreased in hippocampus of patients with schizophrenia (Nadri et al., 2004). In addition, a decrease of β-catenin and γ-catenin was found in hippocampus of schizophrenic patients (Cotter et al., 1998). A recent study using gene knockdown in mice showed that adult neurogenesis in hippocampus is regulated by Wnt signaling pathway via DISC1 (Mao et al., 2009). Other factors implicated in neurodevelopment may play a role in adult neurogenesis and be disturbed in patients with schizophrenia. Neurotrophins, neuregulins, reelin, and retinoid are factors which could be involved in

dysfunction of the neurogenesis in schizophrenic patients and could be investigated for a better understanding of the mechanisms of the illness (Toro and Deakin, 2007).

Regarding functional impairment and reduced volume of the hippocampus observed in early episode of schizophrenia, these findings highlight an involvement of neurodevelopment factors in the mechanism of neurogenesis in adulthood which could be investigated to find new pharmaceutical targets to cure the illness.

1.4 Neurochemical theories of schizophrenia

1.4.1 Dopaminergic theory

Arvid Carlsson and Paul Greengard obtained the Nobel Prize of Physiology and Medicine in 2000 for the discovery of the dopamine and Arvid Carlsson was the first to provide evidence that chlorpromazine functions by blocking dopamine receptors (Iversen and Iversen, 2007). The hyperdopaminergic theory of schizophrenia stemmed from the finding that administration of D-amphetamine, a drug of abuse known to be a dopamine agonist mimics positive symptoms of schizophrenia in healthy individuals. Moreover, recent studies based on cerebral imaging showed that the administration of this drug in small amounts causes a larger release of dopamine in the brains of the schizophrenic patients compared to controls (Iversen and Iversen, 2007).

Dopamine is a neurotransmitter that belong to the catecholamine family and acts at two distinct metabotropic G-coupled receptor families. The D1 (including D1 and D5 receptors) and D2 (including D2, D3, and D4 receptors) receptor families activate and inhibit postsynaptic adenylyl cyclase respectively at the dopamine synapse (Emilien et al., 1999). It is well accepted today that antipsychotic drugs are antagonists of the dopaminergic receptors, in particular D2 (Kapur and Mamo, 2003). Dopamine is known to modulate the glutmatergic system in many regions of the brain such as PFC and hippocampus. Hyperdopaminergy that occurs in schizophrenia and symptoms which ensue from could be explained either by excess of dopamine itself or by an increase of

its receptors. All these data contribute to the hyperdopaminergic theory of schizophrenia. Despite the fact that much evidence implicates dopamine in the neuropathology of schizophrenia, attempts to explain this disease solely in terms of dopaminergic system impairment leaves many aspects unsolved.

1.4.2 Serotonergic theory

The serotonergic theory originally arose from findings of the effect of a drug of abuse, LSD, which is a 5-hydroxytryptamine (5-HT_{2A}) agonist and induces hallucinations in healthy individuals. LSD activates specifically 5-HT_{2A} receptors situated on neocortical pyramidal cells, leading to increased level of glutamate in the cortex. The use of LSD has led to a better understanding of the 5-HT2A receptor which is implicated in cognitive processing such as working memory. Furthermore, brain imaging in humans has shown that hallucinogens increase prefrontal cortical metabolism (Nichols, 2004). In addition, "atypical" antipsychotics such as clozapine, olanzapine, and quetiapine, are known to antagonize 5-HT_{2A} receptor more than dopamine D2 antagonists. These antipsychotics have effect on both positive and negative symptoms of schizophrenia suggesting a role of 5-HT_{2A} receptor in the therapeutic action of these drugs.

Equivocal findings regarding the possible involvement of serotonergic systems in schizophrenia, however, have been reported. A brain imaging study using PET showed no changes in number of 5-HT receptors in schizophrenic patients (Trichard et al., 1998), whilst two other studies using post-mortem 5-HT binding found an increase (Hashimoto et al., 1991) and a decrease number of receptors compared to healthy controls (Burnet et al., 1996). Neuropharmacological evidence suggests that serotonergic system is implied in some aspects of schizophrenia, however the causes of cognitive symptoms in the illness and a possible role of 5-HT_{2A} receptors remains widely unclear and requires further study.

1.4.3 Glutamatergic theory

Glutamate (L-glutamic acid) is a neurotransmitter present in the central nervous system (CNS). It belongs to the amino-acid neurotransmitter family and it is considered as the principal excitatory neurotransmitter in the brain. There are two families of glutamate receptors, the ionotropic receptors which include the *N*-methyl-D-aspartate receptor (NMDAR), the α-amino-3-hydroxy-5-methyl-D-aspartate receptor (AMPAR) and kainate receptors; and glutamate metabotropic receptors. Both families have been implicated in the pathophysiology of schizophrenia.

Pharmacological and in-vivo imaging studies have highlighted that antagonists of NMDAR (e.g. ketamine, Phencyclidine [PCP]) reproduce negative, positive symptoms, and cognitive deficits related to schizophrenia in healthy volunteers (Krystal et al., 1994). Moreover, some suggest that this effect is more transparent than for any other known drug (Parwani et al., 2005). Ketamine administration induces an increase in blood flow in the prefrontal cortex (Lahti et al., 1995), increases quantity of glutamate released in the prefrontal cortex in normal volunteers (Moghaddam et al., 1997) and strongly worsens symptoms in schizophrenic patients (Javitt and Zukin, 1991). These observations contributed to the establishment of the glutamate NMDA receptor hypofunction theory of schizophrenia.

1.5 NMDA receptor and schizophrenia

1.5.1 Structure and function

Glutamate is the principal excitatory neurotransmitter in the mammalian CNS. Most brain neurons express at least one class of glutamate receptors. The NMDAR (see Figure 1-4) is a tetrameric channel which is triggered by the glutamate and co-agonist binding; leading to calcium entry at the postsynaptic membrane. This mechanism is voltage depend, magnesium ions block the channel whilst the postsynaptic membrane remains polarised. The NMDAR is composed of three different subunits, NR1 (GRIN1),

NR2 (GRIN2-A, -B, -C nd -D) and NR3 (GRIN3). The NR1 subunit contains a binding site for glycine and D-serine co-agonists whilst the NR2 subunits contain the binding site for glutamate (Lei and McBain, 2002).

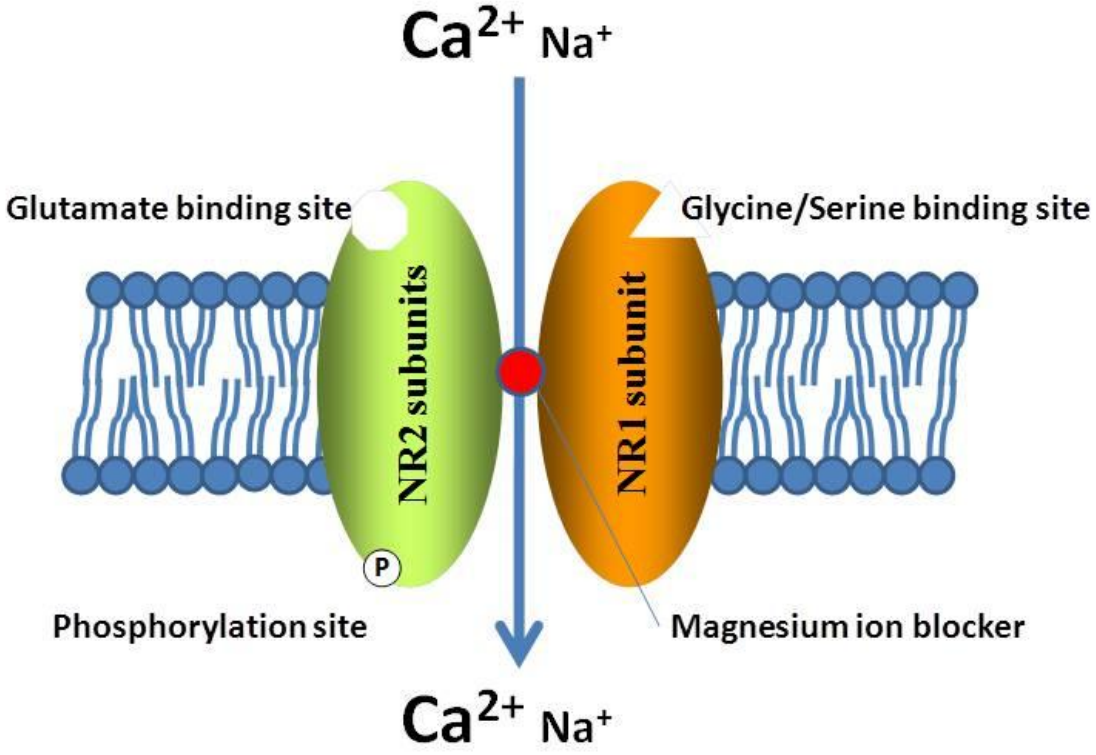

Figure 1-4: The NMDA receptor.

The NMDAR is composed of four or five subunits including at least one copy of the NR1 subunit. The glutamate binding site is on the NR2 subunit, while the Glycine/D-Serine binding site is on the NR1 subunit. The NR2 subunit can be phosphorylated. Opening of the NMDAR channel depends on binding of glutamate and co-agonist (glycine/D-serine) and depolarising excitatory post-synaptic current leading to magnesium release and calcium entry into the post-synaptic dendrite.

The NMDAR is implicated in several neurobiologic mechanisms such as neurodevelopment, cerebral plasticity and excitotoxicity, all of which could play a

major part in schizophrenia pathophysiology. Indeed, schizophrenia is a disease which appears only after adolescence and it was shown that among newly-diagnosed schizophrenic patients, the normal loss of neuronal connections observed in normal individuals is exacerbated by an additional 30% in patients (Bennett, 2008). Moreover the increase in glutamate release in the prefrontal cortex of schizophrenia patients could induce excitotoxic mechanisms (e.g. apoptosis and inflammation) and would explain the loss of cerebral volume observed in this disease.

In order to determine the involvement of NMDA receptors in schizophrenia, a study using genetic methods to induce NMDA hypofunction in rodents showed that a genetically induced reduction of the NR1 subunit NR1 of NMDARs results in deficits in attention, social behaviour and cognitive symptoms (Mohn et al., 1999). Similar results were obtained by changing the co-agonist glycine binding site on NR1 subunit (Ballard et al., 2002). However post-mortem studies have not conclusively shown differences in NMDA subunits expression between schizophrenic patients and controls (Kristiansen et al., 2007a).

1.5.2 NMDAR hypofunction

The NMDAR hypofunction theory is based on the observation that NMDAR antagonists (PCP, MK801 and ketamine) induce schizophrenia symptoms in normal volunteers (Javitt and Zukin, 1991). NMDAR hypofunction theory suggests that co-agonists such as glycine/D-serine should be therapeutically beneficial in schizophrenia. The use of D-cycloserine, a partial NMDAR glycine-site agonist, may improve cognitive functions in schizophrenia (Javitt, 2012). Studies using functional magnetic resonance imaging have made it possible to highlight disturbed brain function in schizophrenic patients. Abnormalities have been observed in cortical and subcortical structures such as the prefrontal cortex, hippocampus, temporal lobe, cingulate gyrus, thalamus and cerebellum (Liddle, 2001). All of these structures are known to have a broad

glutamatergic component. An emerging hypothesis is that dopaminergic dysfunction in schizophrenia is secondary to a fundamental glutamatergic dysfunction.

A particularly interesting study correlates the status of ErbB4 receptor function and NMDA hypofunction in schizophrenia (Hahn et al., 2006). In this study, addition of NRG1 to human brain slices induced phosphorylation (activation) of its ErbB4 receptor leading to decreased NR2A subunit phosphorylation. A decrease in NR2A phosphorylation was exacerbated in hippocampus samples from schizophrenia patients. Furthermore, the interaction between scaffolding protein, post synaptic protein 95 (PSD-95), NMDAR and ErbB4 was increased, leading to a greater reduction in NMDAR phosphorylation in response to NRG1. There was an absence of changes in PSD-95 or ErbB4 protein levels, suggesting that protein-protein interactions in the PSD are responsible for NMDA receptor hypofunction in schizophrenia (Hahn et al., 2006).

Glutamate synapses in the central nervous system are characterised by electron-dense zones under the postsynaptic membrane; called postsynaptic densities (PSD). PSDs are composed of a dense network several hundred proteins, such as receptors, ion-channels, scaffolding proteins, and enzymes such as kinases and phosphatases (Collins et al., 2006a). The study of PSD proteins in schizophrenia is important, especially in light of the findings by Hahn *et al*., 2006 suggesting that NMDAR hypofunction could be related to abnormal protein-protein interactions within the PSD.

1.6 Post synaptic density

1.6.1 Structure and function of the post synaptic density

The post synaptic density is a dense network of proteins localized along the glutamate post synaptic membrane within dendritic spines (see Figure 1-5). The PSD forms a macromolecular complex that plays an essential role in synaptic signaling pathways, receptor trafficking and synaptic plasticity. The whole complex of proteins forms a band of 30 to 40 nanometres thick with a diameter of a few hundred nanometres. Various studies have isolated the PSD using differential centrifugation methods and

have determined that the PSD appears as disc-shaped organelles using electronic microscopy (Ziff, 1997).

Glutamate receptors such as AMPAR, NMDAR and metabotropic receptors are embedded in the PSD and linked to specific clusters of proteins (Mayer and Armstrong, 2004). To identify each of the different receptor-associated protein complexes, proteomic studies were carried out and three protein complexes defined; the NMDAR associated complex (NRC) also called Membranes Associated Guanylate Kinases (MAGUK)-Associated Signalling Complex (MASC), the AMPAR complex (ARC) and the mGluR complex (mGC) (Farr et al., 2004).

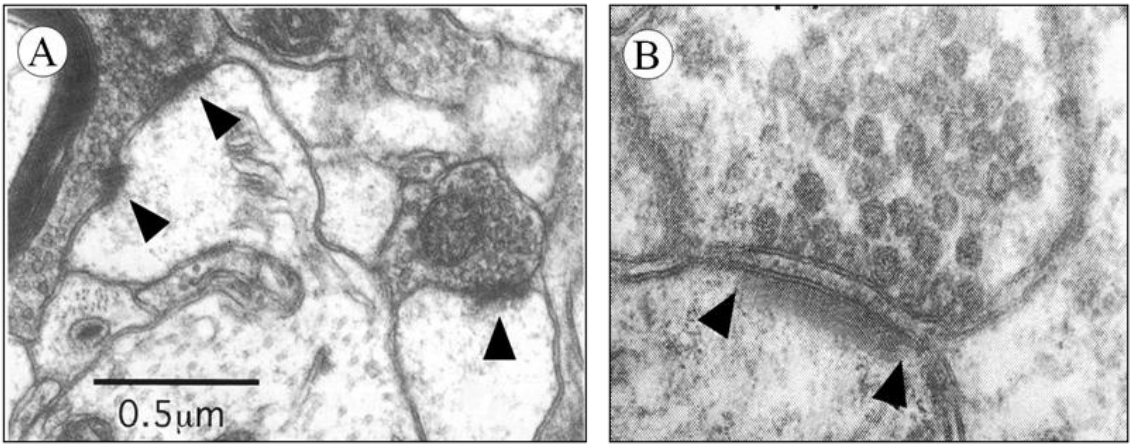

Figure 1-5: Electronic microphotographs of the glutamatergic synapses.

(A) Electron micrograph from the adult hippocampal CA1 region. (B) Synaptic junction formed between a Purkinje cell dendritic spine and a parallel fiber axon in the murine cerebellar cortex. Arrowhead indicates the PSD of the synapses. Taken from (Ziff, 1997).

Within the PSD more than one thousand proteins have been identified and about five hundred have been detected in two or more high-throughput proteomic studies (such as using two dimensional gel electrophoresis followed by liquid chromatography coupled with tandem mass spectrometry (2D LC-MS/MS)) of the PSD (Collins et al., 2006a). PSD proteins have been categorized into functional groups including ion

channel receptors, receptors, cell adhesion and cell-cell interaction proteins, scaffold proteins and signal transduction proteins, amongst many others (Yoshimura et al., 2004a). Amongst these complexes, scaffold proteins such as PSD-95 (Cho et al., 1992a), signalling molecules such as calmodulin and calcium calmodulin dependent protein kinase II (CaMKII) and proteins of the cytoskeleton such as actin and tubulin play a prominent role in synapse formation and function (Kennedy et al., 1983).

Recent studies using comparative proteomics and genomics highlighted the origin of the pro-PSD structure in unicellular organisms and suggested that it plays a role in cell-cell communication, calcium signalling and cytoskeleton regulation (Alié and Manuël, 2010). Moreover a study showed the presence of PSD and MASC orthologs in yeast which regulate structural functions. In this study they also compared PSD composition in different organisms such as unicellular, invertebrate and vertebrate. They showed an increase in structural complexity of the PSD, particularly marked by an expansion of receptors, scaffolding and cytoskeletal proteins which correlated with organism complexity. They also showed differential organisation of the PSD depending on brain localisation in complex organism such as vertebrates (Emes et al., 2008).

In dendritic spines of neurons, the PSD is a dynamic structure which functions as a bridge that constantly reacts to intra- and extracellular signals. A study showed that the PSD thickness increases around two-fold following potassium stimulation in rat cultured neurons and hippocampal slices, due to accumulation of CaMKII within the PSD (Dosemeci et al., 2001). The PSD can be considered as a specialised organelle within the dendrite spine that regulates synaptic interaction between the pre-synaptic terminal and post-synaptic dendrites of neurons.

Modulation of the PSD is essential during neurodevelopment, and allows maintenance and plasticity of spines during adulthood. Neurotrophic factors, cell adhesion proteins and neurotransmitters act on their receptors which are embedded within the PSD to modulate protein-protein interactions between scaffolding proteins within the PSD which trigger molecular mechanisms implicated in the regulation of receptors

trafficking, intracellular cytoskeleton rearrangements, and the strength of the synapse in response to specific activity. The PSD also plays an important role in synaptogenesis and synaptic plasticity. These unique functions of the PSD suggest a central role in disturbances of LTP and LTD and hence learning and memory (Boeckers, 2006).

1.6.2 Receptors within the PSD

Trans-membrane receptors and cell adhesion molecules (CAMs) are embedded within the PSD and regulate synapse formation and maintenance via their interaction with scaffolding and signalling proteins of the PSD.

At glutamate post-synaptic dendrites, NMDAR and AMPAR are the most represented glutamate receptors within the PSD whilst mGluRs (mGluR1/5) are present at a lower concentration (Mayer and Armstrong, 2004). Within the PSD, these receptors are associated with specific proteins to form protein complexes NRC-MASC, ARC, mGC which respectively correspond to NMDAR, AMPAR and mGluR binding complexes.

NR1, NR2A-B and NR3 NMDAR subunits are highly expressed at the dendritic membrane, and their surface trafficking is regulated by their interactions with proteins of the PSD. NR2A subunit interacts with PSD-95/Discs-large/ZO-1 homology (PDZ) domain of scaffold proteins via its C terminus and this interaction is disturbed in experiments using competitive peptide mimicking the NR2A C terminus. The scaffolding proteins PSD-95 and PSD-93 were identified as essential for NR2A membrane surface trafficking (Delint-Ramirez et al., 2010). Both C termini of NR2A and NR2B subunits bind PSD-95 scaffold protein within the PSD. They also bind CaMKII which regulate their interaction with PSD-95 via specific phosphorylation sites (e.g. PDZ1 of PSD-95) (Gardoni et al., 2006). NR1 and NR3 NMDAR subunits interact with the NR2 subunits. NR1 is essential for NMDAR function and localisation at the post-synaptic membrane as it carries the co-agonist binding site. This is exemplified in NR1 knock-down studies, where the NR2A and NR2B subunits no longer localise at the postsynaptic membrane but instead remain in the endoplasmic reticulum (ER) (Forrest et al., 1994; Fukaya et al., 2003).

A study using co-immunoprecipitaion and bioluminescence resonance energy transfert (BRET) demonstrated that NMDAR NR1 subunit interacts with the dopamine D1 receptor within the PSD. They also showed using co-transfection of dopamine D1 receptor and NR1 subunit that NR2B is necessary for the translocation of D1/NR1 complex to the post-synaptic dendrite membrane (Fiorentini et al., 2003). However there is no evidence that NR1 and NR3 interact directly with scaffold proteins of the PSD.

The second most abundant glutamate receptor subtype at glutamate post-synaptic dendrites is the AMPAR which forms ARC complex with proteins of the PSD. The AMPAR is an ionotropic receptor composed of four tetrameric heteromeric subunits termed GluR1, GluR2, GluR3 and GluR4. The C termini of AMPAR GluR2/3/4 subunits interact with the scaffold proteins glutamate receptor-interacting protein 1/2 also called AMPA-receptor-binding protein (GRIP1/2 - ABP) and the protein interacting with C kinase (PICK1) via their PDZ domain (Dong et al., 1997; Nishimune et al., 1998; Xia et al., 1999). In addition, the *N*-ethylmaleimide sensitive factor (NSF) a protein implicated in vesicular membrane fusion is also a partner of AMPAR GluR2 subunits within the PSD (Dong et al., 1997; Nishimune et al., 1998). The GluR1 subunit binds the PDZ of the scaffolding protein Synaptic Associated Protein 97 (SAP-97) (Leonard et al., 1998; Rumbaugh et al., 2003). Although these proteins interact with AMPAR via their PDZ domain, their role within the PSD is AMPAR trafficking and recycling at the post-synaptic membrane. AMPARs can also be associated with proSAP/Shank proteins which are one of the main component of the PSD and act to dock the AMPAR complex at the PSD (Uchino et al., 2006).

Metabotropic GluR receptors (mGluRs) have also been reported to be enriched within the PSD, particularly the mGluR1 family which includes mGluR1 and mGluR5 (Mayer and Armstrong, 2004). These two metabotropic receptors interact with PSD scaffolding protein, Homer, an immediate early gene, which codes a protein with PDZ-like domain, Enabled /VASP homology-1 (EVH1) domain and a C-terminal coiled coil (CC) multimerisation motif that lead to Homer dimerisation (Brakeman et al., 1997). Homer

binds the mGluRs carboxy-terminal intracellular domains and regulates their activity. Disrupted interaction between Homer and mGluRs lead to constitutive activation of mGluRs highlighting that their activation is modulated by intracellular proteins as well as by glutamate binding (Ango et al., 2001). Moreover, Homer also interacts directly or indirectly with other proteins of the PSD such as Shank, PSD-95 and GKAP, linking them with the PSD complex (Tu et al., 1999).

Most dopaminergic neurons are localized in two regions of the brain: the substantia nigra pars compacta (SNc) and the ventral tegmental area (VTA). These neurons project their outputs to the striatum, nucleus accumbens, hippocampus and neocortex. In these latter brain regions, dopaminergic and glutamatergic systems interact at the post-synaptic dendritic spine. Both dopamine D1 (D1/D5) and D2 receptors (D2, D3 and D4) are enriched within the PSD (Yao et al., 2008). Confocal live cell imaging has shown that the D1 dopamine receptor family localises at the head of dendritic spines whereas D5 dopamine receptors concentrate at the neck. Furthermore, NMDAR-triggered stimulation leads to an increase of D1 receptor positive spine heads, possibly due to an interaction between D1/PSD-95/NMDAR (Kruusmägi et al., 2009). A study using co-transfection of D1 or D2 receptors with PSD-95 in HEK-293 cells highlighted an interaction between PSD-95 and D1/D2 receptors. Using functional assays they showed that the PSD-95/D1 complex is disturbed after dopamine stimulation. They also demonstrated the important role of PSD-95 in D1 resensitisation which is accelerated in the presence of PSD-95 (Sun et al., 2009).

PSD-95 interacts with the carboxyl-terminal tail of dopamine D1 receptor via its NH2 terminus domain. The interaction between PSD-95 and D1 plays an important role in internalisation of D1. In the absence of stimulation by D1 receptor agonist, the PSD-95/D1 receptor complex inhibits D1 signalling pathway due to an increased internalisation process via PSD-95 (Zhang et al., 2007). A study reported that PSD-95 stabilise interaction between dopamine D1 receptor and NMDAR which can induce cell death when both receptors are over activated. In this study they also showed that PSD-95 inhibits dopamine D1 receptor-NMDAR NR1 subunit association and NMDAR-

dependent activation of dopamine D1 receptor recycling. Dopamine D1 receptor/NMDAR/PSD-95 complex plays critical role in molecular mechanism underlying neuronal cell survival and neuroplasticity (Zhang et al., 2009). To highlight the role of PSD-95 in the regulation of dopamine D1 receptor induced NMDAR Ca^{2+} release, a study was carried out using co-transfected HEK 293 cells with PSD-95/D1/NR1-NR2B complex. They showed that treatment with dopamine increased NMDAR activity in dose-dependent manner whereas no difference was observed in their controls without co-transfected PSD-95. This study suggests a pivotal role of PSD-95 in dopamine D1 receptor triggered NMDAR activity and LTP (Gu et al., 2007).

Treatment with dopamine D1 receptor agonist leads to AMPAR GluR1 subunit phosphorylation which increase the number of GluR1 subunits at the dendritic spine. Mutation experiments of scaffolding proteins of the PSD such as A-kinase anchoring protein (AKAP79/150) and PSD-95 disturb this molecular mechanism. These results show the involvement of the proteins of the PSD in AMPAR receptor trafficking via dopamine D1 receptor modulation which may have an important role in synaptic plasticity (Swayze et al., 2004). The D2 dopamine receptors family also interacts with the PSD, a study highlighted the role of the interaction between D2 dopamine receptor and NMDAR NR2B subunit in vivo. They showed that recruitment of CaMKII by NR2 subunit phosphrylation site within the PSD is disturbed after dopamine stimulation. In consequence, phosphorylation of the NR2 subunit is reduced which lead to a hypoactivity of the NMDAR (Liu et al., 2006). These studies highlight the importance of PSD proteins such as PSD-95, in mechanisms that regulate dopamine receptor and NMDAR interactions with a potentially important role in dendritic spine plasticity, molecular mechanisms of memory and possibly schizophrenia pathophysiology.

Trophic factors such as Neuregulins (NRG), ephrins and neurotrophins are involved in neuronal development and synaptic plasticity. These factors interact with receptor tyrosine kinases (RTKs) which are embedded within the PSD.

Amongst the six existing subtypes of receptor tyrosine kinases, ErbB (generated by alternative splicing of the gene ERBB and activated by NRG1), ErbB2, ErbB3 and ErbB4 are the three subtypes present at the glutamatergic synapse and interact with scaffolding proteins of the PSD (Bublil and Yarden, 2007). PSD-95 interacts with ErbB4-ErbB4 homodimer and indirectly with ErbB2-ErbB3 heterodimer via erbin, a protein that contains multiple leucine-rich domains and a PDZ domain (Huang et al., 2000; Huang et al., 2001).

Another type of RTKs are the Eph receptors which are activated by cell-surface ligands called Ephrins (Klein, 2004). There are two main types of Eph receptors; EphA (EphA1–8) and EphB (EphB1–4, EphB6) which respectively bind ephrin A (A1-A5) and ephrin B (B1-B3) transmembrane ligands (Kullander and Klein, 2002). EphB2 and EphB4 are present at the post-synaptic dendrites (Dalva et al., 2000). Furthermore, a study highlighted the involvement of the scaffolding protein SAP 97 in a transsynaptic signalling implicated in synaptic plasticity which functions via EphB receptor/ephrinB suggesting interaction between EphB and SAP-97 (Regalado et al., 2006).

The third group of TRKs, activated by neurotrophins consist of two classes of receptors; the tropomyosin-related kinase (Trk) family of receptors and the p75 a member of the tumour necrosis factor family. The neurotrophins nerve growth factor (NGF), brain derived neurotrophic factor (BDNF), neurotrophin-3 (NT-3), and NT-4/5 bind the Trk family (TrkA/B/C) whereas pro-neurotrophins (neurotrophin precursors) bind to p75 (Reichardt, 2006a). Studies have shown that both TrkB and p75 interact with PSD-95 (Sandoval et al., 2007; Yoshii and Constantine-Paton, 2007a).

Synaptic cell adhesion molecules (synCAMs) are transmembrane receptors implicated in cell-cell interactions. These transmembrane receptors contain typically an intra-, a trans- and an extra-cellular domain. The extracellular domain interacts with either the same kind of CAMs (homophilic binding) or other kind of CAMs (heterophilic binding). The synCAMs transmembrane receptors regroup four classes of proteins; the cadherin–catenin, the cadherin-like and cadherin-related neuronal receptor (CNR), the

immunoglobulin-like (Ig) superfamily, and the neurexin–neuroligin. These receptors are enriched at the post-synaptic dendrites and most of them contain specific domains such as PDZ to interact with proteins of the PSD. For instance, a study showed that postsynaptic CAMs such as netrin-G ligand (NGL) and netrin-G (NG) interact with PSD-95 via their cytosolic domain in cultured rat neurons. They also showed that modulation of the expression of these receptors regulate the abundance of PSD-95 leading to a regulation of dendrite spine formation. This study suggests that CAMs are important for the recruitment of PSD-95 during synapse formation and could be implicated in plasticity (Kim et al., 2006). In a more recent study, the CAMs NGL-3 was also identified as an interacting receptor with PSD-95. This CAMs interacts with leukocyte common antigen-related (LAR) which modulate synapse formation and maturation (Woo et al., 2009).

1.6.3 Protein-protein interactions within the PSD

The PSD can be defined as a cluster of specific protein complexes. As mentioned above (see section 1.6.1) glutamate receptors NMDAR, AMPAR and mGluR form protein complex with associated scaffolding proteins called NRC, ARC and mGC respectively. These protein complexes are linked via another molecular structure called Pro-SAP/Shank platform (PSP) which is associated with the cytoskeleton and smooth endoplasmic reticulum (SER) within the dendrite spine (Boeckers, 2006). Scaffolding proteins are characterised by specific protein-protein interacting domains such PDZ (PSD-95/ Discs large/Zona occludens 1), SH3 (src-homology 3), GK (guanylate kinase), EVH1 (*N*-terminal Ena/VASP Homology 1), CC (coiled-coil) and SAM (sterile alpha motif) domains.

Among scaffolding proteins of the PSD, the Membranes Associated Guanylate Kinases (MAGUKs) proteins play an important role in the regulation of the intracellular traffic and the synaptic localization of the ionotropic glutamate receptors. Four homologues have been described; the synapse-associated proteins (SAP) 90/PSD-95, SAP102,

SAP97 and chapsyn-110/PSD-93, all localised at the glutamate synapses of the CNS (Aoki et al., 2001). All of these MAGUK proteins contain three PDZ domains at the *N*-terminus, a SH3 domain and a C-terminal guanylate kinase GK domain. These domains play a key role in protein-protein interactions between receptors of the post-synaptic dendrite, MAGUK proteins, scaffolding proteins of the PSD and signalling proteins implicated in synaptic plasticity (Elias and Nicoll, 2007; Lau and Zukin, 2007).

SAP/PSD-95 was the first scaffolding protein identified within the PSD and studies showed that first and second PDZ domains interact with the NR2 subunit of the NMDAR (Cho et al., 1992a; Kistner et al., 1993; Niethammer et al., 1996). It is well known now that PSD-95 regulates synaptic activity organizing the glutamate ionotropic receptors and their signalling associated proteins in the PSD. PSD-95 interacts also with AMPAR indirectly via stargazin/TARPs which contain the C-terminal PDZ binding motif and play a crucial role in AMPAR trafficking at the glutamate synapse (Schnell et al., 2002). A study also reported that the MAGUK protein SAP-97 could play the same role as stargazin/TARPs allowing interaction between AMPAR and NMDAR/PSD-95 (Chen et al., 2000; El-Husseini et al., 2002). SAP-97 was also identified as partner of NMDAR via NR2A subunit (Gardoni et al., 2003; Mauceri et al., 2007). The scaffolding protein MAGUK SAP102 interacts with NR2B NMDAR subunit and its role is to deliver the subunit to the synaptic membrane (Sans et al., 2003). In addition, studies have highlighted two more binding partners neuroligin and ErbB4 which interact with the third PDZ domain of PSD-95 (Huang et al., 2000; Irie et al., 1997; Song et al., 1999; Naisbitt et al., 1999; Garcia et al., 2000). These studies show the important role of MAGUKs scaffolding proteins in receptor clustering and trafficking at post-synaptic membrane. Furthermore they also have a role in protein-protein interactions with other scaffolding protein of the PSD and signalling proteins implicated in synaptic plasticity.

The other main types of scaffolding proteins within the PSD are the pro-SAP/Shank proteins. All family members are from splice variant of three genes named Shank1/2/3 (Naisbitt et al., 1999; Lim et al., 1999). Typically, proteins coded by these genes contain

six protein-protein interaction domains namely *N*-terminal ankyrin (ANK) repeats SH3 (Src homology 3) and PDZ domains, several proline-rich clusters (PRC), a cortactin binding domain (ppI) and a SAM domain at C-terminal. The PDZ domain of Pro-SAP/Shank binds the C-terminus of GKAP scaffolding protein which interacts with PSD-95/NMDAR complex (Naisbitt et al., 1999). The *N*-terminal ankyrin repeats of Shank are only present in Shank 1 and pro-SAP2/Shank 3 scaffolding proteins which interact with α-fodrin a protein interacting with actin filament and Sharpin a protein implicated in oligomerisation of ProSAP (Lim et al., 2001).

ProSAP/Shank scaffolding proteins were also identified as partners of Homer, another type of scaffolding protein present within the PSD. The proline-rich clusters of Pro-SAP/Shank interacts with the EVH1 domain of Homer which links mGluR1 and mGluR5 with inositol 1,4,5-trisphosphate (IP3) receptors and Shank/GKAP/PSD-95/NMDAR complex (Tu et al., 1999; Tu et al., 1998). These protein-protein binding domains are also implicated in pro-SAP/Shank – cytoskeleton interaction as they allows interaction with cortactin and actin binding protein (Abp1) which regulate actin polymerization (Kim and Sheng, 2004; Qualmann et al., 2004). The SAM domain at C terminus of pro-SAP/Shank was identified as the molecular structure which allows Pro-SAP/Shank – Pro-SAP/Shank binding and give rise to the particular platform within the PSD; PSP (Naisbitt et al., 1999).

As mentioned above (see section1.6.2) the Homer gene was first identified as an IEG which encodes two specific protein-protein interactions domains, EVH1 and CC (Brakeman et al., 1997). A study showed that three Homer genes encode Homer 1/2/3 proteins and generate splice variants Homer 1a/b/c and Homer 2a/b (Xiao et al., 1998). All of these splice variants carry the EVH1 domain which interacts with mGluR1/5, pro-SAP/Shank scaffolding proteins and inositol 1,4,5-trisphosphate (IP3) receptors as mentioned above (Tu et al., 1999; Tu et al., 1998). A study also showed that EVH1 binding partner dynamin III allows the localization of the clathrin endocytic machinery near the PSD through its interaction with Homer and is implicated in AMPAR recycling at post-synaptic membrane (Lu et al., 2007). At the C-terminus the

protein-protein interactions CC domain is known to allow the dimerization of Homer proteins (Xiao et al., 1998).

The GKAP/SAPAP (guanylate kinase-associated protein/synapse-associated protein-associated protein) family of proteins is composed of four isoforms (SAPAP1-4), each containing a C-terminus with a PDZ-binding motifs and a 14-amino acid repeats domain which interacts with GK domain (Takeuchi et al., 1997). Temporal and spatial expression of these proteins varies during brain development (Kindler et al., 2004). GKAP1/SAPAP1 plays a central role in connecting PSD-95 scaffolding proteins of the Pro-SAP/Shank family. The 14-amino acid repeats domain anchors the PSD-95 Guanylate Kinase (GK) domain (Kim et al., 1997) and the synaptic scaffolding molecule (S-SCAM) (Hirao et al., 1998) and the PDZ-binding motifs binds to the PDZ domain of Pro-SAP/Shank molecules (Naisbitt et al., 1999). In addition, a study using immunoprecipitation experiments showed that GKAP/SAPAP protein family can interact with proteins associated with cell-cell adhesion molecules such as adenomatous polyposis coli (APC), beta-catenin (Akiyama, 1997) and nArg BP2 (Kawabe et al., 1999). GKAP/SAPAP also interacts with proteins of the cytoskeleton and associated proteins. Studies have also highlighted GKAP/SAPAP interaction with neurofilament (Hirao et al., 2000) and motor proteins such as myosin Va and dynein (Naisbitt et al., 2000). Thus the GKAP/SAPAP protein family plays central role in protein-protein interactions within the PSD as it links the three complexes NRC-MASC/ARC/mGC to the PSP.

1.6.4 The PSD and its possible role in schizophrenia

Since NMDA receptor hypofunction is implied in the pathophysiology of schizophrenia, it has been suggested that disturbed PSD-95 function may be associated with schizophrenia. However, it does not appear that the NMDA receptor hypofunction is directly related to the level of PSD-95 expression (Tsai et al., 2007). Despite this, a study demonstrated an increase in ErbB4-PSD95 interactions in postmortem tissue

slices of prefrontal cortex obtained from patients with schizophrenia. This study showed significantly increased NRG1-induced activation of ErbB4 compared to controls where protein levels of both proteins remained unchanged. Also NRG1-induced hypophosphorylation of NR2A subunit led to inhibition of NMDAR receptor activation which was more pronounced in schizophrenia subjects compared to controls (Hahn et al., 2006). These findings are the first consistent results which indicate that NMDAR hypofunction may be relevant to explain part of symptoms of schizophrenia.

Another study showed that transcription of DLGAP1 (gene coding for GKAP1) is up-regulated in the nucleus acumbens of rats treated with phencyclidine (a model for schizophrenia). This study also showed an up-regulation of DLGAP1 protein in the same brain area in untreated patients with schizophrenia (Kajimoto et al., 2003). A cytogenetic study showed that GKAP1 is implicated in families with schizophrenia (Pickard et al., 2005). Also, changes in gene copy number (Friedman et al., 2008) and reduced mRNA levels for this gene were associated with schizophrenia (Toro and Deakin, 2008 ; unpublished findings). In addition, a study showed that GKAP1 can potentiate the ionotropic activity of the NMDAR via PSD-95 (Yamada et al., 1999). Furthermore, GKAP1 co-immunoprecipitates with the NR2A subunit of the NMDAR and also with β-catenin (Akiyama, 1997). All of these findings suggest a potential role of GKAP1 as a modulator of the NMDAR and may play a role in NMDAR hypofunction in patients affected with schizophrenia. As previously mentioned, PSD-95 and the scaffolding protein ProSAP/Shank interact via GKAP1 in the PSD. As Shank plays an essential role in the maintenance of the dendritic spines and synapses in cultured hippocampus (Roussignol et al., 2005) and is also known to connect to Homer, a protein linked to mGluRs (see Figure 1-6), these proteins could be investigated as potential modulators of NMDAR function.

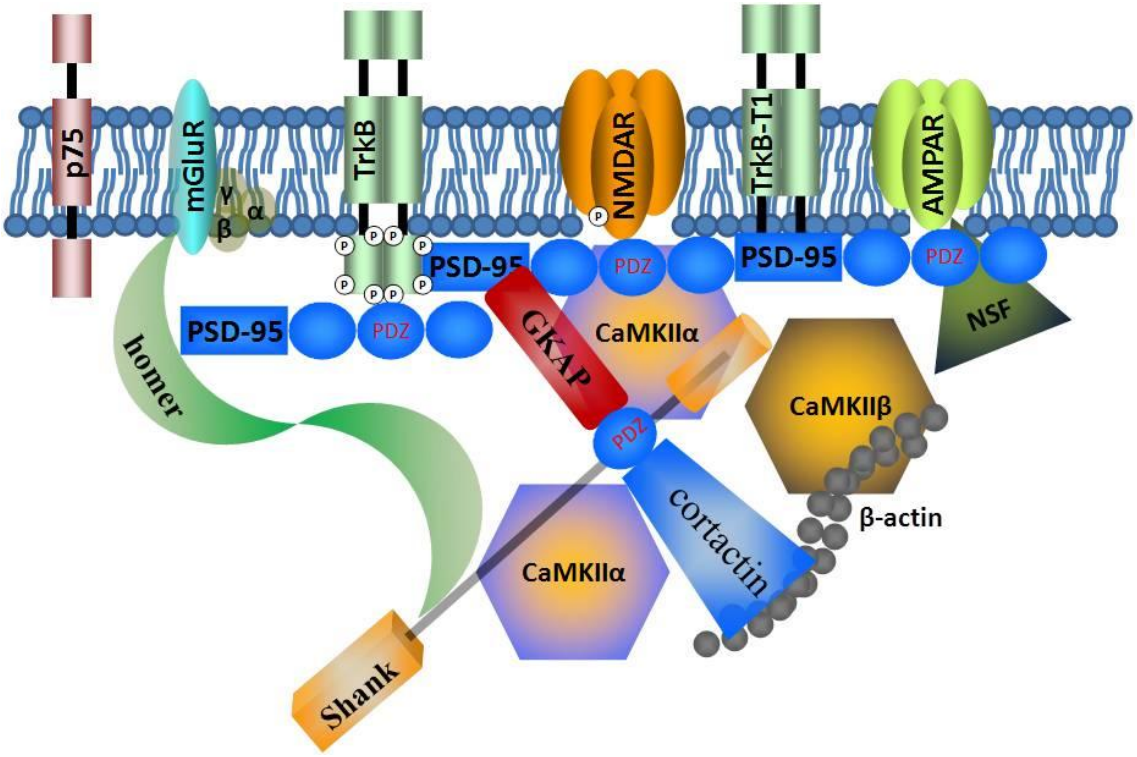

Figure 1-6: Protein-protein interactions at the postsynaptic density.

1.7 Hypothesis and aims

The preceding sections describe the pathophysiology of schizophrenia and some of the most convincing developmental and neurochemical theories of this illness. There is a focus on glutamatergic PSD neurotransmission in schizophrenia and in particular the glutamate NMDAR and associated proteins. Possible aberrations in expression of NMDARs and associated proteins in the brain in schizophrenia may contribute to many of the theories put forward in the present work.

Hypothesis

There is an alteration in the expression of proteins involved in synaptic plasticity within the PSD of premotor cortex from schizophrenics in comparison to major depressive disorder, bipolar disorder and healthy controls.

Aims

1. To optimise and characterise a method for the extraction/purification of the PSD from human premotor cortex.

2. To determine the protein expression of the NMDAR subunit NR2A and associated proteins PSD-95, CaMKIIα, CaMKIIβ and NSF in the PSD of the premotor cortex in schizophrenia compared to major depressive disorder, bipolar disorder and healthy controls.

3. To determine the expression of the neurotrophin receptors TrkB, truncated TrkB T1-TrkB and p75 that regulate synaptic strength and plasticity, in the PSD of the premotor cortex in schizophrenia compared to major depressive disorder, bipolar disorder and healthy controls.

2 Materials and methods

2.1 Human brain samples

Postmortem brain tissue from patients with schizophrenia, major depressive disorder, bipolar disorder and a non-psychiatrically ill comparison group was obtained from the Stanley Consortium postmortem brain collection. The four groups were matched by age, sex, race, postmortem interval, pH, and side of brain. Diagnosis was effectuated according to the Diagnostic and Statistical Manual of Mental Disorders, Fourth Edition, Text Revision (DSM IV-TR) and clinical, demographic and perimortem data were reported (see Table 2-1).

Table 2-1: Clinical and demographical data for Stanley Foundation Neuropathology Consortium (mean ±SEM).

Parameters	Control	Schizophrenia	Major Depression	Bipolar Disorder
№	15	15	15	15
Gender (F/M)	6/9	6/9	5/10	6/9
Age	48.1 (±10.7)	44.5 (±13.1)	46.5 (±9.3)	42.3 (±11.7)
Age Onset	N/A	23.2 (±8.0)	33.9 (±13.3)	21.5 (±8.4)
Duration of Illness (yrs)	N/A	21.3 (±11.4)	12.7 (±11.1)	20.1 (±9.7)
PMI (hrs)	23.7 (±9.9)	33.7 (±14.6)	27.5 (±10.7)	32.5 (±16.1)
pH	6.3 (±0.2)	6.2 (±0.3)	6.2 (±0.2)	6.2 (±0.2)
Mth Form	4.4 (±3.9)	11.2 (±8.5)†	8.4 (±6.6)†	9.7 (±3.6)†
Side (L/R)	8/7	9/6	9/6	7/8
Suicide	0	4	7	9
Antidepresants	0	5	8	7
Antipsychotics	0	15	0	12
Lithium	0	2	2	4

†Different from controls, planned contrast $p<0.05$. PMI - Postmortem Interval; yrs – years; hrs – hours; Mth Form - Months in Formalin; F - Female; M - Male; L - Left; R - Right; Integers are numbers of cases.

Brain specimens were sent to us with a code (IK + number) varying from researcher to researcher to ensure that our studies were blinded. The code was released to us only when all the data were collected and submitted to Stanley Medical Research Institute (SMRI). The brain samples consisted of 15 frozen blocks of premotor cotex (Brodman area 06) from a non-psychiatrically ill comparison group (control), 15 from patients with schizophrenia, 15 from patients with major depressive disorder, and 15 from patients with bipolar disorder. Two collections of 60 frozen blocks of premotor cortex were provided and used to carry out protein extraction, glutamate post-synaptic density enrichment, protein assay, Western blotting and co-immunoprecipitation experiments.

2.2 Enrichment of the glutamate post-synaptic density

The technique that was used for post-synaptic density (PSD) extraction consisted of a succession of centrifugation steps and the use of gradients of different sucrose concentrations to extract PSDs from the synaptosome. The technique used a bench centrifuge with two concentrations of sucrose (see Figure 2-1).

2.2.1 Stock solutions preparation and storage

Prior to PSD extraction, stock solutions were prepared and stored at 4°C (see Table 2-2).

Table 2-2: Stock solutions for PSD extraction using a bench centrifuge.

Compound	Concentration	Volume	pH	Storage
$MgCl_2$	0.5 M	5 ml	N/A	4°C
Hepes	0.5 M	20 ml	7	4°C
KCl	2 M	10 ml	N/A	4°C

$MgCl_2$ – magnesium chloride; Hepes - hydroxyethyl piperazineethanesulfonic acid; KCl - potassium chloride; N/A – not appropriate.

Stock solutions were used to prepare the extraction buffers utilised for extraction of 12 samples (see Table 2-3).

Table 2-3: Buffers for PSD extraction using a bench centrifuge.

Solution	Concentration	Volume	pH	Storage
Sucrose	0.32.M	40 ml	N/A	4°C
Sucrose	0.8 M	10 ml	N/A	4°C
Sucrose, $MgCl_2$	0.32 M, 1 mM	20 ml	N/A	4°C
Hepes	20 mM	20 ml	7	4°C
KCl, Triton X-100	150 mM, 2%	20 ml	N/A	4°C
KCl, Triton X-100	75 mM, 1%	20 ml	N/A	4°C

$MgCl_2$ – magnesium chloride; Hepes - hydroxyethyl piperazineethanesulfonic acid; Triton X-100 - nonionic surfactant; KCl - potassium chloride; N/A – not appropriate.

2.2.2 Preparation of the tubes

The 1.5 ml microcentrifuge tubes used for the different steps of the extraction were coated with Sigmacote (Sigma; SL2) and bovine serum albumin (BSA) to prevent proteins and PSD sticking to the surface of the tubes. Microcentrifuge tubes were coated with 1 ml Sigmacote for 30 seconds and then upside down for another 30 seconds. After discarding the Sigmacote, the tubes were left to dry for 30 minutes under a hood at 25°C. When dried the tubes were washed twice with 1 ml of sterile deionised water. A second coating was carried out with 1 ml of a solution of 10% BSA in sterile deionised water during 30 minutes on a plate shaker at 300 rotations per minute (rpm) and 30 additional minutes with the tubes upside down. Both steps were carried out at 25°C. After removal of the BSA solution the tubes were washed twice with 1 ml of sterile deionised water.

2.2.3 Homogenisation of the human premotor cortex

Frozen blocks of premotor cortex were weighed (100 mg), thinly chopped on ice and placed into homogeniser precellys tubes (Bertin Technologies; 03961-1-003) containing 450 µl of ice-cold 0.32 M sucrose, 1 mM $MgCl_2$ solution containing 2.5 % of protease inhibitor cocktail (Sigma; P8340). Samples were homogenised in a Precellys 24 dual tissue homogenizer (Bertin Technologies; 03119.200.RD010) for 15 seconds at 5000 rpm. After homogenisation the samples were placed on ice and 50 µl of homogenate was pipetted into a labelled tube (Total fraction). Total fractions were placed at -80°C for future analysis.

2.2.4 Extraction of the PSD

For PSD extraction all the centrifugation steps were carried out in a refrigerated centrifuge (Eppendorf 5417R centrifuge; fixed-angle rotor F-45-30-11). The homogenate was transferred into a microcentrifuge tube (tube 1) and centrifuged at 470×g for 2 minutes at 4°C. During this first step of centrifugation the homogeniser Precellys tubes was rinsed with 450 µl of ice-cold 0.32 M sucrose, 1 mM $MgCl_2$ solution containing 2.5% of protease inhibitor cocktail (sigma; P8340). Following the centrifugation the content of the rinsed homogeniser Precellys tube was added into tube 1, the lysate was resuspended by pipetting, then centrifuged at 470×g for 2 minutes at 4°C.

The supernatant was placed into another microcentrifuge tube (tube 2) and the pellet stored at -80°C for future analysis. The supernatant was centrifuged at 10,000×g for 10 minutes at 4°C to collect a synaptosome-enriched pellet. The supernatant collected after this step of centrifugation was pipetted into a labelled microcentrifuge tube (tube 3: cytosolic fraction) and stored at -80°C for future analysis.

The pellet was resuspended with 500 µl of 0.32 M sucrose solution and the suspension was layered onto 750 µl of 0.8 M sucrose solution in a labelled microcentrifuge tube

(tube 4). The samples were centrifuged at 9,100×g for 15 minutes at 4°C. Following centrifugation, the 0.32 M sucrose layer and the myelin/light membrane layer at the 0.32/0.8 M sucrose interface were pipetted into two microcentrifuge tubes, respectively labelled tube 5 and tube 6. Both tubes were stored at -80°C for future analysis.

The collected synaptosomal fraction in 0.8 M sucrose solution (~450 µl into tube 4) was diluted with an equal volume of 20 mM Hepes (pH 7) solution and half of the resultant synaptosomal fraction was poured in a labelled microcentrifuge tube (tube 7). In both, tube 4 and tube 7, an equal volume of 2% Triton X-100, 150 mM KCl solution supplemented with 2.5% protease inhibitor cocktail (sigma; P8340) was added and samples were agitated on a plate shaker for 15 minutes at 4°C and then centrifuged at 20,800×g for 45 minutes at 4°C. The supernatants were collected into two labelled tubes (tube 8 and tube 9) and stored at -80°C for future analysis.

The pellets obtained in tube 4 and tube 7 were resuspended in 500 µl of 1% Triton X-100, 75 mM KCl solution supplemented with 2.5% protease inhibitor cocktail (sigma; P8340) and centrifuged at 20,800×g for 30 minutes at 4°C. The supernatants were collected into two labelled tubes (tube 10 and tube 11) and stored at -80°C for future analysis. The pellets obtained in tube 4 and tube 7 were washed once by resuspending them in 500 µl of 20 mM Hepes (pH 7) and centrifuged as above. The supernatants were collected into two labelled tubes (tube 12 and tube 13) and stored at -80°C for future analysis.

The pellets collected in tubes 4 and 7 were resuspended in 40 µl TBS-T 0.1% supplemented with 2.5% protease inhibitor cocktail (sigma; P8340). Tubes 4 and 7 were defined as the PSD fractions and stored at -80°C until future analysis (see Figure 2-1).

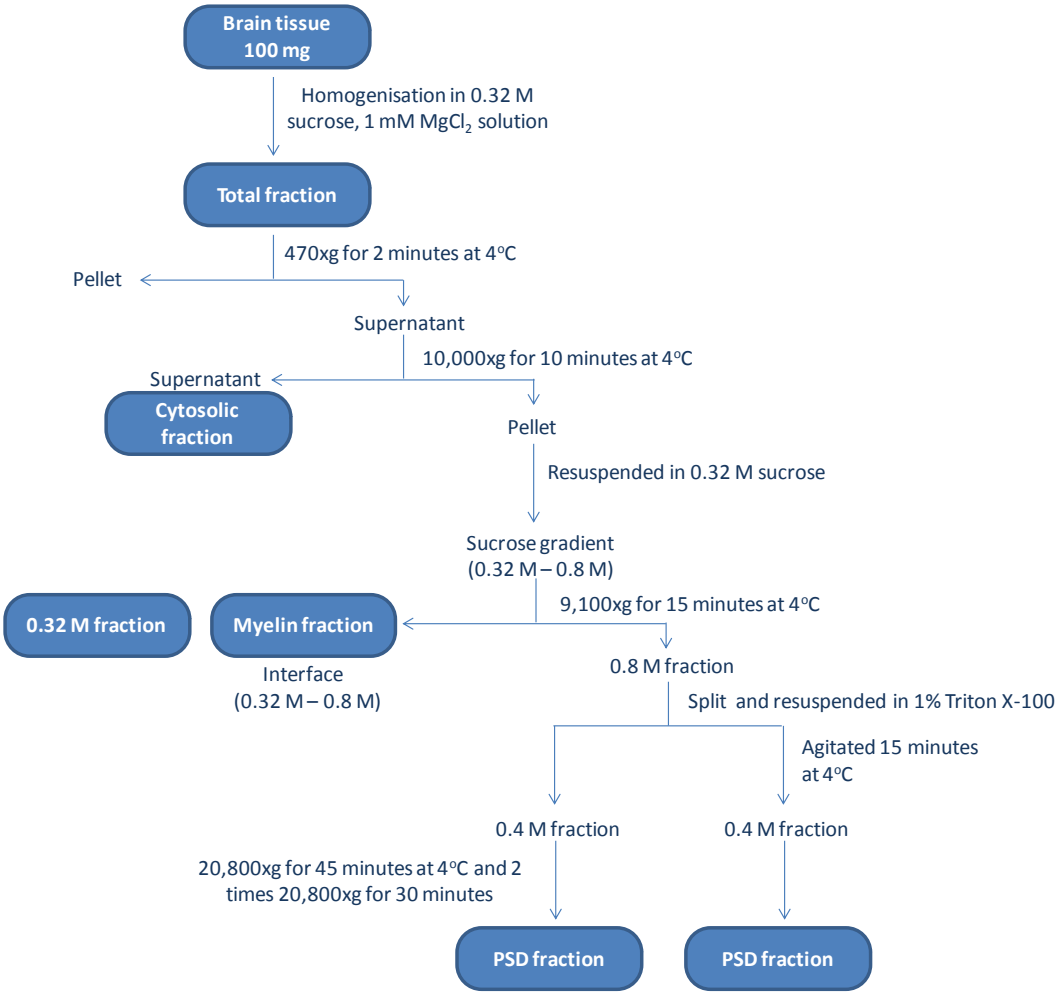

Figure 2-1: Diagram illustrating the different steps of PSD extraction using a bench centrifuge.

2.3 Electron microscopy

PSD fractions were extracted from two samples using a bench centrifuge (see section 2.2) to perform transmission electron microscopy (TEM).

All experiments, described below, were performed at the University of Cambridge (Department of Physiology, Development and Neuroscience) by Dr. Jeremy Skepper.

The samples were fixed, washed, osmicated, dehydrated and embedded in epoxy resin. After embedding, ultrathin sections (50 nm) were prepared with a

ultramicrotome (Leica; Ultracut UCT) using a 45° wedge angle diamond knife (Diatome) and were mounted on metal grids to be viewed in the TEM (FEI Tecnai G2).

2.3.1 Fixation of the PSD fractions

The initial fixation step was carried out in a buffered 0.1 M HEPES solution of 4% glutaraldehyde for 24 hours at 4°C. Samples were centrifuged at 20,800×g for 30 minutes at 4°C and washed in 0.1 M HEPES, 2 mM $CaCl_2$ buffer under agitation for 5 minutes at 4°C. This washing step was repeated three times. Samples were then centrifuged at 20,800×g for 5 minutes at 4°C.

The second fixation step (also called osmication step) was carried out in an HEPES buffered 1% osmium solution supplemented with 1.5% potassium ferricyanide (W/V) and 2 mM $CaCl_2$ during 2 hours under agitation at 4°C. Samples were centrifuged at 20,800×g for 5 minutes at 4°C and were washed in 0.1 M HEPES buffer for 5 minutes under agitation at 4°C. This washing step was repeated three times.

The final fixation (also called "bulk stain") was carried out in 2% uranyl acetate in 0.05M maleate buffer at pH 5.5. Samples were centrifuged at 20,800×g for 5 minutes at 4°C and the pellet was resuspended in deionised water. The samples were then embedded in epoxy resin prior to ultrathin sectioning. As epoxy resin used for our experiment was polymerised in hydrophobic media, the water present in the samples was replaced by ethanol.

2.3.2 Dehydration of the PSD fractions

Dehydration was undertaken in ethanol following the dehydration steps: 50% ethanol for 5 minutes (2 times), 70% ethanol 5 minutes (3 times), 95% ethanol 5 minutes (3 times) and 100% ethanol 10 minutes (3 times). Between each change of solution the samples were centrifuged at 20,800×g for 5 minutes at 4°C and resuspended in the

next dehydration solution. After dehydration of the samples was completed, two additional changes in dry acetonitrile, for 10 minutes each, were performed. Between each change of solution the samples were centrifuged at 20,800×g for 5 minutes at 25°C. The samples were then ready for embedding.

2.3.3 Embedding of the PSD fractions

The samples were infiltrated with solutions of resin in solvent (acetonitrile), with increasing concentrations of resin and finally with the pure epoxy resin mixture. The resin was cured by incubation at 60°C for 48 hours.

Araldite, a high viscosity epoxy resin was used for the embedding of our samples. The hardener (16 mg of dodecenylsuccinic anhydride (DDSA)) and the resin monomer (14 mg of CY 212: mixture of a resin monomer and the plasticiser (dibutyl pthalate)) were pooled into a measuring container, placed in an oven at 60°C and left for 10 minutes before mixing to reduce the viscosity of the components. The mixture was then poured into a warm conical flask and mixed by swirling until the mixture became transparent. After mixing, 600 µl of benzyldimethylamine (BDMA) was added to the mixture and mixed again for 1 minute at which point the colour of the resin turned deep amber and the resin was ready for use.

The pellet obtained after dehydration was resupended in 1-1 acetonitrile and resin mixture (V/V) 18 hours under rotation at 25°C. The samples were then infiltrated with 1-2 acetonitrile and resin mixture (V/V) 6 hours with rotation at 25°C and finally with 100% resin mixture for 24 hours with rotation at 25°C and several changes. Between each change of solution the samples were centrifuged at 20,800×g for 5 minutes at 25°C and resuspended in the next infiltration solution.

After infiltration, the samples were placed in a resin filled embedding capsules and the resin was cured by incubation at 60°C for 48 hours.

2.3.4 Staining of the thin sections of PSDs

The method for staining was based on the use of the heavy metal stains uranyl acetate (U) and lead citrate (Pb). Both U and Pb are cations which bind to anionic sites in the thin sections conferring the ability to scatter electrons thus generating positive contrast.

After sectioning the embedded PSD fractions, ultrathin sections of the samples were dried down onto a support grid and were floated on a drop of 50% methanol containing 2% uranyl acetate solution during 4 minutes. The grid and the sample were then jet washed with 50% methanol solution followed by deionised water. This was followed by staining for 4 minutes with Reynolds lead citrate and further rinsing with DIW. The samples were then ready for TEM imaging.

2.3.5 Imaging of the PSDs

The ultrathin section of the samples sitting on a grid was clamped into a single tilt, specimen rod which was inserted, via an airlock, into the microscope (FEI Tecnai G2). Inside the column of the TEM, which was maintained at high vacuum, the ultrathin section was imaged at 120kv and a magnified image of the interior of the ultrathin section of the samples was projected onto a viewing screen. A CCD camera was used to record the images which were digitised and archived by a computer.

2.4 Protein assay

After extraction of the different fractions from premotor cortex (see section 2.2.4), proteins concentrations were assessed using the bicinchoninic acid (BCA) assay (Pierce; 23235). This protein assay is a detergent-compatible BCA formulation for the colorimetric detection and quantification of the total amount of proteins in a sample. The technique is based on the detection Cu^{+1}, which is formed when Cu^{+2} is reduced by protein in an alkaline environment. A purple-colored reaction product is formed by the chelation of two molecules of BCA with one cuprous ion (Cu^{+1}). This water-soluble

complex exhibits a strong absorbance at 562 nm that is linear with increasing protein concentrations.

2.4.1 Standard curve and sampling

Initially, a range of different known concentrations of bovine serum albumin (BSA) were prepared to establish a standard curve of protein concentration which was used to determine the concentration of protein in our samples. A solution of BSA at 2 mg/ml (Pierce; 23209) was used to prepare the seven different concentrations (2.5, 5, 10, 20, 40, 80 and 100 µg/ml) of the standard curve (see Table 2-4).

Table 2-4: BSA solutions for the standard curve.

Final concentration of BSA	BSA	Added water
100 µg/ml	50 µl of BSA at 2mg/ml	950 µl
80 µg/ml	120 µl of BSA at 2mg/ml	2.880 ml
40 µg/ml	1 ml of BSA at 80 µg/ml	1 ml
20 µg/ml	1 ml of BSA at 40 µg/ml	1 ml
10 µg/ml	1 ml of BSA at 20 µg/ml	1 ml
5 µg/ml	1 ml of BSA at 10 µg/ml	1 ml
2.5 µg/ml	1 ml of BSA at 5 µg/ml	1 ml

BSA – bovine serum albumin.

All protein assay experiments were carried out in 96 well plates (Fishers Scientific; DIS-971-030J). The solutions of BSA at known concentrations were pipetted in duplicate into the first two columns of the 96 well plates. The first two wells of the first row of the 96 well plates were loaded with 150 µl of solution of BSA at 100 µg/ml and 150 µl of solution of BSA at 80, 40, 20, 10, 5 and 2.5 µg/ml was loaded in a same manner in the first two wells of the six following rows. The two first wells of the last row of the 96 well plates were loaded with 2 µl of lysis buffer used for the extraction of the PSD and 148 µl of water was added (Blank). The samples were then pipetted in duplicate, 2 µl

of sample was loaded in a well for each replicate and 148 µl of water was added in each well.

2.4.2 Measurement of the protein concentration

The BCA solution was prepared by mixing the 3 following reagents (80 wells):

- Reagent A (Pierce; 23231): 6.25 ml of 0.2 M NaOH containing sodium carbonate, sodium bicarbonate and sodium tartrate.
- Reagent B (Pierce; 23231): 6 ml of 4% BCA in water.
- Reagent C (Pierce; 23231): 250 µl of 4% cupric sulfate, pentahydrate in water.

In each well (standards and samples), 150 µl of the BCA solution was added within 5 minutes. The plates were agitated at 300 rpm on a plate shaker for 30 seconds at 25°C. The plates were covered with foil and incubated during 1 hour at 37°C. After incubation the plates were left at 25°C for 10 minutes and the absorbance measured with a plate reader (Thermo Fisher Scientific; Varioskan Flash Multimode Reader) at 562 nm.

The software of the plate reader was set to calculate the average of each duplicate, to subtract the blank from the standards, to calculate the coefficient of correlation of the standard curve and the protein concentration of our samples in µg/µl.

2.5 Western Blotting

2.5.1 Sample denaturing

The proteins were denatured by adding 4 µl of 500 mM dithiothreitol reducing agent (Invitrogen; NP0004) and 12.5 µl of loading sample buffer (Invitrogen; NP0007) in 25 µl

of sample containing 60 µg of protein, followed by 10 minutes incubation in a air dry heater at 70°C.

2.5.2 Proteins separation

To separate the denatured proteins a sodium dodecyl sulfate (SDS) polyacrylamid gel 1.5 mm in thickness was prepared. The gel was composed of two gels, the main and the stacking gel respectively with 8% and 5% acrylamid-bisacrylamid (29:1) (See Table 2-5). The main gel (8%) at the bottom was first poured between the glass plates with permanent bonded gel spacers sealed on a casting stand and left 20 minutes for polymerisation at 25°C. The stacking gel (5%) at the top in which the denatured proteins were concentrated was then poured on top of the main gel. A polycarbonate comb was added between the glass plates in order to mould the 10 wells of the gel and left 20 minutes for polymerisation at 25°C. After polymerisation, the glass plates containing the polyacrylamid gel were placed in an electrophoresis apparatus for protein separation.

The running buffer composed of 25 mM Tris, 192 mM glycine, 0.1% SDS (W/V) in water (see Table 2-6) was poured in the electrophoresis apparatus to cover the wells of the gel. The first well was loaded with 4 µl of the ladder of molecular weight (LI-COR; 928-40000) and 40 µl of denatured proteins were loaded in the subsequent wells of the polyacrylamid gel. Migration of the proteins through the polyacrylamid gel occured during 2 and 10 minutes respectively at 200 and 75 volts to concentrate proteins into the stacking gel, and then for 1 hour at 170 volts to separate proteins according to their molecular weight.

Table 2-5: Buffers for main and stacking polyacrylamid gels.

2 gels	Main gel 8%	Stacking gel 5%
Acrylamid-Bisacrylamid 40%	4 ml	625 µl
Tris-HCl 1 M pH 6.8	-	1.250 ml
Tris-HCl 1.5 M pH 8.8	7,5 ml	-
SDS 10%	200 µl	50 µl
APS 10%	200 µl	50 µl
Temed	8 µl	4 µl
H_2O	8.100 ml	3 ml

Tris HCl - Tris-buffered saline (TBS) with hydrochloric acid; SDS - sodium dodecyl sulfate; APS – ammonium persulfate; Temed - ; H_2O - water.

2.5.3 Proteins transfer and unspecific sites blocking

At the end of the separation, proteins in the gel were transferred onto a polyvinylidene difluoride (PVDF) membrane using an electro-blotter for 90 minutes at 350 mA. All non-specific binding sites of the membrane were saturated by incubation 1 hour under agitation in Tris Buffer Saline (TBS) supplemented with 10% low fat milk (W/V) and 0.1% Tween (V/V) blocking buffer at 25°C (see Table 2-6). A solution of TBS 5X composed of 20 mM Tris and 150 mM NaCl was prepared prior to transfer and stored at 4°C (see Table 2-6). The PVDF membranes were soaked in 100% methanol for 2 minutes and rinsed in 25 mM Tris, 192 mM glycine, 20% methanol transfer buffer (see Table 2-6). After migration and separation of the proteins the polyacrylamid gels were placed on top of two sponges and a sheet of Whatman filter paper before being soaked in transfer buffer. In the gel holder cassettes the PVDF membranes were placed on top of the gels and any bubbles that appeared between the gels and the membranes were removed. One additional sheet of Whatman filter paper and a sponge soaked in transfer buffer were added on top of the membranes. The gel holder cassettes were closed and placed into an electro-blotter and a container with iced water was added to cool down the system. The transfer buffer was then poured into

the buffer chamber to completely cover the gel holder cassettes. The electro-blotter was then plugged to the generator and transfer was carried out at 350 mA for 90 minutes at 25°C. After transfer the membranes were removed from the gel holder cassettes and rinsed in TBS-0.1% Tween. The membranes were then blocked with the blocking buffer 1 (Table 2-6) for 1 hour at 25°C and washed 3 times with TBS-Tween for 10 minutes at 20°C. The membranes were then ready for immunodetection.

Table 2-6: Buffers for Western blotting.

Compounds	Running	Transfer	TBS 5X	TBS-tween	Blocking 1	Blocking 2
Tris	3.02 g	3.02 g	24.2 g	-	-	-
Glycine	14.4 g	14.4 g	-	-	-	-
NaCl	-	-	87.6 g		-	-
Methanol	-	200 ml	-	-	-	-
SDS	1 g	-	-	-	-	-
Tween 20	-	-	-	1 ml	-	-
TBS 5X	-	-	-	200 ml	-	-
TBS-Tween	-	-	-	-	up to 10 ml	up to 10 ml
Low fat milk	-	-	-	-	1 g	-
BSA	-	-	-	-		1 g
H_2O	up to 1 l	up to 1 l	up to 2 l	up to 1 l	-	-

Tris - Tris-buffered saline (TBS); NaCl – sodium chloride; SDS - sodium dodecyl sulfate; Tween 20 - polysorbate surfactant; TBS 5X - Tris-buffered saline 5X; TBS-Tween - Tris-buffered saline -polysorbate surfactant; BSA - bovine serum albumin; H2O - water.

2.5.4 Immunodetection

Immunodetection was performed with primary antibodies directed against proteins of interest. The primary antibodies were diluted in blocking buffer 2 (Table 2-6), and incubated for 16 hours at 4°C (Table 2-7). At the end of the incubation with the

primary antibodies, the membranes were washed 3 times in TBS 0.1% Tween to eliminate unlinked primary antibodies. Then membranes were incubated in the dark with secondary antibodies, diluted in blocking buffer 1 (Table 2-6), directed against the species in which were produced the primary antibodies (Table 2-7). Membranes were again washed three times in TBS 0.1% Tween.

Table 2-7: Antibodies for Western blotting.

Antibodies	Dilution	Time of incubation	Type of secondary antibody
Anti PSD-95 (Cell Signaling; #3450)	1/4,000	16 hours at 4°C	Anti rabbit
Anti Trk B (Cell Signaling; #4607S)	1/4,000	16 hours at 4°C	Anti rabbit
Anti-CaMKII (Cell Signaling; #3362)	1/4,000	16 hours at 4°C	Anti rabbit
Anti-p75 (R&D system; MAB 367)	1/4,000	16 hours at 4°C	Anti mouse
Anti-NSF (Cell Signaling; #2145)	1/4,000	16 hours at 4°C	Anti rabbit
Anti-NR2A (Cell Signaling; #4205)	1/4,000	16 hours at 4°C	Anti rabbit
Anti-AMPAR (Cell Signaling; # 2460)	1/4,000	16 hours at 4°C	Anti rabbit
Anti-Synaptophysin (Cell Signaling; #4329)	1/4,000	16 hours at 4°C	Anti rabbit
Anti-GFAP (Cell Signaling; #3670)	1/4,000	16 hours at 4°C	Anti mouse
Anti β-actin (Sigma, A3516)	1/10,000	16 hours at 4°C	Anti mouse
Anti β-III-tubulin (Sigma, T8578)	1/5,000	16 hours at 4°C	Anti mouse
Anti-rabbit (LI-COR; 926-32210)	1/10,000	1 hour at 25°C	-
Anti-mouse (LI-COR; 926-32220)	1/10,000	1 hour at 25°C	-

2.5.5 Detection by immunofluorescence « Western Odyssey »

This technique is based on the detection of the emission of fluorescence after excitation by near-infrared of a fluorophore linked to the secondary antibodies. It provides the following benefits: the ability to quantify several proteins on a single membrane and the conservation of stable and consistent signal during a long time. To read the emission of fluorescence a scanner (Odyssey Infrared Imaging System; LI-COR)

was used, which retransmits digital image of the emitted fluorescence and allows detection either one or the other of the proteins, or both simultaneously.

After washes, the membranes were placed on the glass of the scanner proteins facing the glass and scanned at 6 and 7.5 intensity respectively for 700 nm (red) and 800 nm (green) emissions.

2.6 Co-immunoprecipitation

Magnetic beads (Invitrogen; 100-02D) were used to co-immunoprcipitate PSDs. Magnetic beads are covalently linked to proteins A which are proteins that have the capacity to bind constant fragment Fc of the antibody directed against one of the protein of the PSD complex. For our experiments we used an antibody against PSD-95 (Table 2-7).

2.6.1 Tubes coating

The microcentrifuge tubes used for the co-immunoprecipitation were coated with sigmacote (Sigma; SL2) and bovine serum albumin (BSA) in order to avoid the PSDs to stick to the hedge of the microcentrifuge tubes. Prior to co-immunoprecipitate the PSDs, 1.5 ml microcentrifuge tubes were coated with 1 ml sigmacote during 30 seconds and the tube upside down for another 30 seconds. After discard of the sigmacote, the tubes were left to dry 30 minutes under hood at 25°C. When dried the tubes were washed twice with 1 ml of sterile deionised water. A second coating was carried out with 1 ml of a solution of 10% BSA in sterile deionised water during 30 minutes on a plate shaker at 300 rpm and 30 additional minutes with the tubes upside down. Both steps were carried out at 25°C. After removal of the BSA solution the tubes were washed twice with 1 ml of sterile deionised water and ready for co-immunoprecipitation of the PSDs.

2.6.2 Cross linking of the magnetic beads with antibodies directed to PSD-95

After coating of the tubes, 50 µl of magnetic beads were resuspended in 700 µl of TBS 0.1% Tween and 10 µl of antibody directed against PSD-95 were incubated for 20 minutes on a tilting rotator at 25°C. After incubation with the antibody the tubes were placed on a magnet and the supernatant was discarded. The beads were then washed 3 times with 200 µl of TBS 0.1% Tween to eliminate unlinked antibodies.

2.6.3 Immuno-purification of the PSD fraction

After washes, the beads-PSD-95 antibodies complexes were resuspended 700 µl of TBS 0.1% Tween and 60 µg of protein from the PSD fraction was added. The tubes were then placed on a tilting rotator and incubated 20 minutes at 25°C. After incubation, tubes were placed on a magnet and the supernatant was removed.

2.6.4 Wash of the beads-antibodies-PSDs complexes and elution by denaturation

The beads-antibodies-PSDs complexes were resuspended in 500 µl of TBS 1% tween, placed on a tilting rotator and incubated for 15 minutes at 25°C. This step was repeated four times in order to remove any proteins that would not have bound the beads or the antibody directed to PSD-95 specifically. After removal of the unspecific binding, the tubes were placed on a magnet and rinsed three times with 200 µl of TBS 0.1% Tween to eliminate the excess of Tween. The beads-antibodies-PSDs complexes were resuspended in 40 µl of TBS 0.1% Tween and 4 µl of 500 mM dithiothreitol (DTT) reducing agent and 12.5 µl of loading sample buffer followed by 10 minutes incubation in a air dry bath at 70°C. After denaturing elution 40 µl of elute was loaded in polyacrylamid gel for Western blot (see section 2.5).

2.7 Data and statistical analysis

The fluorescence emitted by the secondary antibodies on the membranes was recorded with the software of the scanner (Odyssey Infrared Imaging System; LI-COR) and was used for data analysis. Data were transferred and analysed on excel tables. Statistic analyses were performed using SPSS statistical analysis software.

2.7.1 Data analysis

For each band detected corresponding to the targeted protein on a membrane the signal was quantified using a squared area having the same surface for each sample. This squared area was replicated 5 times and the squared areas were disposed on different part of the membrane where no protein was detected to define the value of the background. The average of the background for the defined squared area was subtracted from each value obtained for all the samples on the same membrane. To normalise our results, a ratio between the protein of interest and β-actin and β-III-tubulin was carried out.

2.7.2 Removal of outliers

After data analysis, the data were pasted in SPSS for statistical analysis. For each protein and for each group tested the intensity of fluorescence was represented on a boxplot chart in order to remove the outlier values. Outliers were removed for each protein concerned and in each ratio where the outlier was involved. In a same way, outliers of the ratios were removed.

2.7.3 Statistical test

After analysis of the normal distribution of our samples and study of the homogeneity of variance an ANOVA test was chosen to compare the four different groups for each

protein studied. ANOVA and Spearman's correlation coefficient were used for the analysis of covariables and when these tests were significant an ANCOVA was performed to compare the four different groups for each protein studied.

3 Enrichment and characterisation of the glutamate post-synaptic density

3.1 Aims and objectives

The aims of the present study are to characterise the integrity and the purity of the PSD fraction following fractionation of homogenates of frozen human frontal cortex. A comparison between the different steps of fractionation will also be done. The integrity and morphology of the PSDs will also be determined using osmication staining and TEM imaging. Western blotting analysis will be used to determine the presence of expected constituents of the PSD such as the scaffolding protein PSD-95, the NR2A subunit of the NMDAR and subunits 2, 3 and 4 of AMPARs. Western blotting analysis will also be utilised to evaluate the purity of the obtained PSD fractions by assessing known contaminants such as the pre-synaptic vesicles marker, synaptophysin, the cytoskeletal protein β-III-tubulin and the marker of glial cells, glial fibrillary acidic protein (GFAP).

3.2 Introduction

Glutamate neurons are polarised cells with defined regions consisting of a cell body, an axon ending with a synaptic terminal, and the post-synaptic dendrites that receive impulses from other neurons. Glutamate neurons receive, conduct, and transmit electrochemical impulses in the nervous system via highly differentiated structures called excitatory synapses (see Figure 3-1). These excitatory synapses are characterised by an electron-dense structure forming a thickening of the postsynaptic membrane of dendritic spines, called the PSD (Kennedy, 2000; Sheng and Sala, 2001).

The PSD is a highly organized multi-protein complex with disk-like structure, 30-40 nm thick and 250-500 nm wide, which contains receptors, receptor-associated scaffold proteins, cytoskeleton elements, and regulatory enzymes. The PSD plays a crucial role in the re-organisation of the receptors at the postsynaptic dendrites and the induction of signal transduction molecules in response to presynaptic terminal glutamate release (Dosemeci et al., 2006). These changes in the molecular organisation of the post-

synaptic dendrites modulate the excitability of the neurones and their ability to make new synaptic connections by rearrangement of their cytoskeleton (Ho et al., 2011). This mechanism is called synaptic plasticity and maybe disturbed in psychiatric disorders (Eastwood, 2003; Lewis and Moghaddam, 2006).

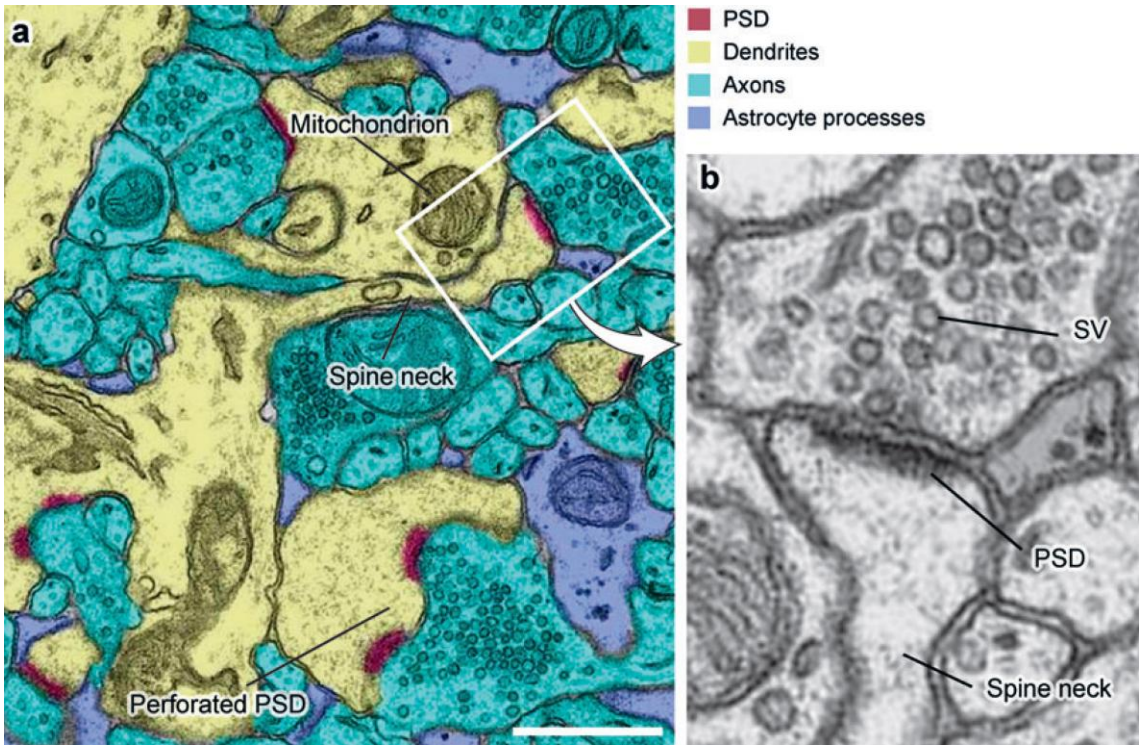

Figure 3-1: Electron micrograph of glutamate synapses.

(a)Region of the hippocampus highlighted with illustrative colours (scale bar: 1 µm). (b) High magnification of an excitatory synapse. (Taken from (Sheng and Hoogenraad, 2007)).

During the 20th and beginning of the 21th century several methods were developed to isolate the PSD and combined with proteomic methods to analyse protein content of the PSD. Most of these studies were carried out using non-human mammalian brains (Dosemeci et al., 2007; Cohen et al., 1977; Cotman et al., 1974) .

3.2.1 Enrichment of the glutamate post-synaptic density

Isolation of the PSD is based on a technique, developed at the beginning of the fifties, which uses sucrose density gradient followed by centrifugation. This method consists of centrifugation of a mixed population of particles with different densities in a discontinuous sucrose gradient containing two or more layers of sucrose, the top layer having the lowest concentrated solution of sucrose. A mixture of particles with different densities are layered onto the sucrose density gradient and centrifuged. The particles are separated at the interfaces of the sucrose density gradient depending on their density, the particles with high density passing further through the sucrose density gradient while particles with low density are retained at the interfaces of the sucrose density gradient (Brakke, 1951).

In the mid seventies, a first attempt to use this technique to isolate the PSD was developed. Rat brains were homogenised in an isotonic 0.32 M sucrose solution and the resulting mixture submitted to several steps of centrifugation for separation and isolation of the PSD. The method that was developed to isolate a PSD fraction involved the preparation of a synaptosomal fraction containing synaptic junctions using a sucrose density gradient (0.8, 1, 1.2 M sucrose). The synaptosomal fraction was collected at the interface between 1 and 1.2 M sucrose layers and incubated with *N*-lauroyl sarcosinate to detach the PSD from the synaptosomal membranes which remained insoluble in this detergent. The dissolved synaptosomal fraction was then layered on a second sucrose density gradient (1, 1.4, 2.2 M sucrose) to separate the PSD from other residual contaminants (see Figure 3-2). The purity and the integrity of the isolated PSDs were assessed respectively by electron microscopy and enzymatic assays. They showed that the isolated PSDs were structurally intact and exhibited properties which characterise them *in situ*. They also showed that the size, shape, and electron opacity of the isolated PSDs were those seen in tissue; and that the purity of the PSD fraction was better than 85% (Cotman et al., 1974).

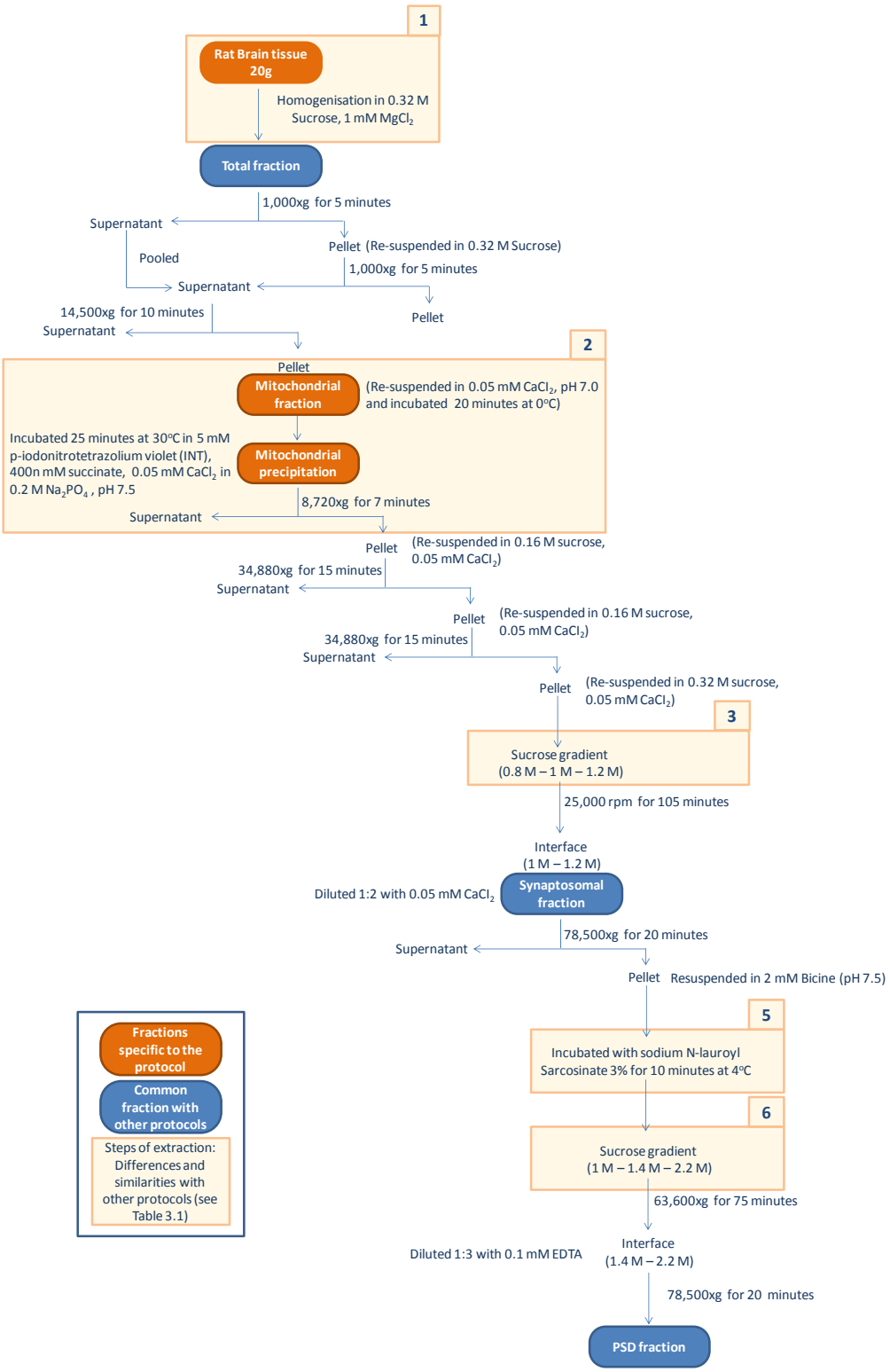

Figure 3-2: Diagram illustrating the steps of fractionation to enrich and purify the post-synaptic density (Adapted from (Cotman et al., 1974)).

Another study showed that the detergent Triton X-100 could be used as an alternative to *N*-lauroyl sarcosinate detergent and introduced ultracentrifugation (100,000g) to extract the PSD fraction from dog cerebral cortex. In this study they compared two methods of isolation of the PSDs, one with a short procedure of isolation (see Figure 3-3) and one with a long procedure of isolation (see Figure 3-4), both based on Cotman *et al.,* 1974 method with slight modifications. For the long procedure of isolation of the PSDs one sucrose density gradient separation was added after collection of the synaptosomal fraction as described by Cotman *et al.,* 1974 method. They obtained similar results with both short and long procedure for the isolation of the PSDs regarding the purity and integrity of the PSDs determined by electron microscopy, enzymatic assays, and gel electrophoresis of the proteins (Cohen et al., 1977).

A study demonstrated that the previous short procedure of extraction developed by Cohen *et al.*, 1977 could be used for the isolation of the PSDs in different regions of the dog brain. In this study they extracted PSDs from cerebral cortex, midbrain, cerebellum, and brain stem using the Triton X-100 method (see Figure 3-5). They compared the protein composition, the protein phosphorylation, and the morphology of the PSDs in the different regions of the brain. They showed using electron microscopy and gel electrophoresis of the proteins that PSDs had different molecular phenotype depending on their localisation into the brain. The shape and the protein content of the PSDs were similar in cerebral cortex and midbrain whereas the shape and protein content were different in cerebellum of dog brain than the two regions previously mentioned (Carlin et al., 1980).

Previous techniques to isolate the PSDs mentioned above were utilised either for whole brain or brain regions of relatively large mammals such as dogs and rats. In those studies they were using between 20 and 80 grams of brain tissue. For the isolation of the PSDs from human post-mortem brain tissue a reduction in the amount of tissue used for extraction of the PSD is desirable as human brain tissue samples are precious.

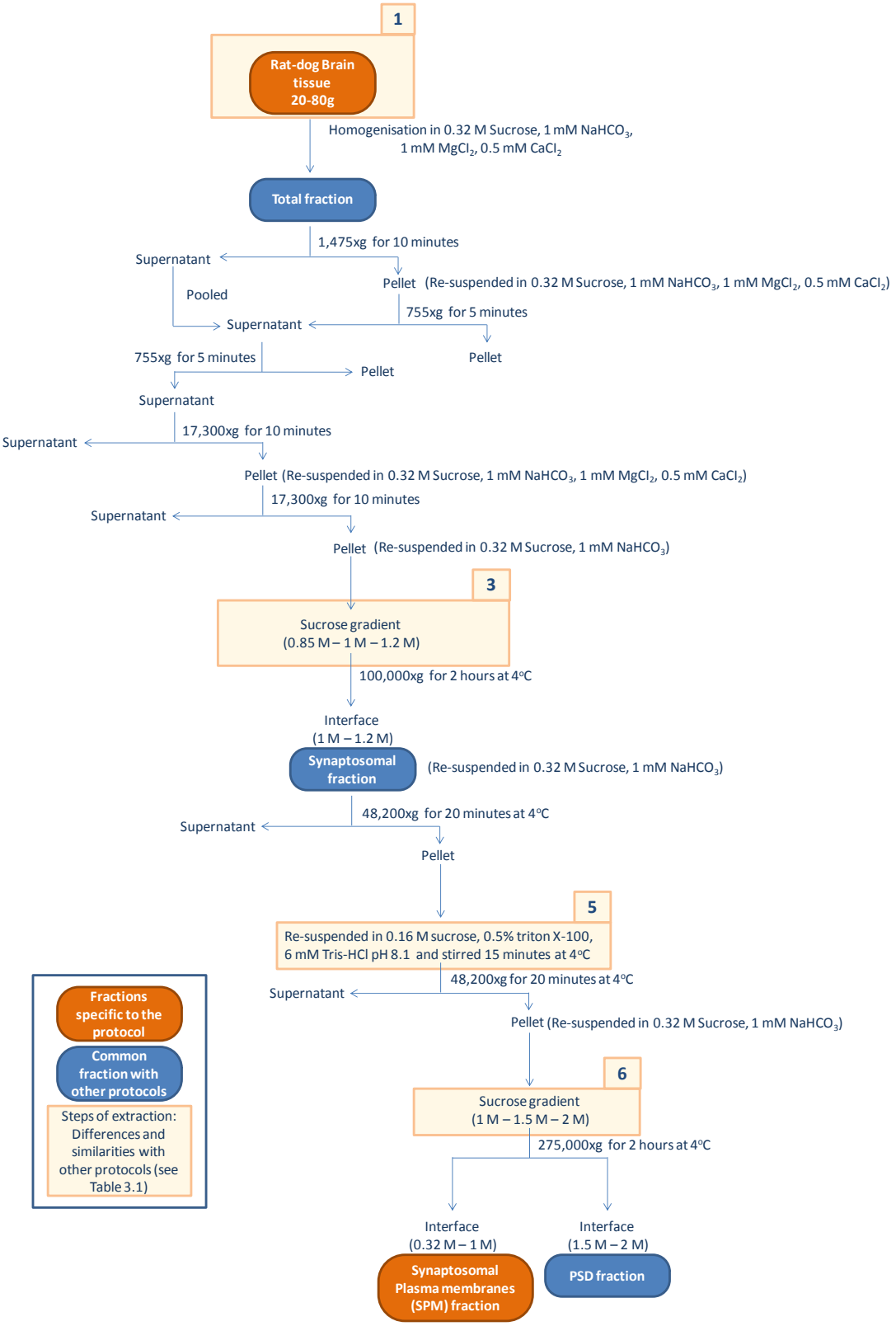

Figure 3-3: Diagram illustrating the steps of fractionation (short procedure) to enrich and purify the post-synaptic density (Adapted from (Cohen et al., 1977)).

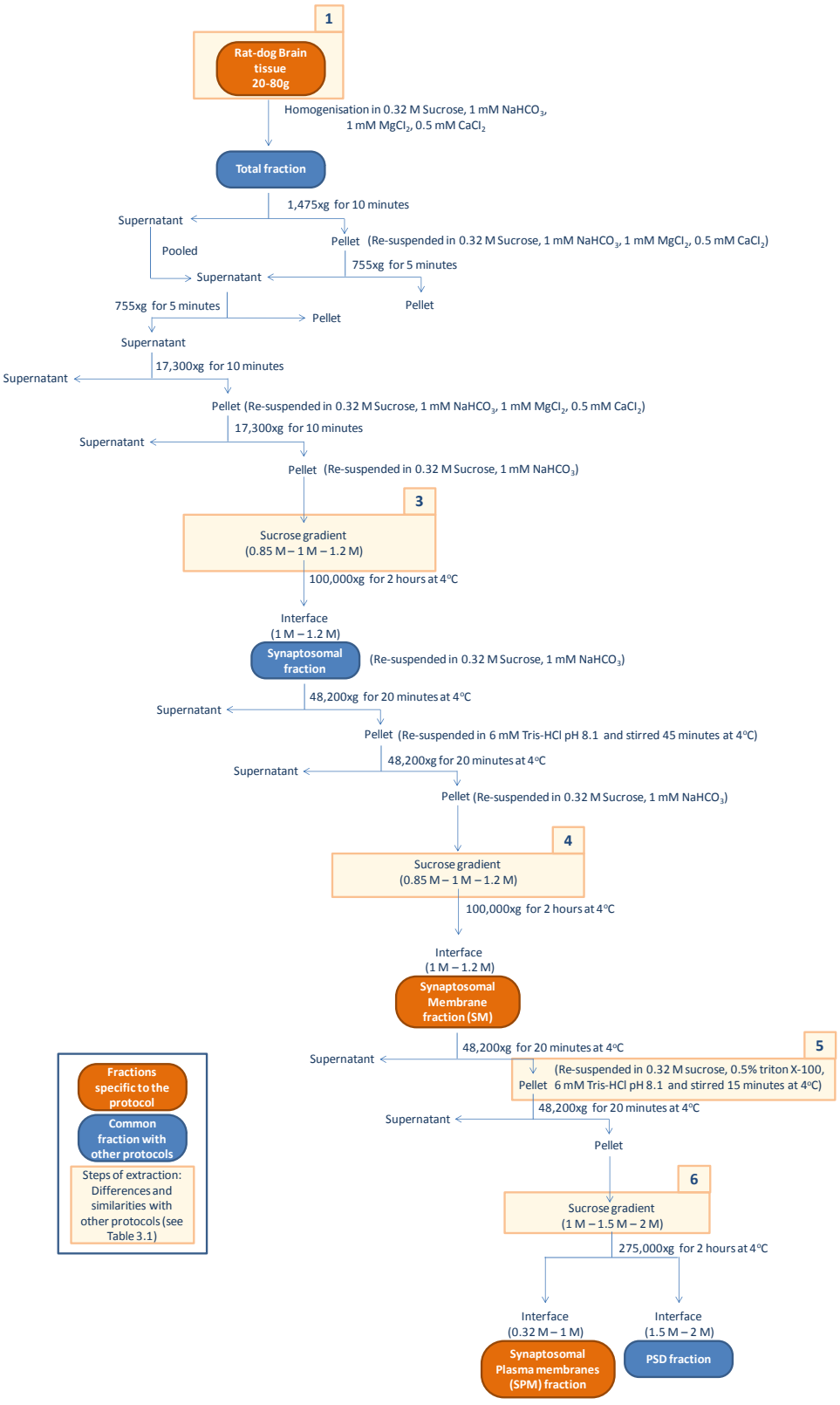

Figure 3-4: Diagram illustrating the steps of fractionation (long procedure) to enrich and purify the post-synaptic density (Adapted from (Cohen et al., 1977)).

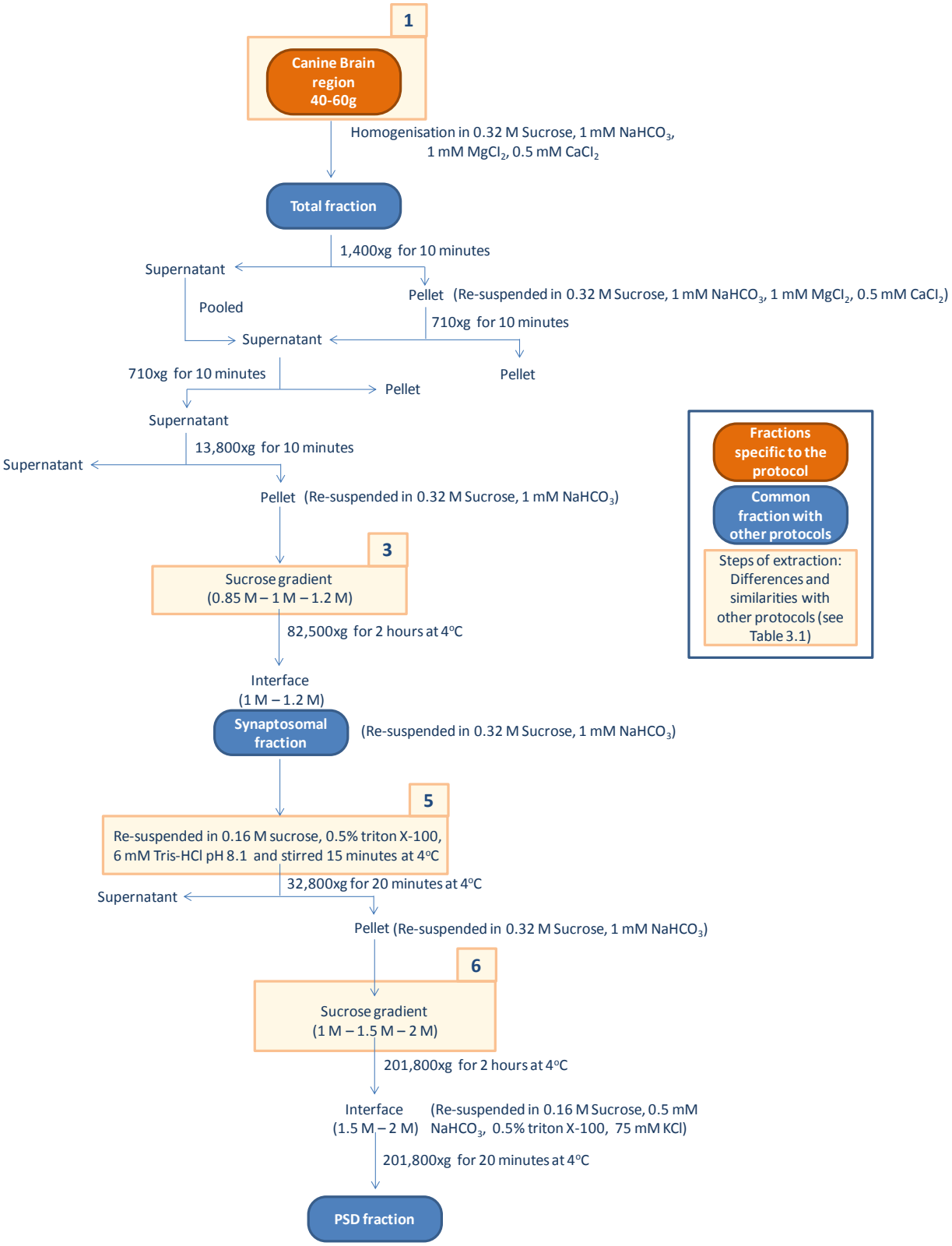

Figure 3-5: Diagram illustrating the steps of fractionation to enrich and purify the post-synaptic density (Adapted from (Carlin et al., 1980)).

Two recent studies present new approaches to reduce the amount of starting tissue and the time needed for the isolation of the PSDs. The first study reported a simple and highly effective procedure for the rapid isolation of PSDs from 200 mg of adult mouse hippocampus (see Figure 3-6). In this study the authors replaced the first sucrose density gradient (0.8, 1, 1.2 M sucrose) previously described to isolate the synaptosomal fraction by two successive filtrations using 100 and 5 µm filters. After filtration of the hippocampus homogenate they used the same second sucrose density gradient (1, 1.4, 2 M sucrose) previously utilised to isolate the PSDs. They characterised the obtained PSD fractions using electron micrographs and Western blot analysis and showed that this technique yields purified PSD fraction sample. Moreover, they compared two different protocols using swing and fixed bucket rotors for PSD isolation and both resulted in very pure PSD fractions (Villasana et al., 2006). Although the amount of starting tissue required for the isolation of the PSDs using the technique presented above was substantially reduced, the amount of tissue remained too important for human post-mortem brain studies. A second technique was recently developed to isolate the PSDs from 5-6 slices (400 µm thick) of rat hippocampus (see Figure 3-7).

In this study the authors described a simple and convenient method based on the fractionation of the tissue homogenate by sucrose density gradient (0.32, 0.8 M sucrose), followed by two consecutive extractions of a synaptosomal fraction with Triton X-100 for the preparation of PSD fractions. They showed that PSD fractions obtained were significantly enriched in the protein PSD-95, one of the most abundant protein of the PSD, using Western blotting and that the shape of the PSDs after isolation was similar to those observed *in situ* using electron microscopy. They studied the composition of the PSD fraction by 2D LC-MS/MS and they identified PSD-scaffolding proteins, signaling molecules, cytoskeletal elements known to be present in the PSD. In addition, they showed that further purification of PSDs was possible using magnetic beads coated with a PSD-95 antibody (Dosemeci et al., 2006).

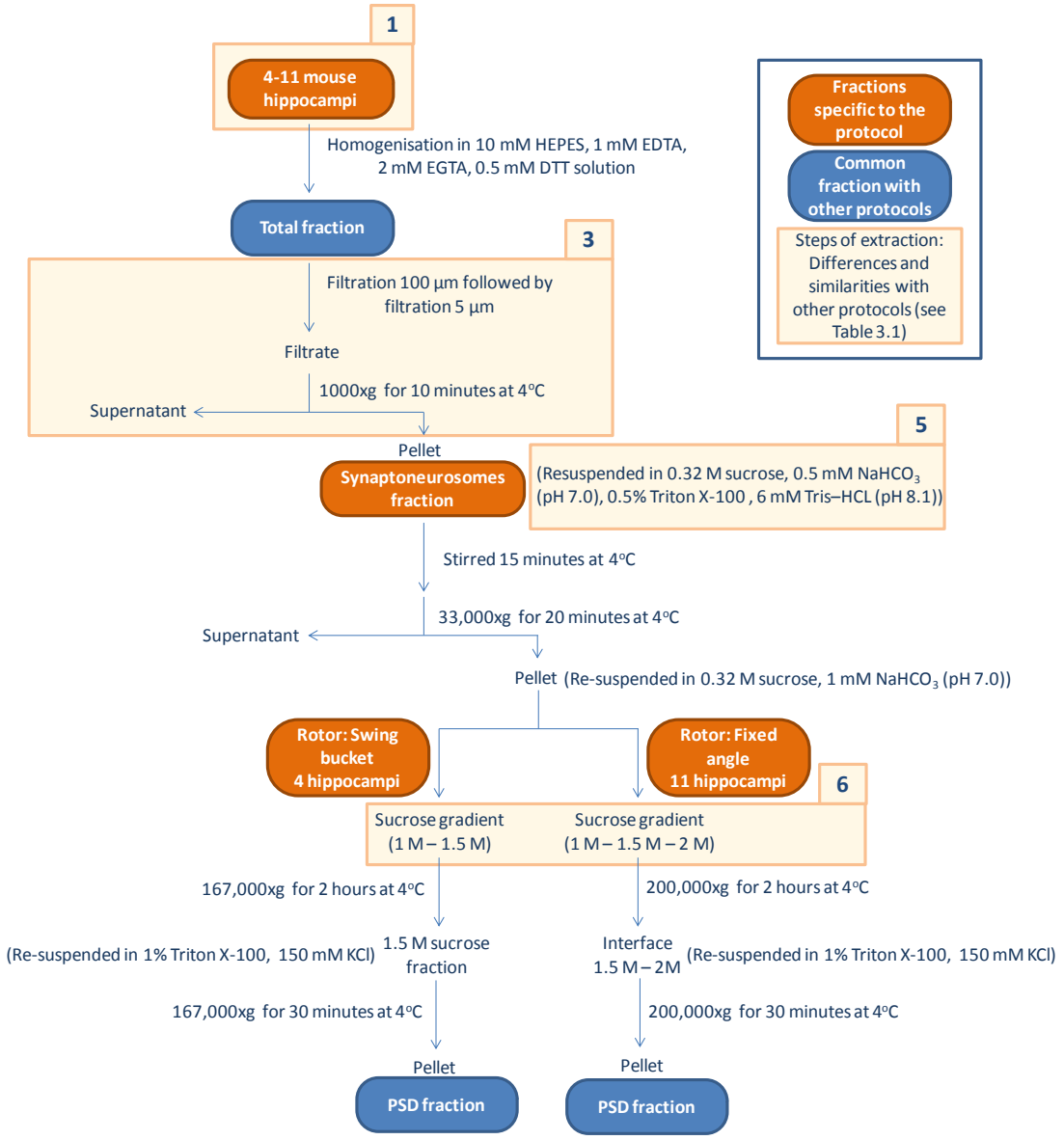

Figure 3-6: Diagram illustrating the steps of fractionation to enrich and purify the post-synaptic density (Adapted from (Villasana et al., 2006)).

All the previous methods described above were used for the extraction of non human brain samples and the PSD fractions were prepared from tissue freshly removed from the host. Biochemical fractionation of postmortem brain tissues faces special challenges due to the impact of the agonal state, complicating medical conditions, the post-mortem interval (PMI), inconsistent pH, and duration of storage. These conditions

may affect the integrity of the PSDs by modifying the structure of the proteins inside the complex (Hunsucker et al., 2008).

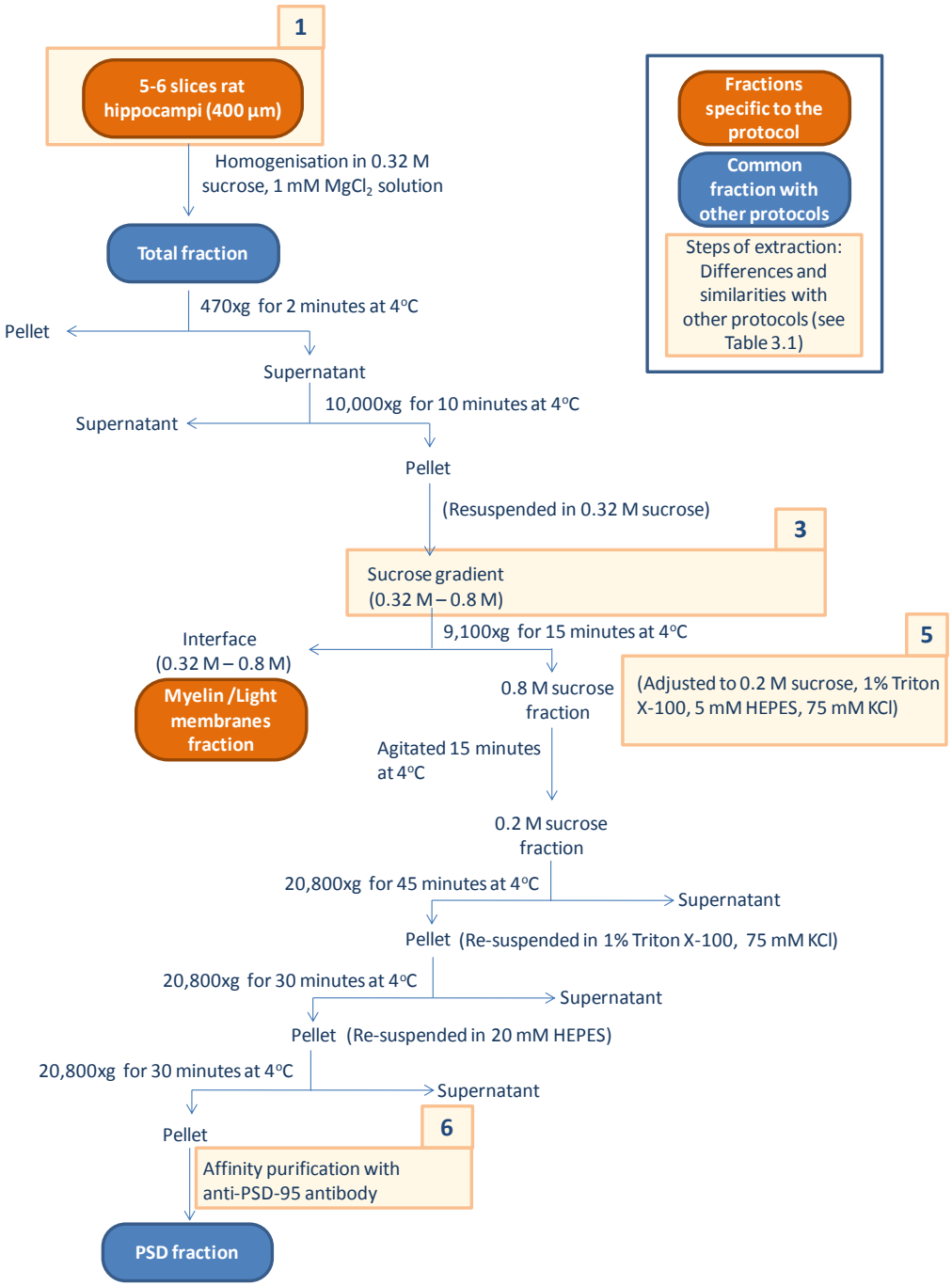

Figure 3-7: Diagram illustrating the steps of fractionation to enrich and purify the post-synaptic density (Adapted from (Dosemeci et al., 2006)).

A study recently assessed the feasibility of the isolation of PSDs from human post-mortem tissue and the integrity of the PSDs after extraction. In their study they examined three different methods: 1) Method 1, using the a slightly modified version of the short procedure previously developed by Cohen *et al.* 1977 (see Figure 3-8); 2) Method 2, a sucrose density gradient based purification of synaptosomes, followed by detergent extraction and pH based differential extraction of synaptic membranes (see Figure 3-9); and 3) Method 3, a mixture of the two precedent methods (see Figure 3-10).

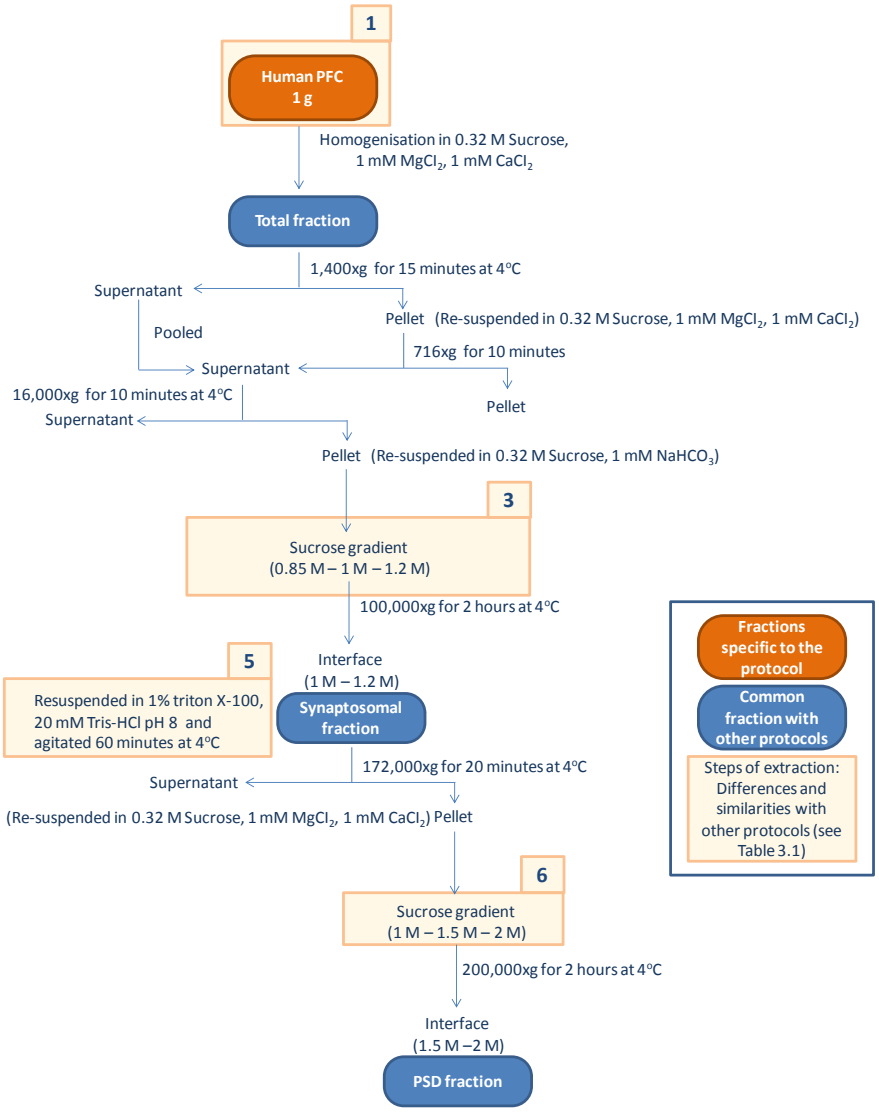

Figure 3-8: Diagram illustrating the steps of fractionation (method 1) to enrich and purify the post-synaptic density (Adapted from (Hahn et al., 2009)).

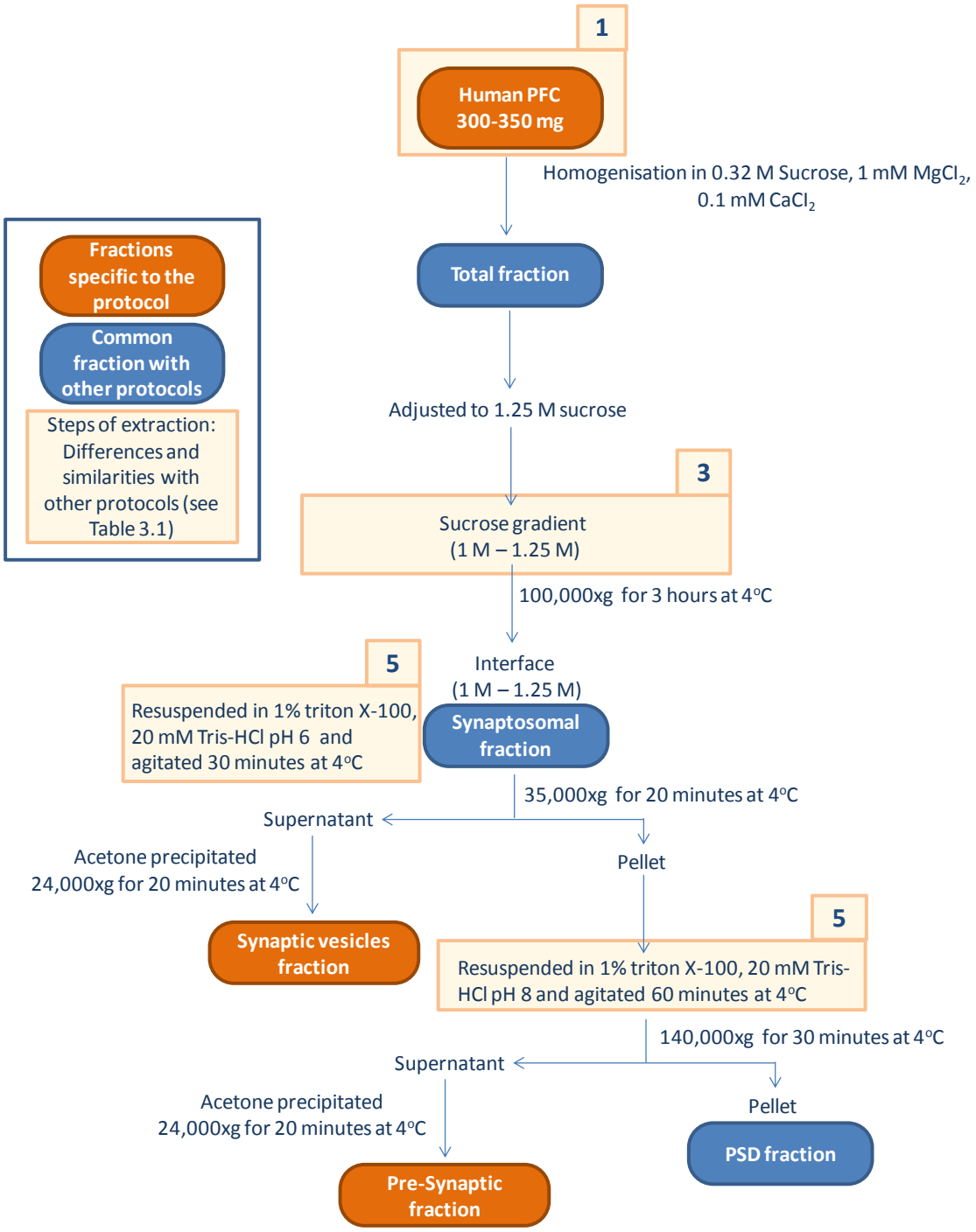

Figure 3-9: Diagram illustrating the steps of fractionation (method 2) to enrich and purify the post-synaptic density (Adapted from (Hahn et al., 2009)).

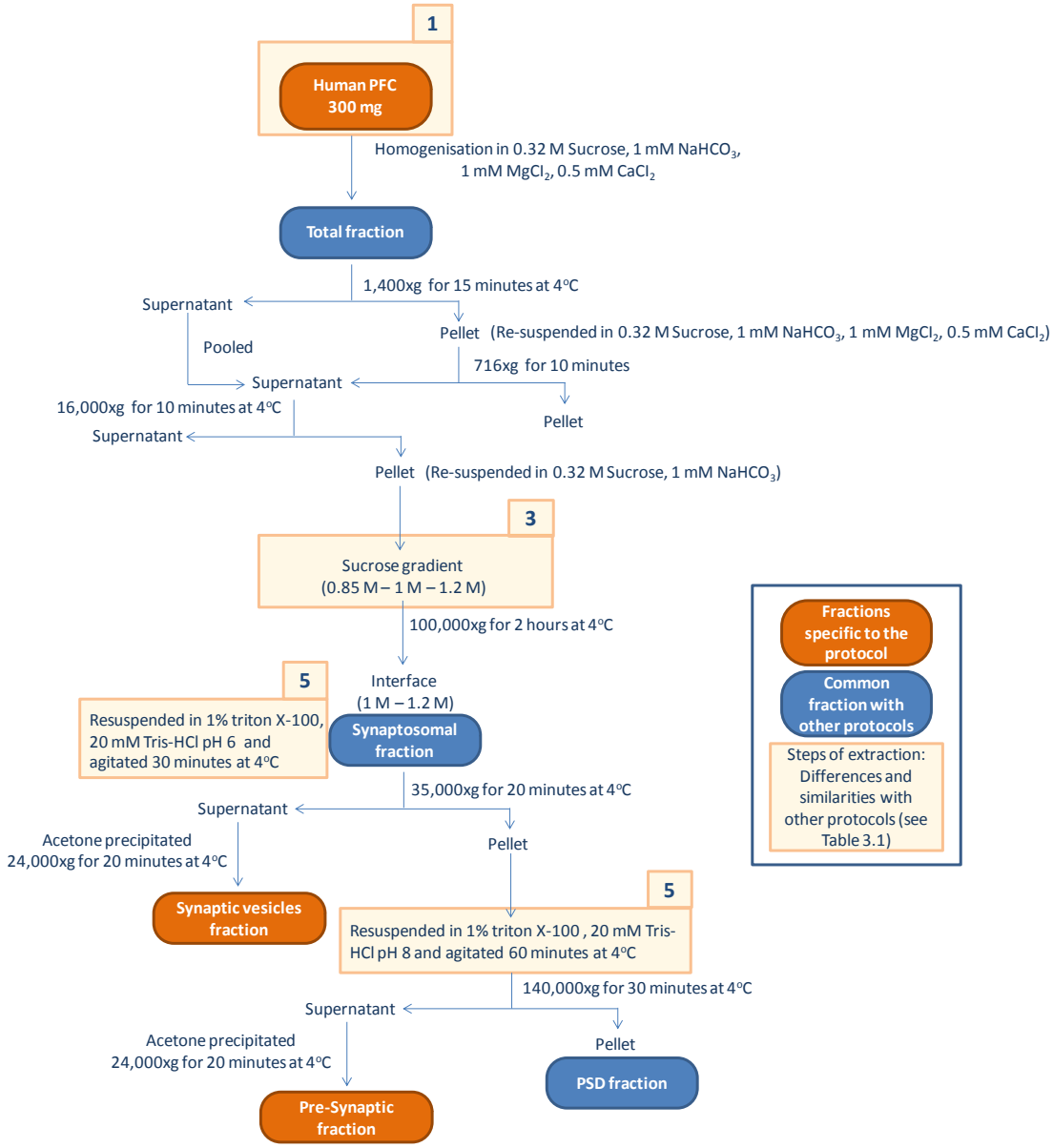

Figure 3-10: Diagram illustrating the steps of fractionation (method 3) to enrich and purify the post-synaptic density (Adapted from (Hahn et al., 2009).

For all three methods electron microscopy experiments showed that the integrity of the PSDs was conserved after their extraction and that the typical PSD proteins were present and enriched after isolation of the PSDs using western blotting and 2D LC-MS/MS (Hahn et al., 2009).

Table 3-1: Summary of main differences (orange) and similarities (blue) between protocols developed to extract the PSD.

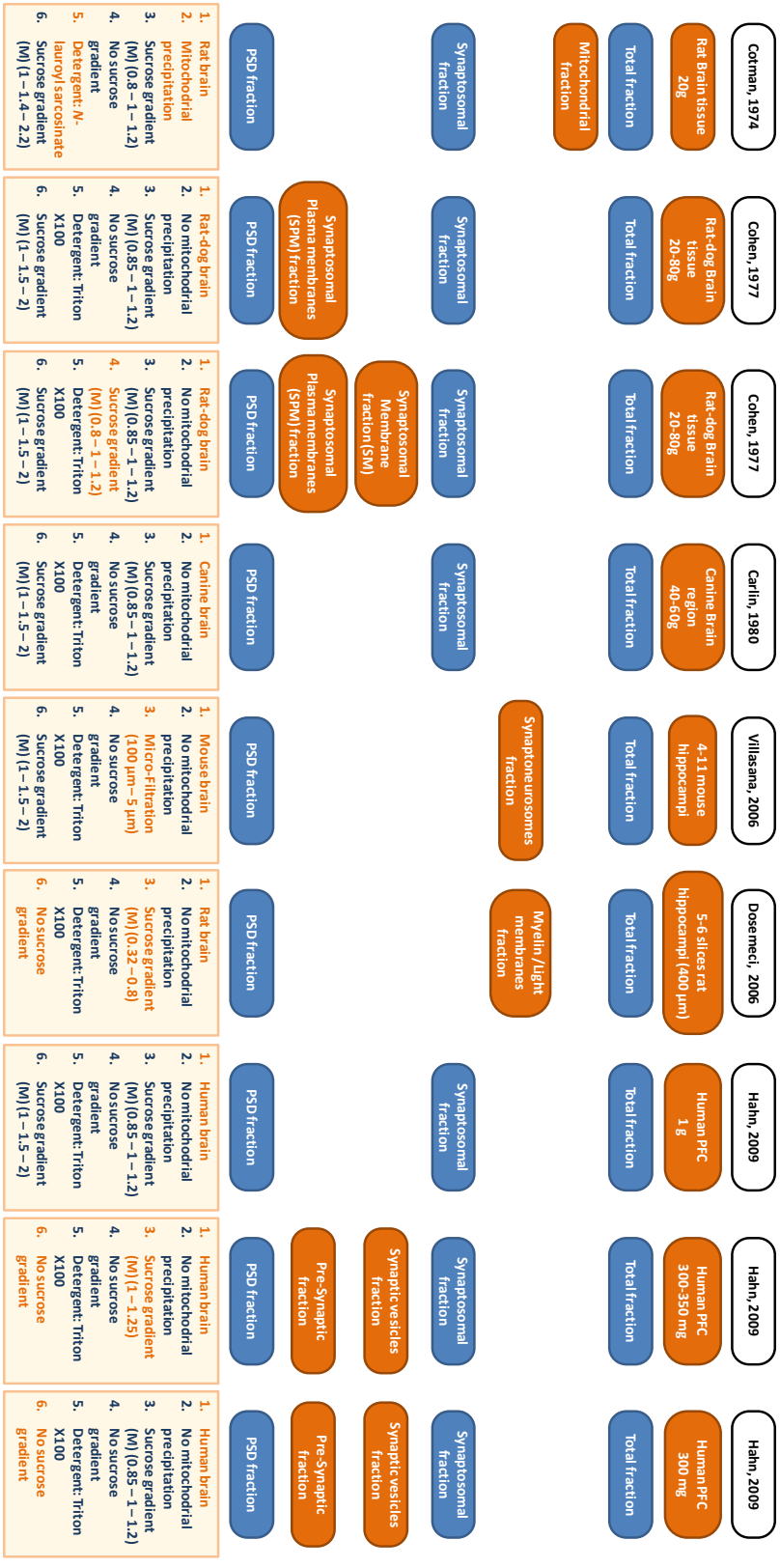

All techniques presented above have been intensively used during the last two decades to isolate the PSDs and have been combined with proteomic methods to analyse and characterise the content of the PSDs.

3.2.2 Characterisation of the glutamate post-synaptic density

Several methods such as electron microscopy, gel electrophoresis, Western blotting and liquid chromatography coupled with mass spectrometry can be used to characterise the morphology and the composition of the isolated PSDs.

The morphology of the PSDs can be assessed using negative staining and TEM and was widely described by many studies (Dosemeci et al., 2006; Cohen et al., 1977; Cotman et al., 1974; Hahn et al., 2009). All these studies referenced an electron dense disk-shaped structure with 200-500 nm diameter and 20-40 nm in thickness. A recent study demonstrated that the PSDs can be extracted from human brain samples (see Figure 3-11) and could be used for further proteomic analyses (Hahn et al., 2009).

Electron micrographs of the synaptosomal fraction are often presented to characterise the different steps of purification of the isolation of the PSD (see Figure 3-11). It consists of a fraction rich in membrane vesicles and organelles with electron dense opacity (see Figure 3-11 A). Within this synaptosomal fraction pre- and post-synaptic structures such as neurotransmitter vesicles and PSD can be observed. The PSD is often associated with presynaptic dense zone rich in proteins with high electron opacity (see Figure 3-11 B). In the PSD fraction this symetric structure can be observed after PSD isolation at pH 8 (see Figure 3-11 C). Depending on the method of extraction (pH 6) the pre-synaptic structure can be removed and the symmetric structures do not appear anymore in the electron micrograph images of the PSD fraction (see Figure 3-11 D).

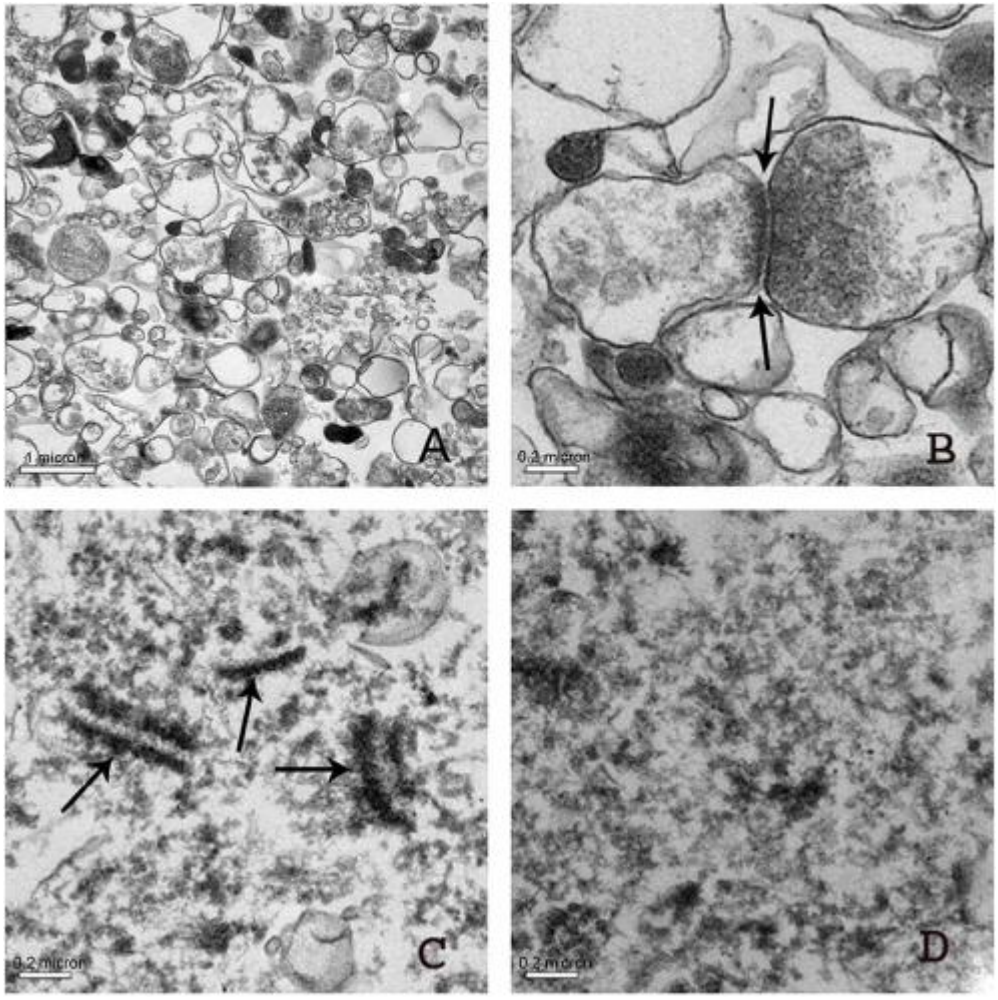

Figure 3-11: Electron micrographs of the synaptosomal and PSD fractions obtain after fraction of human brain samples.

(A) Thin section of synaptosomal fraction. (B) High magnification of the synaptosomal fraction. (C) PSD fraction extracted with Triton X-100 at pH 6 from synaptic membranes. (D) PSD fraction extracted with Triton X-100 at pH 6 from synaptic membranes. Arrows show the PSDs (Taken from (Hahn et al., 2009)).

Other studies used gold immunolabelling and TEM, rotary shadow electron microscopy or rotary shadow electron microscopy coupled with gold immunolabelling to describe the three dimensional morphology of the PSDs (see Figure 3-12) and to determine the

arrangement of receptors, scaffold proteins and kinases such as NMDAR, PSD-95 and CaMKII within the PSD (Carlin et al., 1980; Dosemeci et al., 2000; Chen et al., 2005).

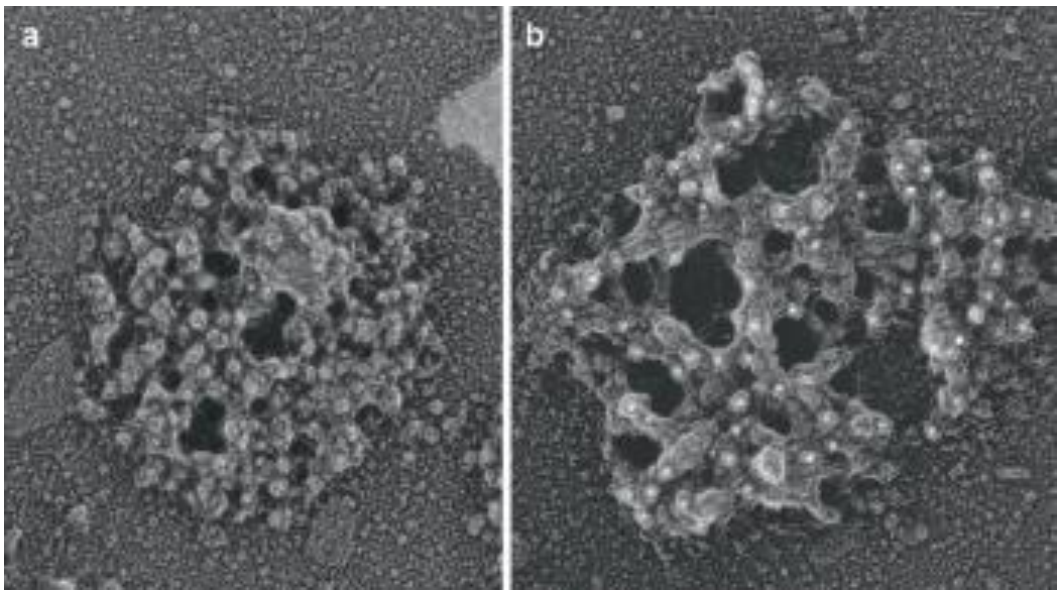

Figure 3-12: Micrographs of the PSD obtained by rotary shadow electron microscopy.

(a) Granular surface of the PSD facing the synaptic cleft. (b) Intra-cytoplasm surface of the PSD. (Taken from (Sheng and Hoogenraad, 2007)).

Although electron microscopy gives information on the morphology of the PSD and the localisation of specific proteins at the PSD, this technique is not appropriated to identify and to quantify the proteins in the PSD. Isolation of the PSDs coupled with proteomic techniques such as gel electrophoresis, Western blotting and LC-MS/MS give more qualitative and quantitative information regarding the protein composition of the PSD.

Studies using LC-MS/MS have been critical to identify specific markers of the PSD such as receptors and scaffolding proteins (Yoshimura et al., 2004b; Collins et al., 2006b), such as NMDAR subunits, AMPAR subunits and PSD-95. Moreover LC-MS/MS and Western blotting were used to assess the purity of the PSD fraction by the

identification of contaminants coming from the presynaptic terminal and mitochondria such as synaptophysin, SNAP-25 and proteins involved in metabolic processes.

3.3 Materials and methods

3.3.1 Enrichment of the glutamate post-synaptic density

Six frozen blocks of human brain were weighed (100 mg), thinly chopped on ice and placed into homogeniser tubes (Precellys Bertin Technologies) containing 450 µl of ice-cold 0.32 M sucrose, 1 mM $MgCl_2$ solution containing 2.5 % of protease inhibitor cocktail (Sigma). Samples were homogenised in a Precellys 24 dual tissue homogenizer (Bertin Technologies) for 15 seconds at 5000 rpm. After homogenisation the samples were placed on ice and 50 µl of homogenate was pipetted into a labelled tube (Total fraction). The homogenates were fractionated using the extraction protocol described in section 2.2.

At the end the procedure 12 PSD fractions were obtained. Two PSD fractions were used for electron microscopy analysis and all fractions collected during the fractionation of the 6 samples were used for Western blotting analysis.

3.3.2 Electron microscopy

Two PSD fractions extracted from two different frozen premotor cortex samples were used to perform transmission electron microscopy (TEM).

All experiments were performed at the University of Cambridge (Department of Physiology, Development and Neuroscience) by Dr. Jeremy Skepper.

The samples were fixed, washed, osmicated, dehydrated and embedded in epoxy resin. After embedding, ultrathin sections (50 nm) were prepared and were mounted on metal grids to be viewed in the TEM as described in section 2.3.

3.3.3 Protein concentration and protein assay

Before assaying the protein concentration for each fraction collected after PSDs isolation, the collected washing steps were concentrated in a vacuum drier for 1 hour at 60°C. The dried pellet obtained was then re-suspended in 50 µl of sterile deionised water.

A protein assay was then carried out on each fraction (Total fraction, cytosolic fraction, 0.32 M sucrose fraction, light membrane/myelin fraction, washing 1, 2 and 3 fractions, and PSD fractions) during the PSD extraction of the six samples as described in section 2.4.

3.3.4 Western blotting

For each fraction collected, 60 µg of protein was denatured and loaded onto 5-8% polyacrylamid gel. Proteins were separated and transferred on PVDF membranes for immunodectection of PSD-95, NR2A, AMPAR, synaptopysin, GFAP, β-III-tubulin and β-actin. Western blotting was performed as described in section 2.5.

Synaptophysin, Beta-III-tubulin and beta-actin were first detected and the membranes were then probed with PSD-95 and NR2A. The membranes were stripped 1 hour at 25°C on a plate agitator, and probed with AMPAR and GFAP antibodies.

3.3.5 Data analysis

For each protein detected the background signed was substracted and a ratio of each protein with β-actin was calculated. An average of the ratio for the 6 experiments was calculated and total, cytosolic, myelin/light membranes and PSD fraction were compared. Statistical analysis was performed using SPSS-ANOVA test to assess the significant differences between each fraction compared.

3.4 Results

3.4.1 Electron microscopy

Electron microscopy was carried out on the pelleted PSD fraction and thin section were stained and visualised by TEM. Amongst all pictures recorded, two of them were selected to show the content of the PSD fraction.

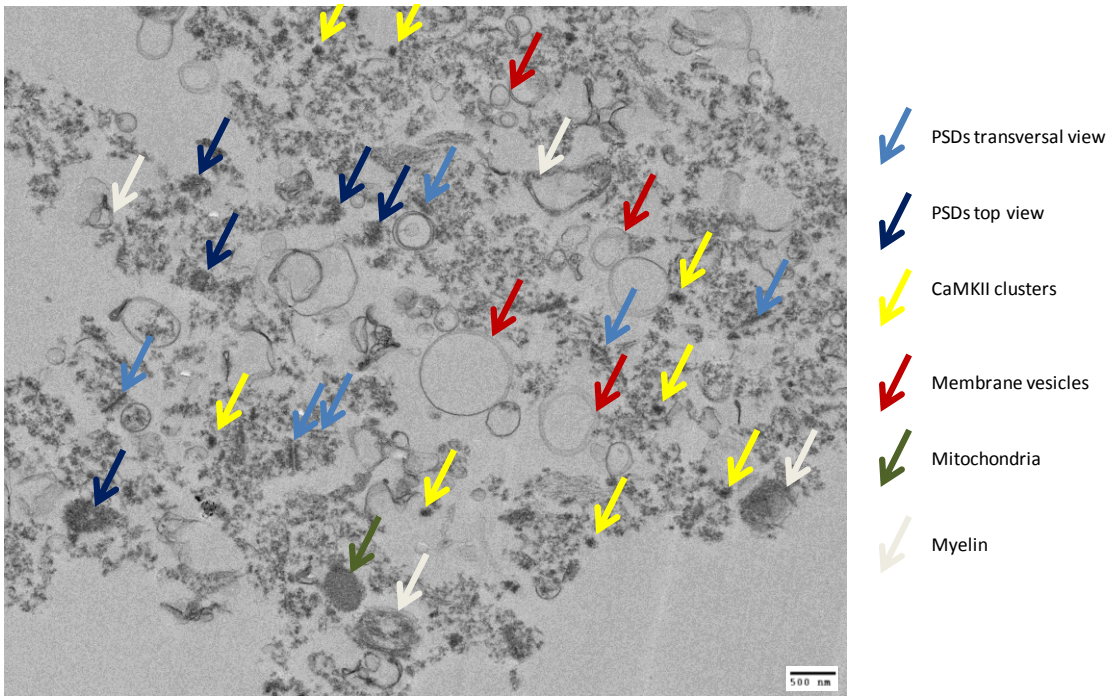

Figure 3-13: Electron micrograph of the PSD fraction.

(magnification x 3,500).

Electron micrographs showed a heterogenic composition of the PSD fraction with circular structures with low density (light grey) surrounded by particulate structures with higher density (dark grey). Amongst the particles with higher density, some have a symmetrical structure separated by a white gap (200-500 µm wide). These structures are the PSDs in transversal view (light blue arrows). Near circular shaped structures with high electron density indicated by the dark blue arrows show the PSDs via a top view. Additional circular shaped structures with smaller diameter and higher electron

density than the PSDs shown by the yellow arrows are the CaMKII clusters. Also, contaminants such as membrane vesicles (red arrows), mitochondrion (green arrow) and myelin (light grey arrows) were present in the PSD fractions (see Figure 3-13). The mitochondrion was differentiated from PSDs top view because of its regular ovoidal shape compared to the PSDs top view and the presence of internal membranes (visible on the digital picture).

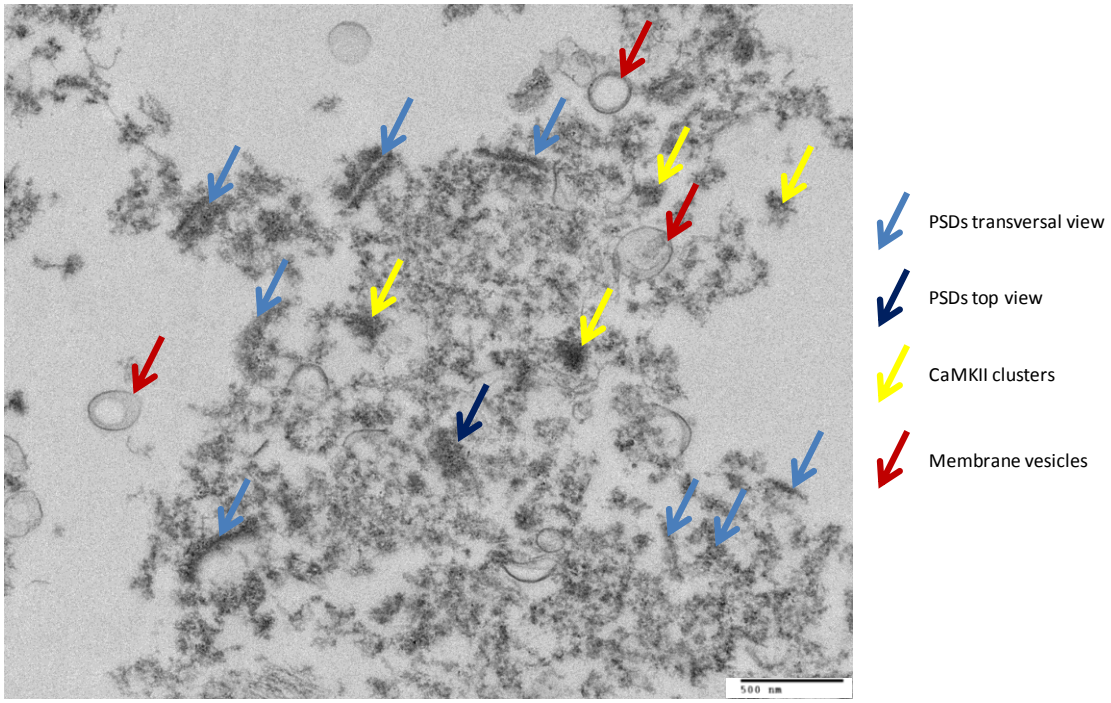

Figure 3-14: Electron micrograph of the PSD fraction with higher magnification.

(magnification x 7,800).

Observation of the PSD fraction with higher magnification (see Figure 3-14) showed the presence of the isolated PSDs. Three symmetrical PSDs separated by the synaptic cleft were observed and at least five PSDs without pre-synaptic dense electron opacity were also visible (light blue arrows). Disk-shaped structures were distinguishable and were designed either as transversal view of the PSD (dark blue arrow) or as CaMKII clusters (yellow arrows) depending on their electron opacity and diameter.

Contaminants such as membrane vesicles were also observed as indicated by red arrows (see Figure 3-14).

3.4.2 Expression of PSD-95

Each fraction separated and collected after PSD isolation was blotted on a PVDF membrane and PSD-95 was immunodetected (see Figure 3-15). The experiment was repeated 6 times (see Figure A-1) and the average of the ratio PSD-95/β-actin (β-actin being the protein used to normalise our results) for each fraction was compared to the ratio PSD-95/β-actin of the total fraction (see Figure 3-16).

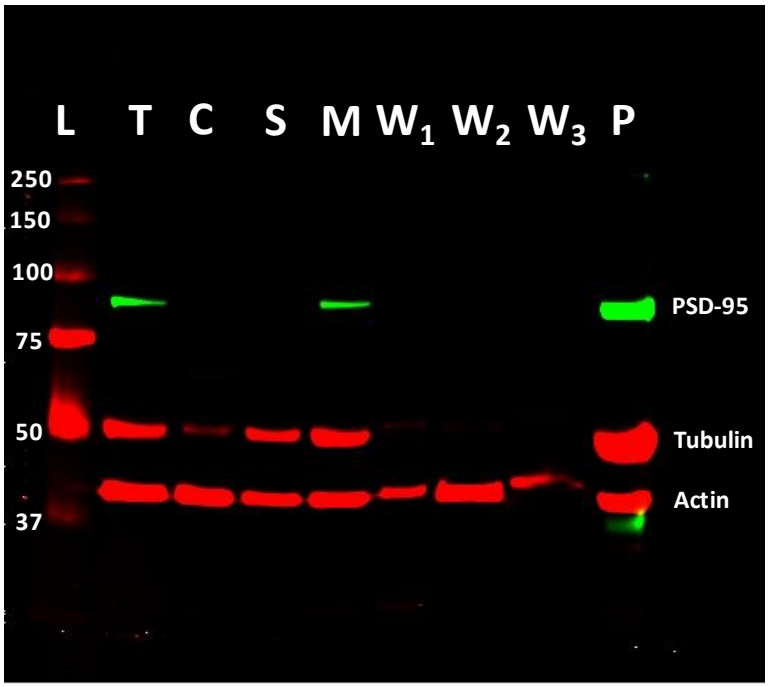

Figure 3-15: Digital image of a representative membrane after detection of PSD-95, tubulin, and actin.

(L) ladder; (T) Total fraction; (C) Cytosolic fraction; (S) Sucrose 0.32 M fraction; (M) Myelin/light membranes fractions; (W_1) wash 1 fraction; (W_2) wash 2 fraction; (W_3) wash 3 fraction; (P) PSD fraction.

Immunodetection of PSD-95 showed visible green bands at 95 KDa which is the expected size of the target protein (see Figure 3-15). These bands were observed in the total, myelin/light membranes and PSD fractions. The signal observed in the PSD fraction was much stronger than in any other fraction. The signal for PSD-95 in the total and myelin/light membranes fractions was similar in both.

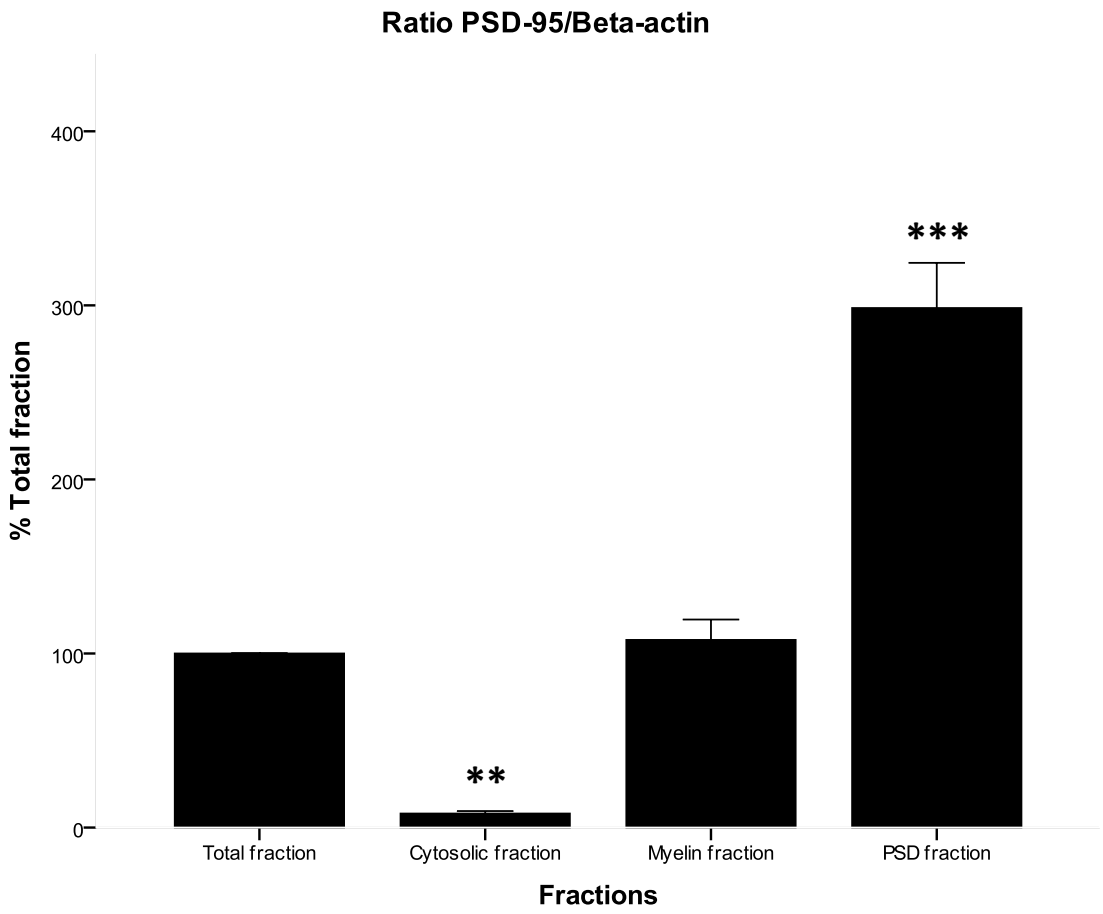

Figure 3-16: Mean (± SEM) of the ratio PSD-95/β-actin in percentage of the total fraction.

Statistical test ANOVA with Bonfferoni correction. Comparison with the total fraction (p<0.01; *** p<0.001)**

The analysis of the results obtained from 6 experiments showed a significant increase in the ratio PSD-95/β-actin (up to 200 %; p<0.001) in the PSD fractions compared to

the total fractions. Moreover, the ratio PSD-95/β-actin was significantly decreased in the cytosolic fraction compared to the total fraction ($p<0.01$). No significant change was observed for the myelin/light membranes fractions compared to the total fractions (see Figure 3-16).

3.4.3 Expression of NR2A

The NR2A subunit of the NMDAR receptor was immunodetected at the same time as PSD-95 (see Figure 3-17). The experiment was repeated 6 times (see Figure A-3) and the average NR2A/β-actin ratio for each fraction was compared to the NR2A/β-actin ratio of the total fraction (see Figure 3-18).

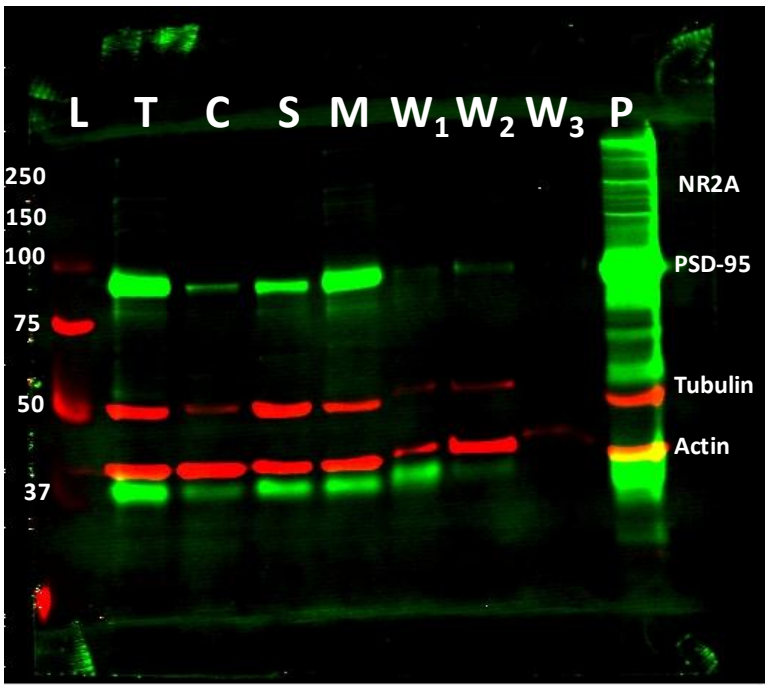

Figure 3-17: Digital picture of the membrane after detection of NR2A.

(L) ladder; (T) Total fraction; (C) Cytosolic fraction; (S) Sucrose 0.32 M fraction; (M) Myelin/light membranes fractions; (W_1) wash 1 fraction; (W_2) wash 2 fraction; (W_3) wash 3 fraction; (P) PSD fraction. NR2A specificity (See Figure A-2).

As PSD-95 and NR2A were detected at the same time and the NR2A signal was much lower than PSD-95, the image showed very high unspecific binding (extra bands) due to the immunodetection of PSD-95. However, visible green bands were detected at the expected size (180 KDa) of NR2A (see Figure 3-17). These bands were observed with very weak intensity in the total, myelin/light membranes fractions and with much higher intensity in the PSD fractions. NR2A could not be visually detected in any other fraction.

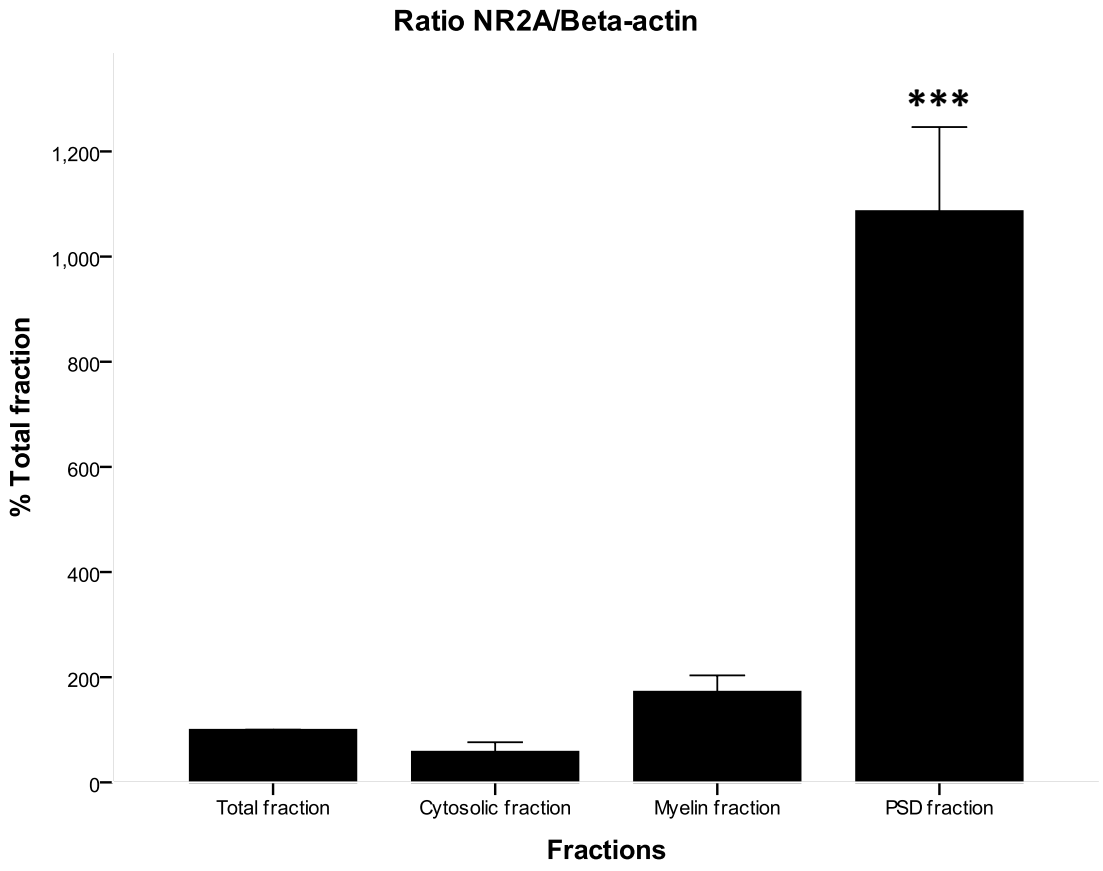

Figure 3-18: Mean (± SEM) of the ratio NR2A/β-actin in percentage of the total fraction.

Statistical test ANOVA with Bonfferoni correction. Comparison with the total fraction (*p<0.001)**

Comparison between fractions showed a significant increase of the amount of NR2A in the PSD fractions. No significant change was observed for the cytosolic and myelin/light membranes fractions compared to the total fraction (see Figure 3-16).

3.4.4 Expression of AMPAR

After detection of PSD-95 and NR2A the membranes were stripped and re-probed with an antibody directed to AMPAR subunits 2, 3 and 4 (see Figure 3-19).

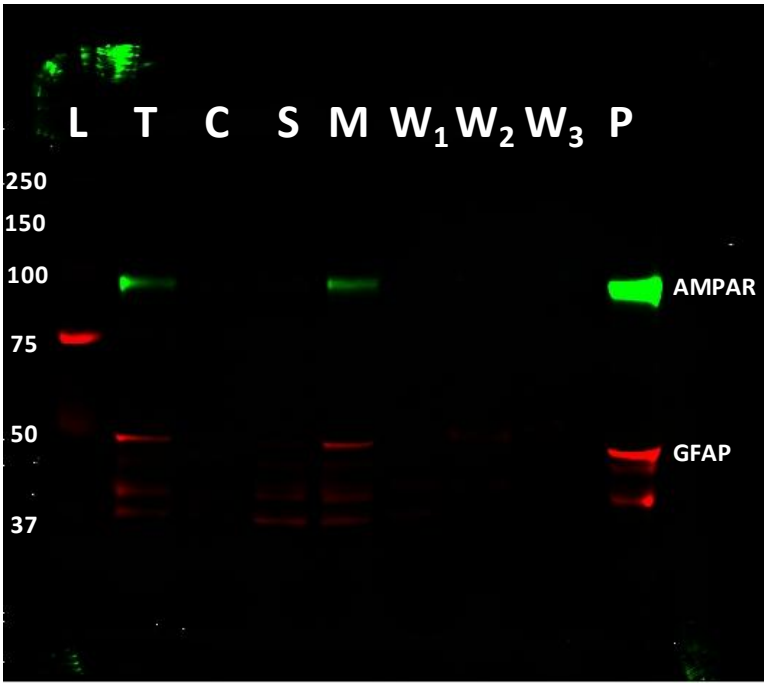

Figure 3-19: Digital picture of the membrane after detection of AMPAR.

(L) ladder; (T) Total fraction; (C) Cytosolic fraction; (S) Sucrose 0.32 M fraction; (M) Myelin/light membranes fractions; (W_1) wash 1 fraction; (W_2) wash 2 fraction; (W_3) wash 3 fraction; (P) PSD fraction.

Subunits 2,3,4 of the AMPAR have an expected size of 90 KDa. Immunodetection of AMPAR subunits showed visible green bands at 90 KDa in the total, myelin/light membranes and PSD fractions (see Figure 3-19). A much higher intensity of the signal

was observed for the PSD fraction than in any other fraction. The signal detected for AMPAR subunits in the total and myelin/light membranes fractions was similar in both fractions. No signal was detected in the other fractions.

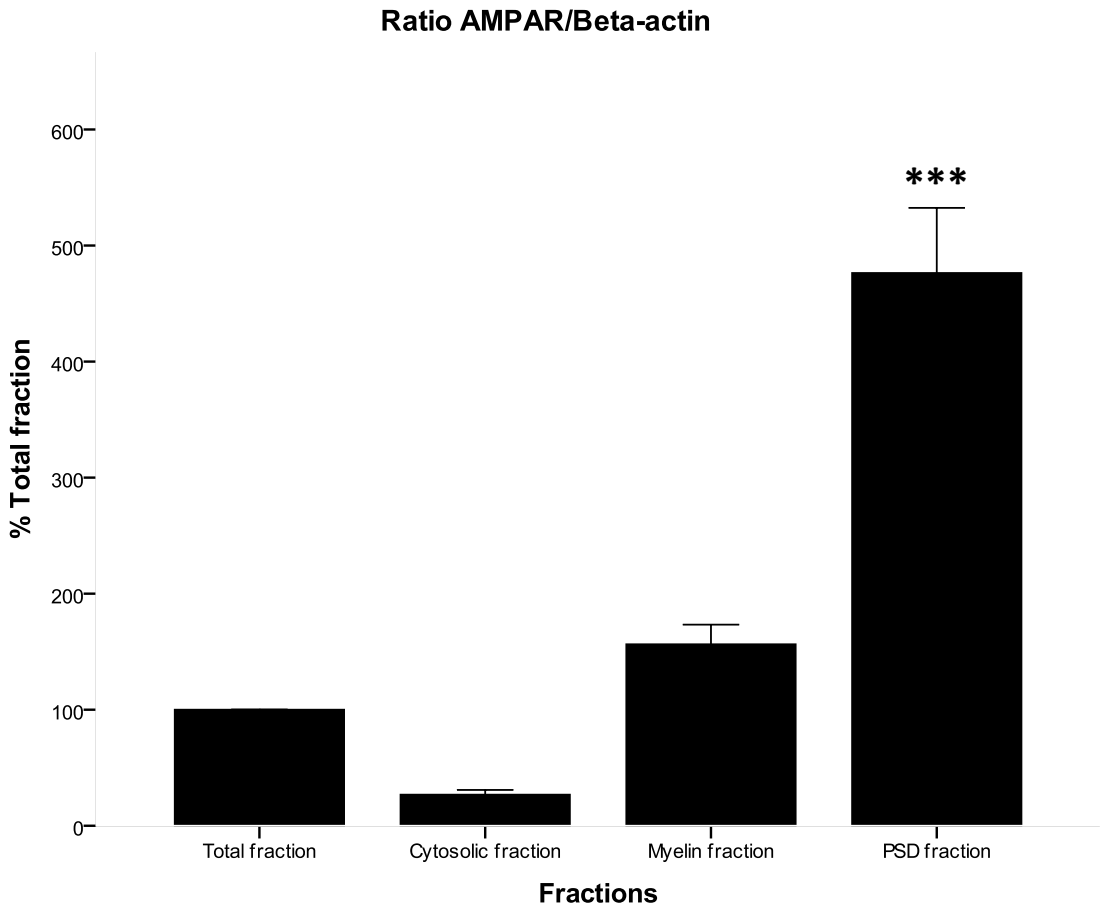

Figure 3-20: Mean (± SEM) of the ratio AMPAR/β-actin in percentage of the total fraction.

Statistical test ANOVA with Bonfferoni correction. Comparisons with the total fraction (*p<0.001)**

Repeated measurements of the 6 experiments showed a significant increase of the AMPAR subunits ($p<0.001$) in the PSD fractions compared to the total fractions. No significant change was observed for the cytosolic and myelin/light membranes

fractions. However a decreasing trend could be observed for the cytosolic fraction compared to the other fractions (see Figure 3-20).

3.4.5 Expression of synaptophysin, beta-III-tubulin and GFAP

In order to determine the purity of the PSD fraction, synaptophysin, β-III-tubulin, and GFAP were detected on the membranes (see Figure 3-21). β-actin was detected at the same time as used for normalisation of the expression of each protein. GFAP was detected at the same time as AMPAR subunits after the membranes were stripped.

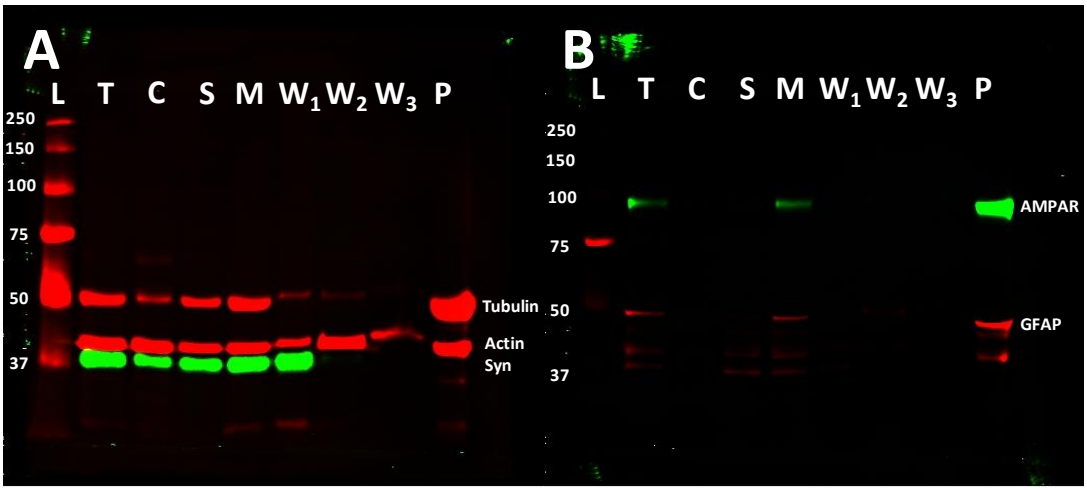

Figure 3-21: Digital picture of the membranes after detection of synaptophysin, GFAP, β-III-tubulin and β-actin.

(A) Detection of synaptophysin and β-III-tubulin. (B) Detection of GFAP. (L) ladder; (T) Total fraction; (C) Cytosolic fraction; (S) Sucrose 0.32 M fraction; (M) Myelin/light membranes fractions; (W_1) wash 1 fraction; (W_2) wash 2 fraction; (W_3) wash 3 fraction; (P) PSD fraction.

Immunodetection of synaptophysin (green), β-III-tubulin and β-actin showed specific bands for all three proteins at their expected size, respectively 37, 52 and 42 KDa. β-

actin was detectable in each fraction, whilst synaptophysin and β-III-tubulin did not appear in all fractions. β-III-tubulin was detected in almost all fractions but with very weak intensity in washes fractions. Synaptophysin, a maker of the pre-synaptic terminal was not detected in the last washes fractions nor the PSD fractions (see Figure 3-21 A). Astroglial cell marker GFAP, showed between 3 and 5 main bands indicating the one at expected size of GFAP (50 KDa). GFAP was detected in the total and myelin/light membranes fractions with similar intensities and with higher intensity in the PSD fractions.

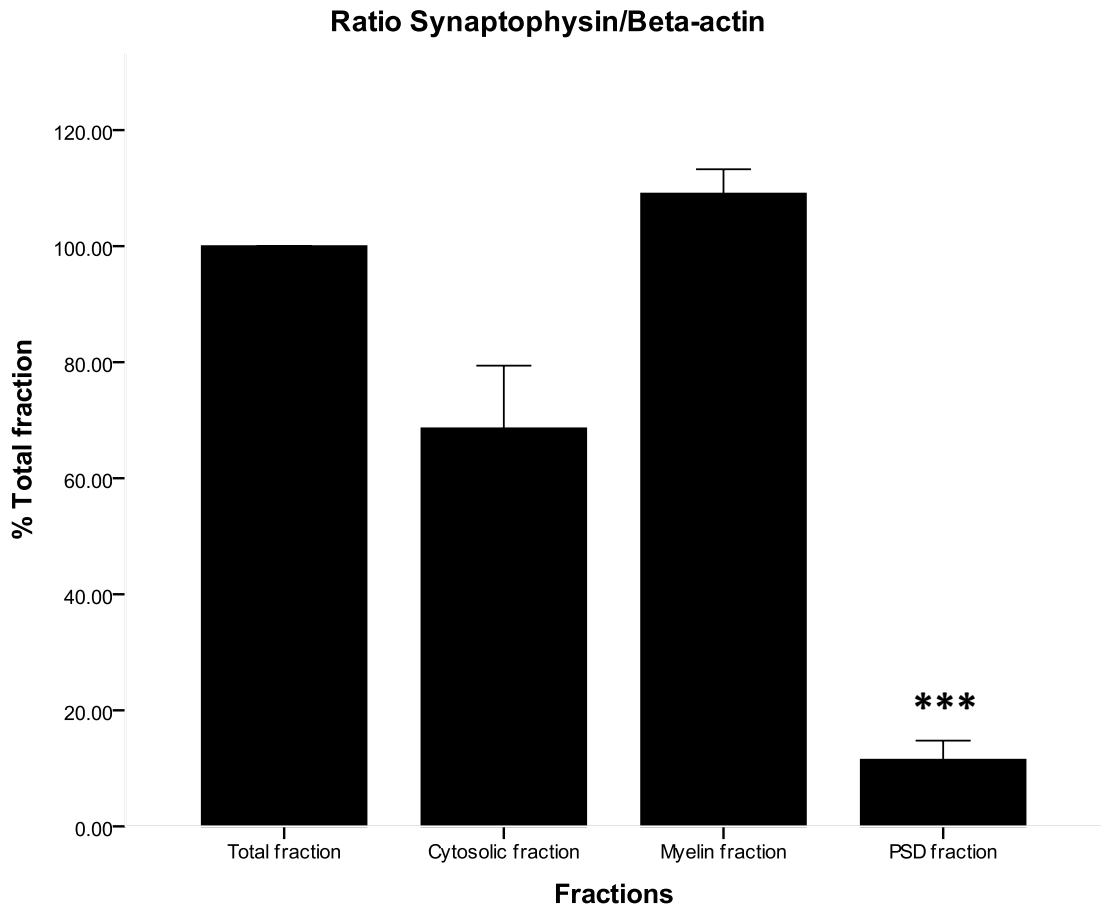

Figure 3-22: Mean of the ratio synaptophysin/β-actin in percentage of the total fraction.

Statistical test ANOVA with Bonfferoni correction. Comparison with the total fraction (* p<0.001)**

Comparison of synaptophysin expression in total, cytosolic, myelin/light membranes and PSD fractions showed a significant decrease of synaptophysin expression in the PSD fractions (p<0.001). No further differences in expression of synaptophysin were found between the total, cytosolic and myelin/light membrane fractions. However a trend decrease of expression of synaptophysin was observed in the cytosolic fractions compared to the total and myelin/light membranes fractions (see Figure 3-22).

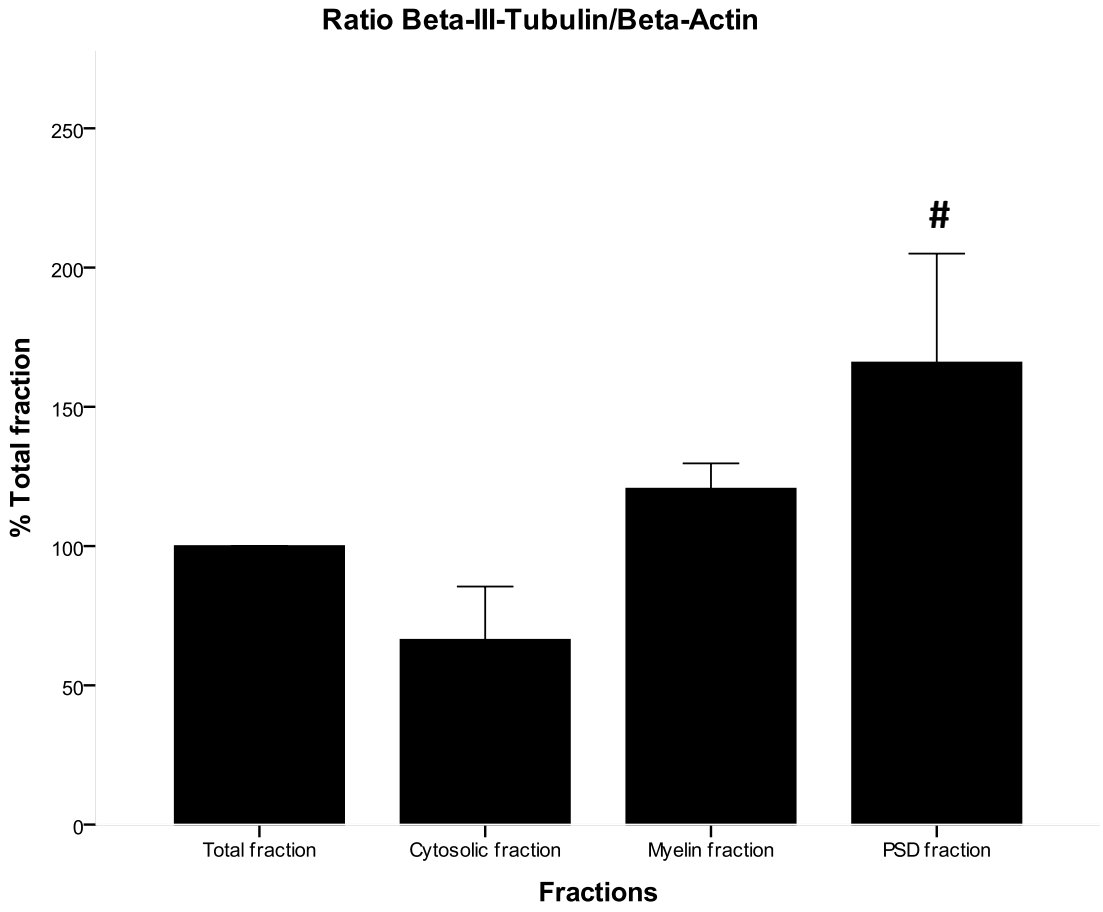

Figure 3-23: Mean of the ratio β-III-tubulin/β-actin in percentage of the total fraction.

Statistical test ANOVA with Bonfferoni correction (# p<0.05;Comparison with cytosolic fraction).

No significant difference was found for the expression of β-III-tubulin between the different fractions compared to the total fraction. However a significant increase of the expression of β-III-tubulin (# p<0.05) was found in the PSD fraction compared to the cytosolic fraction (see Figure 3-23).

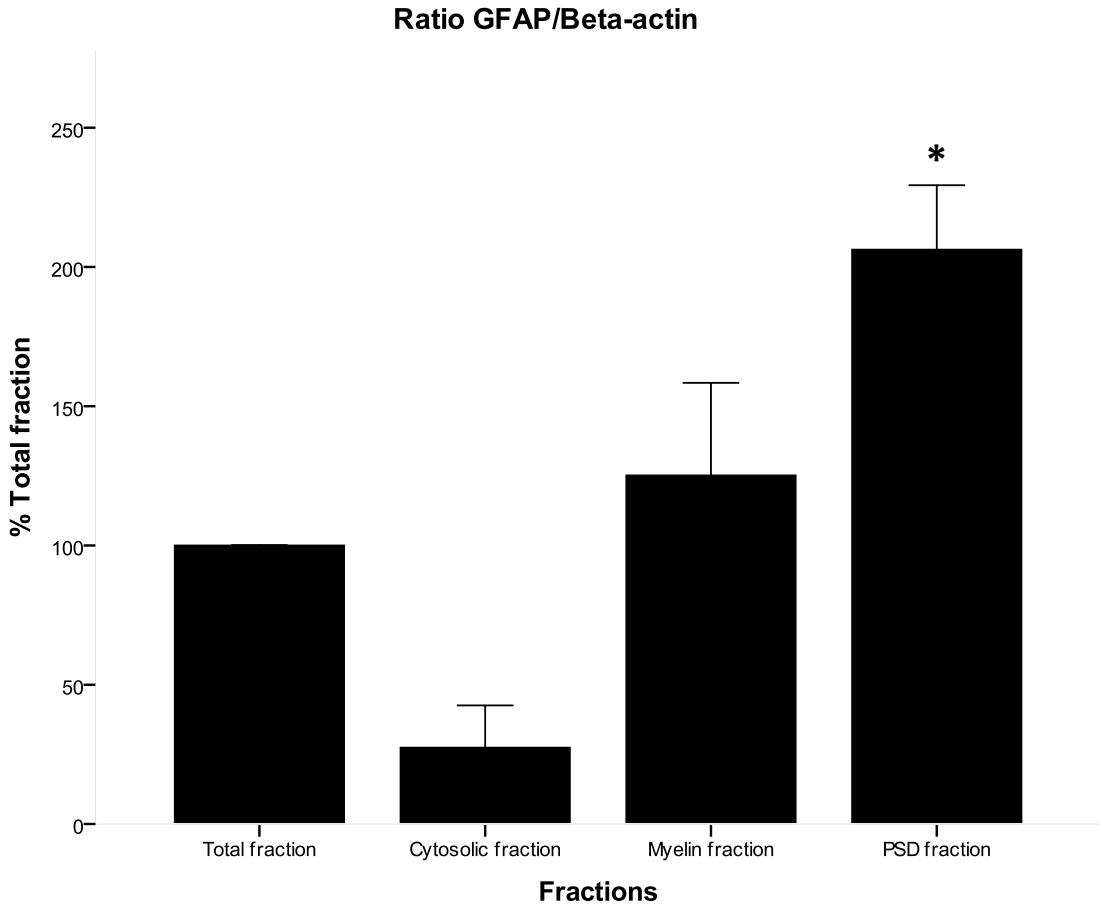

Figure 3-24: Mean (± SEM) of the ratio GFAP/β-actin in percentage of the total fraction.

Statistical test: ANOVA with Bonfferoni correction. Comparison with the total fraction (*p<0.05)

The expression of the marker of glial cells GFAP showed a significant increase in the PSD fraction compared to the total fraction ($p<0.05$). A trend decrease of the expression of GFAP can also be observed in the cytosolic fraction compared to the other fractions.

3.5 Discussion and conclusion

This part of the study has verified:

1. **That it is possibility to extract PSDs from frozen human premotor cortex using sucrose gradient separation and bench centrifugation.**
2. **That the developped method leads to PSD fraction with an acceptable yield and PSD integrity.**
3. **That proteins expressed mainly at the post-synaptic terminals are enriched in the PSD fraction compared to the whole homogenate.**

The characterisation of the PSD fraction using electron microscopy showed a heterogenic composition of the PSD. Indeed PSDs were detected in the PSD fractions with contaminants that resembled CaMKII clusters, mitochondria, myelin and membrane vesicles. These results were previously reported in a study using the same technique of PSD isolation (Dosemeci et al., 2006). The presence of PSDs in transverse view with or without symmetrical structures and disk-like shaped structures with high electron density indicated that integrity of the PSDs seems to be conserved after isolation from frozen blocks human brain (see Figure 3-14) as reported previously in a study using a different PSD isolation method on human PFC (Hahn et al., 2009). These results suggest the presence of both asymmetrical and symmetrical synapses in the

cerebral cortex as reported in other studies in the cerebral cortex of non-human mammalians (Carlin et al., 1980; Peters et al., 2008).

Proteins of the PSD such as NMDAR, AMPAR and the scaffolding protein PSD-95 play a crucial role into the complex machinery of the PSD and their function maybe disturbed in psychiatric diseases such schizophrenia, major depressive and bipolar disorders (Petrie et al., 2000; Stahl, 2007). Detection of these proteins in the PSDs isolated from post-mortem frozen blocks of human brain was crucial for our study. The protein PSD-95, the subunit NR2A of the NMDAR, the subunits 2, 3, 4 of the AMPAR were all detected in the PSD fractions (see Figure 3-15; Figure 3-17 and Figure 3-19). Moreover all of these proteins were enriched in the PSD fraction compared to the total fractions as previously mentioned in other studies (Dosemeci et al., 2006; Villasana et al., 2006; Hahn et al., 2009).

Semi-quantitative analysis of the amount of PSD-95, NR2A and AMPAR subunits was carried out on six independent experiments of the isolation of the PSDs. The results showed a significant increase of the ratio PSD-95/β-actin ($p<0.001$) (see Figure 3-16), NR2A/β-actin ($p<0.001$) (see Figure 3-18) and AMPAR/ β-actin ($p<0.001$) (see Figure 3-20) in the PSD fractions compared to the total fractions. These results concord with previous studies (Villasana et al., 2006; Hahn et al., 2009).

As mentioned above electron micrographs showed that the PSD fractions contained contaminants. The pre-synaptic vesicles marker synaptophysin, the cytoskeletal protein β-III-tubulin and the marker of glial cells GFAP were immunodetected to determine the nature of the contaminants in the PSD fractions (see Figure 3-21). β-actin was also detected and the intensity detected was used as a denominator to normalise our results.

Comparison of synaptophysin expression in total, cytosolic, myelin/light membranes and PSD fractions showed a significant decrease of synaptophysin expression in the PSD fractions ($p<0.001$) (see Figure 3-22). No significant difference was found for the expression of β-III-tubulin between the different fractions compared to the total

fraction. However a significant increase of the expression of β-III-tubulin (# $p<0.05$) (see Figure 3-23) was found in the PSD fraction compared to the cytosolic fraction. The expression of the marker of glial cells GFAP showed a significant increase in the PSD fraction compared to the total fraction ($p<0.05$) (see Figure 3-24). These results were similar to results obtained in previous studies (Dosemeci et al., 2006; Hahn et al., 2009), and also contradictory with a study using another type of isolation (Villasana et al., 2006).

Our results establish that PSDs can be isolated from frozen blocks of human brain in reasonable purity using the protocol developed by Dosemeci *et al,.* 2006. Electron micrographs showed the presence of the PSDs in the PSD fractions and Western blotting analysis of the PSD fraction demonstrated an enrichment of the most common scaffolding protein of the PSD, PSD-95, and the subunits of the two more important receptors implicated in synaptic plasticity, NR2A and AMPAR subunits. Contaminants such as mitochondria and myelin were also detected in the PSD fraction. The marker of the pre-synaptic vesicles, the protein synaptophysin was absent in our PSD fractions.

The method used in our study allowed us to use a minimum amount of human brain sample and to get reasonable purity of the PSD fraction. Moreover this technique of isolation maybe followed with PSD-95 immunoprecipitation in order to increase the purity of the PSD and study protein-protein interactions within the PSD with better efficacy (Dosemeci et al., 2006).

4 Expression of proteins involved in neuronal plasticity in the premotor cortex in schizophrenia

4.1 Aims and objectives

The aims of the present study are to quantify the level of protein expression of the NR2A subunit of the NMDAR, the scaffolding protein PSD-95, the protein kinases CaMKIIα and CaMKIIβ and the vesicle transporter NSF in the BA 6 in schizophrenia and to compare the findings with patients with major depressive disorder, bipolar disorder and healthy controls. Expression of the proteins mentioned above shall be quantified using Western blotting on BA 6 homogenate PSD fractions. Protein expression shall also be assessed after co-immunoprecipited PSD and the findings compared to direct Western blotting of the BA 6 homogenate PSD fractions.

4.2 Introduction

The human neocortex is a thick 6-layered structure containing neuronal cell bodies that cover the cerebrum and form sulci, gyry and lobuli that define the four cerebral lobes: the frontal lobe, the parietal lobe, the temporal lobe and the occipital lobe (see Figure 4-1). The frontal lobe is phylogenetically and ontogenically the latest developed part of the cortex and it occupies nearly a third of the neocortex (Fuster, 2002).

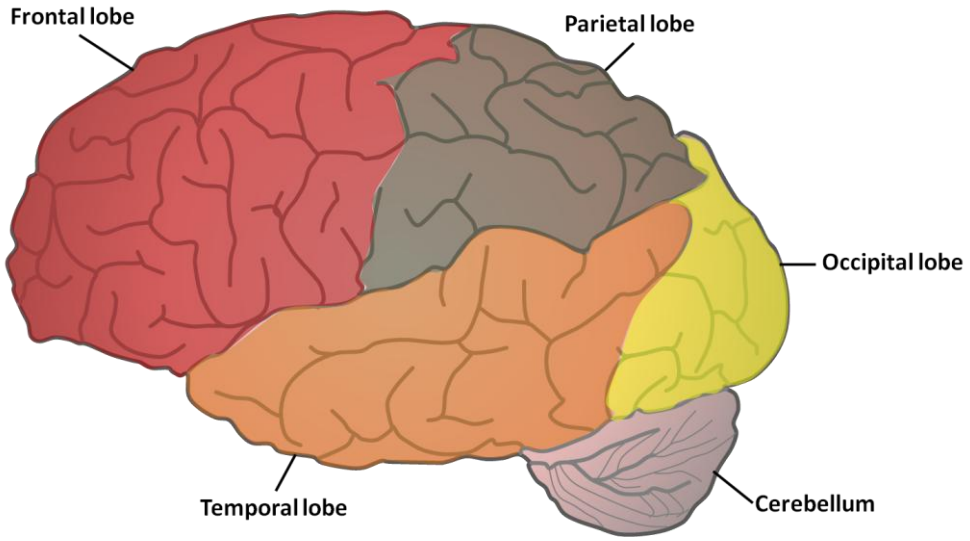

Figure 4-1: Diagram illustrating the localisation of the cerebral lobes.

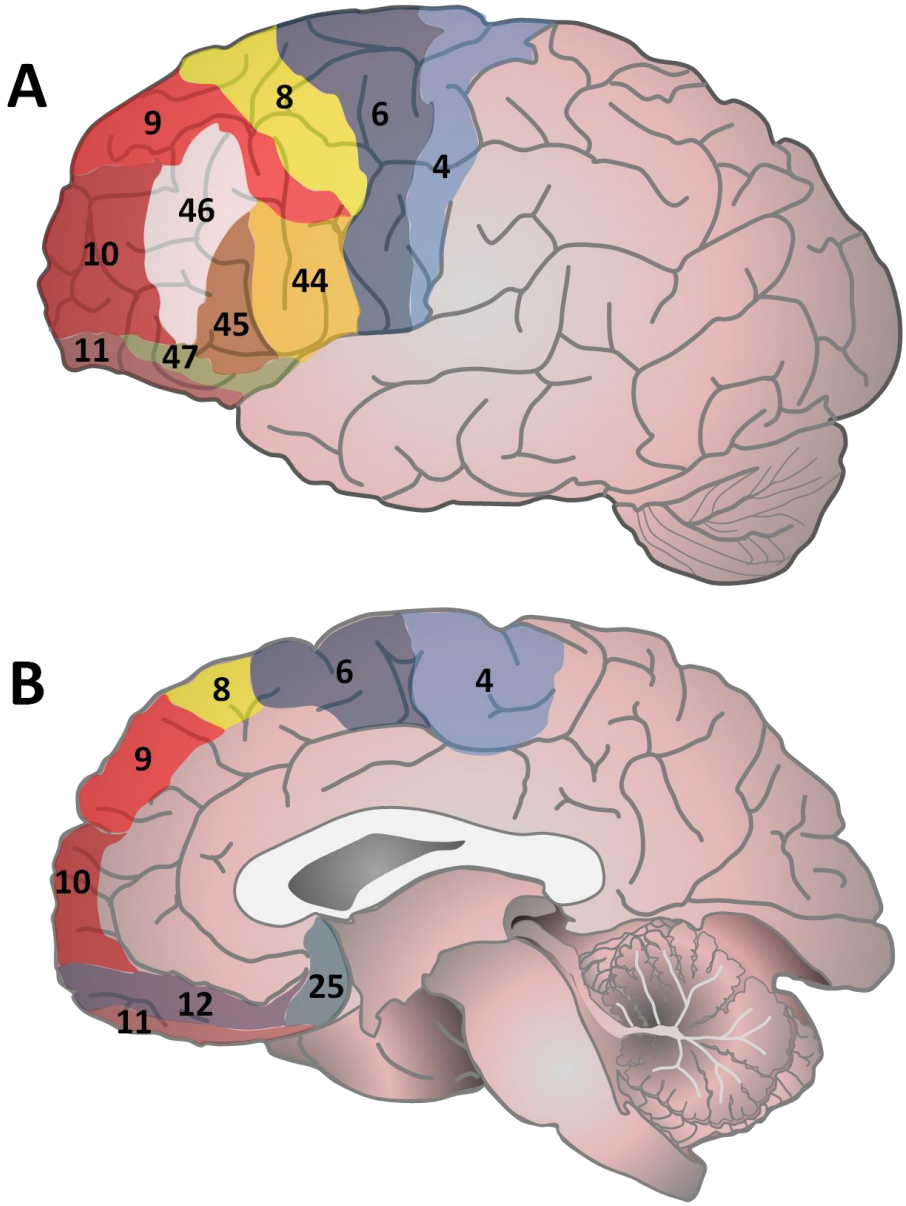

Figure 4-2: Diagram illustrating the position of the Brodmann's areas of the frontal cortex.

(A) Lateral part of the left hemisphere of the brain. (B) Medial part of the right hemisphere of the brain. (4) BA 4 (Primary motor cortex), (6) BA 6 (Premotor cortex and supplementary motor cortex), (8) BA 8 (Dorsomedial frontal cortex), (9) BA 9 (Dorsolateral prefrontal cortex), (10) BA 10 (Anterior prefrontal cortex), (11) BA 11 (Orbitofrontal cortex), (12) BA 12 (Orbitofrontal cortex), (25) BA 25 (Ventromedial prefrontal cortex), (44) BA 44 (Broca's area), (45) BA 45 (Broca's area), (46) BA 46 (Dorsolateral prefrontal cortex), (47) BA 47 (Ventrolateral prefrontal cortex).

The frontal lobe is composed of areas anatomically and functionally heterogeneous that play key roles in motor, emotional and cognitive functions. In the early 20th century several regions (Brodmann's area; BA) of the cortex were described depending on their cytoarchitectonic structure by Brodmann (see Figure 4-2). The frontal lobe consists of two sub-regions called the motor cortex (BA 4 and BA 6) and the PFC (BA 8 to 12, BA 25 and BA 44 to 47) (Brodmann, 1909).

4.2.1 Structure of the premotor cortex

In humans, Brodmann's area 6 (BA 6) is located in the precentral region of cerebral cortex at the caudal part of the superior, the middle and the inferior frontal gyri and the rostral part of the precentral gyrus that is not occupied by the BA 4. It also covers the medial side of the hemisphere down to the cingulate sulcus. Cytoarchitecturally, BA 6 is bounded rostrally by the PFC and caudally by BA 4. The main cytoarchitectural feature of the BA 6 is its characteristic agranular structure (Friederici, 2006). BA 6, also called premotor cortex, is composed of several functionally heterogeneous regions (see Figure 4-3). The premotor cortex which lies to the lateral aspect of the frontal lobe is divided into four sections, the premotor cortex dorsal (PMd) rostral, the PMd caudal, the premotor ventral (PMv) rostral (BA 44 in human) and the PMv caudal. In addition the supplemental motor area (SMA) is located on the medial aspect of the brain in the dorsomedial frontal cortex (Picard and Strick, 2001) and is divided into three sections, the pre-supplemental motor area (Pre-SMA), the supplemental motor area proper (SMA proper) and the supplemental eye field (SEF) which lies at the border of the SMA and the pre-SMA, close to the paracentral sulcus (Grosbras et al., 1999).

The premotor cortex constitutes a separate fronto-parietal cortical network and is also directly or indirectly connected to the subcortical nuclei, cerebellum and spinal cord. These projections, interconnections and loops which have been mostly studied in non-human primates are discribed below.

The PMd receives a combination of somatosensory and visual information from the medial intraparietal area in the superior parietal lobule (Colby and Duhamel, 1991; Galletti, 1996). The rostral portion of PMd is strongly interconnected with the prefrontal cortex (BA 46) (Lu et al., 1994; Barbas, 2000) whereas the caudal portion of PMd has strong interconnections with the primary motor cortex (M1) (Dum and Strick, 2005).

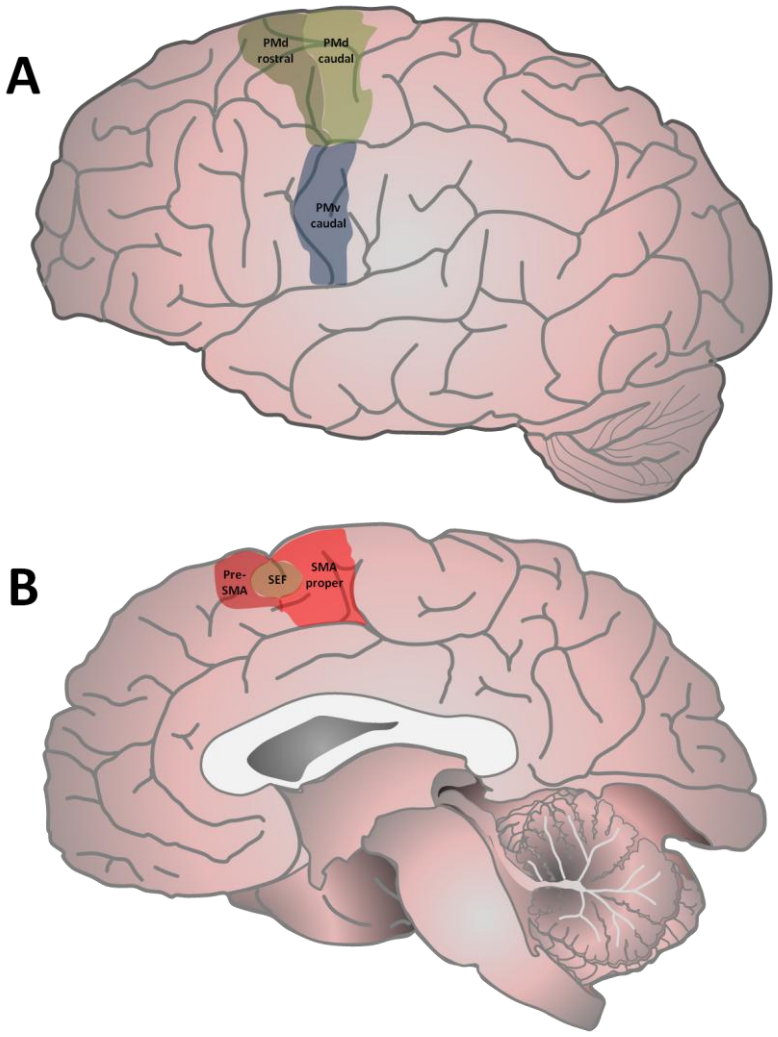

Figure 4-3: Diagram illustrating the parcellation of the Brodmann area 6.

(A) Lateral part of the left hemisphere of the brain. (B) Medial part of the right hemisphere of the brain. Pre-supplementary motor area (Pre-SMA); Supplementary motor area (SMA); Supplementary eye field (SEF); Premotor cortex dorsal (PMd); Premotor cortex ventral (PMv).

The caudal portion of the PMd projects outputs to M1 and directly to the spinal cord (Muakkassa and Strick, 1979; Dum and Strick, 1991) and does not have connections with the prefrontal cortex (Lu et al., 1994). In contrast, the rostral portion of the PMd does not project to M1 or to the spinal cord (Muakkassa and Strick, 1979; Dum and Strick, 1991). The rostral portion of the PMd is interconnected with areas of prefrontal cortex (BA 46) and with the reticular formation of the cerebellum (Lu et al., 1994). In addition, the rostral portion of the PMd does not appear to have any substantial interconnections with the caudal portion of the PMd (Kurata, 1991).

The caudal and rostral portions of the PMv receive input from the ventral and anterior intraparietal cortex respectively (Rizzolatti et al., 1988; Murata et al., 1997; Luppino et al., 1999). Both portions of the PMv receive inputs from the secondary somatosensory cortex (SII). The caudal portion of the PMv is connected more strongly with the SMA proper than with the pre-SMA. In contrast, the rostral portion of the PMv is connected more strongly with the pre-SMA than the SMA (Geyer et al., 2000). M1 receives dense input from the caudal portion of the PMv (Dum and Strick, 2005; Godschalk et al., 1984). The rostral portion of the PMv receives inputs from the lateral prefrontal cortex, especially from the opercular and the ventral prefrontal cortex (Dum and Strick, 2005). In addition, the caudal portion of the PMv sends outputs to the reticular formation of the cerebellum, spinal cord and facial nucleus of the brainstem (Geyer et al., 2000).

Input sources from the dorsolateral prefrontal cortex are different depending on the region of the PM cortex implicated. The PMd receives main inputs from the dorsal area of the PFC, whereas the PMv receives inputs from the ventral area of the PFC (Barbas and Pandya, 1987; Wang et al., 2002; Hoshi, 2006). The same differences are observed for the inputs from the parietal cortex. The PMd receives main inputs from the superior parietal lobule (Johnson et al., 1996; Matelli et al., 1998) whereas the PMv receives inputs from the inferior parietal lobule (Rozzi et al., 2006). Thus, neuroanatomical considerations suggest that the PMd and PMv are involved in

networks that are distinct (Tanné-Gariépy et al., 2002; Rizzolatti and Matelli, 2003; Stepniewska et al., 2006).

The SMA send outputs that makes a direct and substantial contribution to the corticospinal tract as it comprises approximately 10 % of all corticospinal cells (Dum and Strick, 1991; He et al., 1995; Wise, 1996). By comparison, the pre-SMA has a sparse projection in the corticospinal system (Dum and Strick, 1991; Luppino et al., 1994). The SMA has reciprocal connections with M1, whereas the pre-SMA does not (Luppino et al., 1993). Also, as the rostral portions of the PMd and PMv, the pre-SMA and the SEF project to the dorsolateral prefrontal cortex (BA 46 mainly) (Lu et al., 1994; Luppino et al., 1993; Wang et al., 2005).

The premotor cortex has also connections to sub-cortical nuclei giving rise to direct or indirect loops connecting the premotor cortex to the basal ganglia. These inter-connections are defined as the basal ganglia-thalamo-cortical loops. The premotor and the supplementary motor loops are similar. The premotor, the SMA, the pre-SMA and the SEF all send outputs to the caudate nucleus/putamen which send outputs onto the the internal segment of the globus pallidus both directly and indirectly (through the external segment of the globus pallidus). In turn, the internal segment of the globus pallidus send outputs to the motor areas of the thalamus which return the information received back to the premotor areas (Nakano et al., 2000; Nachev et al., 2008). In addition, both the SMA and the pre-SMA have a "hyperdirect" connection to the subthalamic nucleus which interacts with internal and external segment of the globus pallidus (Nambu et al., 1996).

4.2.2 Functions of the premotor cortex

The basic function of the premotor cortex is clearly the motor sequencing and the planning of movements. For instance, damage in the human lateral premotor area by stroke results in kinetic apraxia and other motor impairments, which include defects in planning, initiating, and sequencing (Miyai et al., 1999). A study using whole-brain

fMRI showed that in the absence of any movement, attending to and predicting increasingly complex target motion rely on premotor cortices. Serial prediction caused activations in premotor and parietal cortices (Schubotz and Von Cramon, 2002). The Tower of London task is a test of motor planning in which subjects must move coloured balls on a computer screen to match a specified arrangement in a minimum of number of moves. This test was used in a study using to map the network of brain structures involved in planning movement. In this study they demonstrated that BA 6, particularly the lateral premotor cortex, with other areas of the cortex forms a network implicated in motor planning (Dagher et al., 1999). In addition to motor sequencing and planning movement the BA 6 is also involved in processes such as movement initiation (Jenkins et al., 2000), movement preparation and imagined movement (Stephan et al., 1995), motor learning (Halsband and Lange, 2006), horizontal saccadic eye movements (Tanaka and Kunimatsu, 2011) and interlimb coordination (Henrik Ehrsson et al., 2000).

The left premotor cortex, particularly the left SMA, participates in language initiation and maintenance of voluntary speech production. A study utilising fMRI blood-oxygen-level-dependent (BOLD) response showed that left premotor cortex was involved with other areas of the cortex in speech production (Shuster and Lemieux, 2005). Another study using scan PET demonstrated the involvement of the SMA in speech desorder such as stuttering (Fox et al., 2000). Imaging studies also revealed the activation of the SMA during language processing such as verbal fluency, phonological and semantic language tasks (Basho et al., 2007; De Carli et al., 2007). Furthermore the premotor cortex is involved in diverse language processes such as language switching (Price et al., 1999), reading novel words (Dietz et al., 2005), updating verbal information (Tanaka et al., 2005), phonological processing (McDermott et al., 2003), object naming (Baciu et al., 1999), lipreading (Paulesu et al., 2003), word retrieval (Warburton et al., 1996) and lexical decision on words and pseudowords (Price et al., 1994).

The BA6 also participate in memory, attention, and executive functions due to the activation of an extended brain network, that sometimes involves BA6. Many

neuroimaging studies have highlighted the role of prefrontal regions in the sustained maintenance and manipulation of information over short delays, or working memory. In addition, neuroimaging findings have highlighted the role of prefrontal regions in the formation and retrieval of memories for events, or episodic long-term memory. Studies also showed co-activation of the BA 6 during both long term and short term memory (Tulving et al., 1994; Rämä et al., 2001; Ranganath et al., 2003). The BA 6 has also been reported to be involved in mnemonic rehearsal (Goldberg et al., 1996; Kapur et al., 1996) and topographic memory (Berthoz, 1997).

Functional neuroimaging studies also revealed the neural system underlying visuospatial attention and dynamic visuospatial imagery. These studies provide strong and consistent evidence that the human premotor mesial and lateral premotor cortices are involved in visuospatial attention and dynamic visuospatial imagery (Nobre et al., 1997; Lamm et al., 2001). In human, the left ventral premotor cortex was also reported to be activated when alphabetical characters were passively observed and that the same region was also involved in handwriting. Visual presentation of letters and pseudoletters activated a part of the left premotor cortex, more ventrally and medially, compared to the area activated when the letters were being written by the subjects (Longcamp et al., 2003; Longcamp et al., 2005). In addition to visuospatial attention functional neuroimaging studies also reported the involvement of the premotor cortex in selective attention to rhythm and processing sequential sounds as well as attention to human voices (Platel et al., 1997; Nakai et al., 2005).

Executive functions define the cognitive processes that regulate, control, and manage cognitive processes, such as planning, working memory, attention, problem solving, verbal reasoning, inhibition, mental flexibility, multi-tasking, and initiation and monitoring of actions (Chan et al., 2008). Neuropsychological studies have shown that the PFC plays a crucial role in executive functions; however functional neuroimaging studies seem to reveal the activation of a more extended brain network during executive functions which sometimes involves the BA 6. For instance, imaging studies showed a bilateral activation of the premotor cortex as well as the left supplementary

motor area in planning and solving novel problems (Crozier et al., 1999; Fincham et al., 2002). The BA 6 was also reported to be activated in processes such as executive control of the behavior (Burton et al., 2001) and deductive reasonning (Knauff et al., 2002; Reverberi et al., 2007).

4.2.3 The premotor cortex and the pathophysiology of schizophrenia

Research exploring the cognitive impairments in schizophrenia generally focuses on dysfunction of association cortices such as the PFC, the temporal cortex and the parietal cortex. However several lines of evidence suggest that these impairments are reflective of a dysfunction of a more extended neural network which may imply the premotor cortex.

Motor sequencing and motor planning seems to be disturbed in schizophrenia. For instance, when patients with schizophrenia are required to reproduce relatively simple drawings of geometric shapes, their performance is significantly worse than controls when visual feedback of their movements is removed (Mlakar et al., 1994). Furthermore, minor abnormalities in motor coordination and motor sequencing are readily identified for tasks such as finger tapping and finger–thumb alternation. Increased incidence of minor abnormalities in motor coordination and motor sequencing have been observed in first-episode psychosis patients and in people identified as having a high risk for developing psychosis (Dazzan and Murray, 2002). In addition studies demonstrated deficits in motor control and motor imagery in patients with schizophrenia (Danckert et al., 2002; Franck et al., 2001; Maruff et al., 2003).

Neuroimaging studies also revealed reduced activation of the SMA in simple motor tasks in catatonic or akinetic patients with schizophrenia (Payoux et al., 2004; Scheuerecker et al., 2009). Reduced volumes of the left SMA was reported in patients with schizophrenia presenting persistent negative symptoms compared to non-deficit patients (Galderisi et al., 2008; Cascella et al., 2010). Furthermore, alterations in the premotor areas such as reduced pre-SMA (Exner et al., 2006) and premotor cortex

(Baudendistel et al., 1997; Kodama et al., 2001; Rowland et al., 2008) gray matter volume were linked to disturbances in motor skill learning in schizophrenia. In addition to alteration of higher motor functions such as coordination, planning, fine-tuning, and learning of motion sequences, disturbances in intention or volition might originate from both cognitive and premotor deficits. For instance, voliton has been connected with the function of the pre-SMA (Haggard, 2008). In summary, neuroimaging studies of different modalities support the view of an altered structure and function of the premotor system in schizophrenia. These studies suggest that disturbed volition, learning, initiation and execution of movements in schizophrenia may result from dysfunctions of the premotor cortex and of impaired structural connectivity with association cortices such as PFC and parietal cortex.

4.2.4 Summary

The human premotor system in the brain includes the dorsal and ventral premotor areas, the supplemental motor area, the pre-supplemental motor area and the supplemental eye field. The system is organised in different parallel loops interconnected the basal ganglia, the M1, the PFC, the parietal cortex, the cerebellum and the spinal cord. The lateral premotor cotex (PMd and PMv) is involved in goal-directed movements, whilst the medial premotor cortex (SMA proper, pre-SMA) is engaged in motor planning and execution. Furthermore, the pre-SMA has been implicated in volitional aspects of behavior and drive.

A recent study using repetitive transcranial magnetic stimulation in the premotor cortex which suppresses cortical excitability in M1 in healthy subjects showed reduced motor cortical inhibition in patients with schizophrenia (Oxley et al., 2004). This study suggests that abnormal neural plasticity in the premotor cortex may be involved in the pathophysiology of schizophrenia. Furthermore, altered NRG1-ErbB4 signalling was associated with NMDAR hypofunction in the prefrontal cortex in schizophrenia (Hahn et al., 2006). In the BA 6 of schizophrenic patients reduced NRG1 C-terminal fragments

has been reported, indicating altered NRG1 signalling in this premotor cortex (Barakat et al., 2010). These findings suggest that the glutamate system, particularly disturbances in molecular processes involved in synaptic plasticity, may be involved in the dysfunction of the premotor cortex in schizophrenia.

4.3 Materials and methods

4.3.1 Enrichment of the glutamate post-synaptic density

Sixty frozen blocks of human brain were weighed, thinly chopped on ice and homogenised (see section 2.2.3). The homogenates were fractionated as described in section 2.2.4. The extraction was carried out three times. PSD fractions were collected and used for both direct Western blotting analyses and co-immunoprecipitations.

4.3.2 Protein concentration and protein assay

A protein assay was carried out on the PSD fractions as described in section 2.4. Sixty micrograms of protein of each fraction were used either for direct Western blotting or co-IP experiments.

4.3.3 Co-immunoprecipitation

The tubes used for co-IP were coated, then the magnetic beads were cross linked with antibodies directed to PSD-95 and the PSDs were immuno-purified, washed and eluted by denaturation as described in section 2.6.

4.3.4 Western blotting

For direct WB of the PSD fractions, 60 µg of protein was denatured and loaded onto 5-8% polyacrylamid gel. Proteins were separated and transferred on PVDF membranes for immunodectection of PSD-95, NR2A, CaMKIIα and CaMKIIβ, NSF, β-III-tubulin and β-actin. Western blotting was performed as described in section 2.5. For the co-immunoprecipited PSDs WB was carried out after denaturing elution of the complex beads-antibodies-PSDs and PSD-95, NR2A, CaMKIIβ, NSF, β-III-tubulin and β-actin were detected as described above.

4.3.5 Data analysis

For each membrane an average of the background was substracted from the signal quantified for each protein detected. A ratio between the protein of interest and either β-actin or β-III-tubulin was calculated. An average of the ratio of three experiments was calculated for WB experiments on the PSD fraction. Co-IP experiment was carried out once. Expression of NR2A, PSD-95, CaMKIIα, CaMKIIβ and NSF in PSD fractions and co-immunoprecipited PSDs were compared.

Effects of demographic and peri-mortem factors were assessed using ANOVA, Student's t-test and Spearman's correlation statistical analysis. When no significant effect of the demographic and peri-mortem factors was found ANOVA statistical analysis was performed to assess the effect of diagnosis, and Bonferroni post-hoc tests were used to assess interactions between teh diagnostic groups. When significant effect of demographic or peri-mortem variables were found, ANCOVA statistical analysis was performed with the associated co-variable.

4.4 Results

Western blotting using IR-dye secondary antibodies and primary antibodies directed to NMDAR NR2A subunit, PSD-95, CamKIIα and β, NSF, β-actin and β-III-tubulin revealed the presence of all six proteins in the PSD fraction and five of them co-immunoprecipited with PSD-95. For the co-immunoprecipited PSDs the signal from CamKIIα protein was indistinguishable from the primary antibody heavy chain. Consequently, CamKIIαwas excluded from the co-IP study.

The first part of the analysis consisted of identifying the most appropriate protein (β-actin or β-III-tubulin) for normalisation of the WB and co-IP data. Expression of the NMDAR subunits NR2A, PSD-95, CamKIIα and β and NSF was then presented as a ratio of these proteins with β-actin or β-III-tubulin respectively for WB and co-IP experiments (see section 4.4.1).

4.4.1 Expression of β-actin and β-III-tubulin in the PSD fraction and within the PSD

The mean of the fluorescence intensity of β-actin and β-III-tubulin was compared between the four diagnostic groups for both WB and co-IP experiments using one-way ANOVA (see Figure 4-4). For both β-actin and β-III-tubulin, no significant main effects of diagnosis were found for WB (β-actin $F(3, 54) = 0.847$, $p = 0.474$; β-III-tubulin $F(3, 56) = 1.034$, $p = 0.385$) or co-IP experiments (β-actin $F(3, 54) = 1.604$, $p = 0.199$; β-III-tubulin $F(3, 54) = 0.545$, $p = 0.654$)

By observing the bar charts (Figure 4.4) the variance from the mean for β-actin was more homogeneous in the WB experiments (see Figure 4-4 A and C), while for the co-IP PSD, the variance from the mean for β-III-tubulin was more homogeneous between diagnostic groups. Therefore, β-actin was chosen as the denominator to normalise data from WB experiments and β-III-tubulin was used as the denominator to normalise data from co-IP experiments.

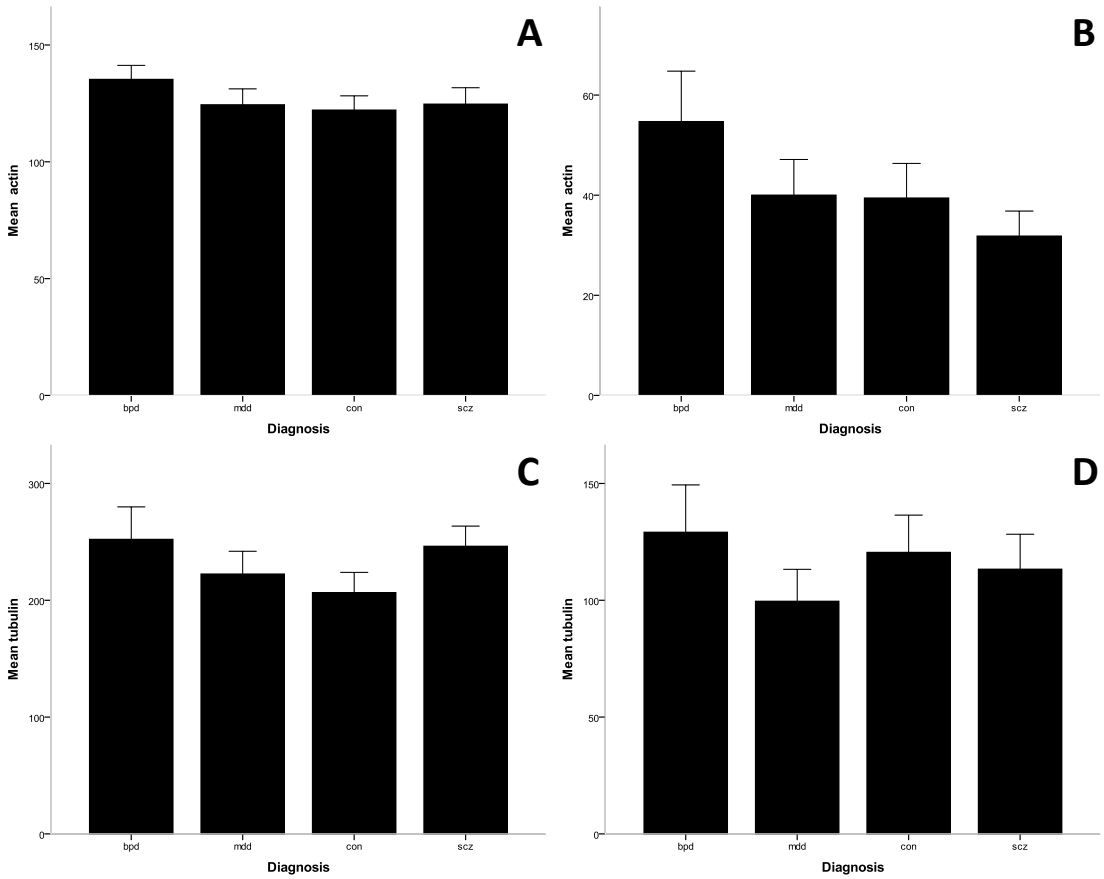

Figure 4-4: Mean (± SEM) fluorescence intensity for β-actin and β-III-tubulin in the PSD fraction and co-IP PSD depending on diagnosis.

(A) Mean fluorescence intensity for β-actin after WB of the PSD fraction. (B) Mean fluorescence intensity for β-actin after co-IP of the PSD fraction. (C) Mean fluorescence intensity for β-III-tubulin after WB of the PSD fraction. (D) Mean fluorescence intensity for β-III-tubulin after co-IP of the PSD fraction. (bpd) bipolar disorder ; (mdd) major depressive disorder ; (con) control ; (scz) schizophrenia

The effects of gender (see Figure 4-5 A and B) and cerebral hemisphere (see Figure 4-5 C and D) on dependent variables β-actin and β-III-tubulin for WB and co-IP experiments respectively, were examined using Student's T-test. No significant effect of gender was found for β-actin ($t(56) = 0.011$, $p = 0.991$) or β-III-tubulin ($t(56) = 0.786$,

p = 0.435). Similarly, no effect of brain hemisphere was foundfor both WB (β-actin; t(56) = 0.135, p = 0.893) and co-IP (β-III-tubulin; t(56) = 0.110, p = 0.913) experiments.

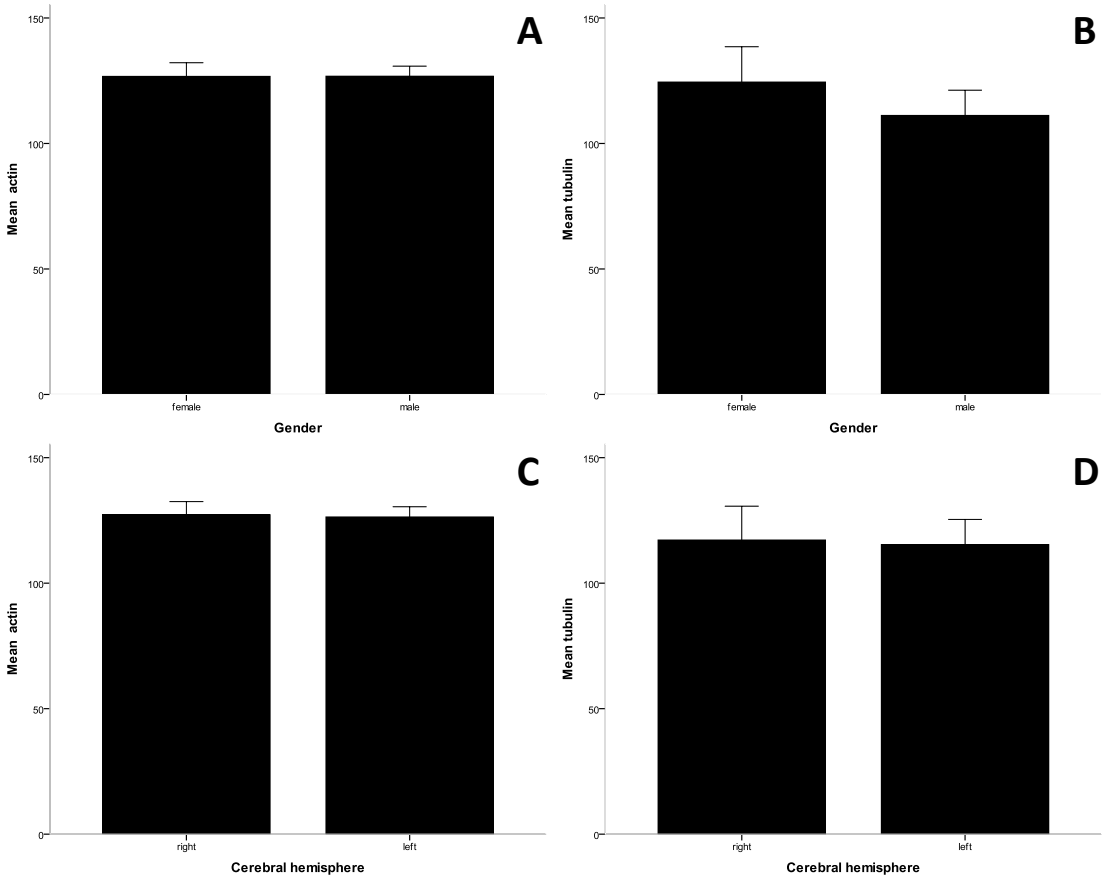

Figure 4-5: Mean (± SEM) fluorescence intensity for β-actin and β-III-tubulin in the PSD fraction and co-IP PSD depending on gender and side of the cerebral hemisphere.

(A) Mean fluorescence intensity for β-actin after WB of the PSD fraction. (B) Mean fluorescence intensity for β-III-tubulin after co-IP of the PSD fraction. (C) Mean fluorescence intensity for β-actin after WB of the PSD fraction. (D) Mean fluorescence intensity for β-III-tubulin after co-IP of the PSD fraction.

The effect of psychotic symptoms on tdependent variables β-actin and β-III-tubulin for WB (see Figure 4-6 A) and co-IP experiments respectively (see Figure 4-6 B) were also

examined using Student's T-test. However, in this case the group control was removed from the analysis. No significant effect of psychosis was found for both β-actin ($t(42) = 0.232$, $p = 0.818$) and β-III-tubulin ($t(41) = 0.188$, $p = 0.852$).

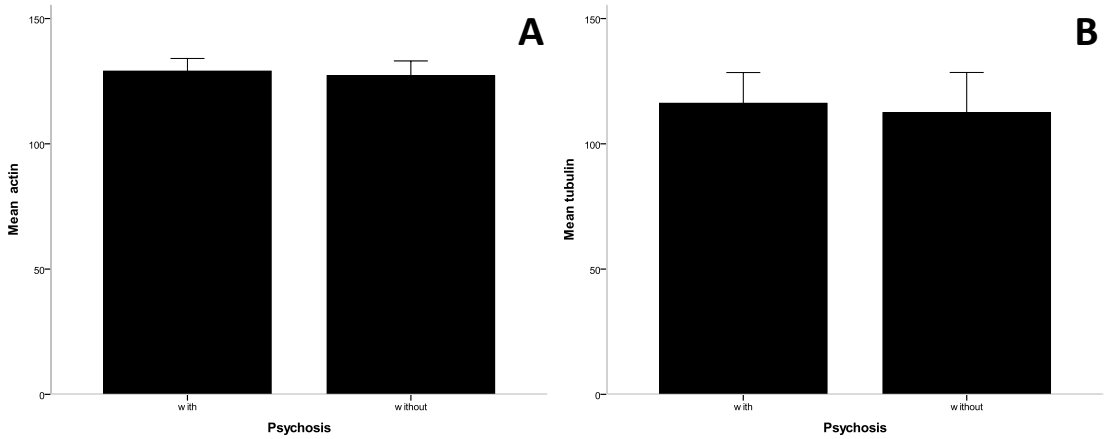

Figure 4-6: Mean (± SEM) fluorescence intensity for β-actin and β-III-tubulin in the PSD fraction and co-IP PSD depending on psychotic symptoms.

(A) Mean fluorescence intensity for β-actin after WB of the PSD fraction. (B) Mean of the fluorescence intensity for β-III-tubulin after co-IP of the PSD fraction.

To assess potentially confounding effects of death by suicide on the β-actin and β-III-tubulin for WB (see Figure 4-7 A and C) and co-IP experiments respectively (see Figure 4-7 B and D), a Student's t-test analysis was carried out with and without the group control. No significant effect of death by suicide was found for both β-actin ($t(56) = 1.121$, $p = 0.267$) and β-actin ($t(42) = 0.839$, $p = 0.406$) respectively with or without the control group. Student's t-test for both with ($t(48.34) = 1.972$, $p = 0.054$) or without ($t(40.16) = 1.819$, $p = 0.076$) the control group revealed a trend towards a significant decrease in the group with death by suicide for β-III-tubulin.

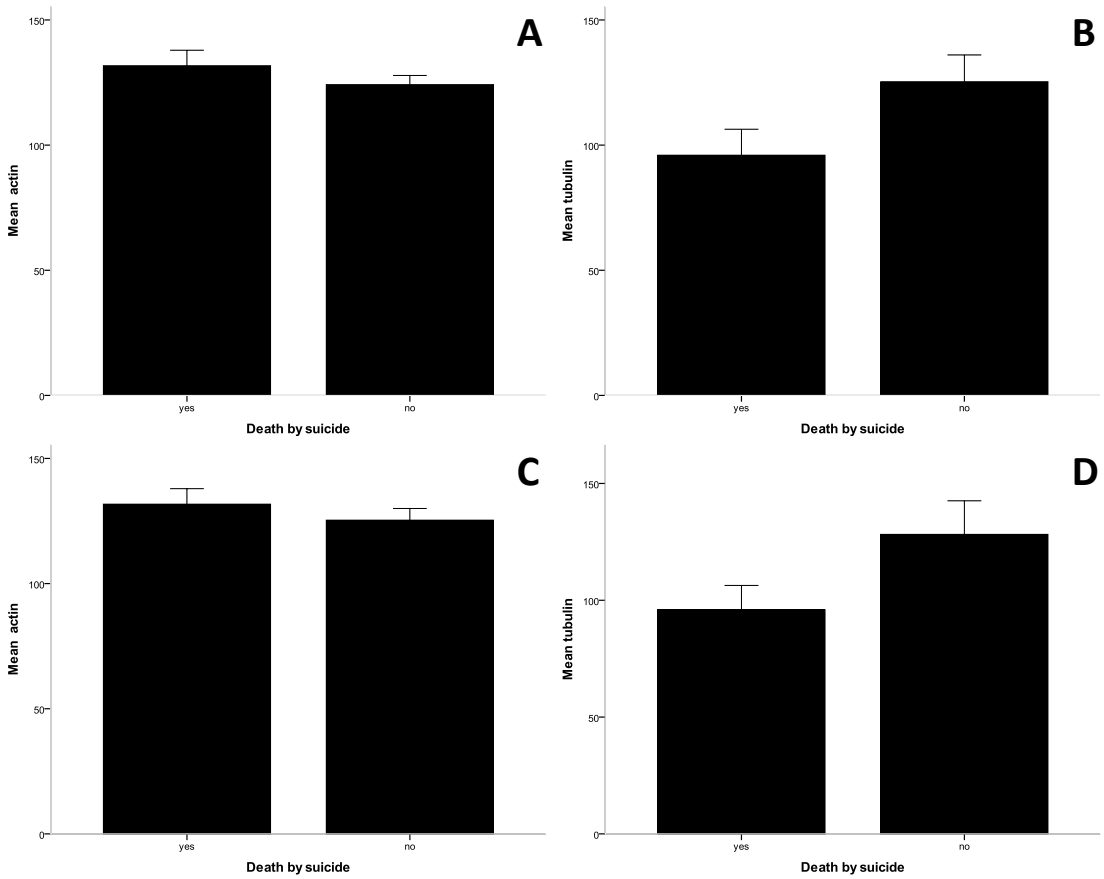

Figure 4-7: Mean (± SEM) fluorescence intensity for β-actin and β-III- in the PSD fraction and co-IP PSD depending on death by suicide.

(A) Mean fluorescence intensity for β-actin after WB of the PSD fraction. (B) Mean fluorescence intensity for β-III-tubulin after co-IP of the PSD fraction. (C) Mean fluorescence intensity for β-actin after WB of the PSD fraction (without controls). (D) Mean fluorescence intensity of β-III-tubulin after co-IP for the PSD fraction (without controls).

One-way ANOVA was used to compare the mean fluorescence intensity for β-actin and β-III-tubulin between substance and alcohol abuse groups for both WB (see Figure 4-8 A and C) and co-IP (see Figure 4-8 B and D) experiments. A significant increase of expression of β-actin ($F(4, 52) = 3.921$, $p = 0.017$) for WB experiments (see Figure 4-8 A) was found for the group that was taking drug of abuse at present and moderately compared to the group with none or little consummation of drug abuse. For the co-IP

experiments no significant difference (F(4, 52) = 0.702, p = 0.594) between the severity of substance abuse was found for β-III-tubulin (see Figure 4-8 B). For both β-actin (F(5, 52) = 1.148, p = 0.347) and β-III-tubulin (F(5, 52) = 0.783, p = 0.567) respectively for WB and co-IP experiments, no significant effect of the severity of alcohol abuse was observed (see Figure 4-8 C and D).

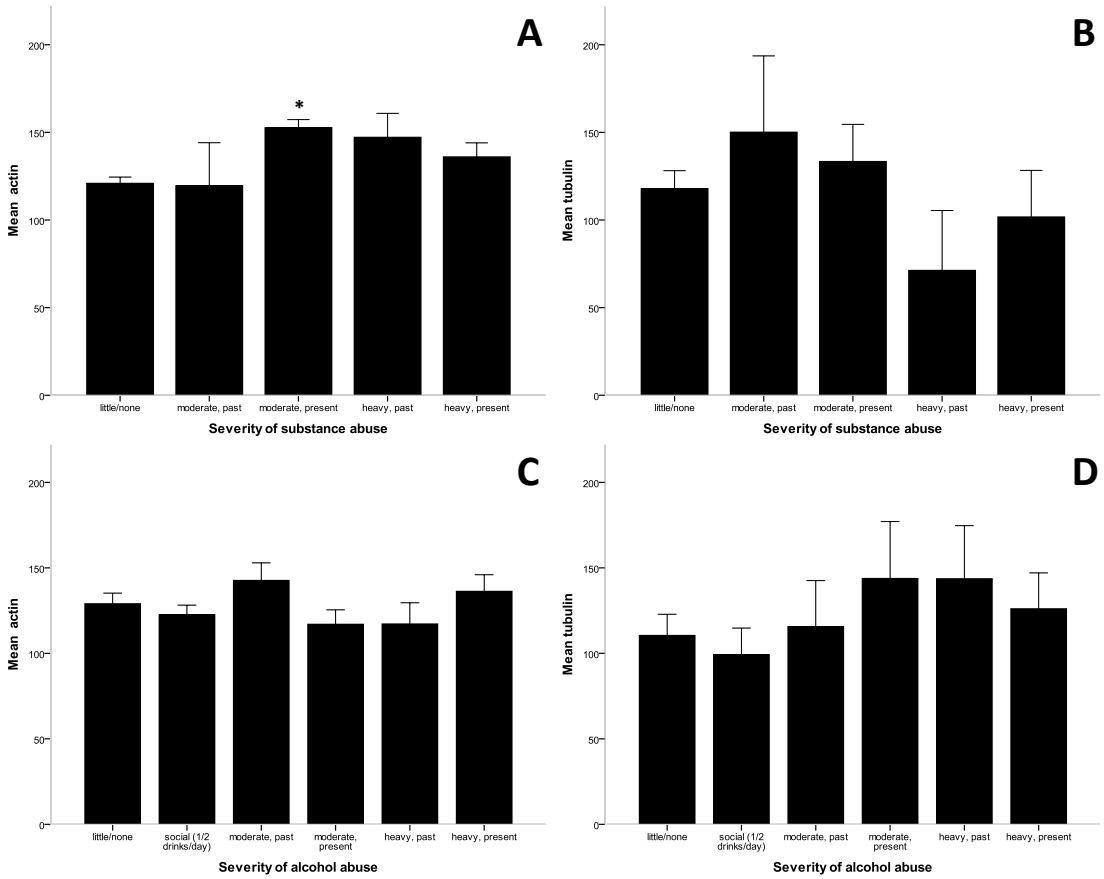

Figure 4-8: Mean (± SEM) fluorescence intensity for β-actin and β-III- in the PSD fraction and co-IP PSD depending on severity of substance and alcohol abuse.

(A) Mean fluorescence intensity for β-actin after WB of the PSD fraction. (B) Mean fluorescence intensity for β-III-tubulin after co-IP of the PSD fraction. (C) Mean fluorescence intensity for β-actin after WB of the PSD fraction. (D) Mean fluorescence intensity for β-III-tubulin after co-IP of the PSD fraction. Statistical test ANOVA with Bonferroni correction. Comparison with little/none (* p<0.05).

In order to identify an eventual correlation between the expression of β-actin and β-III-tubulin with the effect of the severity of substance and alcohol abuse a non-parametric Spearman's correlation analysis was performed. An increase of β-actin was significantly correlated with an increase of the severity of substance ($\rho(57) = 0.385$; $p = 0.002$) whereas no correlation was observed for β-III-tubulin ($\rho(57) = -0.011$; $p = 0.933$). Neither the expression of β-actin ($\rho(58) = -0.012$; $p = 0.927$) or β-III-tubulin ($\rho(58) = 0.168$; $p = 0.208$) were significantly correlated with an increase of the severity of alcohol abuse.

Table 4-1: Correlational effects of demographic and peri-mortem factors on the expression of β-actin and β-III-tubulin.

Spearman's correlation	Age at death	pH	Mass of the brain	PMI	Storage
β-actin (n=58)	**-0.374****	-0.237	0.258	0.131	0.190
β-III-tubulin (n=58)	0.089	-0.173	0.063	0.124	0.087

****p<0.01**

The effects of age at death, pH of the brain, mass of the brain, PMI and duration of storage of the brain for both β-actin and β-III-tubulin were examined with non-parametric Spearman's correlation analysis. A significant negative correlation was found between age at death and expression of β-actin ($\rho(58) = -0.374$; $p = 0.004$) whereas pH of the brain, mass of the brain, PMI and duration of storage of the brain were found to have no effect. Age at death, pH of the brain, mass of the brain, PMI and duration of storage of the brain were found to have no effect on expression of β-III-tubulin (see Table 4-1).

Table 4-2: Correlational effects of demographic and peri-mortem factors on the expression of β-actin and β-III-tubulin (without controls).

Spearman's correlation	Age at death	Age of onset of disease	Duration of disease	Life time quantity of fluphenazine or equivalent
β-actin (n=44)	**-0.389****	-0.131	-0.267	-0.059
β-III-tubulin (n=43)	0.467	0.335	0.443	0.352

****p<0.01**

The effects of age at death, age of onset of disease, duration of diseases and life time quantity of fluphenazine or equivalent for both β-actin and β-III-tubulin were also examined with non-parametric correlation analysis. However in this case the group control was removed. As previously observed a significant negative correlation was found between age at death and expression of β-actin ($\rho(44) = -0.389$; $p = 0.009$). Age of onset of disease, duration of diseases and life time quantity of fluphenazine or equivalent were found to have no effect on the expression of β-actin. Age at death, age of onset of disease, duration of diseases and life time quantity of fluphenazine or equivalent were found to have no effect on the expression of β-III-tubulin (see Table 4-2).

To summarise the expression of β-III-tubulin was not significantly affected by demographic and peri-mortem factors for the co-IP experiments whereas the expression of β-actin was affected by severity of substance abuse and age at death. Consequently an ANCOVA statistical analysis was performed to assess whether any significant difference of the mean of β-actin for each diagnosis group would appear with the effect of severity of substance abuse and the age at death as co-variables. No significant difference between diagnosis was found for β-actin ($F(3, 51) = 0.283$, $p = 0.837$) with the effect of severity of substance abuse and the age at death as co-

variables. Subsequently β-actin was then chosen as denominator to normalise data from WB experiments and β-III-tubulin to normalise data from co-IP experiments.

4.4.2 Expression of NR2A in the PSD fraction and within the PSD

The ratios NR2A/β-actin and NR2A/β-III-tubulin were compared between each diagnostic group for both WB and co-IP experiments using one-way ANOVA. A significant difference in the mean ratios NR2A/β-actin and NR2A/β-III-tubulin between diagnosis was found for both WB and co-IP experiments (see Figure 4-9).

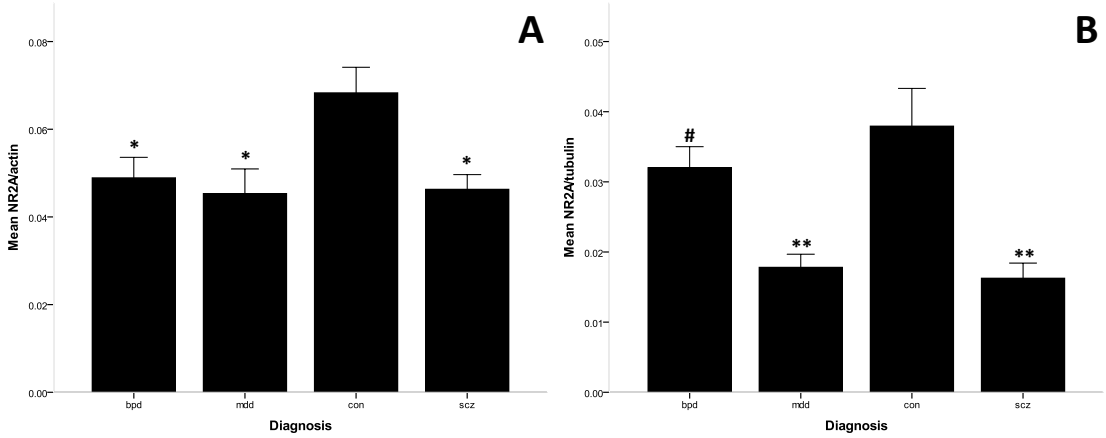

Figure 4-9: Mean (± SEM) ratios NR2A/β-actin and NR2A/β-III-tubulin in the PSD fraction and co-IP PSD depending on diagnosis.

(A) Mean ratio NR2A/β-actin after WB of the PSD fraction. (B) Mean ratio NR2A/β-III-tubulin after co-IP of the PSD fraction. (bpd) bipolar disorder ; (mdd) major depressive disorder ; (con) control ; (scz) schizophrenia. Statistical test ANOVA with Bonferroni correction. Comparison with control (* $p<0.05$; ** $p<0.01$) or schizophrenia ($^{\#}p<0.05$). Statistical ANCOVA was also perfomed with co-variable (see Figure 4-20).

Bonferroni post-hoc analysis of the WB data revealed a significant decrease in the mean ratio NR2A/β-actin in bipolar disorder disorder ($F(3, 53) = 4.817$, $p = 0.047$), major depressive disorder disorder ($F(3, 53) = 4.817$, $p = 0.011$) and schizophrenia ($F(3, 53) = 4.817$, $p = 0.014$) compared to the group control (see Figure 4-9 A).

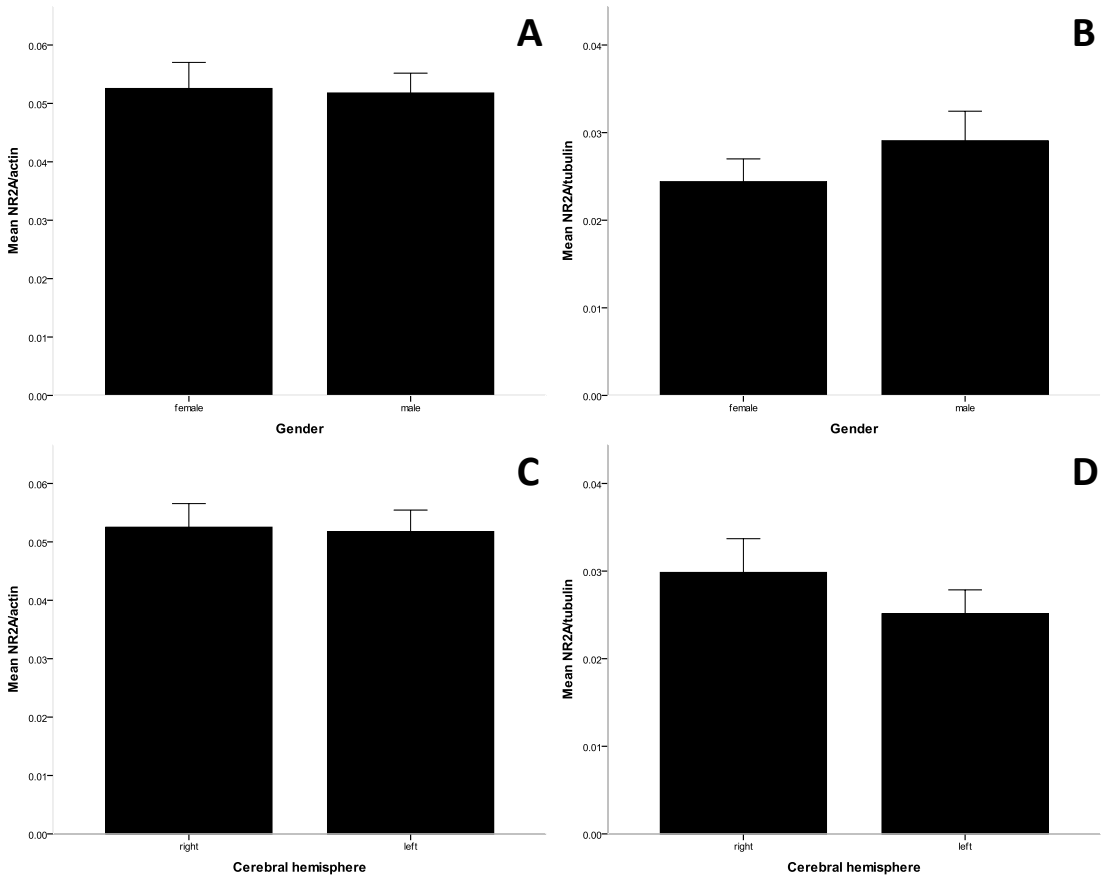

Figure 4-10: Mean (± SEM) ratios NR2A/β-actin and NR2A/β-III-tubulin in the PSD fraction and co-IP PSD depending on gender and side of the cerebral hemisphere.

(A) Mean ratio NR2A/β-actin after WB of the PSD fraction. (B) Mean ratio NR2A/β-III-tubulin after co-IP of the PSD fraction. (C) Mean ratio NR2A/β-actin after WB of the PSD fraction. (D) Mean of the ratio NR2A/β-III-tubulin after co-IP of the PSD fraction.

In addition, a significant decrease in the mean ratio NR2A/β-III-tubulin in major depressive disorder ($F(3, 46) = 7.927$, $p = 0.003$) and schizophrenia ($F(3, 46) = 7.927$, $p = 0.001$) but not in bipolar disorder ($F(3, 46) = 7.927$, $p = 1.000$) compared to controls was found in the co-IP experiment (see Figure 4-9 B). Also the mean ratio NR2A/β-III-tubulin was lower in schizophrenia ($F(3, 46) = 7.927$, $p = 0.039$) and major depressive disorder (trend: $F(3, 46) = 7.927$, $p = 0.080$) relative to bipolar disorder in the co-IP experiment.

The effects of gender (see Figure 4-10 A and B) and cerebral hemisphere (see Figure 4-10 C and D) on dependent variables NR2A/β-actin and NR2A/β-III-tubulin for WB and co-IP experiments respectively were examined using Student's T-test analysis. No significant effects of gender were found for NR2A/β-actin ($t(55) = 0.140$, $p = 0.889$) and NR2A/β-III-tubulin ($t(48) = 1.007$, $p = 0.319$) or cerebral lateralisation for WB (NR2A/β-actin; $t(55) = 0.136$, $p = 0.892$) and co-IP (NR2A/β-III-tubulin; $t(48) = 1.029$, $p = 0.308$) experiments.

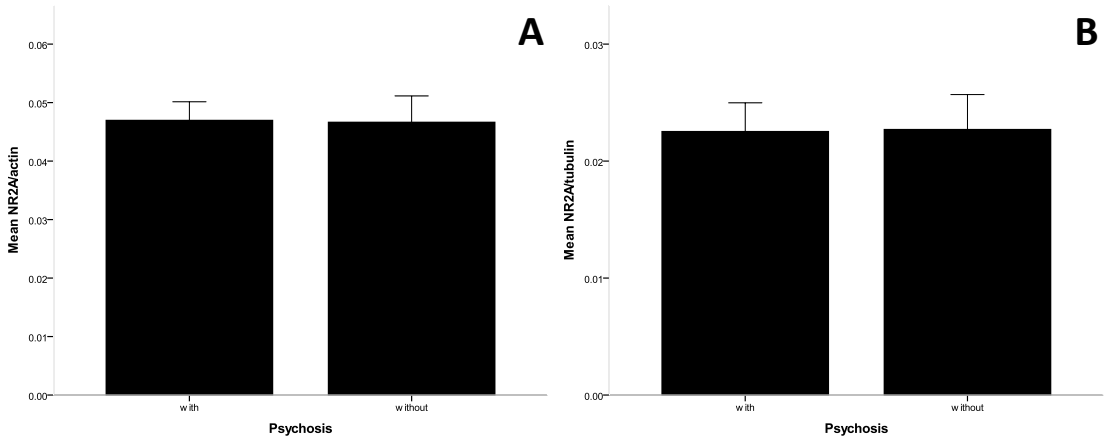

Figure 4-11: Mean (± SEM) ratios NR2A/β-actin and NR2A/β-III- in the PSD fraction and co-IP PSD depending on psychotic symptoms.

(A) Mean ratio NR2A/β-actin after WB of the PSD fraction. (B) Mean NR2A/β-III-tubulin after co-IP of the PSD fraction.

The effect of psychotic symptoms on NR2A/β-actin and NR2A/β-III-tubulin for WB (see Figure 4-11 A) and co-IP experiments respectively (see Figure 4-11 B) were also examined using Student's T-test analysis and omission of the control group from the analysis. No significant effect of psychosis was found for both NR2A/β-actin (t(41) = 0.061, p = 0.952) or NR2A/β-III-tubulin (t(33) = 0.045, p = 0.964).

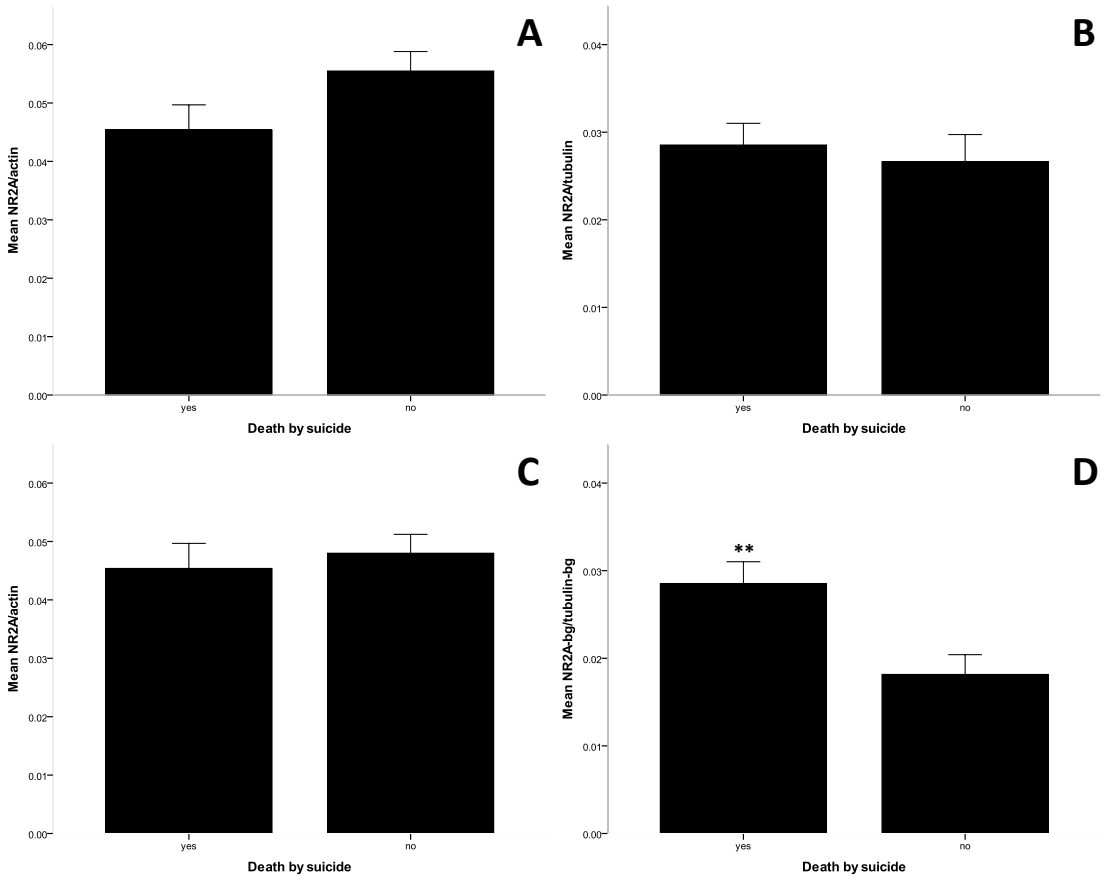

Figure 4-12: Mean (± SEM) ratios NR2A/β-actin and NR2A/β-III-tubulin in the PSD fraction and co-IP PSD depending on death by suicide.

(A) Mean ratio NR2A/β-actin after WB of the PSD fraction. (B) Mean ratio NR2A/β-III-tubulin after co-IP of the PSD fraction. (C) Mean ratio NR2A/β-actin after WB of the PSD fraction (without controls). (D) Mean ratio NR2A/β-III-tubulin after co-IP of the PSD fraction (without controls). Statistical Student's t test (p<0.01).**

For the effect of death by suicide on NR2A/β-actin and NR2A/β-III-tubulin rfor WB (see Figure 4-12 A and C) and co-IP experiments respectively (see Figure 4-12 B and D), a Student's t-test analysis was carried out with and without the control group. A trend towards a significant decrease in the suicide group for NR2A/β-actin (t(55) = 1.800, p = 0.077) was found when controls were included, however this was no longer significant when the controls were excluded (t(41) = 0.495, p = 0.624).

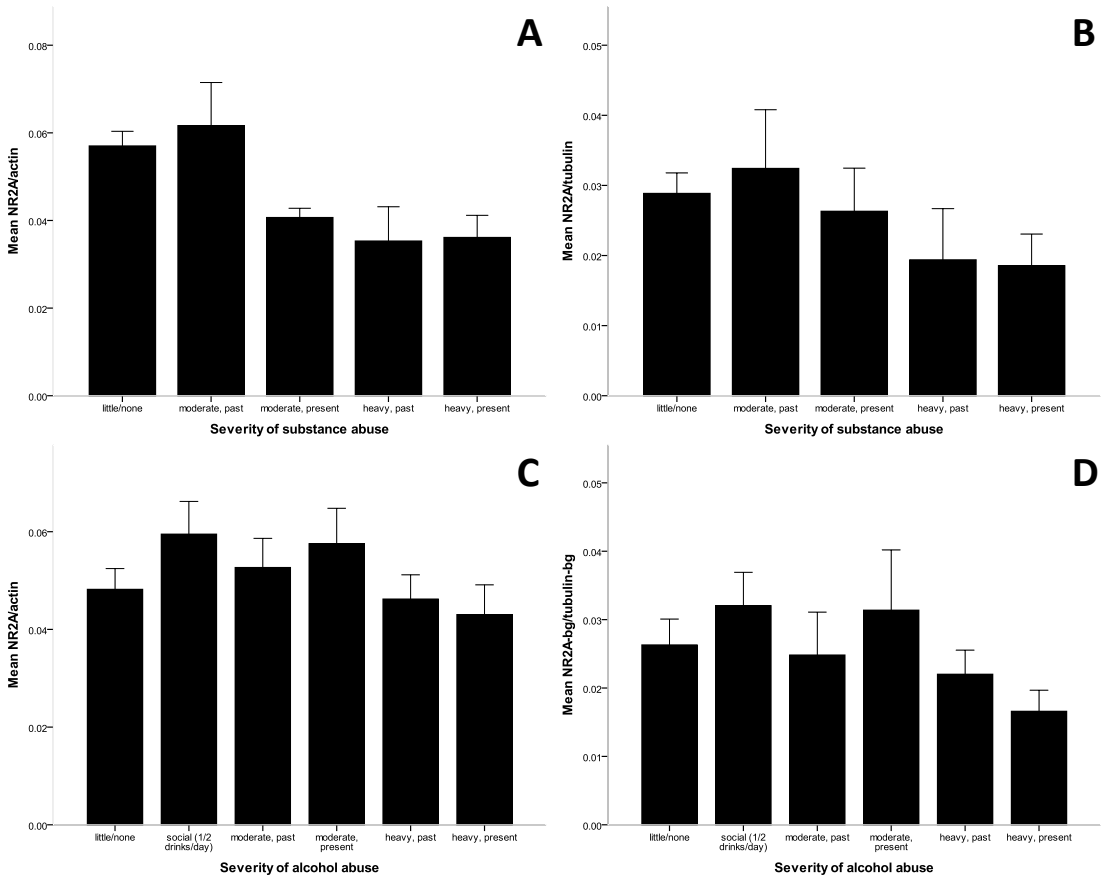

Figure 4-13: Mean (± SEM) ratios NR2A/β-actin and NR2A/β-III-tubulin in the PSD fraction and co-IP PSD depending on severity of substance and alcohol abuse.

(A) Mean ratio NR2A/β-actin after WB of the PSD fraction. (B) Mean ratio NR2A/β-III-tubulin after co-IP of the PSD fraction. (C) Mean ratio NR2A/β-actin after WB of the PSD fraction. (D) Mean ratio NR2A/β-III-tubulin after co-IP of the PSD fraction.

A significant increase in NR2A/β-III-tubulin ($t(33) = 3.082$, $p = 0.004$) was found in the suicide group when controls were excluded, but not when they were included ($t(45.78) = 0.480$, $p = 0.634$). One-way ANOVA was used to assess the effects of severity of substance and alcohol abuse on NR2A/β-actin and NR2A/β-III-tubulin respectively for WB (see Figure 4-13 A and C) and co-IP (see Figure 4-13 B and D) experiments.

A significant difference of the mean of NR2A/β-actin ($F(4, 52) = 2.992$, $p = 0.027$) was found using ANOVA on the effect of substance abuse, however there was no significant change after Bonferroni correction (see Figure 4-13 A). For the co-IP experiments no significant difference ($F(4, 45) = 0.672$, $p = 0.615$) between the severity of substance abuse was found for NR2A/β-III-tubulin (see Figure 4-13 B). For both ratios NR2A/β-actin ($F(5, 51) = 1.037$, $p = 0.406$) and NR2A/β-III-tubulin ($F(5, 44) = 0.933$, $p = 0.469$) respectively for WB and co-IP experiments, no significant effect of the severity of alcohol abuse was observed (see Figure 4-13 C and D).

Table 4-3: Correlational effects of demographic and peri-mortem factors on the ratios NR2A/β-actin and NR2A/β-III-tubulin.

Spearman's correlation	Age at death	pH	Mass of the brain	PMI	Storage
NR2A/β-actin (n=57)	**0.307***	-0.028	-0.191	-0.122	-0.189
NR2A/β-III-tubulin (n=50)	-0.083	-0.082	-0.106	-0.051	-0.062

***p<0.05**

The correlation of both ratios NR2A/β-actin and NR2A/β-III-tubulin with the effect of the severity of substance and alcohol abuse was assessed with a non-parametric correlation analysis of Spearman. A negative correlation of the ratio NR2A/β-actin was found significant with the severity of substance ($\rho(57) = -0.425$; $p = 0.001$) whereas no correlation was observed for NR2A/β-III-tubulin ($\rho(50) = -0.144$; $p = 0.320$). Neither the

ratio NR2A/β-actin (ρ(57) = -0.057; p = 0.676) or the ratio NR2A/β-III-tubulin (ρ(50) = -0.142; p = 0.326) were significantly correlated with an increase of the severity of alcohol abuse.

The effects of age at death, pH of the brain, mass of the brain, PMI and duration of storage of the brain for both ratios NR2A/β-actin and NR2A/β-III-tubulin were examined with non-parametric correlation analysis. A significant positive correlation was found between age at death and the ratio NR2A/β-actin (ρ(57) = 0.307; p = 0.020) whereas pH of the brain, mass of the brain, PMI and duration of storage of the brain were found to have no effect. Age at death, pH of the brain, mass of the brain, PMI and duration of storage of the brain were not found to have any effect on the ratio NR2A/β-III-tubulin (see Table 4-3).

Table 4-4: Correlational effects of demographic and peri-mortem factors on the ratios NR2A/β-actin and NR2A/β-III-tubulin (without controls).

Spearman's correlation	Age at death	Age of onset of disease	Duration of disease	Life time quantity of fluphenazine or equivalent
NR2A/β-actin (n=43)	0.232	0.015	0.300	0.287
NR2A/β-III-tubulin (n=35)	-0.244	**-0.375***	0.153	0.024

***p<0.05**

The effects of age at death, age of onset of disease, duration of diseases and life time quantity of fluphenazine or equivalent for both ratios NR2A/β-actin and NR2A/β-III-tubulin were also examined with non-parametric correlation analysis. In this study the group control was removed. Age at death, age of onset of disease, duration of diseases

and life time quantity of fluphenazine or equivalent were found to have no effect on the expression of NR2A/β-actin. A significant negative correlation was observed between age of onset of the disease and the mean of the ratio NR2A/β-III-tubulin ($\rho(35) = -0.375$; $p = 0.026$). Age at death, duration of the disease and life time quantity of fluphenazine or equivalent were not found to have any effect on the mean of the ratio NR2A/β-III-tubulin (see Table 4-4).

The mean of the ratio NR2A/β-III-tubulin was found to not be significantly affected by any of the demographic and peri-mortem factors for the co-IP experiments whereas the ratio NR2A/β-actin was affected by the age at death. Subsequently an ANCOVA was performed to assess whether the ratio NR2A/β-actin was affected for each diagnosis group with the effect of the age at death as co-variable.

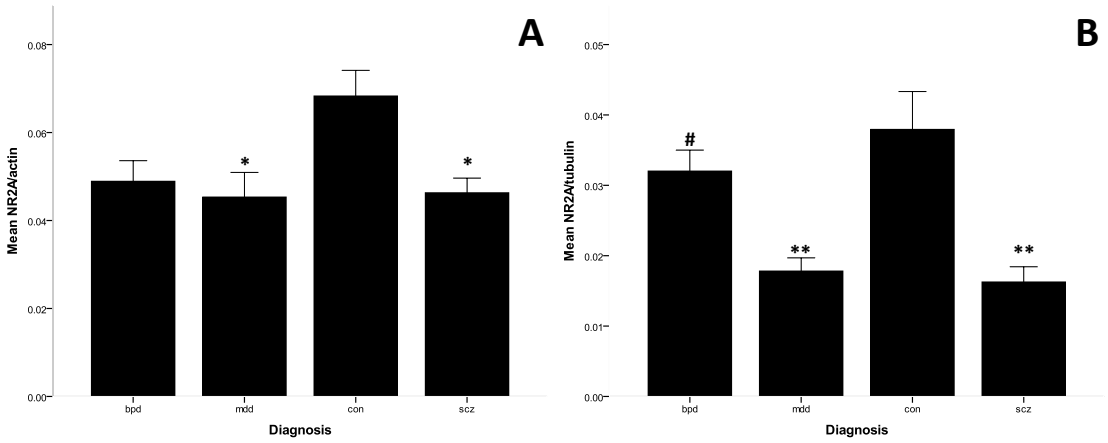

Figure 4-14: Mean (± SEM) ratios NR2A/β-actin (ANCOVA) and NR2A/β-III-tubulin (ANOVA) in the PSD fraction and co-IP PSD depending on diagnosis.

(A) Mean ratio NR2A/β-actin after WB of the PSD fraction. (B) Mean ratio NR2A/β-III-tubulin after co-IP of the PSD fraction. (bpd) bipolar disorder ; (mdd) major depressive disorder ; (con) control ; (scz) schizophrenia. Statistical test ANCOVA with age at death as co-variable for NR2A/β-actin was performed with Bonferroni correction. Comparison with control (*p<0.05; **p<0.01) or schizophrenia ($^{\#}$p<0.05).

A significant difference between the different diagnosis group was found for NR2A/β-actin ($F(3, 52) = 4.597$, $p = 0.006$) with the effect of the age at death as co-variables. In order to determine which diagnosis groups were different from the others a Bonferroni correction was carried out. A significant decrease of the mean of the ratio NR2A/β-actin ($F(3, 52) = 4.597$, $p = 0.010$) for the diagnosis group with major depressive disorder compared to the group control. A significant decrease in the group with schizophrenia (NR2A/β-actin: $F(3, 52) = 4.597$, $p = 0.021$) was found with the group control but not for the diagnosis group with bipolar disorder (NR2A/β-actin: $F(3, 52) = 4.597$, $p = 0.088$) (see Figure 4-14 A).

4.4.3 Expression of PSD-95 in the PSD fraction and within the PSD

The mean of the ratios of PSD-95/β-actin and PSD-95/β-III-tubulin was compared between each diagnosis groups for both WB and co-IP (see Figure 4-15). For both PSD-95/β-actin ($F(3, 51) = 0.704$, $p = 0.554$) and PSD-95/β-III-tubulin ($F(3, 51) = 2.358$, $p = 0.080$) no significant difference between diagnosis was found for both respectively WB and co-IP experiments using ANOVA (see Figure 4-15 A and B). However the chart representing the difference of the means of the ratio PSD-95/ β-III-tubulin for each group of diagnosis showed a decrease of the ratio PSD-95/β-III-tubulin between the group of diagnosis with schizophrenia and the group (see Figure 4-15 B).

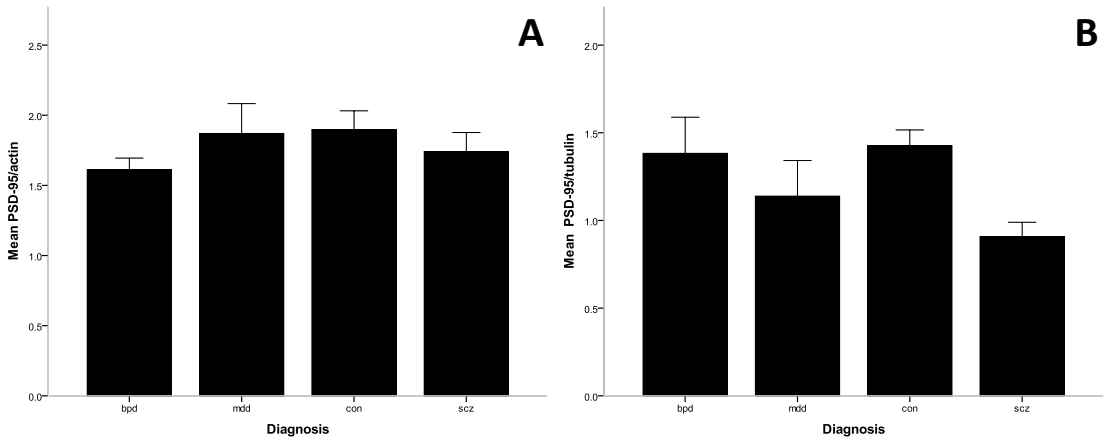

Figure 4-15: Mean (± SEM) ratios PSD-95/β-actin and PSD-95/β-III-tubulin in the PSD fraction and co-IP PSD depending on diagnosis.

(A) Mean ratio PSD-95/β-actin after WB of the PSD fraction. (B) Mean ratio PSD-95/β-III-tubulin after co-IP of the PSD fraction. (bpd) bipolar disorder ; (mdd) major depressive disorder ; (con) control ; (scz) schizophrenia. Statistical test ANOVA with Bonferroni correction. Statistical test ANCOVA was also perfomed with co-variables (see Figure 4-20).

This difference of the mean of the ratio PSD-95/β-III-tubulin between these two groups was also assessed with Student's t-test and revealed a significant decrease of the ratio PSD-95/β-III-tubulin ($t(26) = 4.214$, $p = 0.0003$) for the group of diagnosis with schizophrenia compared to the group control.

The difference of the mean of the two dependent variables PSD-95/β-actin and PSD-95/β-III-tubulin respectively for WB experiments and co-IP experiments depending on gender (see Figure 4-16 A and B) and the side of the cerebral hemisphere (see Figure 4-16 C and D) was assessed with Student's T-test analysis. Neither significant difference of the mean of the ratio PSD-95/β-actin was revealed for gender ($t(53) = 0.404$, $p = 0.688$) or the side of the cerebral hemisphere ($t(53) = 0.018$, $p = 0.985$). A significant decrease of the mean of the ratio PSD-95/β-III-tubulin was found in female ($t(53) = 2.077$, $p = 0.043$) and a trend towards a significant decrease in the left hemisphere of the cerebrum ($t(53) = 1.828$, $p = 0.073$).

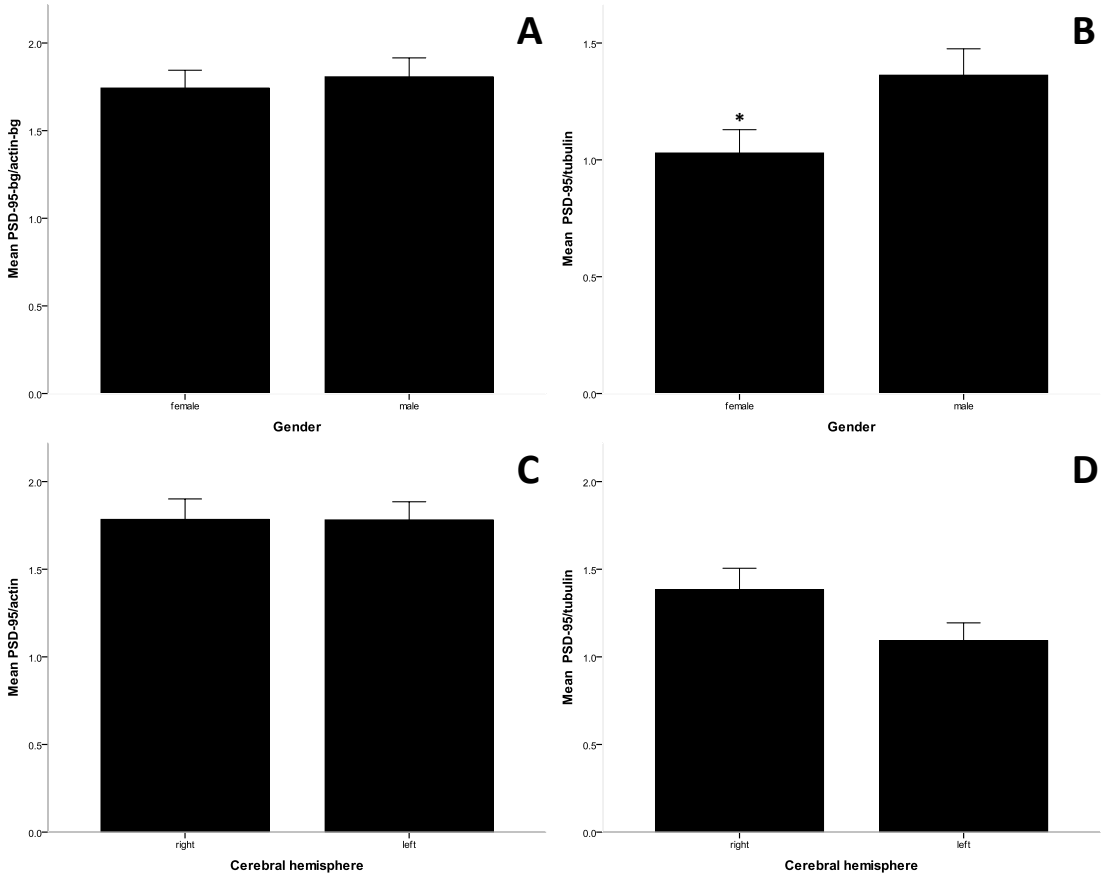

Figure 4-16: Mean (± SEM) ratios PSD-95/β-actin and PSD-95/β-III-tubulin in the PSD fraction and co-IP PSD depending on gender and side of the cerebral hemisphere.

(A) Mean ratio PSD-95/β-actin after WB of the PSD fraction. (B) Mean ratio PSD-95/β-III-tubulin after co-IP of the PSD fraction. (C) Mean ratio PSD-95/β-actin after WB of the PSD fraction. (D) Mean ratio PSD-95/β-III-tubulin after co-IP of the PSD fraction.

The effect of psychotic symptoms on the dependent variables PSD-95/β-actin and PSD-95/β-III-tubulin respectively for WB experiments (see Figure 4-17 A) and co-IP experiments (see Figure 4-17 B) were also examined with Student's T-test analysis. The group control was removed from the analysis and no significant difference was found for both ratios PSD-95/β-actin ($t(24.63) = 0.328$, $p = 0.745$) and PSD-95/β-III-tubulin ($t(38) = 0.234$, $p = 0.816$).

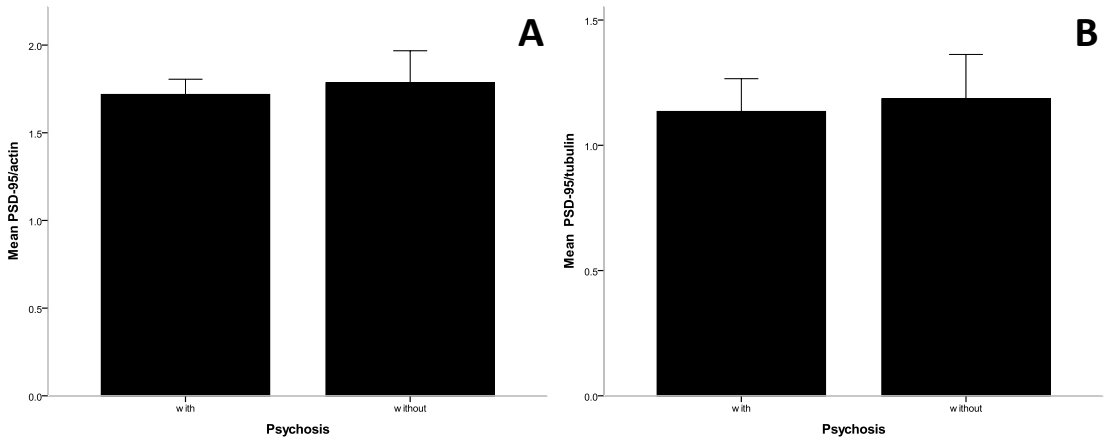

Figure 4-17: Mean (± SEM) ratios PSD-95/β-actin and PSD-95/β-III-tubulin in the PSD fraction and co-IP PSD depending on psychotic symptoms.

(A) Mean ratio PSD-95/β-actin after WB of the PSD fraction. (B) Mean ratio PSD-95/β-III-tubulin after co-IP of the PSD fraction.

Study of the incidence of death by suicide on the dependent variables PSD-95/β-actin and PSD-95/β-III-tubulin respectively for WB experiments (see Figure 4-18 A and C) and co-IP experiments (see Figure 4-18 B and D) was also assessed using Student's t-test analysis for both with and without the group control. No significant difference was found for both the ratio PSD-95/β-actin with ($t(53) = 0.122$, $p = 0.903$) or without ($t(40) = 0.479$, $p = 0.635$) the control group. Student's t-test for both with ($t(53) = 2.696$, $p = 0.009$) or without ($t(38) = 3.530$, $p = 0.001$) the control group revealed a significant increase in the group with death by suicide for PSD-95/β-III-tubulin. The means of the ratios PSD-95/β-actin and PSD-95/β-III-tubulin obtained for each degree of severity of substance and alcohol abuse for both WB (see Figure 4-19 A and C) and co-IP (see Figure 4-19 B and D) experiments were compared with one-way ANOVA. No significant difference of the mean of the ratios PSD-95/β-actin and PSD-95/β-III-tubulin for both WB and co-IP experiments, neither for the degree of severity of drug abuse (PSD-95/β-actin: $F(4, 49) = 1.489$, $p = 0.220$; PSD-95/β-III-tubulin: $F(4, 50) = 1.078$, $p = 0.377$) nor

alcohol abuse (PSD-95/β-actin: F(5, 49) = 0.641, p = 0.670; PSD-95/β-III-tubulin: F(5, 49) = 0.737, p = 0.599), was observed.

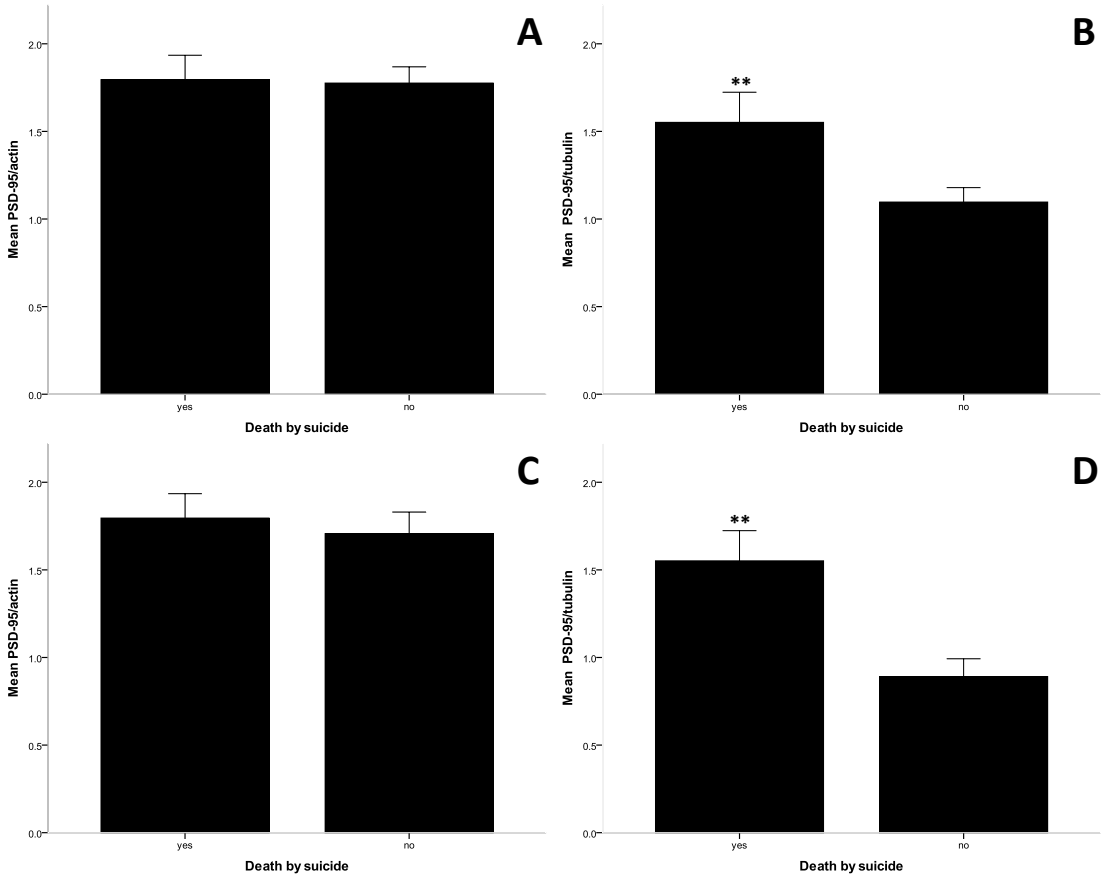

Figure 4-18: Mean (± SEM) ratios PSD-95/β-actin and PSD-95/β-III-tubulin in the PSD fraction and co-IP PSD depending on death by suicide.

(A) Mean ratio PSD-95/β-actin after WB of the PSD fraction. (B) Mean ratio PSD-95/β-III-tubulin after co-IP of the PSD fraction. (C) Mean ratio PSD-95/β-actin after WB of the PSD fraction (without controls). (D) Mean ratio PSD-95/β-III-tubulin after co-IP of the PSD fraction (without controls). Statistical Student's t-test (p<0.01).**

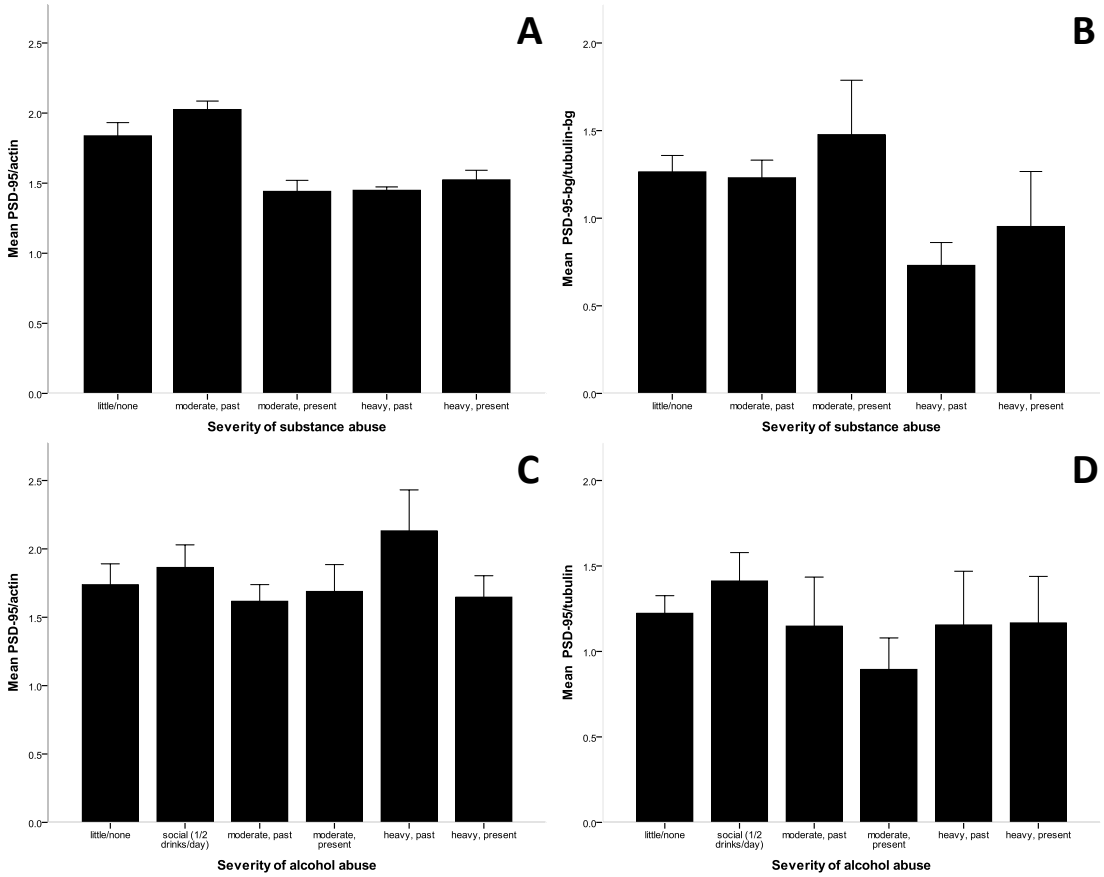

Figure 4-19: Mean (± SEM) ratios PSD-95/β-actin and PSD-95/β-III-tubulin in the PSD fraction and co-IP PSD depending on severity of substance and alcohol abuse.

(A) Mean ratio PSD-95/β-actin after WB of the PSD fraction. (B) Mean ratio PSD-95/β-III-tubulin after co-IP of the PSD fraction. (C) Mean ratio PSD-95/β-actin after WB of the PSD fraction. (D) Mean ratio PSD-95/β-III-tubulin after co-IP of the PSD fraction.

Correlation between the mean of the ratios PSD-95/β-actin and PSD-95/β-III-tubulin and the level of the severity of substance and alcohol abuse were assessed with a non-parametric correlation analysis of Spearman. A trend towards a decrease of the ratio PSD-95/β-actin was correlated with an increase of the severity of substance abuse ($\rho(54) = -0.239$; $p = 0.082$) whereas no correlation was found for the ratio PSD-95/β-III-tubulin ($\rho(55) = -0.137$; $p = 0.319$). Neither the mean of the ratio of PSD-95/β-actin ($\rho(55) = 0.026$; $p = 0.851$) nor the mean of the ratio PSD-95/β-III-tubulin ($\rho(55) = -$

0.132; p = 0.336) were significantly correlated with an increase of the severity of alcohol abuse.

The effects of age at death, pH of the brain, mass of the brain, PMI and duration of storage of the brain for both ratios PSD-95/β-actin and PSD-95/β-III-tubulin were examined with non-parametric correlation analysis of Spearman. Age at death, pH of the brain, mass of the brain, PMI and duration of storage of the brain were found to have no effect on the ratio PSD-95/β-actin. A significant decrease of the mean of the ratio PSD-95/β-III-tubulin (ρ(55) = -0.343; p = 0.010) was correlated with an increase of the post-mortem interval. Age at death, pH of the brain, mass of the brain and duration of storage of the brain were found to have no effect the ratio PSD-95/β-III-tubulin (see Table 4-5).

Table 4-5: Correlational effects of demographic and peri-mortem factors on the ratios PSD-95/β-actin and PSD-95/β-III-tubulin.

Spearman's correlation	Age at death	pH	Mass of the brain	PMI	Storage
PSD-95/β-actin (n=55)	0.206	0.075	-0.138	-0.112	-0.045
PSD-95/β-III-tubulin (n=55)	-0.125	0.189	0.209	**-0.343***	-0.168

***p<0.05**

The group control was removed to study the effect of age at death, age of onset of disease, duration of diseases and life time quantity of fluphenazine or equivalent on both ratios PSD-95/β-actin and PSD-95/β-III-tubulin using non-parametric correlation analysis. No effect of the age at death, the age of onset of the disease, the duration of

the disease and the life time quantity of fluphenazine or equivalent were revealed neither for the ratio PSD-95/β-actin nor the ratio PSD-95/β-III-tubulin (see Table 4-6).

Table 4-6: Correlational effects of demographic and peri-mortem factors on the ratios PSD-95/β-actin and PSD-95/β-III-tubulin (without controls).

Spearman's correlation	Age at death	Age of onset of disease	Duration of disease	Life time quantity of fluphenazine or equivalent
PSD-95/β-actin (n=42)	0.186	0.279	-0.052	-0.045
PSD-95/β-III-tubulin (n=40)	-0.159	-0.231	0.006	-0.154

To summarise there was no effect of the demographic and peri-mortem factors on the ratio PSD-95/β-actin whereas gender, death by suicide and post-mortem interval were found to have an effect on the mean of the ratio PSD-95/β-III-tubulin for the co-IP experiments. ANCOVA statistical analysis showed a significant difference of the mean of the ratio PSD-95/β-III-tubulin between diagnosis groups ($F(3, 48) = 2.995$, $p = 0.040$). The post-hoc test with Bonferroni's correction revealed that the mean of the ratio PSD-95/β-III-tubulin was significantly reduced in schizophrenia compared to control ($F(3, 48) = 2.995$, $p = 0.049$) (see Figure 4-20 B).

In contrast no significant difference was found either for the group with bipolar disorder ($F(3, 48) = 2.995$, $p = 0.824$) or the group with major depressive disorder ($F(3, 48) = 2.995$, $p = 0.155$) for the mean of the ratio PSD-95/β-III-tubulin compared to the group control (Figure 4-20 A).

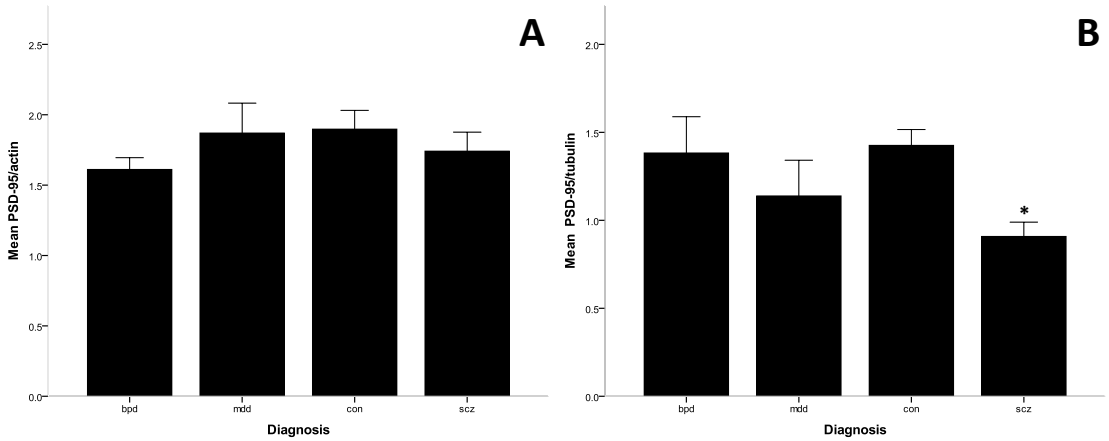

Figure 4-20: Mean (± SEM) ratios PSD-95/β-actin and PSD-95/β-III-tubulin in the PSD fraction and co-IP PSD depending on diagnosis (ANCOVA).

(**A) Mean ratio PSD-95/β-actin after WB of the PSD fraction. (B) Mean ratio PSD-95/β-III-tubulin after co-IP of the PSD fraction. (bpd) bipolar disorder ; (mdd) major depressive disorder ; (con) control ; (scz) schizophrenia. Statistical test ANCOVA with gender, death by suicide and post-mortem interval as co-variables for PSD-95/β-III-tubulin was performed with Bonferroni correction. Comparison with control (* p<0.05).**

4.4.4 Expression of CaMKIIα in the PSD fraction

The signal for the detection of CaMKIIα was undistinguishable from the signal emitted from the detection of the heavy chain of the primary antibody used to carry out the co-IP experiments.

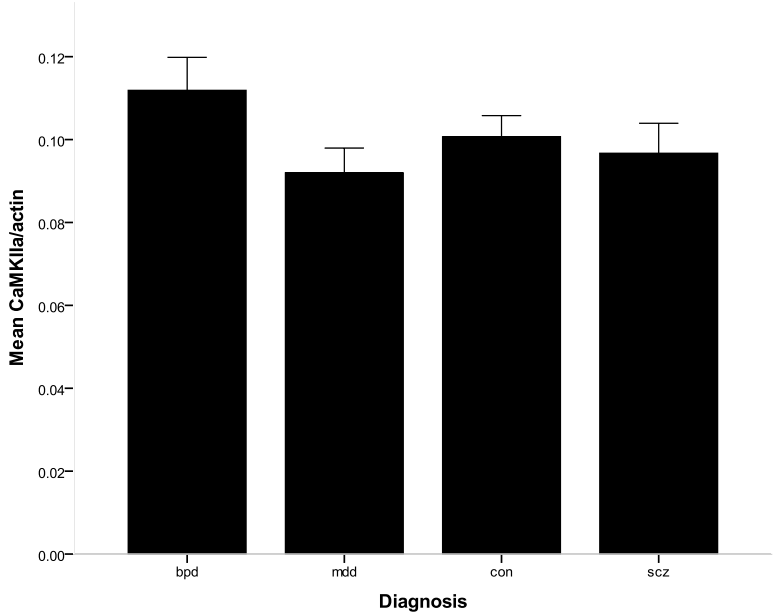

Figure 4-21: Mean (± SEM) ratio CaMKIIα/β-actin in the PSD fraction (WB) depending on diagnosis.

(bpd) bipolar disorder ; (mdd) major depressive disorder ; (con) control ; (scz) schizophrenia.

Consequently in this study the expression of CaMKIIα was only assessed in the PSD fraction by WB. The mean of the ratio CaMKIIα/β-actin was compared for each diagnosis groups with one-way ANOVA statistical test (see Figure 4-21). No significant difference between diagnosis was found for the ratio CaMKIIα/β-actin ($F(3, 50) = 1.557$, $p = 0.211$) by WB experiments in the PSD fraction. However the chart representing the difference of the means of the ratio CaMKIIα/β-actin for each group of diagnosis showed a decrease of the ratio CaMKIIα/β-actin between the group of diagnosis with major depressive disorder and the group with bipolar disorder. This difference of the mean of the ratio CaMKIIα/β-actin between these two groups was assessed with Student's t-test and revealed a trend towards a decrease of the ratio CaMKIIα/β-actin ($t(25) = 1.914$, $p = 0.067$) for the group with major depressive disorder and the group with bipolar disorder.

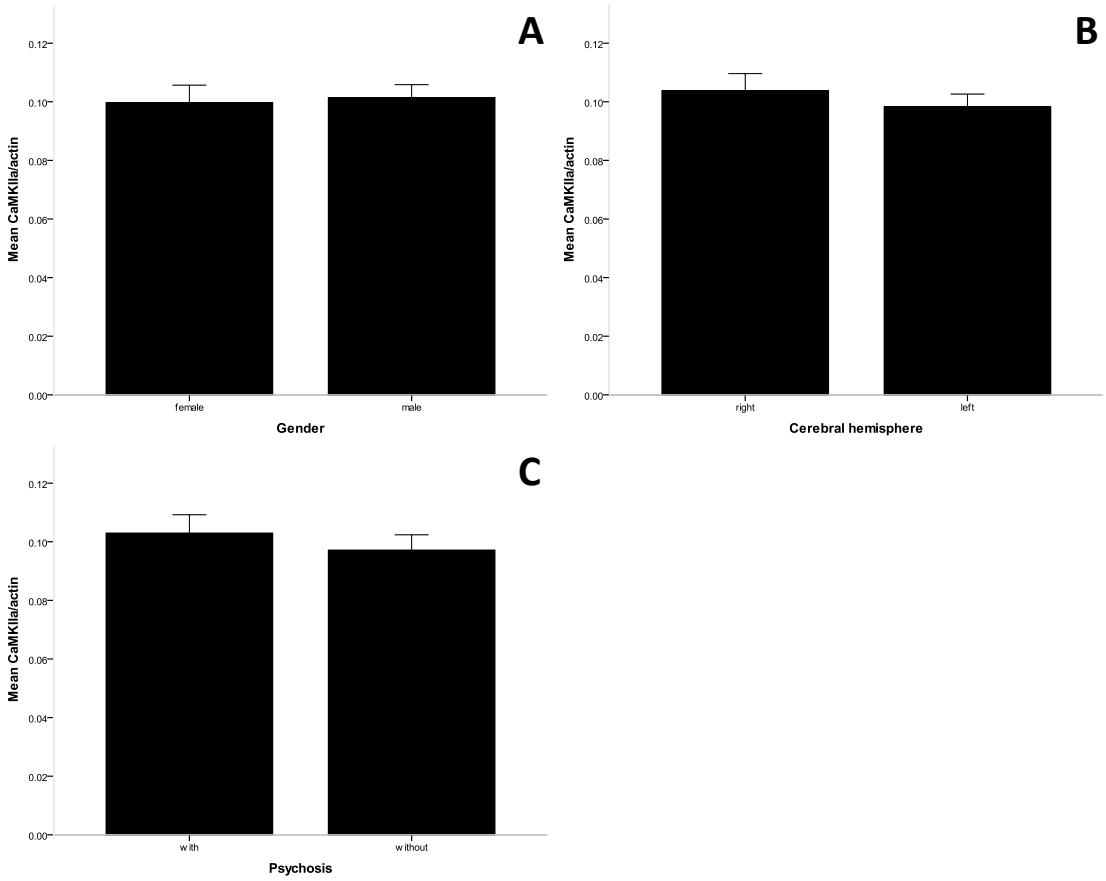

Figure 4-22: Mean (± SEM) ratio CaMKIIα/β-actin in the PSD fraction depending on gender, side of the cerebral hemisphere and psychotic symptoms.

(A) Mean ratio CaMKIIα/β-actin after WB of the PSD fraction (gender). (B) Mean ratio CaMKIIα/β-actin after WB of the PSD fraction (cerebral hemisphere) (C) Mean ratio CaMKIIα/β-actin after WB of the PSD fraction (psychosis).

Student's T-test analysis was performed to assess the level of expression of CaMKIIα depending on gender (see Figure 4-22 A) and the side of the cerebral hemisphere (see Figure 4-22 B). No significant effect of gender was found for the ratio CaMKIIα/β-actin ($t(52) = 0.241$, $p = 0.811$) or cerebral lateralisation by WB ($t(523) = 0.773$, $p = 0.443$) experiments. The group control was removed from the analysis and the effect of psychotic symptoms on the dependent variable CaMKIIα/β-actin was also examined

with Student's t-test analysis (see Figure 4-22 C). No significant effect of psychosis was found for the ratio CaMKIIα/β-actin (t(40) = 0.648, p = 0.520).

For the effect of death by suicide on the dependent variable CaMKIIα/β-actin for WB experiments (see Figure 4-23 A and C) a Student's t-test analysis was carried out with and without the group control. No significant effect of death by suicide was found for the mean of the ratio CaMKIIα/β-actin with (t(52) = 1.112, p = 0.271) or without (t(40) = 0.648, p = 0.520) the control group.

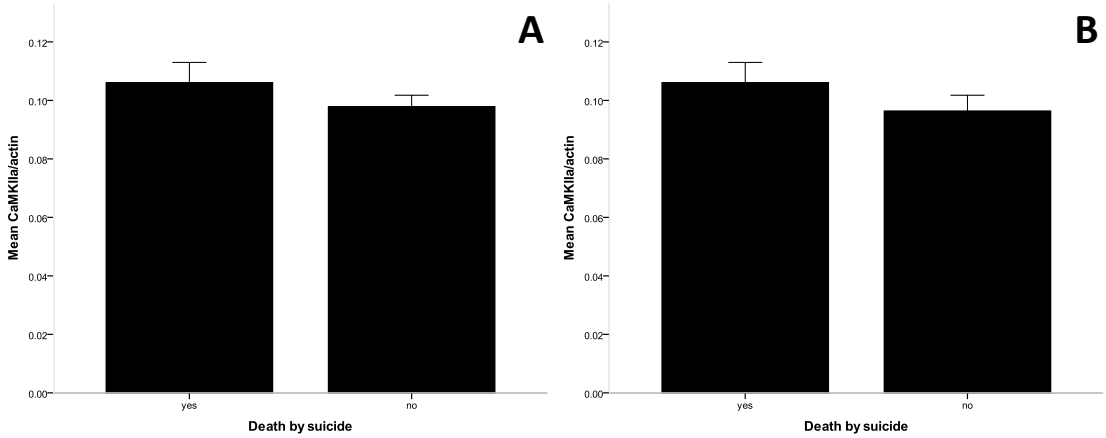

Figure 4-23: Mean (± SEM) ratio CaMKIIα/β-actin in the PSD fraction depending on death by suicide (WB).

(A) Mean ratio CaMKIIα/β-actin after WB of the PSD fraction. (B) Mean ratio CaMKIIα/β-actin after WB of the PSD fraction (without controls).

The effects of the severity of substance and alcohol abuse on the mean of the ratio CaMKIIα/β-actin were tested using one-way ANOVA statistical test (see Figure 4-24 A and B). No significant difference of the mean of the ratio CaMKIIα/β-actin was found either for the effect of the severity of substance abuse (F(4, 48) = 2.552, p = 0.051) or alcohol abuse (F(5, 48) = 0.456, p = 0.807). Because of the trend observed for the effect of the severity of substance abuse on the mean of the ratio CaMKIIα/β-actin a

post-hoc with Bonferroni's correction was performed. A trend towards a decrease of CaMKIIα/β-actin (F(4, 48) = 2.552, p = 0.078) between moderate present and heavy present consummation of drug abuse (see Figure 4-24 A).

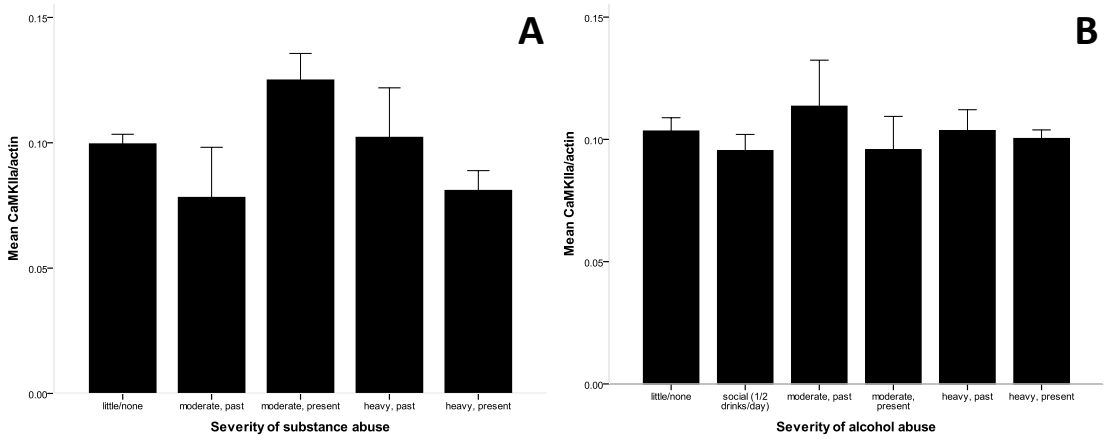

Figure 4-24: Mean (± SEM) ratio CaMKIIα/β-actin in the PSD fraction depending on severity of substance and alcohol abuse.

(A) Mean ratio CaMKIIα/β-actin after WB of the PSD fraction (substance abuse). (B) Mean ratio CaMKIIα/β-actin after WB of the PSD fraction (alcohol abuse).

Non-parametric correlation analysis of Spearman was carried out to identify an eventual correlation between the difference of the mean of the ratio CaMKIIα/β-actin and the severity of substance and alcohol abuse. No correlation was observed for the ratio CaMKIIα/β-actin either for the severity of substance abuse (ρ(53) = -0.015; p = 0.917) or the severity of alcohol abuse (ρ(54) = -0.045; p = 0.745).

Table 4-7: Correlational effects of demographic and peri-mortem factors on the ratio CaMKIIα/β-actin.

Spearman's correlation	Age at death	pH	Mass of the brain	PMI	Storage
CaMKIIα/β-actin (n=54)	-0.172	-0.008	-0.057	0.215	0.107

Table 4-8: Correlational effects of demographic and peri-mortem factors on the ratio CaMKIIα/β-actin (without controls).

Spearman's correlation	Age at death	Age of onset of disease	Duration of disease	Life time quantity of fluphenazine or equivalent
CaMKIIα/β-actin (n=42)	-0.184	-0.105	-0.073	0.106

The effects of age at death, pH of the brain, mass of the brain, PMI and duration of storage of the brain for CaMKIIα/β-actin were examined with non-parametric correlation analysis (see Table 4-7). The effects of age at death, age of onset of disease, duration of diseases and life time quantity of fluphenazine or equivalent for CaMKIIα/β-actin were also examined with non-parametric correlation analysis with the group control removed (see Table 4-8). None of these demographic and peri-mortem factors had any correlation with the expression of CaMKIIα by WB.

To summarise the expression of CaMKIIα was not significantly affected by any of the demographic and peri-mortem factors and subsequently no ANCOVA statistical analysis was performed.

4.4.5 Expression of CaMKIIβ in the PSD fraction and within the PSD

The expression of CaMKIIβ in each diagnosis groups was compared by measuring the difference of the mean of the ratios CaMKIIβ/β-actin and CaMKIIβ/β-III-tubulin respectively for both WB and co-IP experiments using one-way ANOVA statistical test (see Figure 4-25). The ratio CaMKIIβ/β-actin ($F(3, 50) = 2.025$, $p = 0.122$) was found to have no significant difference between diagnosis with WB experiments (see Figure 4-25 A).

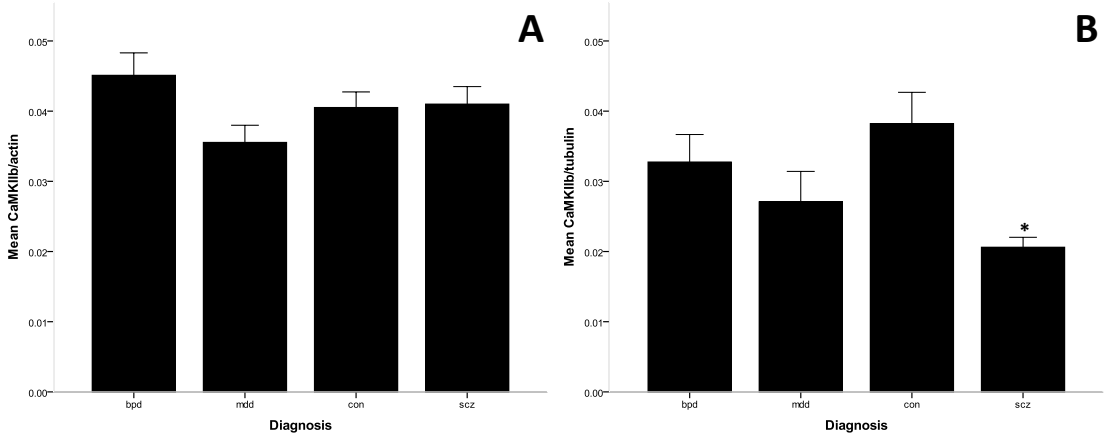

Figure 4-25: Mean (± SEM) ratios CaMKIIβ/β-actin and CaMKIIβ/β-III-tubulin in the PSD fraction and co-IP PSD depending on diagnosis.

(A) Mean ratio CaMKIIβ/β-actin after WB of the PSD fraction. (B) Mean ratio CaMKIIβ/β-III-tubulin after co-IP of the PSD fraction. (bpd) bipolar disorder ; (mdd) major depressive disorder ; (con) control ; (scz) schizophrenia. Statistical test ANOVA with Bonfferoni correction. Comparison with control (* $p<0.05$). ANCOVA statistical analysis was also performed CaMKIIβ/β-actin including post mortem interval as co-variable (see Table 4-9), No significant difference was found between diagnosis.

In contrast, a significant one-way ANOVA was found for the mean of the ratio CaMKIIβ/β-III-tubulin ($F(3, 48) = 3.876$, $p = 0.015$) and a post hoc test with Bonferroni's

correction was carried out in order to distinguish which groups of diagnosis were significantly different. Post-hoc analysis showed a significant decrease of the mean of the ratio CaMKIIβ/β-III-tubulin in the group with schizophrenia compared to the group control ($F(3, 48) = 3.876$, $p = 0.013$). The groups with bipolar disorder ($F(3, 48) = 3.876$, $p = 1.000$) and major depressive disorder ($F(3, 48) = 3.876$, $p = 0.273$) were not found to have any significant difference with the group control (see Figure 4-25 B).

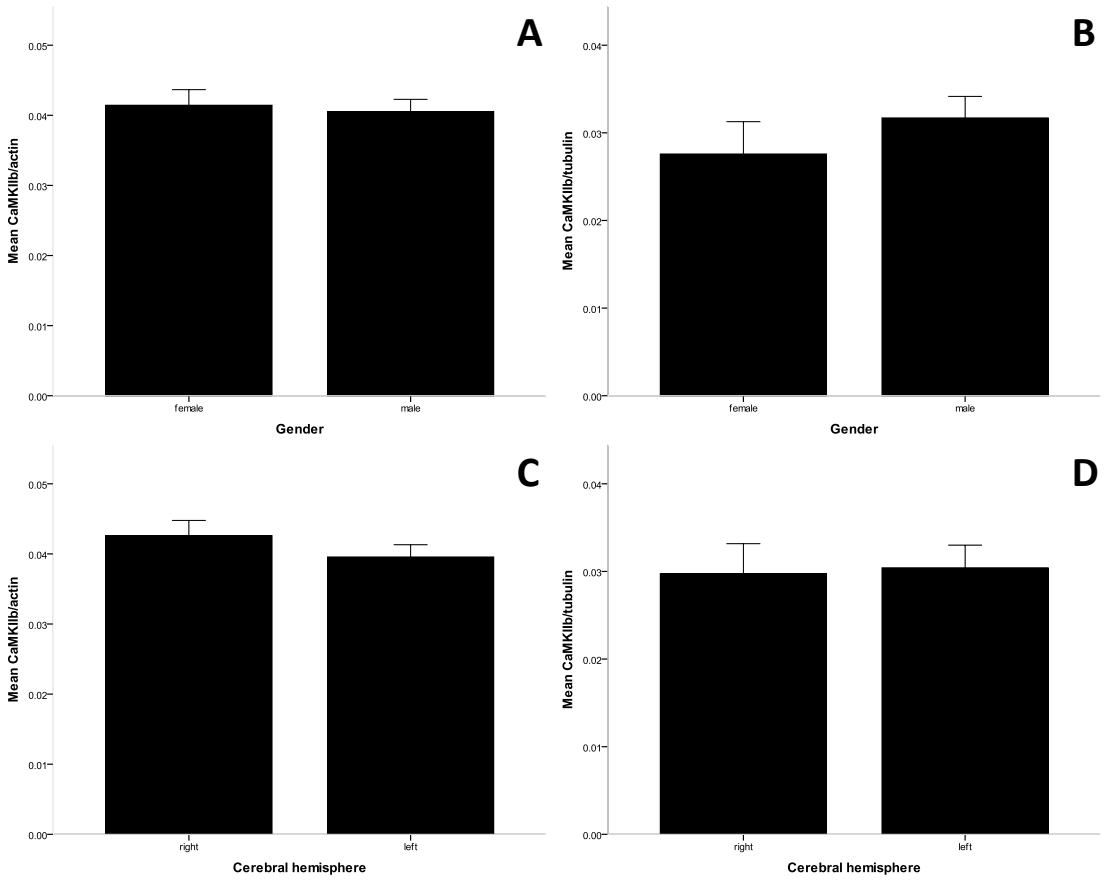

Figure 4-26: Mean (± SEM) ratios CaMKIIβ/β-actin and CaMKIIβ/β-III-tubulin in the PSD fraction and co-IP PSD depending on gender and side of the cerebral hemisphere.

(A) Mean ratio CaMKIIβ/β-actin after WB of the PSD fraction. (B) Mean ratio CaMKIIβ/β-III-tubulin after co-IP of the PSD fraction. (C) Mean ratio CaMKIIβ/β-actin after WB of the PSD fraction. (D) Mean of the ratio CaMKIIβ/β-III-tubulin after co-IP of the PSD fraction.

The expression of CaMKIIβ depending on gender (see Figure 4-26 A and B) and the side of the cerebral hemisphere (see Figure 4-26 C and D) was assessed for CaMKIIβ/β-actin and CaMKIIβ/β-III-tubulin respectively for WB experiments and co-IP experiments with Student's t-test analysis. There was no significant different level of expression of CaMKIIβ between male and female ($t(52) = 0.329$, $p = 0.744$) or right and left hemisphere of the cerebrum ($t(52) = 1.102$, $p = 0.275$) using WB analysis. Same results were found for the expression of CaMKIIβ measured by co-IP for both gender ($t(50) = 0.968$, $p = 0.338$) and cerebral hemisphere ($t(50) = 0.159$, $p = 0.874$).

The effect of psychotic symptoms on the dependent variables CaMKIIβ/β-actin and CaMKIIβ/β-III-tubulin respectively for WB experiments (see Figure 4-27 A) and co-IP experiments (see Figure 4-27 B). The group control was removed and the difference between the means of the ratios CaMKIIβ/β-actin and CaMKIIβ/β-III-tubulin was also examined with Student's T-test analysis. No significant effect of psychosis was found for both CaMKIIβ/β-actin ($t(38) = 0.897$, $p = 0.375$) and CaMKIIβ/β-III-tubulin ($t(36) = 0.302$, $p = 0.765$).

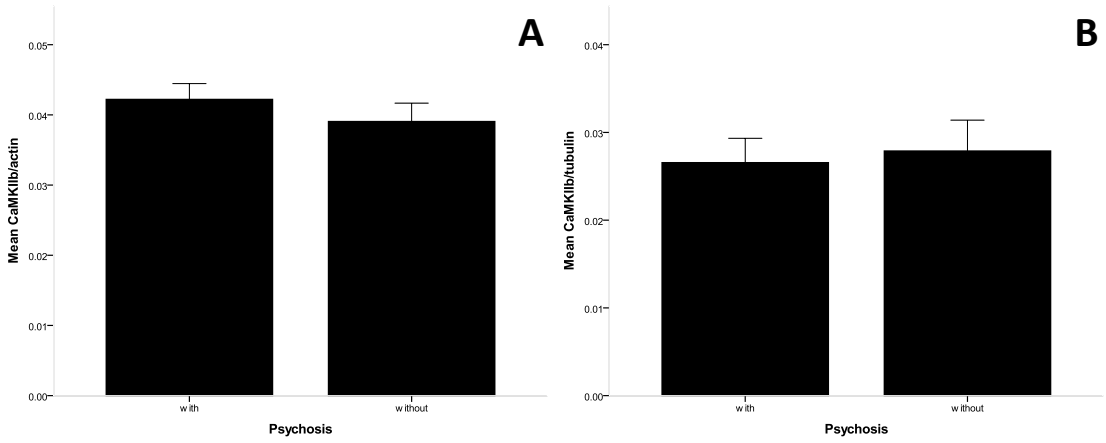

Figure 4-27: Mean (± SEM) ratios CaMKIIβ/β-actin and CaMKIIβ/β-III-tubulin in the PSD fraction and co-IP PSD depending on psychotic symptoms.

(A) Mean ratio CaMKIIβ/β-actin after WB PSD fraction. (B) Mean of the ratio CaMKIIβ/β-III-tubulin after co-IP of the PSD fraction.

Student's t-test analysis was also carried out with and without the group control to determine the effect of death by suicide on the dependent variables CaMKIIβ/β-actin and CaMKIIβ/β-III-tubulin respectively for WB experiments (see Figure 4-28 A and C) and co-IP experiments (see Figure 4-28 B and D).

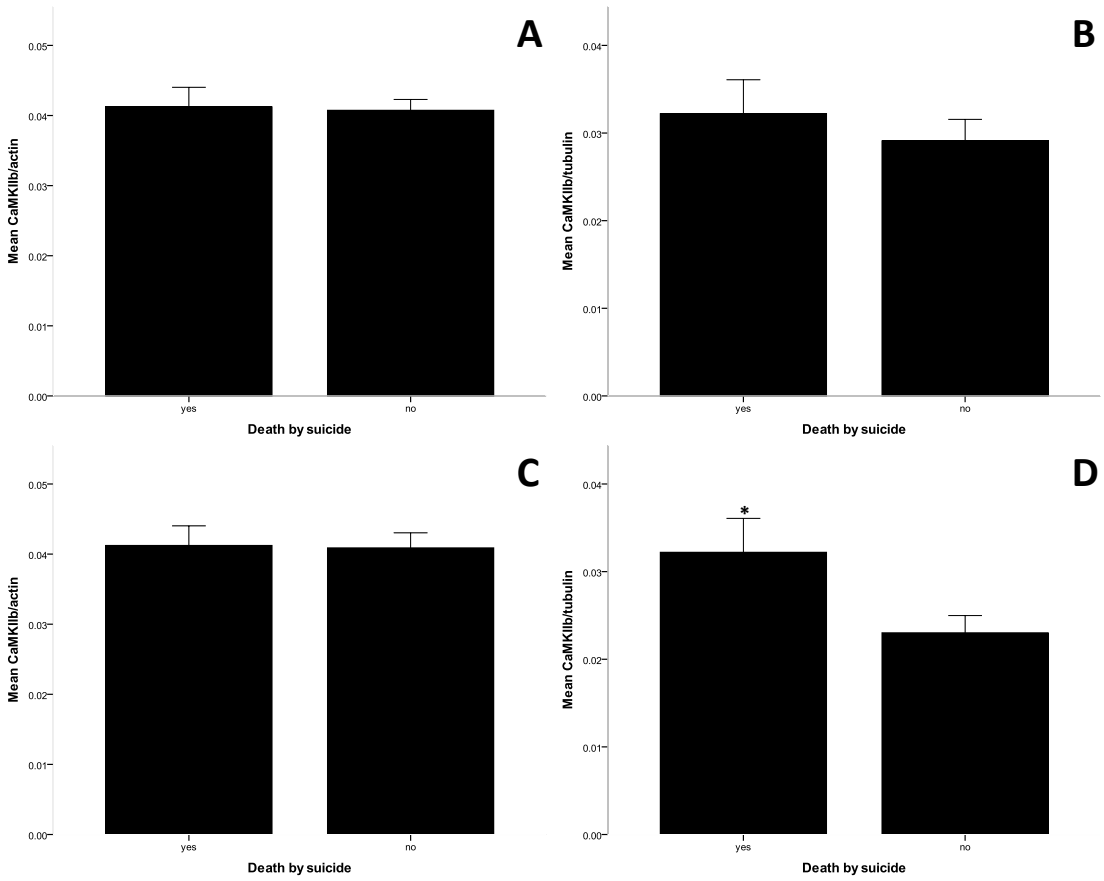

Figure 4-28: Mean (± SEM) ratios CaMKIIβ/β-actin and CaMKIIβ/β-III-tubulin in the PSD fraction and co-IP PSD depending on death by suicide.

(A) Mean ratio CaMKIIβ/β-actin after WB of the PSD fraction. (B) Mean ratio CaMKIIβ/β-III-tubulin after co-IP of the PSD fraction. (C) Mean ratio CaMKIIβ/β-actin after WB of the PSD fraction (without controls). (D) Mean ratio CaMKIIβ/β-III-tubulin after co-IP of the PSD fraction (without controls). Statistical Student's t test (* $p<0.05$).

No significant effect of death by suicide was found for both CaMKIIβ/β-actin ($t(52) = 0.166$, $p = 0.869$) and CaMKIIβ/β-actin ($t(38) = 0.100$, $p = 0.921$) respectively with or without the control group (see Figure 4-28 A and C). There was also no significant difference of the mean of the ratio CaMKIIβ/β-III-tubulin between the groups with or without psychosis when the group control was included in the statistical analysis ($t(50) = 0.700$, $p = 0.487$). In contrast Student's t-test revealed a significant increase in the group with death by suicide for CaMKIIβ/β-III-tubulin ($t(24.03) = 2.119$, $p = 0.045$) when the group control was removed (see Figure 4-28 B and D).

One-way ANOVA statistical test was performed to compare the mean of the ratios CaMKIIβ/β-actin and CaMKIIβ/β-III-tubulin between each degree of severity of substance abuse and alcohol abuse for both WB (see Figure 4-29 A and C) and co-IP (see Figure 4-29 B and D) experiments. One-way ANOVA statistical test for WB experiments revealed a trend of difference between groups with different degrees of substance abuse ($F(4, 49) = 2.119$, $p = 0.093$) whereas no significant difference was found for the expression of CaMKIIβ ($F(5, 48) = 0.366$, $p = 0.869$) looking at the severity of alcohol abuse (see Figure 4-29 A and C).

Because of the trend observed for the effect of the severity of substance abuse on the mean of the ratio CaMKIIβ/β-actin a post-hoc with Bonferroni's correction was performed. A trend towards a decrease of CaMKIIα/β-actin ($F(4, 49) = 2.119$, $p = 0.082$) between moderate present and heavy present consummation of drug abuse (see Figure 4-29 A). For the co-IP experiments there was no significant difference between the expression of CaMKIIβ either when considering the severity of substance abuse ($F(4, 46) = 0.493$, $p = 0.741$) or the severity of alcohol abuse ($F(5, 46) = 0.875$, $p = 0.505$) (see Figure 4-29 B and D).

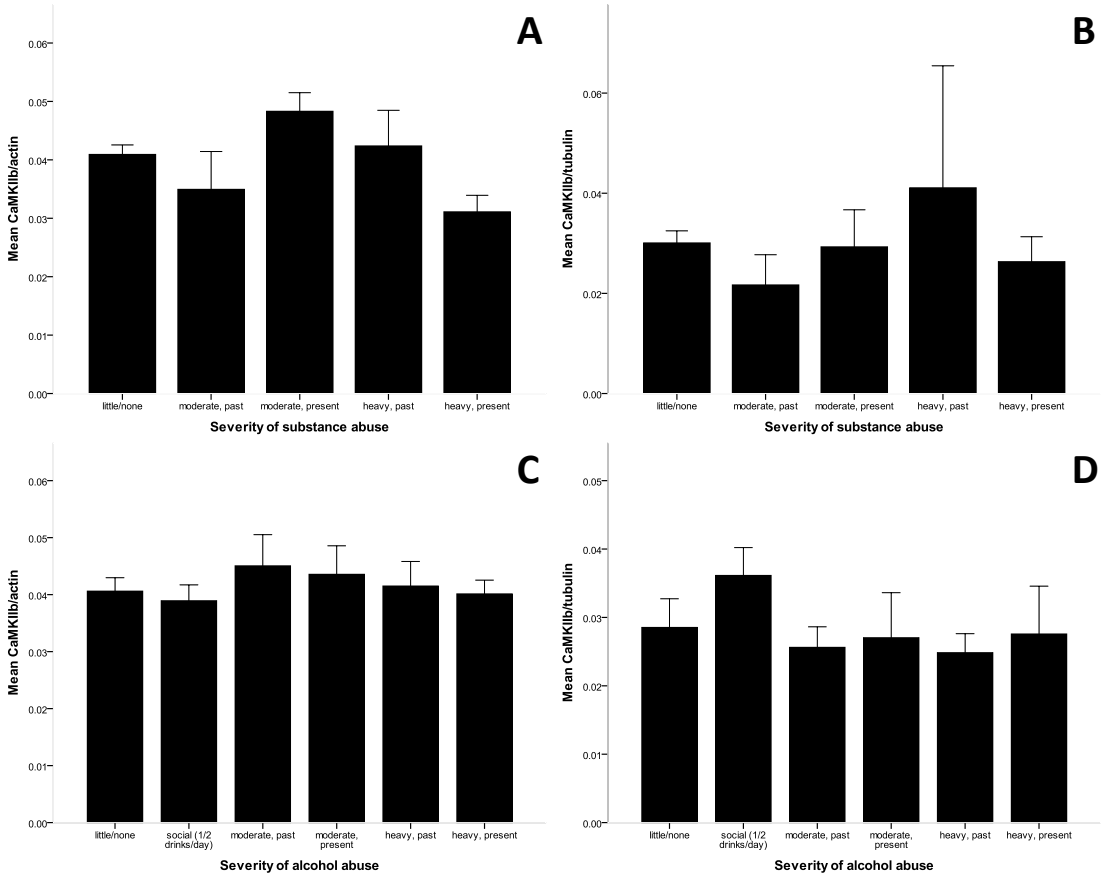

Figure 4-29: Mean (± SEM) ratios CaMKIIβ/β-actin and CaMKIIβ/β-III-tubulin in the PSD fraction and co-IP PSD depending on severity of substance and alcohol abuse.

(A) Mean ratio CaMKIIβ/β-actin after WB of the PSD fraction. (B) Mean ratio CaMKIIβ/β-III-tubulin after co-IP of the PSD fraction. (C) Mean ratio CaMKIIβ/β-actin after WB of the PSD fraction. (D) Mean ratio CaMKIIβ/β-III-tubulin after co-IP of the PSD fraction.

Correlation between the expression of CaMKIIβ with the the severity of substance abuse and alcohol abuse was also assessed by non-parametric correlation analysis of Spearman. Neither the difference of the means of the ratio CaMKIIβ/β-actin ($\rho(54) = -0.060$; $p = 0.664$) nor the ratio CaMKIIβ/β-III-tubulin ($\rho(52) = -0.075$; $p = 0.602$) were significantly correlated with an increase of the severity of substance abuse. In addition neither the difference of expression of CaMKIIβ was significantly correlated with an

increase of the severity of alcohol abuse with WB analysis (ρ(54) = 0.058; p = 0.676) nor with co-IP analysis (ρ(52) = -0.100; p = 0.481).

Table 4-9: Correlational effects of demographic and peri-mortem factors on the ratios CaMKIIβ/β-actin and CaMKIIβ/β-III-tubulin.

Spearman's correlation	Age at death	pH	Mass of the brain	PMI	Storage
CaMKIIβ/β-actin (n=54)	0.030	-0.070	-0.090	**0.268***	0.229
CaMKIIβ/β-III-tubulin (n=52)	-0.097	0.255	0.003	-0.115	-0.058

***p<0.05**

Correlational effects of demographic and peri-mortem factors were assessed for the age at death, the pH of the brain, the mass of the brain, the PMI and the duration of storage of the brain for both CaMKIIβ/β-actin and CaMKIIβ/β-III-tubulin with non-parametric correlation analysis. A significant increase of the mean of the ratio CaMKIIβ/β-actin was significantly correlated with an increase of the post-mortem interval (ρ(44) = -0.389; p = 0.009). No significant correlation was found between the ratio CaMKIIβ/β-actin and the demographic and peri-mortem factors such as pH of the brain, mass of the brain, PMI and duration of storage of the brain. Age at death, pH of the brain, mass of the brain, PMI and duration of storage of the brain were found to have no effect on the ratio CaMKIIβ/β-III-tubulin (see Table 4-9).

For both WB and co-IP experiments the effects of age at death, age of onset of disease, duration of diseases and life time quantity of fluphenazine or equivalent on the expression of CaMKIIβ were also examined with non-parametric correlation analysis. For this study the group control was removed. None of the demographic and peri-

mortem factors mentioned above were found to be significantly correlated with the level of expression of CaMKIIβ either for WB or co-IP experiments (see Table 4-10).

Table 4-10: Correlational effects of demographic and peri-mortem factors on the ratios CaMKIIβ/β-actin and CaMKIIβ/β-III-tubulin (without controls).

Spearman's correlation	Age at death	Age of onset of disease	Duration of disease	Life time quantity of fluphenazine or equivalent
CaMKIIβ/β-actin (n=40)	-0.044	-0.124	0.147	0.216
CaMKIIβ/β-III-tubulin (n=38)	-0.210	-0.127	0.017	-0.071

None of the demographic and peri-mortem factors that were tested were found to affect the ratio CaMKIIβ/β-III-tubulin whereas the ratio CaMKIIβ/β-actin was affected by an increase of the post-mortem interval. Consequently an ANCOVA statistical analysis was performed including post mortem interval as co-variable. No significant difference between each group of diagnosis for the mean of the ratio CaMKIIβ/β-actin ($F(3, 49) = 2.027$, $p = 0.122$) was found with the effect of the post-mortem interval as co-variable.

4.4.6 Expression of NSF in the PSD fraction and within the PSD

The means of the ratios NSF/β-actin and NSF/β-III-tubulin were compared between each diagnosis groups for both WB and co-IP experiments using one-way ANOVA statistical test (see Figure 4-30). For both NSF/β-actin ($F(3, 53) = 0.586$, $p = 0.627$) and NSF/β-III-tubulin ($F(3, 50) = 1.109$, $p = 0.354$) no significant difference between diagnosis was found (see Figure 4-30 A and B).

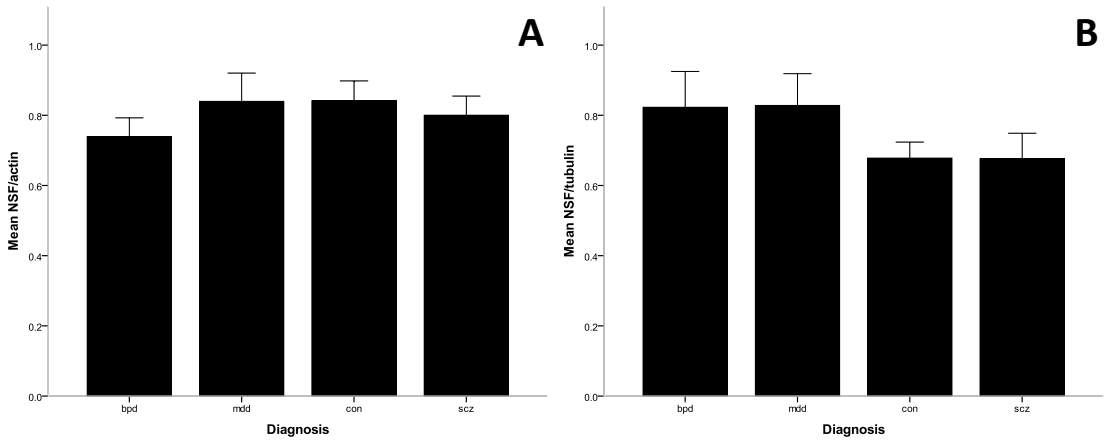

Figure 4-30: Mean (± SEM) ratios NSF/β-actin and NSF/β-III-tubulin in the PSD fraction and co-IP PSD depending on diagnosis.

(A) Mean ratio NSF/β-actin after WB of the PSD fraction. (B) Mean ratio NSF/β-III-tubulin after co-IP of the PSD fraction. (bpd) bipolar disorder ; (mdd) major depressive disorder ; (con) control ; (scz) schizophrenia. ANCOVA statistical analysis with death by suicide as co-variable was performed for the mean ratio NSF/β-III-tubulin (see Figure 4-33 B), no significant difference was found between diagnosis.

Using Student's T-test analysis the effects of gender (see Figure 4-31 A and B) and of the side of the cerebral hemisphere (see Figure 4-31 C and D) were determined on the dependent variables NSF/β-actin and NSF/β-III-tubulin respectively for WB experiments and co-IP experiments.

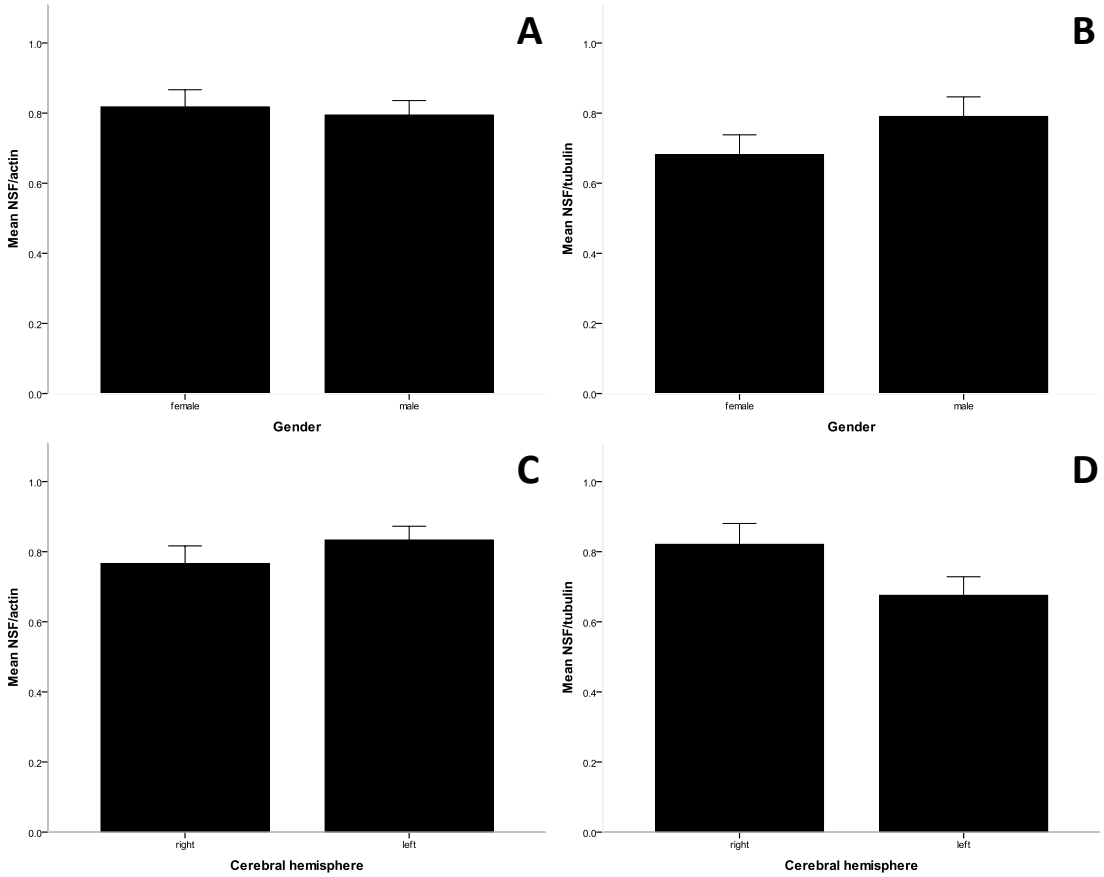

Figure 4-31: Mean (± SEM) ratios NSF/β-actin and NSF/β-III-tubulin in the PSD fraction and co-IP PSD depending on gender and side of the cerebral hemisphere.

(A) Mean ratio NSF/β-actin after WB of the PSD fraction. (B) Mean ratio NSF/β-III-tubulin after co-IP of the PSD fraction. (C) Mean ratio NSF/β-actin after WB of the PSD fraction. (D) Mean ratio NSF/β-III-tubulin after co-IP of the PSD fraction.

Neither significant effect of gender was found for both NSF/β-actin ($t(55) = 0.363$, $p = 0.718$) and NSF/β-III-tubulin ($t(52) = 1.310$, $p = 0.196$) or cerebral lateralisation for WB (NSF/β-actin; $t(55) = 1.070$, $p = 0.289$). For the co-IP experiment a trend towards a decrease of the mean of the ratio NSF/β-III-tubulin ($t(52) = 1.828$, $p = 0.073$) was found in the left hemisphere of the cerebrum (see Figure 4-31 D).

To determine the effect of psychotic symptoms on the dependent variables NSF/β-actin and NSF/β-III-tubulin respectively for WB experiments (see Figure 4-32 A) and co-IP experiments (see Figure 4-32 B) the group control was removed and Student's t-test analysis was performed. There was no significant difference between the expression of NSF with or without psychosis for both WB (NSF/β-actin: t(42) = 0.683, p = 0.498) and co-IP (NSF/β-III-tubulin: t(38) = 0.402, p = 0.690).

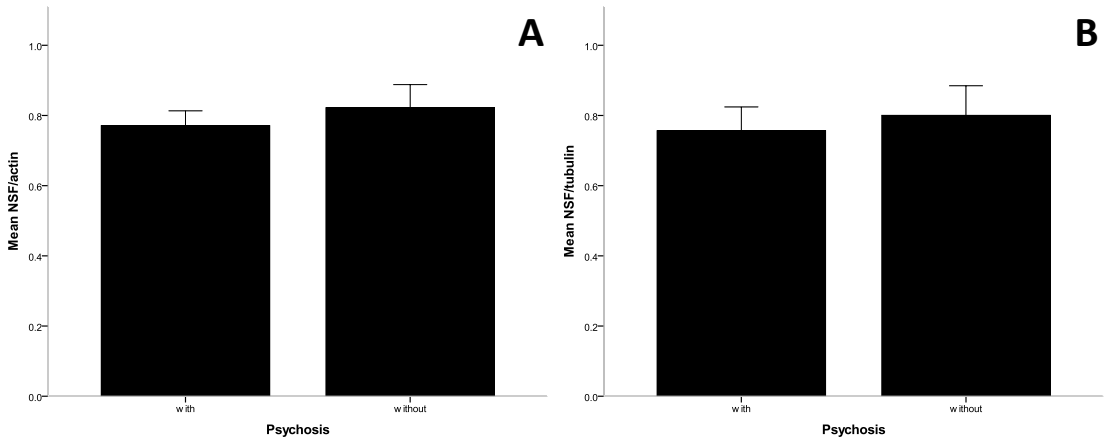

Figure 4-32: Mean (± SEM) ratios NSF/β-actin and NSF/β-III-tubulin in the PSD fraction and co-IP PSD depending on psychotic symptoms.

(A) Mean ratio NSF/β-actin after WB of the PSD fraction. (B) Mean ratio NSF/β-III-tubulin after co-IP of the PSD fraction.

For the effect of death by suicide on the dependent variables NSF/β-actin and NSF/β-III-tubulin respectively for WB (see Figure 4-33 A and C) and co-IP experiments (see Figure 4-33 B and D), a Student's t-test analysis was carried out with (see Figure 4-33 A and B) and without (see Figure 4-33 C and D) the group control. No significant effect of death by suicide was found for both NSF/β-actin (t(55) = 1.006, p = 0.319) and NSF/β-actin (t(42) = 0.779, p = 0.440) respectively with or without the control group. Student's t-test for both with (t(52) = 4.149, p = 0.0001) or without (t(38) = 3.634, p =

0.001) the control group revealed a significant increase in the group with death by suicide for NSF/β-III-tubulin.

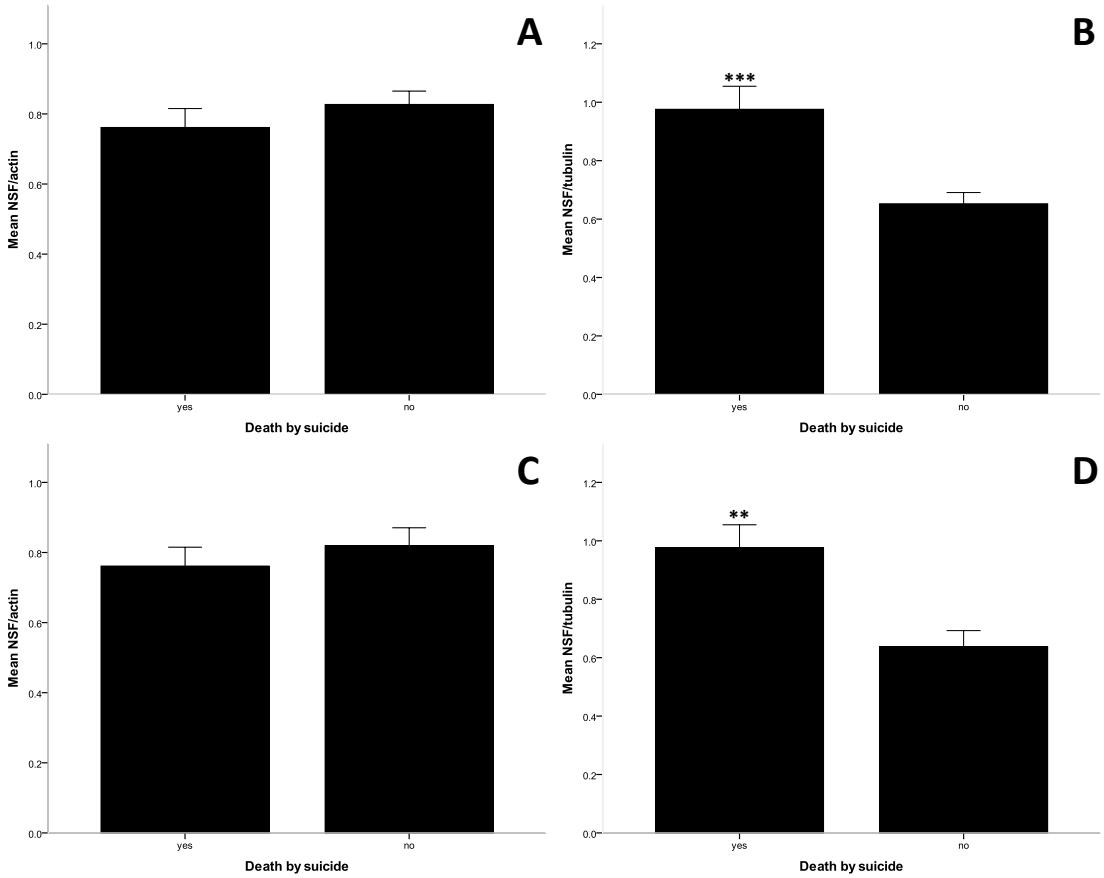

Figure 4-33: Mean (± SEM) ratios NSF/β-actin and NSF/β-III-tubulin in the PSD fraction and co-IP PSD depending on death by suicide.

(A) Mean ratio NSF/β-actin after WB of the PSD fraction. (B) Mean ratio NSF/β-III-tubulin after co-IP of the PSD fraction. (C) Mean ratio NSF/β-actin after WB of the PSD fraction (without controls). (D) Mean ratio NSF/β-III-tubulin after co-IP of the PSD fraction (without controls). Statistical Student's t test (p<0.01; *** p<0.001).**

The effects of the severity of substance abuse (see Figure 4-34 A and B) and the severity of alcohol abuse (see Figure 4-34 C and D) were examined with one-way

ANOVA statistical for both ratios NSF/β-actin (see Figure 4-34 A and C) and NSF/β-III-tubulin (see Figure 4-34 B and D).

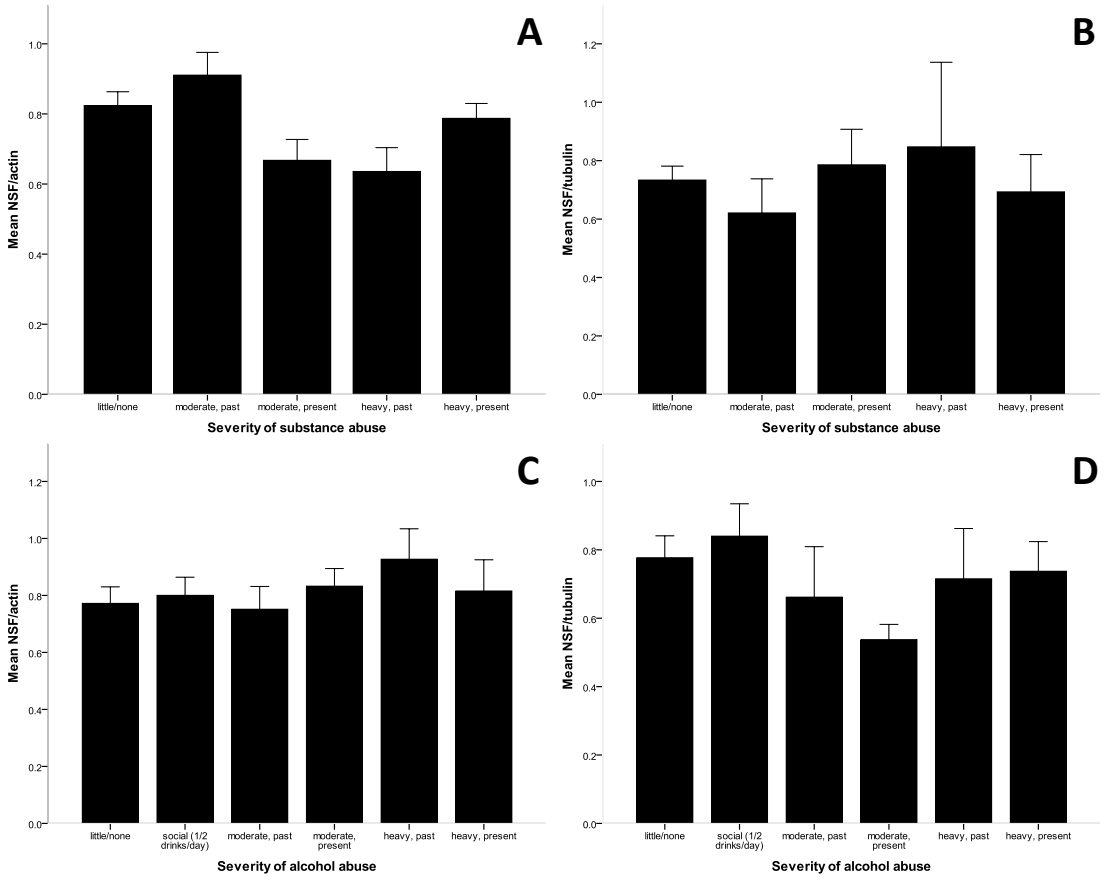

Figure 4-34: Mean (± SEM) ratios NSF/β-actin and NSF/β-III- in the PSD fraction and co-IP PSD depending on severity of substance and alcohol abuse.

(A) Mean ratio NSF/β-actin after WB of the PSD fraction. (B) Mean ratio NSF/β-III-tubulin after co-IP of the PSD fraction. (C) Mean ratio NSF/β-actin after WB of the PSD fraction. (D) Mean ratio NSF/β-III-tubulin after co-IP of the PSD fraction.

No significant difference of the level of expression of NSF was revealed for both WB ($F(4, 51) = 1.319$, $p = 0.275$) and co-IP ($F(4, 48) = 0.235$, $p = 0.917$) experiments considering the degree of severity of substance abuse (see Figure 4-34 A and B). For

both NSF/β-actin ($F(5, 51) = 0.385$, $p = 0.857$) and NSF/β-III-tubulin ($F(5, 48) = 1.029$, $p = 0.412$) respectively for WB and co-IP experiments, no significant effect of the severity of alcohol abuse was observed (see Figure 4-34 C and D).

Non-parametric correlation analysis of Spearman was performed to determine an eventual correlation between the expression of NSF with the effect of the severity of substance and alcohol abuse. No effect either with the severity of substance abuse (NSF/β-actin: $\rho(56) = -0.154$, $p = 0.256$; NSF/β-III-tubulin: ($\rho(53) = 0.031$, $p = 0.825$) or for the severity of alcohol abuse (NSF/β-actin: $\rho(57) = 0.136$, $p = 0.314$; NSF/β-III-tubulin: $\rho(54) = -0.160$, $p = 0.246$) on the expression of NSF with both WB and co-IP experiments.

The effects of age at death, pH of the brain, mass of the brain, PMI and duration of storage of the brain for both ratios NSF/β-actin and NSF/β-III-tubulin were examined with non-parametric correlation analysis. No significant correlation was found for any of the demographic and peri-mortem factors with both ratios NSF/β-actin and NSF/β-III-tubulin (see Table 4-11).

Table 4-11: Correlational effects of demographic and peri-mortem factors on the ratios NSF/β-actin and NSF/β-III-tubulin.

Spearman's correlation	Age at death	pH	Mass of the brain	PMI	Storage
NSF/β-actin (n=57)	0.259	0.009	-0.058	0.019	-0.107
NSF/β-III-tubulin (n=54)	-0.177	0.158	-0.045	-0.228	-0.054

Non-parametric correlation analysis was also carried out to correlate the effects of age at death, age of onset of disease, duration of diseases and life time quantity of fluphenazine or equivalent on both NSF/β-actin and NSF/β-III-tubulin. For this study

the group control was removed. None of the demographic and peri-mortem factors was found to be correlated with with the expression of (see Table 4-12).

Table 4-12: Correlational effects of demographic and peri-mortem factors on the ratios NSF/β-actin and NSF/β-III-tubulin (without controls).

Spearman's correlation	Age at death	Age of onset of disease	Duration of disease	Life time quantity of fluphenazine or equivalent
NSF/β-actin (n=44)	0.215	0.040	0.235	0.005
NSF/β-III-tubulin(n=40)	-0.129	-0.262	0.067	-0.259

To summarise the expression of NSF was not significantly affected by any demographic and peri-mortem factors for the WB experiments whereas the ratio NSF/β-III-tubulin by the effect of death by suicide. ANCOVA statistical analysis with death by suicide as co-variable was performed and no significant difference of the mean of the ratio NSF/β-III-tubulin ($F(3, 49) = 0.402$, $p = 0.752$) was revealed between diagnosis.

4.5 Discussion and conclusions

This part of the investigation has demonstrated:

1. **That expression of proteins involved in synaptic plasticity NR2A, PSD-95 and CaMKIIβ is decreased in schizophrenia compared to healthy control.**
2. **That expression of the protein NSF involved in AMPAR trafficking is not affected in any psychiatric disorder tested in this study compared to control.**

3. **That proteins mentioned above are differentialy expressed and disturbed depending on their cellular localisation (extra-post-synaptic density (WB) and intra-post-synaptic density (co-IP)) in schizophrenia.**
4. **That β-actin is more appropriated to normalise direct WB of the PSD compared to β-III-tubulin whereas β-III-tubulin is more appropriated to normalise WB after co-IP of the PSD compared to β-actin.**

Utilising co-IP, the present study revealed a significant decrease of the expression of the NMDAR subunit NR2A within the PSD in the premotor cortex of patients with schizophrenia ($F(3, 46) = 7.927$, $p = 0.001$) and major depressive disorder ($F(3, 46) = 7.927$, $p = 0.003$) compared to healthy control. This study also revealed that the expression of NR2A within the PSD is significantly reduced in the premotor cortex of patients with schizophrenia compared to patients with bipolar disorder ($F(3, 46) = 7.927$, $p = 0.039$). Using WB of the PSD fraction the results showed a significant decrease of the expression of NR2A in the premotor cortex of patients with major depressive disorder compared to control ($F(3, 51) = 0.601$, $p = 0.025$). In addition a trend towards a significant decrease of the expression of NR2A was found in the premotor cortex of patients with schizophrenia compared to control ($F(3, 51) = 0.601$, $p = 0.058$) (see section 4.4.2).

Previous postmortem studies of NR2A mRNA and protein in schizophrenia have yielded variable results depending on the region of the brain studied, the techniques used and the variable effects of demographical/clinical factors.

A study using *in situ* hybridisation showed a decrease in NR2A mRNA in the DLPFC of patients with schizophrenia and major depressive disorder but not in bipolar disorder relative to controls. In the same study, using receptor autoradiography, the authors revealed no alterations in receptor binding in any of the illnesses (Beneyto and Meador-Woodruff, 2008). This suggests that there is no change in the number of NMDAR in the DLPFC of patients with schizophrenia, major depressive disorder and

bipolar disorder but an abnormal NMDAR stoechiometry in the DLPFC of patients with schizophrenia and major depressive disorder. Our findings of decreased NR2A in PSD are in accordance with this study. However, other studies report conflicting findings. For example, one study found increased mRNA levels for NR2A in the DLPFC and occipital cortex of elderly patients with schizophrenia compared to matched healthy subjects (Dracheva et al., 2001). Whereas, another study found no significant changes of the expression of NR2A proteins in the DLPFC and other regions investigated in schizophrenia compared to healthy subjects (Kristiansen et al., 2007b).

Other studies have focused on the expression of NR2A in interneurons. A recent study found that the density of interneurons that expressed NR2A mRNA was significantly decreased by 48-50% in layers 3 and 4 in PFC (BA 9) of subjects with schizophrenia, but the cellular expression of NR2A mRNA in the neurons that exhibited a detectable level of this transcript was unchanged (Bitanihirwe et al., 2009). Another study found similar findings, reporting that interneurons that expressed NR2A mRNA were decreased by 73% and 52%, in layers 2 and 5, respectively, in anterior cingulate cortex (BA 24) of subjects with schizophrenia. However the expression level of NR2A mRNA was unaltered (Woo et al., 2004).

Animal studies have been useful to observe potential links between reduced NR2A and the pathophysiology of schizophrenia. One study used lentivirus mediated RNA-interference (RNAi) to knockdown the glial enzyme DAO in the mouse cerebellum and showed a 22% decrease in NR2A mRNA relative to controls in cerebellum (Burnet et al., 2011). Another study that used NR2A knockout mice to model schizophrenia demonstrated that these mice had impaired locomotor activity. Impairment of the locomotor activity was attenuated by treatment with antipsychotics such as haloperidol and risperidone (Miyamoto et al., 2001).

The studies mentioned above illustrate the complexities of postmortem studies. Consideration needs to be given to the regional, cellular and subcellular origins of the

brain samples, the potentially confounding effects of numerous demographical, perimortem and clinical factors and also the techniques used.

In the present study, co-IP and WB of the PSD occasionally showed similar findings, however, more often than not, the findings were different. Co-IP (with PSD-95) of the PSD fraction, may represent proteins of interest specifically docked at the synapse, whereas, WB of the PSD may also include proteins that are present at extra-synaptic regions or in the process of intracellular recycling. The differences between WB and co-IP data could also be due to the removal of more contaminants in the co-IP experiments. Previous studies and our results together, suggest that NR2A may be downregulated without changes in NMDAR number in premotor cortex of patients with schizophrenia and major depressive disorder. This change in the stoechiometry of the NMDAR may lead to a dysfunction of the PSD machinery in these two psychiatric illnesses.

The present study also revealed a significant decrease ($F(3, 48) = 2.995$, $p = 0.049$) in the expression of scaffolding protein PSD-95 within the PSD in the premotor cortex of patients with schizophrenia compared to healthy subjects, utilising co-IP. In contrast to the findings for NR2A in major depressive disorder, no significant changes for PSD-95 within the PSD were found. In addition no changes in the expression of PSD-95 were found in the premotor cortex of patients with bipolar disorder. WB analysis of the PSD fraction did not reveal any changes in PSD-95 for all three psychiatric illnesses compared to the control group (see section 4.4.3).

Postmortem studies of PSD-95 mRNA and protein in different regions of the brain of patients with schizophrenia have reported heterogenous results. Studies using *in situ* hybridisation reported changes in the expression of PSD-95 mRNA in schizophrenia dependant on brain region. In the DLPFC, one study reported no changes in PSD-95 mRNA expression in schizophrenia, major depressive disorder and bipolar disorder (Beneyto and Meador-Woodruff, 2008). Another study reported increased PSD-95 mRNA in thalamus of elderly patients with schizophrenia (Clinton et al., 2003),

whereas a decreased PSD-95 mRNA was observed in thalamus of young patients with schizophrenia and bipolar disorder but not in patients with major depressive disorder (Clinton and Meadow-Woodruff, 2004). In the anterior cingulate cortex, PSD-95 mRNA was increased in patients with schizophrenia (Kristiansen et al., 2006). Furthermore, an increased expression of PSD-95 mRNA was found in the occipital cortex of patients with schizophrenia compared to healthy subjects (Dracheva et al., 2001).

Studies comparing the expression of the PSD-95 protein between patients with schizophrenia and healthy subjects or others psychiatric groups have also reported conflicting results. A study using WB showed increased PSD-95 protein expression in the dorsomedial thalamus of patients with schizophrenia compared to healthy subjects (Clinton et al., 2006). Other studies reported decreased expression of PSD-95 protein in the anterior cigulate cortex of patients with schizophrenia compared to healthy controls (Kristiansen et al., 2006; Funk et al., 2009). In the hippocampus, a study using immunoautoradiographical techniques showed a decrease in PSD-95 protein in the dentate molecular layer in both schizophrenia and bipolar disorder relative to major depression (Toro and Deakin, 2005). Other studies reported no change in the expression PSD-95 proteins in the orbitofrontal cortex, the DLPFC and ventral thalamus of patients with schizophrenia compared to healthy subjects (Kristiansen et al., 2007b).

In the present study, decreased expression of the scaffolding protein PSD-95 was reported in schizophrenia. There have been no previous studies that have assessed the expression of PSD-95 within the PSD. Both NR2A and PSD-95 that are known to interact within the PSD are significantly reduced in schizophrenia whereas no significant change in the expression of PSD-95 was found in patients with major depressive disorder. These findings suggest that distinct interactions/signalling pathways within the PSD may be disturbed in these two different psychiatric illnesses.

The present study also revealed a significant decrease in the expression of the signalling protein CaMKIIβ within the PSD in the premotor cortex of patients with schizophrenia compared to the group control utilising co-IP. No significant difference

in the expression of CaMKIIβ within the PSD was found in the premotor cortex of patients with major depressive disorder or bipolar disorder. Using WB no significant differences between diagnosis was found for the expression CaMKIIα in the PSD fraction (see sections 4.4.4 and 4.4.5).

Few postmortem studies have been carried out previously to assess the expression of CaMKIIα and CaMKIIβ in schizophrenia. A preliminary study using qPCR showed that mRNA for CaMKIIβ was significantly elevated in the DLPFC in the schizophrenia (Novak et al., 2000). In frontal cortex the same authors showed that the expression of CaMKIIα was significantly elevated in major depressive disorder but not in schizophrenia and that the expression of CaMKIIβ was significantly elevated in schizophrenia and in major depressive disorder (Novak et al., 2006). Another study using *in situ* hybridisation in the PFC reported no changes in the expression of CaMKIIα mRNA in schizophrenia and major depressive disorder whereas a significant decrease was found in bipolar disorder compared to healthy subjects (Xing et al., 2002). A behavioural study that assessed memory performances showed that phosphorylation of CaMKII proteins was significantly reduced in PCP animal model of schizophrenia compared to controls (Nabeshima et al., 2006).

The previous finding of increased CaMKIIβ mRNA in schizophrenia (Novak et al., 2006) is in contradiction with our results. However the Novak et al study assessed mRNA levels in PFC, whereas protein levels in PSD of BA6 were assessed here. The present study highlights a decrease in CaMKIIβ expression specifically in schizophrenia and not major depressive disoder or bipolar disorder.

Previous postmortem studies of NSF in patients with schizophrenia have reported conflicting results. A study using *in situ* hybridisation showed a significant decrease of NSF in PFC of subjects with schizophrenia compared to healthy controls (Mirnics et al., 2000). Others studies reported no change in the expression of NSF in same brain area in schizophrenia. For instance, one study used qPCR and WB to measure NSF and found that expression was not altered significantly in the prefrontal cortex of

schizophrenic patients compared to subjects controls (Imai et al., 2001). In addition, another study confirmed the results of the latter study using WB in a different BA region of the PFC (Gray et al., 2006).

Our findings for the expression of NSF in the premotor cortex of patients with schizophrenia are in concordance with last two studies. The expression of the vesicular protein NSF was not affected within the PSD in the premotor cortex in any of the psychiatric illnesses compared to the healthy subjects either using co-IP or WB (see section 4.4.6). As NSF is known to regulate trafficking of GluR2 at the post synaptic membrane it is possible that AMPAR trafficking is not disturbed in the premotor cortex of patients with schizophrenia. However, other components of the trafficking machinery would need to be studied to make any firm conclusions.

Overall, the results from the present study suggest that both schizophrenia and major depressive disorder share in common, disturbed NMDAR subunit stochiometry with less NR2A subunits. In addition, a decrease in NR2A, PSD-95 and CaMKIIβ expression within the PSD seems to be a specific feature of schizophrenia. All together, our findings confirm that glutamatergic system may be disturbed in schizophrenia and that disturbance in the premotor cortex may be due to a disturbed signalling pathway implicated in synaptic plasticity.

5 Expression of neurotrophin receptors in the premotor cortex in schizophrenia

5.1 Aims and objectives

The aims of the present study are to semi-quantify protein expression of the neurotrophin receptors TrkB, TrkB-T1 and p75 in BA 6 in schizophrenia relative to major depressive disorder, bipolar disorder and healthy controls. Protein expression will be assessed using WB and co-IP of the PSD fraction. New WB will be carried out for the detection of TrkB, TrkB-T1 and p75 on BA 6 homogenate PSD fractions whereas detection of TrkB, TrkB-T1 and p75 after co-IP will be performed on the membranes used for the previous study (Chapter 4).

5.2 Introduction

Neurotrophins, namely nerve growth factor (NGF), brain-derived neurotrophic factor (BDNF), neurotrophin-3 (NT-3), and neurotrophin-4/5 (NT-4/5), are neurotrophic factors that bind to the high affinity tropomyosin receptor kinase (Trk) receptors, as well as to the low affinity p75 receptor. NGF binds to TrkA, BDNF and NT-4/5 to TrkB, and NT-3 to TrkC (and weakly to TrkB). Activation of these receptors stimulates various intracellular signalling pathways such as mitogen-activated protein kinase/extracellular signal-regulated kinases (MAPK/ERK), phospholipase Cγ (PLCγ), and phosphoinositide 3-kinase (PI3K) pathways, involved in cell survival, proliferation, differentiation and apoptosis (Huang and Reichardt, 2003).

BDNF plays a crucial role in neurodevelopment and function of the mammalian central nervous system. BDNF is released from neurons and regulates synaptic plasticity, which is thought to underlie learning and memory (Chao, 2003; Lu et al., 2005). BDNF is translated as a precursor protein (pro-BDNF) which is subsequently cleaved to produce a mature protein (BDNF) (Matsumoto et al., 2008). Pro-BDNF binds the p75 neurotrophin receptor with high affinity whereas BDNF binds TrkB with high affinity (Lee et al., 2001). In addition a recent study reported that neurons release both pro-BDNF and BDNF (Yang et al., 2009).

Several studies have reported that the expression of BDNF is decreased in schizophrenia, bipolar disorder and major depressive disorder relative to healthy controls (Knable et al., 2004; Gervasoni et al., 2005; Karege et al., 2005; Pillai, 2008).

5.2.1 Function of TrkB receptor within the PSD

The full-length TrkB isoform (TrkB) is a tyrosine kinase that forms homodimers during ligand binding. The homodimerisation triggers tyrosine phosphorylations in the intracellular Trk domains thereby activating transduction of the BDNF signal. These phosphorylations activate MAPK, PI3K or PLCγ intracellular signaling pathways that regulate the assembling of TrkB within the PSD, gene transcription, protein translation and trafficking. TrkB activation of the three signalling pathways is described in more detail below.

Phosphorylation of tyrosine residue 785 of TrkB, recruits and activates PLCγ which in turn hydrolyses phosphatidylinositol 4,5-bisphosphate, to produce diacylglycerol (DAG) and inositol 1,4,5-trisphosphate (IP3) (Huang and Reichardt, 2003; Reichardt, 2006b). DAG activates protein kinase C (PKC), and IP3 receptor releases Ca^{2+} from intracellular reticulum endoplasmic stores. A study has shown that BDNF triggers intracellular Ca^{2+} release at postsynaptic sites of cultured hippocampal neurons (Lang et al., 2007). Then, both Ca^{2+} and DAG activate the plasma membrane transient receptor potential canonical subfamily channel 3/6 (TRPC3/6) that contribute to BDNF-induced Ca^{2+} elevations at growth cones and synapses (Li et al., 2005; Amaral and Pozzo-Miller, 2007).

A study using cultured cortical pyramidal neurons showed that TrkB-BDNF-triggered Ca^{2+} transients translocate GluR1 subunit of AMPAR, but not NMDAR subunits to synapses (Nakata and Nakamura, 2007). Another study using (HEK) 293 cells carrying TrkB and transfected with GluR2 cDNA or GluR1 cDNA, showed that BDNF triggered the translocation of GluR2 but not that of GluR1 via NSF (Narisawa-Saito et al., 2002). These finding suggest a direct involvement of triggered-TrkB-BDNF in synaptic

plasticity. In addition, the elevated Ca^{2+} concentration triggered by PLCγ also increases Ca^{2+}-sensitive adenyl cylclase (AC) activity which is involved in the formation of PSD-95-TrkB complexes (Ji et al., 2005). Ca^{2+}-sensitive AC also activates the cyclic AMP responsive element binding (CREB) which is involved in nuclear transcription (Nguyen et al., 1994; Shaywitz and Greenberg, 1999).

Phosphorylation of TrkB also occurs at tyrosine residue 515 which recruits and phophorylates Shc. Phosphorylated Shc interacts with the adaptor protein Grb2 that recruits and activates the guanine nucleotide exchange factor SOS which promotes the removal of GDP from Ras that can then bind GTP and become active. Ras activates the downstream kinase B-raf, MEK and MAPK/Erk (Huang and Reichardt, 2003; Reichardt, 2006b). MEK-MAPK/Erk signalling pathway also activates CREB (Shaywitz and Greenberg, 1999). Protein-synthesis also occurs via phosphorylation of eukaryotic initiation factor 4E (eIF4E), the 4E-binding protein 1 (4E-BP1) and ribosomal protein S6 triggered by MAPK/Erk (Kelleher III et al., 2004; Klann and Dever, 2004). These findings emphasise the crucial role played by MAPK/Erk signalling pathway in synaptic plasticity.

The PI3K pathway is also activated by TrkB via Shc, Grb2 and Ras as previously described (Reichardt, 2006b). Activation of PI3K changes the composition of inositol phospholipids which leads to the translocation of Akt/protein kinase B to the plasma membrane. Akt activates translation within the post-synaptic dendrite via the mammalian target of rapamycin (mTOR) which regulates protein synthesis (Sarbassov et al., 2005). Then mTOR phosphorylates the protein kinases p70S6K and 4E-BP1 allowing mRNA translation by ribosomes located in the post-synaptic dendrite. The PI3K-Akt pathway also regulates the trafficking of synaptic proteins (Yoshii and Constantine-Paton, 2007b). This pathway also plays a pivotal role synaptic plasticity through translation and transport of synaptic proteins.

The TrkB receptor is present within the PSD of rat cerebral cortex and hippocampus (Wu et al., 1996). TrkB also co-localises with NMDAR at the PSD of cultured cortical

neurons (Gomes et al., 2006). Activation of the TrkB-PLCγ pathway, or direct application of BDNF to cultured neurons, increased synaptic co-localisation of TrkB with PSD-95 and co-IP of PSD-95 and TrkB is correlated with increased synaptic activity (Ji et al., 2005; Yoshii and Constantine-Paton, 2007b). Furthermore BDNF triggered TrkB also induces a rapid transport of PSD-95 from the soma to the dendritic regions of developing neurons in a PI3K-AKT- and microtubule- dependent, protein synthesis-independent, process (Yoshii and Constantine-Paton, 2007b). A study demonstrated that over-expression of PSD-95 increases spine number, size and synaptic efficacy (El-Husseini et al., 2000).

Taken together these studies emphasise the crucial role of TrkB at the post-synaptic dendrite and its contribution to synaptic plasticity and the organisation of the glutamatergic synapse through stabilisation of PSD-95 within the PSD.

5.2.2 Functions of truncated TrkB receptor

Truncated TrkB (TrkB-T1) is a splice variant of TrkB in which alternative splicing removes the exons that code for the intracellular tyrosine kinase domain. Therefore, TrkB-T1 binds to BDNF but it does not undergo autophosphorylation. TrkB-T1 was considered as a dominant-negative form of TrkB as several studies showed negative functions against TrkB, such as TrkB phosphorylation (Knüsel et al., 1994), calcium efflux (Eide et al., 1996), neurite outgrowth (Fryer et al., 1997), cell survival activity (Haapasalo et al., 2001), and gene expression by BDNF (Renn et al., 2009).

TrkB-T1 can form a homodimer or a heterodimer with TrkB, which suppresses TrkB signalling pathway or reduces the availability of BDNF to neurons by binding excess of BDNF (Biffo et al., 1995). However the suggestion that TrkB-T1 is a dominant-negative form of TrkB remains controversial and other functions have also been suggested. For instance several studies revealed that the expression of TrkB-T1 increases markedly at various important periods of neuronal development such as axonal remodelling and synaptogenesis (Ohira et al., 1999; Ohira et al., 2001). In addition several studies

reported that BDNF-triggered TrkB-T1 activates its own signalling pathway. TrkB-T1 binds directly to Rho GDI1, a Rho guanine nucleotide dissociation inhibitor, which in turn promotes the removal of GDP from Rho GTPase that can then bind GTP and become active (Ohira et al., 2006). The Rho signalling pathway regulates the arrangement of microfilaments, intermediate filaments, and microtubules (Etienne-Manneville and Hall, 2002). A study reported that in the BDNF-triggered TrkB-T1 signalling pathway, Rho GDI1 is released from TrkB-T1 in a BDNF-dependent manner, which causes decreases of the activities of Rho-signalling molecules such as RhoA, Rho-associated kinase (ROCK), p21-activated kinase (PAK), and ERK 1/2 (Ohira et al., 2006). These studies suggest that TrkB-T1 regulates the Rho-signalling pathways and the actin cytoskeleton and may be implicated in synaptic plasticity. Other studies showed that TrkB-T1 induces neurite outgrowth (Yacoubian and Lo, 2000; Haapasalo et al., 1999), regulates cytoskeletal changes in astrocytes and may stimulate PLCγ and MAPK signalling (Ohira et al., 2007).

The ratio of cortical TrkB to TrkB-T1 decreases with age as TrkB-T1 protein levels are higher in infants. This increase corresponds with the period of cellular and synaptic pruning (Bracken and Tyrrigiano, 2009). Furthermore the level of expression and localisation seem to vary in different cortical regions. For instance, TrkB-T1 is preferentially localised to pyramidal neurons in the motor cortex layers II–VI (Ohira et al., 2005), but evenly distributed between pyramidal and interneurons in the visual cortex (Bracken and Tyrrigiano, 2009). The differential distribution of TrkB-T1 between brain regions may regulate localised BDNF function.

The positive or negative effect of BDNF-triggered TrkB-T1 on synaptic plasticity remains unclear. However, these studies show its involvement in cytoskeletal rearrangement which may be disturbed in psychiatric disorders.

5.2.3 Function of the p75 receptor within the PSD

The p75 receptor was originally described as a low-affinity receptor for neurotrophins. Recent studies have demonstrated that p75 can promote cell death or survival and modulate neurite outgrowth depending on the operative ligands and co-receptors. Increased expression of p75 has been shown to be involved in neuronal cell death in cultured cells. In addition, studies showed that p75 is disturbed in major depressive disorder and schizophrenia (Fujii and Kunugi, 2009).

Animal studies using p75 mutant mice show impairments in water maze learning, inhibitory avoidance and habituation tasks, which indicates that p75 signalling might modulate synaptic plasticity (Peterson et al., 1999; Wright et al., 2004). Studies also revealed that $p75^{-/-}$ mice have increased hippocampal neuron spine numbers (Koshimizu et al., 2009) and that over-expression of p75 in these neurons reduced the number of dendritic spines (Zagrebelsky et al., 2005). Similarly treatment with a cleavage-resistant proBDNF in cultured neurons decreased the number of spines (Koshimizu et al., 2009). Spine retraction is a mechanism that regulates dendritic arborisation.

Recent studies revealed that activation of p75 receptor is necessary for NMDAR-dependent LTD in CA1 hippocampal neurons (Rösch et al., 2005; Woo et al., 2005). NMDAR-dependent LTD is also absent in the hippocampal CA1 region of p75-knockout mice without affecting NMDAR-dependent LTP or NMDAR-independent LTD (Rösch et al., 2005; Woo et al., 2005). During synaptic depression p75 seems to involve a specific NMDAR subunit NR2B that is implicated in LTD but not in LTP (Massey et al., 2004; Liu et al., 2004). A study using immunostaining and Western blot experiments showed that there was a significant decrease in expression of NR2B in the hippocampus of $p75^{-/-}$ mice. In addition whole-cell recordings revealed that the NR2B-mediated synaptic currents were reduced in CA1 neurons of $p75^{-/-}$ mice. Finally, application of proBDNF to wild-type slices increased the NR2B-mediated synaptic currents and the proBDNF-induced enhancement of LTD was reversed by an NR2B-specific antagonist.

This study demonstrates that proBDNF activates p75 to promote NMDAR-dependent hippocampal LTD, and that this is achieved primarily by enhancing the expression of the NR2B subunit (Woo et al., 2005).

5.3 Materials and methods

5.3.1 Enrichment of the glutamate post-synaptic density

The extraction and purification of PSDs was performed as described in Chapter 4 (see section 4.3.1, page 109).

5.3.2 Protein concentration and protein assay

A protein assay was carried out on the PSD fractions as described in in Chapter 4 (see section 4.3.2, page 109).

5.3.3 Co-immunoprecipitation

The co-immunoprecipitation of PSDs was performed as described in Chapter 4 (see section 4.3.3, page 109).

5.3.4 Western blotting

The WB of PSDs was performed as described in Chapter 4 (see section 4.3.4, page 110), exept that TrkB, TrkB-T1, p75 were immunodetected instead of NR2A, PSD-95, CaMKIIα, CaMKIIβ and NSF. New membranes were immunoblotted for WB experiments. Consequently novel statistical analysis for β-actin was performed (see section 5.4.1, page 172).

5.3.5 Data analysis

Data analysis was performed as described in Chapter 4 (see section 4.3.5, page 110).

5.4 Results

Co-immunprecipitation experiments revealed the presence TrkB, T-TrkB, p75, β-actin and β-III-tubulin. The receptor p75 was indistinguishable from the background of the membranes for the western blotting experiments. Therefore this receptor was excluded from the WB study. The first result analysis consisted on confirming that β-actin was appropriate for the normalisation of the results for WB experiments. Expression of TrkB, T-TrkB and were then measured as a ratio of these proteins with β-actin or β-III-tubulin respectively for WB and co-IP experiments. For the co-IP experiment β-III-tubulin used to normalise our results was the same used in co-IP experiments presented above (see section 4.4.1)

5.4.1 Expression of β-actin in the PSD fraction

The mean of the fluorescence intensity of β-actin was compared between each diagnosis groups using one-way ANOVA statistical test. No significant difference between diagnosis was found for the mean of the fluorescence of β-actin ($F(3, 55) = 1.907$, $p = 0.139$) by WB. The chart representing the difference of the means of the flurescence of β-actin between each group of diagnosis showed an appropriate homogeneity of variance of the mean (see Figure 5-1). However the expression of β-actin was assessed for each demographic and peri-mortem factors in order to determine wether β-actin could be used as denominator to normalise data from WB experiments.

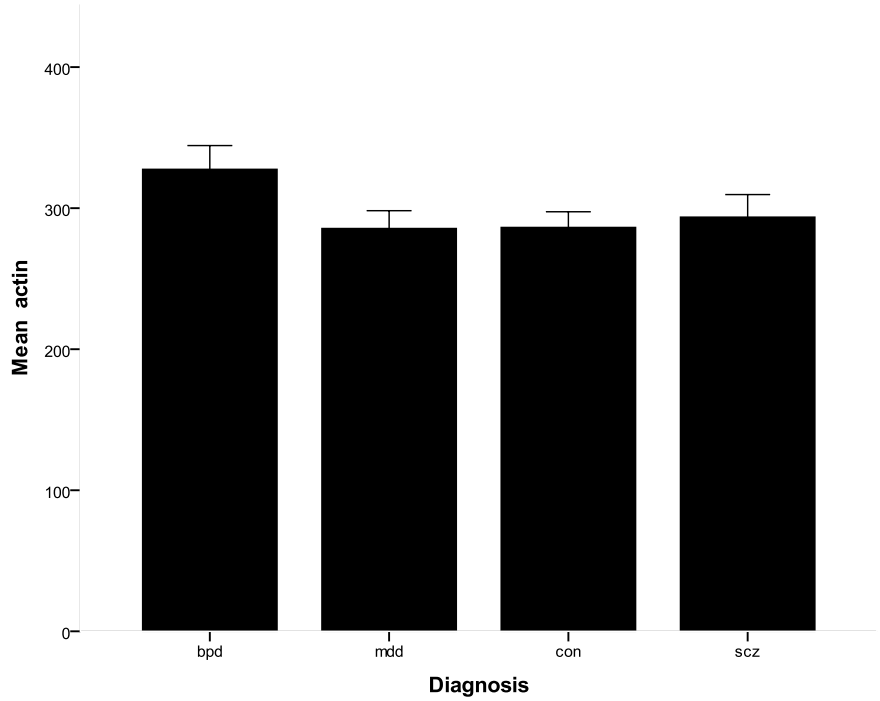

Figure 5-1: Mean (± SEM) fluorescence intensity for β-actin in the PSD fraction.

(bpd) bipolar disorder ; (mdd) major depressive disorder ; (con) control ; (scz) schizophrenia

Student's T-test analysis was performed in order to determine an eventual difference of expression of β-actin between male and female (see Figure 5-2 A) and between the right and the left side of the cerebral hemisphere (see Figure 5-2 B). No significant difference in the expression of β-actin was found either for gender ($t(57) = 0.167$, $p = 0.868$) or for the right and left hemisphere of the cerebrum ($t(57) = 1.122$, $p = 0.267$). The group control was removed and the effect of psychotic symptoms on the dependent variable β-actin was also examined with Student's T-test analysis. No significant difference of the expression of β-actin ($t(43) = 0.636$, $p = 0.528$) was found between both groups with and without psychosis (see Figure 5-2 C).

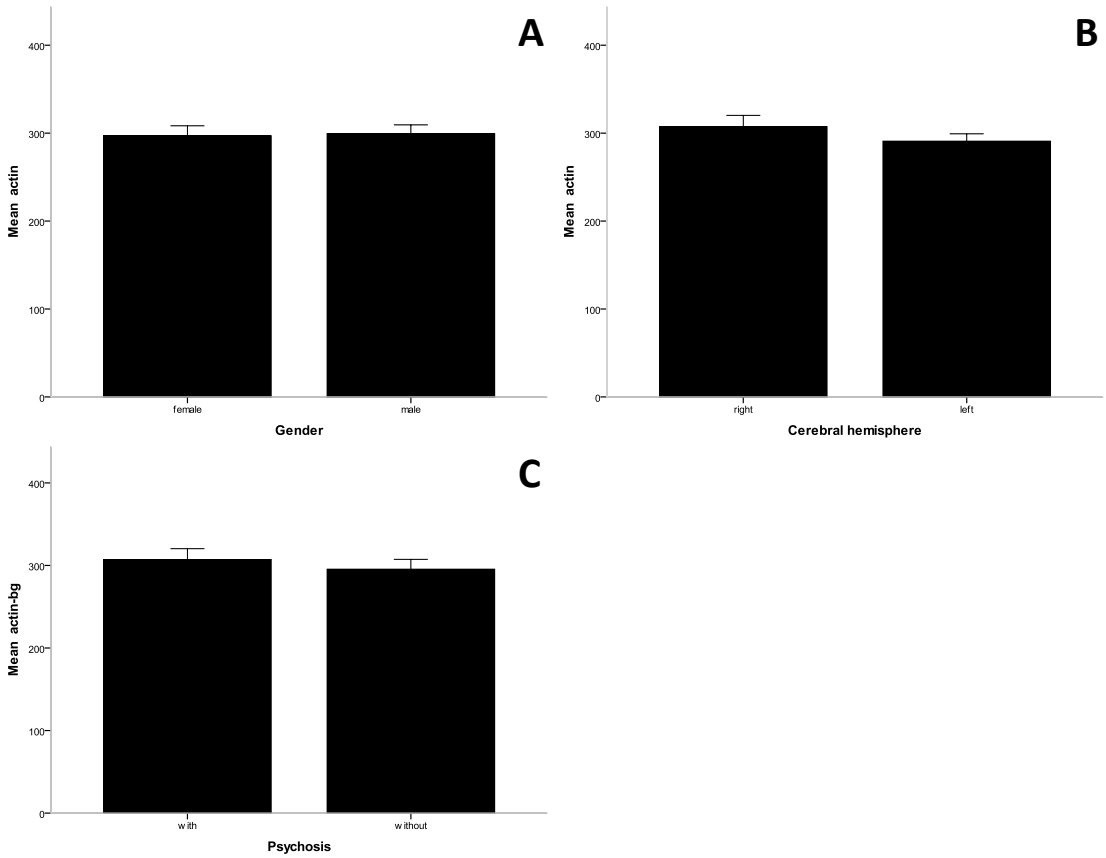

Figure 5-2: Mean (± SEM) fluorescence intensity for β-actin in the PSD depending on gender, side of the cerebral hemisphere and psychosis.

(A) Mean fluorescence intensity for β-actin after WB of the PSD fraction (Gender). (B) Mean fluorescence intensity for β-actin after WB of the PSD fraction (Cerebral hemisphere). (C) Mean fluorescence intensity for β-actin after WB of the PSD fraction (Psychosis).

The expression of β-actin was compared between groups of individu that died by suicide or not with Student's t-test analysis. In this study both expression of β-actin with (see Figure 5-3 A) and without (see Figure 5-3 B) the group control were compared. No significant effect of death by suicide was found for β-actin either with ($t(29.18) = 1.135$, $p = 0.266$) or without the group control ($t(43) = 0.908$, $p = 0.369$).

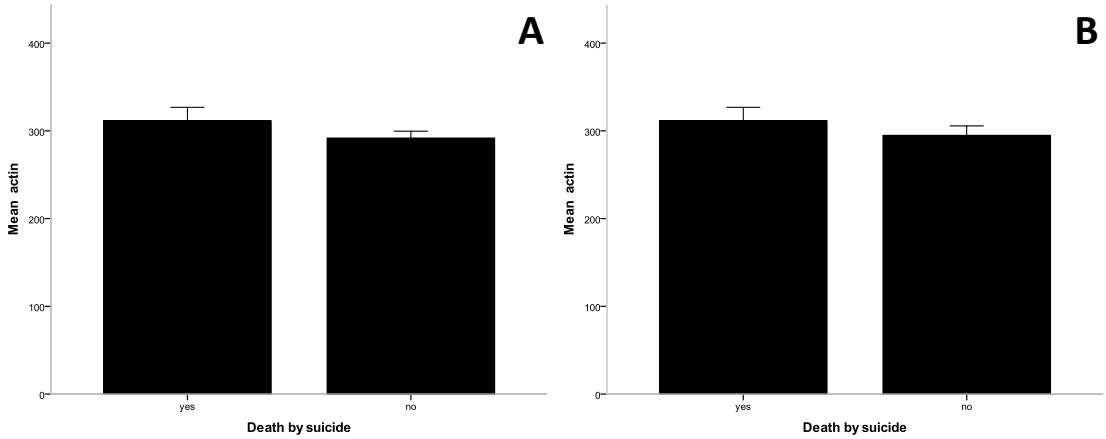

Figure 5-3: Mean (± SEM) fluorescence intensity for β-actin in the PSD fraction depending on death by suicide.

(A) Mean fluorescence intensity for β-actin after WB of the PSD fraction. (B) Mean fluorescence intensity for β-actin after WB of the PSD fraction (without controls).

One-way ANOVA statistical test was performed to compare the mean of the fluorescence intensity of β-actin between each of the degrees of severity of substance and alcohol abuse (see Figure 5-4 A). A trend towards a significant increase of the expression of β-actin ($F(4, 53) = 3.524$, $p = 0.064$) was found in the group moderate/present compared to the group none/little consummation of drug abuse. No significant effect of the severity of alcohol abuse ($F(5, 53) = 0.623$, $p = 0.683$) was observed on the expression of β-actin (see Figure 5-4 B).

Non-parametric correlation analysis of Spearman was performed to identify an eventual correlation between the expression of β-actin with the effect of the severity of substance and alcohol abuse. An increase of β-actin was significantly correlated with an increase of the severity of substance ($\rho(58) = 0.413$; $p = 0.001$) whereas no correlation was observed for the severity of alcohol abuse ($\rho(59) = 0.074$; $p = 0.579$).

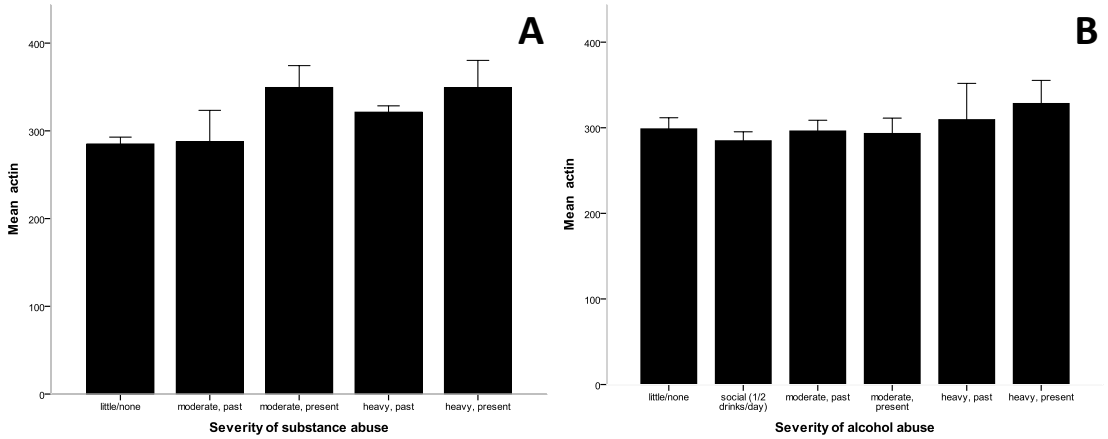

Figure 5-4: Mean (± SEM) fluorescence intensity for β-actin and β-III-tubulin in the PSD fraction depending on severity of substance and alcohol abuse.

(A) Mean fluorescence intensity for β-actin after WB of the PSD fraction. (B) Mean fluorescence intensity for β-III-tubulin after co-IP of the PSD fraction. (C) Mean fluorescence intensity for β-actin after WB of the PSD fraction. (D) Mean fluorescence intensity for β-III-tubulin after co-IP of the PSD fraction.

The effects of age at death, pH of the brain, mass of the brain, PMI and duration of storage of the brain on the expression of β-actin were examined with non-parametric correlation analysis. A significant negative correlation was found between age at death and expression of β-actin ($\rho(59) = -0.319$; $p = 0.014$) whereas pH of the brain, mass of the brain, PMI and duration of storage of the brain were found to have no effect (see Table 5-1).

The group control was removed and the effects of age at death, age of onset of disease, duration of diseases and life time quantity of fluphenazine or equivalent for the expression of β-actin were also examined with non-parametric correlation analysis. As previously observed in the study with the group control a significant negative correlation was found between age at death and the expression of β-actin ($\rho(45) = -0.375$; $p = 0.011$). Age of onset of disease, duration of diseases and life time quantity of

fluphenazine or equivalent were found to have no effect on the expression of β-actin (see Table 5-2).

Table 5-1: Correlational effects of demographic and peri-mortem factors on the expression of β-actin.

Spearman's correlation	Age at death	pH	Mass of the brain	PMI	Storage
β-actin (n=59)	**-0.319***	-0.174	0.151	0.213	0.177

***p<0.05**

Table 5-2: Correlational effects of demographic and peri-mortem factors on the expression of β-actin (without controls).

Spearman's correlation	Age at death	Age of onset of disease	Duration of disease	Life time quantity of fluphenazine or equivalent
β-actin (n=45)	**-0.375***	-0.186	-0.161	0.027

***p<0.05**

The expression of β-actin was affected by the effect of severity of substance abuse and the age at death. Consequently an ANCOVA statistical analysis was performed in order to reveal any significant difference of the mean of β-actin between diagnosis. No significant difference between diagnosis was found for β-actin ($F(3, 52) = 0.713$, $p = 0.549$) with the effect of severity of substance abuse and the age at death as co-variables. Subsequently β-actin was then used as denominator to normalise data from WB experiments.

5.4.2 Expression of TrkB in the PSD fraction and within the PSD

Means of the ratios TrkB/β-actin and TrkB/β-III-tubulin were compared between each diagnosis groups for both WB and co-IP experiments using one-way ANOVA statistical test (see Figure 5-5 A and B).

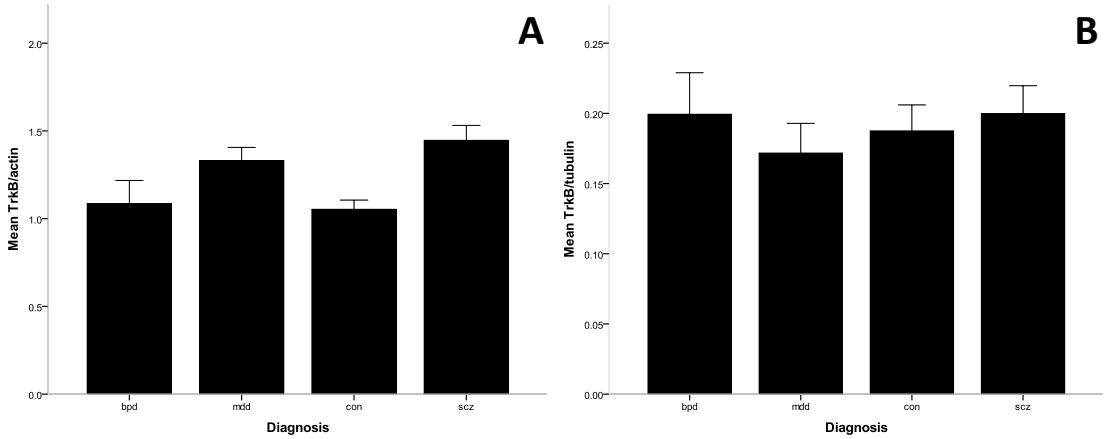

Figure 5-5: Mean (± SEM) ratios TrkB/β-actin and TrkB/β-III-tubulin in the PSD fraction and co-IP PSD epending on diagnosis.

(A) Mean ratio TrkB/β-actin after WB of the PSD fraction. (B) Mean ratio TrkB/β-III-tubulin after co-IP of the PSD fraction. (bpd) bipolar disorder ; (mdd) major depressive disorder ; (con) control ; (scz) schizophrenia. ANCOVA statistical analysis was performed with the pH of the brain and severity of substance abuse, the age at death as co-variables respectively for TrkB/β-actin (see Table 5-3) and TrkB/β-III-tubulin (see Figure 5-9 B and Table 5-4), no significant differences were found between diagnosis.

ANOVA revealed a trend towards an increase of the mean of the ratio TrkB/β-actin for the group with schizophrenia compared to the group control ($F(3, 50) = 3.675$, $p = 0.066$) and the group with bipolar disorder($F(3, 50) = 3.675$, $p = 0.057$). In contrast no significant difference of the means between diagnosis was observed for for the ratio TrkB/β-III-tubulin ($F(3, 52) = 0.330$, $p = 0.804$).

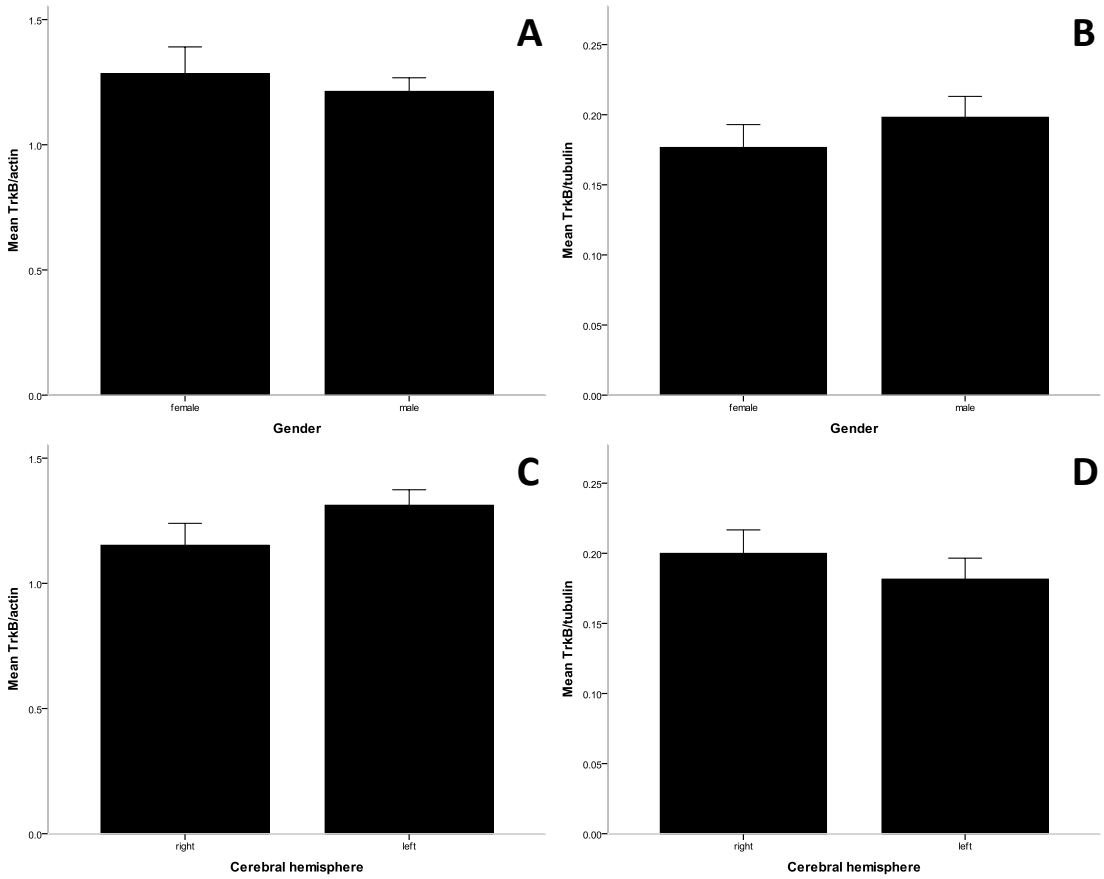

Figure 5-6: Mean (± SEM) ratios TrkB/β-actin and TrkB/β-III-tubulin in the PSD fraction and co-IP PSD depending on gender and side of the cerebral hemisphere.

(A) Mean ratio TrkB/β-actin after WB of the PSD fraction. (B) Mean ratio TrkB/β-III-tubulin after co-IP of the PSD fraction. (C) Mean ratio TrkB/β-actin after WB of the PSD fraction. (D) Mean ratio TrkB/β-III-tubulin after co-IP of the PSD fraction.

The expression of TrkB was compared in both genders (see Figure 5-6 A and B) and in both cerebral hemispheres (see Figure 5-6 C and D) for WB experiments and co-IP experiments with Student's t-test analysis. No significant difference was found between gender for both TrkB/β-actin ($t(52) = 0.659$, $p = 0.513$) and TrkB/β-III-tubulin ($t(54) = 0.937$, $p = 0.435$). No cerebral lateralisation was observed for both WB (TrkB/β-

actin: t(52) = 1.533, p = 0.131) and co-IP (TrkB/β-III-tubulin: t(54) = 0.822, p = 0.415) experiments.

The expression of TrkB was also compared in group of patients presenting or not psychotic symptoms for both WB experiments (see Figure 5-7 A) and co-IP experiments (see Figure 5-7 B) with Student's T-test analysis. As psychotic symptoms occur only in groups with psychiatric disorders the group control was removed from the analysis. No significant difference was found between groups with or without psychosis for both TrkB/β-actin (t(40.10) = 0.481, p = 0.633) and TrkB/β-III-tubulin (t(40) = 0.375, p = 0.710).

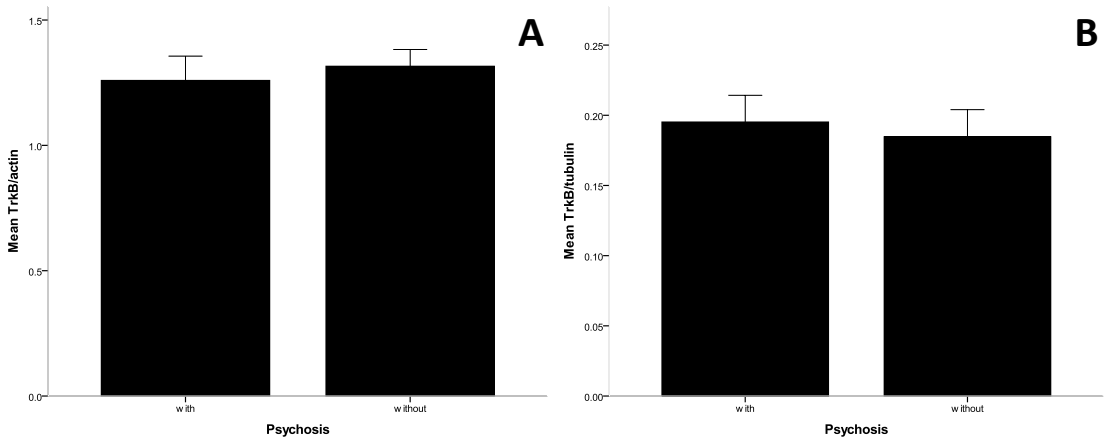

Figure 5-7: Mean (± SEM) ratios TrkB/β-actin and TrkB/β-III- in the PSD fraction and co-IP PSD depending on psychotic symptoms.

(A) Mean ratio TrkB/β-actin after WB of the PSD fraction. (B) Mean ratio TrkB/β-III-tubulin after co-IP of the PSD fraction.

Student's t-test analysis was also carried out to determine whether the expression of TrkB is different in groups of individuals that had death by suicide. This study was carried out with and without the group control and WB experiments (see Figure 5-8 A and C) and co-IP experiments (see Figure 5-8 B and D) were compared.

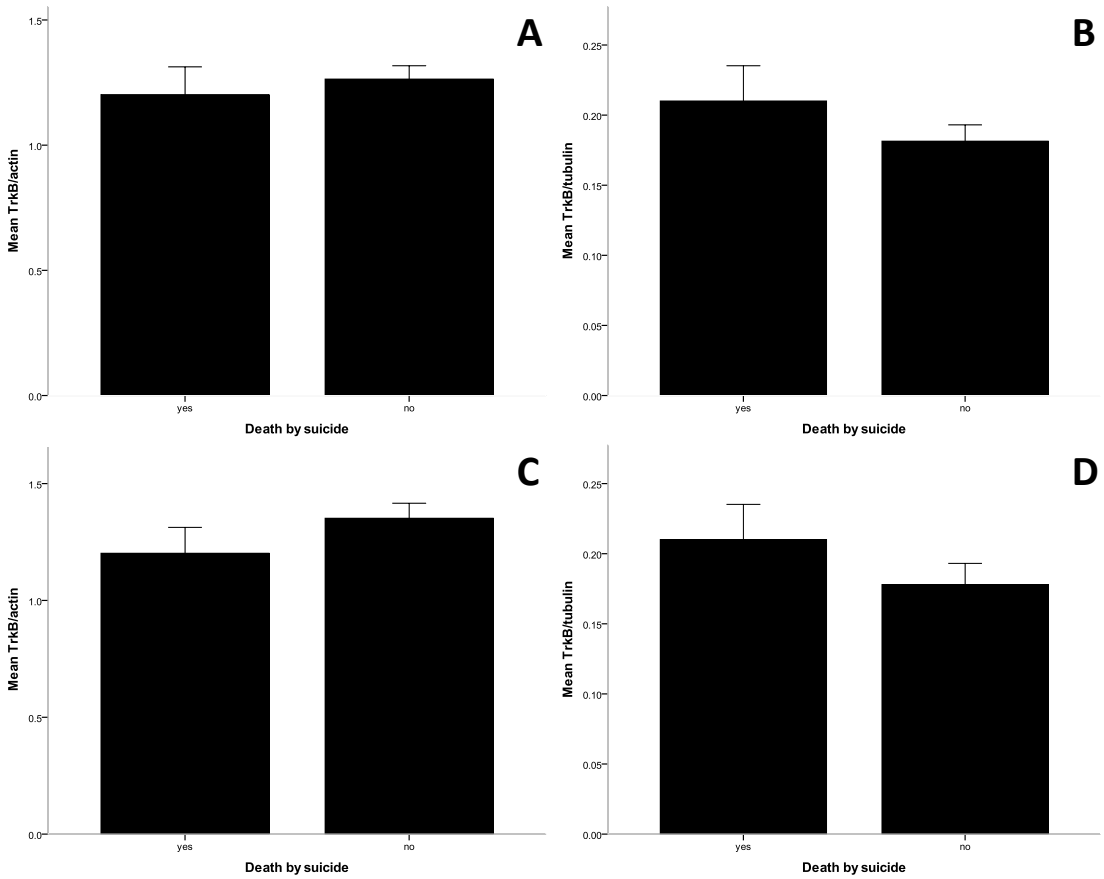

Figure 5-8: Mean (± SEM) ratios TrkB/β-actin and TrkB/β-III-tubulin in the PSD fraction and co-IP PSD depending on death by suicide.

(A) Mean ratio TrkB/β-actin after WB of the PSD fraction. (B) Mean ratio TrkB/β-III-tubulin after co-IP of the PSD fraction. (C) Mean ratio TrkB/β-actin after WB of the PSD fraction (without controls). (D) Mean ratio TrkB/β-III-tubulin after co-IP of the PSD fraction (without controls).

Student's t-test did not reveal any difference between the groups with death by suicide or not for both TrkB/β-actin ($t(27.91) = 0.505$, $p = 0.618$) and TrkB/β-actin ($t(42) = 1.217$, $p = 0.231$) respectively with or without the control group. For the co-IP Student's t-test for both with ($t(54) = 1.189$, $p = 0.240$) or without ($t(40) = 1.162$, $p = 0.252$) the control group showed no significant difference in the group with death by suicide for TrkB/β-III-tubulin.

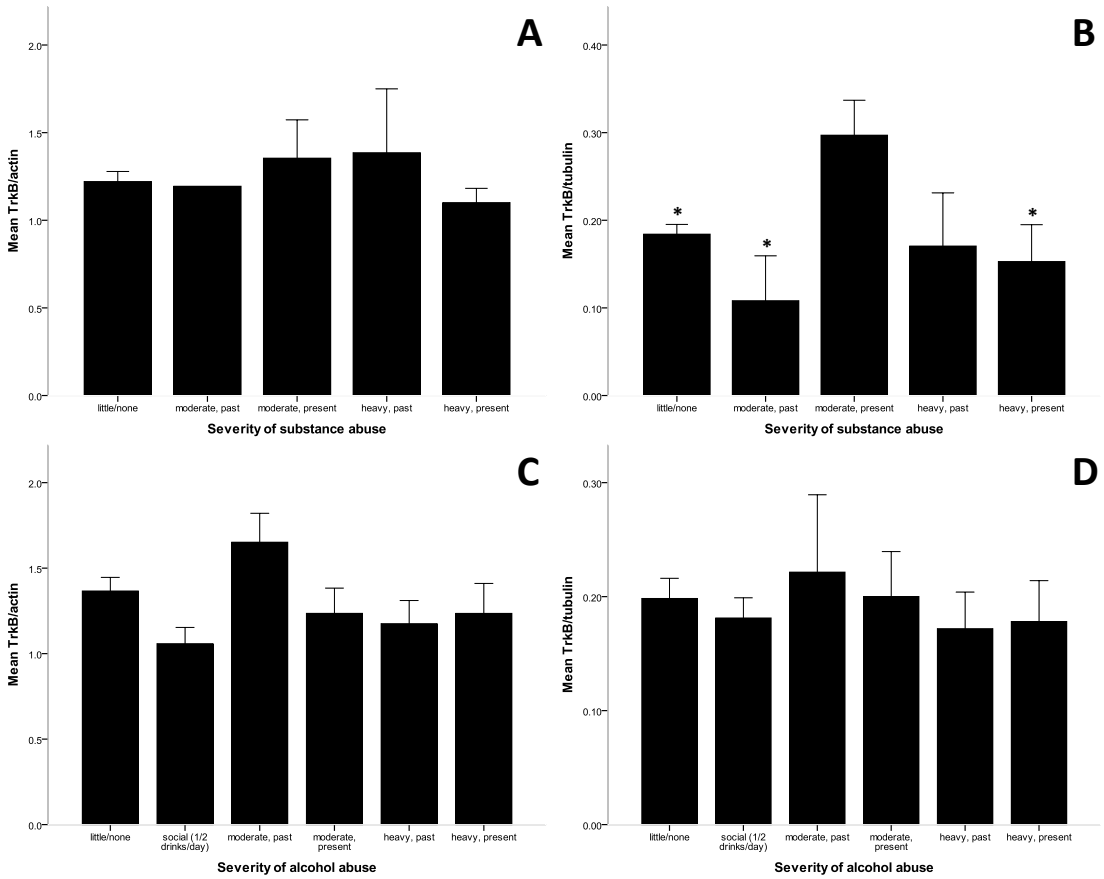

Figure 5-9: Mean (± SEM) ratios TrkB/β-actin and TrkB/β-III- in the PSD fraction and co-IP PSD depending on severity of substance and alcohol abuse.

(A) Mean ratio TrkB/β-actin after WB of the PSD fraction. (B) Mean ratio TrkB/β-III-tubulin after co-IP of the PSD fraction. (C) Mean ratio TrkB/β-actin after WB of the PSD fraction. (D) Mean ratio TrkB/β-III-tubulin after co-IP of the PSD fraction. Statistical test ANOVA with Bonferroni correction. Comparison with moderate, present substance abuse (* $p<0.05$).

One-way ANOVA statistical test was performed to compare the means of the ratios TrkB/β-actin and TrkB/β-III-tubulin between each group with different severity of substance and alcohol abuse for both WB (see Figure 5-9 A and C) and co-IP (see Figure 5-9 B and D) experiments. No significant difference was found between the groups with different severity of substance abuse for the ratio TrkB/β-actin ($F(3, 48) = 0.579$, $p = 0.632$) (see Figure 5-9 A) whereas a significant decrease of the mean of the ratio

TrkB/β-III-tubulin was found for the groups "none/little" ($F(4, 50) = 3.469$, $p = 0.029$), "moderate past" ($F(4, 50) = 3.469$, $p = 0.045$) and "heavy present" ($F(4, 50) = 3.469$, $p = 0.042$) compared to "moderate present" (see Figure 5-9 B). For the severity of alcohol abuse a trend towards a significant increase of the expression of TrkB ($F(5, 48) = 2.175$, $p = 0.084$) was revealed for the group "moderate present" compared to the group "social (1/2 drinks/day)" with WB experiments (see Figure 5-9 B). No significant effect of the severity of alcohol abuse ($F(5, 50) = 0.292$, $p = 0.915$) was observed with the co-IP experiments (see Figure 5-9 D).

Table 5-3: Correlational effects of demographic and peri-mortem factors on the ratios TrkB/β-actin and TrkB/β-III-tubulin.

Spearman's correlation	Age at death	pH	Mass of the brain	PMI	Storage
TrkB/β-actin (n=54)	-0.048	**-0.275***	-0.075	0.108	0.088
TrkB/β-III-tubulin (n=56)	-0.257	-0.129	-0.053	-0.182	0.104

***p<0.05**

Non-parametric correlation analysis of Spearman was performed in order to identify an eventual correlation between the expression of TrkB with the effect of the severity of substance and alcohol abuse. No correlation was found between the expression of TrkB and the severity of substance and acohol abuse either for WB (TrkB/β-actin: substance abuse: $\rho(53) = 0.073$; $p = 0.604$; alcohol abuse: $\rho(54) = -0.099$; $p = 0.478$) or co-IP experiments (TrkB/β-III-tubulin: substance abuse: $\rho(55) = -0.007$; $p = 0.960$; alcohol abuse: $\rho(56) = -0.074$; $p = 0.586$).

The effects of age at death, pH of the brain, mass of the brain, PMI and duration of storage of the brain for both TrkB/β-actin and TrkB/β-III-tubulin were examined with

non-parametric correlation analysis. A significant negative correlation was found between pH of the brain and expression of TrkB ($\rho(54) = -0.275$; $p = 0.044$) whereas age at death, mass of the brain, PMI and duration of storage of the brain were found to have no effect with WB experiments. Age at death, pH of the brain, mass of the brain, PMI and duration of storage of the brain were found to have no effect on the ratio TrkB/β-III-tubulin (see Table 5-3).

Table 5-4: Correlational effects of demographic and peri-mortem factors on the ratios TrkB/β-actin and TrkB/β-III-tubulin (without controls).

Spearman's correlation	Age at death	Age of onset of disease	Duration of disease	Life time quantity of fluphenazine or equivalent
TrkB/β-actin (n=44)	-0.084	0.056	-0.076	0.008
TrkB/β-III-tubulin (n=42)	**-0.311***	-0.124	-0.147	-0.044

***p<0.05**

For the effects of age at death, age of onset of disease, duration of diseases and life time quantity of fluphenazine or equivalent for both TrkB/β-actin and TrkB/β-III-tubulin the group control was removed. Non-parametric correlation analysis showed a significant negative correlation was found between age at death and the ratio TrkB/β-III-tubulin ($\rho(42) = -0.311$; $p = 0.045$). Age of onset of disease, duration of diseases and life time quantity of fluphenazine or equivalent were found to have no effect on the expression of TrkB/β-III-tubulin. Age at death, age of onset of disease, duration of diseases and life time quantity of fluphenazine or equivalent were found to have no effect on the expression of TrkB/β-actin (see Table 5-4).

To summarise the expression of TrkB was significantly affected by demographic and peri-mortem factors for both WB and co-IP experiments. A decrease of the ratio TrkB/β-actin was correlated with an increase of the pH of the brain and the ratio TrkB/β-III-tubulin wasd affected by the effect of severity of substance abuse and the age at death. Consequently an ANCOVA statistical analysis was performed for both WB and co-IP experiments. ANCOVA revealed a trend towards an increase of the mean of the ratio TrkB/β-actin for the group with schizophrenia compared to the group control ($F(3, 49) = 3.411$, $p = 0.078$) and the group with bipolar disorder($F(3, 49) = 3.411$, $p = 0.059$) and significant difference for the ratio TrkB/β-III-tubulin ($F(3, 49) = 0.391$, $p = 0.760$) between diagnosis groups.

5.4.3 Expression of TrkB-T1 in the PSD fraction and within the PSD

One-way ANOVA statistical test was used to compare the means of the ratios TrkB-T1/β-actin and TrkB-T1/β-III-tubulin for both WB and co-IP experiments (see Figure 5-10). One-way ANOVA statistical test was used to compare the means of the ratios TrkB-T1/β-actin and TrkB-T1/β-III-tubulin respectively for both WB and co-IP experiments (see Figure 5-10). For both WB and co-IP experiments no significant difference was revealed for the ratios TrkB-T1/β-actin ($F(3, 46) = 1.888$, $p = 0.145$) and TrkB-T1/β-III-tubulin ($F(3, 52) = 1.957$, $p = 0.132$) between diagnosis. The chart representing the mean of the ratio TrkB-T1/β-actin for each group of diagnosis showed an increase of the expression TrkB-T1 in the group with schizophrenia compared to the group control by WB (see Figure 5-10 A). Therefore a Student's t-test was performed to determinate whether the difference between the two groups was significant. A significant increase of the mean of the ratio TrkB-T1/β-actin ($t(21) = 2.741$, $p = 0.012$) was revealed using Student's t-test in the group with schizophrenia compared to control. For the co-IP experiments the chart representing the the difference of the means of TrkB-T1 between diagnosis showed a decrease of the ratio TrkB-T1 in the group with schizophrenia compared to the group control (see Figure 5-10 B). Student's

t-test revealed a significant decrease of the expression of TrkB-T1 for the group with schizophrenia compared to the group control (t(26) = 2.384, p = 0.025) and the group with bipolar disorder (t(20.60) = 2.101, p = 0.048). No significant difference of the mean of the ratio T-TrkB/β-III-tubulin was observed for the group with major depressive disorder compared to the group control or the group with bipolar disorder.

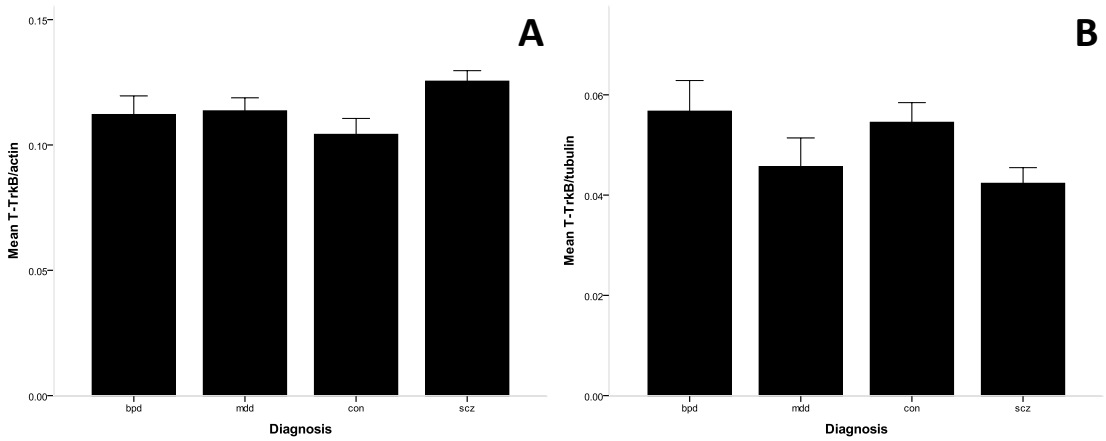

Figure 5-10: Mean (± SEM) ratios TrkB-T1/β-actin and TrkB-T1/β-III-tubulin in the PSD fraction and co-IP PSD depending on diagnosis.

(A) Mean ratio TrkB-T1/β-actin after WB of the PSD fraction. (B) Mean ratio TrkB-T1/β-III-tubulin after co-IP of the PSD fraction. (bpd) bipolar disorder ; (mdd) major depressive disorder ; (con) control ; (scz) schizophrenia. An ANCOVA statistical analysis was performed with the pH of the brain and the age at death, PMI, death by suicide as co-variables respectively for TrkB/β-actin (see Table 5-5) and TrkB/β-III-tubulin (see Table 5-5 and Figure 5-13 B), no significant differences were found between diagnosis.

The expression of TrkB-T1 by gender was compared for both WB and co-IP experiments (see Figure 5-11 A and B). No significant difference of the expression of TrkB-T1 (t(48) = 0.910, p = 0.367) was observed by WB whereas a trend towards a significant decrease of the expression of TrkB-T1 (t(54) = 1.879, p = 0.435) in female was revealed with the co-IP experiment. Comparison of the mean of the ratios TrkB-

T1/β-actin (t(48) = 1.161, p = 0.252) and TrkB-T1/β-III-tubulin (t(54) = 1.050, p = 0.299) in the right or the left cerebral hemisphere did not reveal any cerebral laterisation of the expression of TrkB-T1 with both WB and co-IP experiments (see Figure 5-11 C and D).

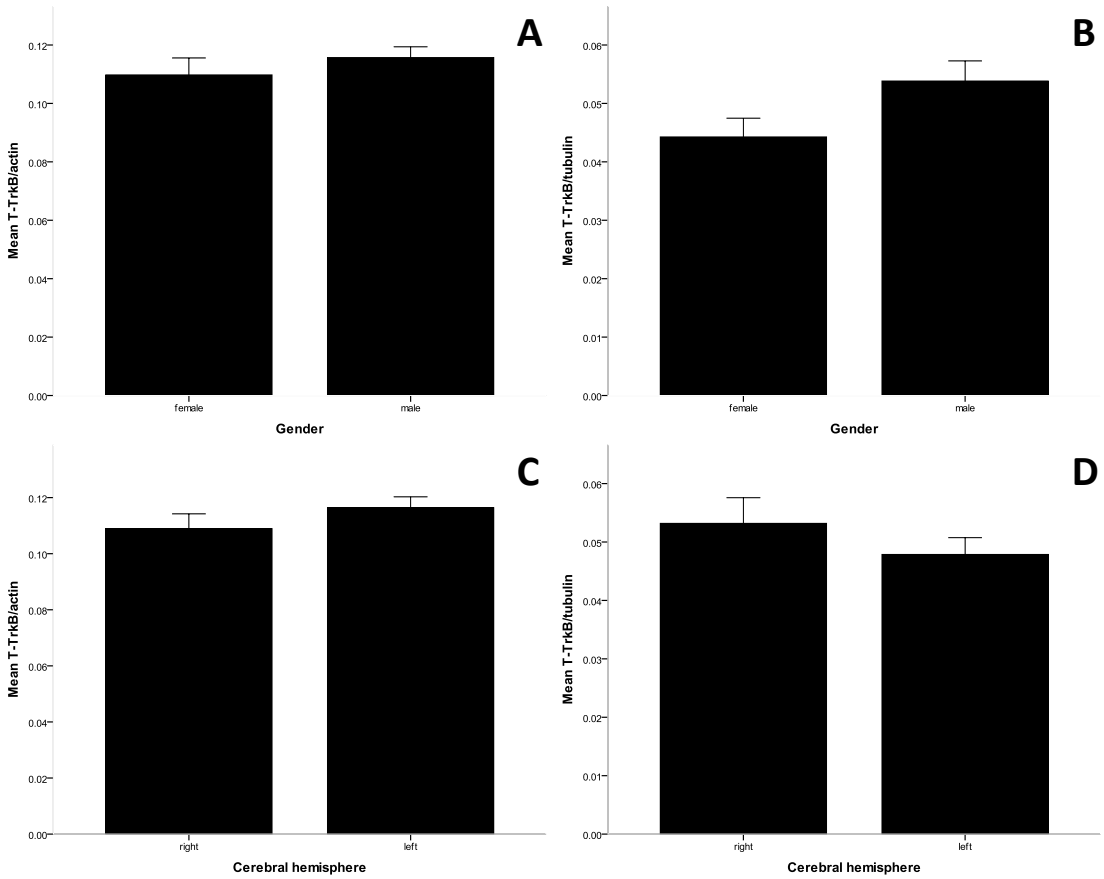

Figure 5-11: Mean (± SEM) ratios TrkB-T1/β-actin and TrkB-T1/β-III-tubulin in the PSD fraction and co-IP PSD depending on gender and side of the cerebral hemisphere.

(A) Mean ratio TrkB-T1/β-actin after WB of the PSD fraction. (B) Mean ratio TrkB-T1/β-III-tubulin after co-IP of the PSD fraction. (C) Mean ratio TrkB-T1/β-actin after WB of the PSD fraction. (D) Mean ratio TrkB-T1/β-III-tubulin after co-IP of the PSD fraction.

To determine whether the psychotic symptoms have an effect on the dependent variables TrkB-T1/β-actin and TrkB-T1/β-III-tubulin respectively for WB experiments (see Figure 5-12 A) and co-IP experiments (see Figure 5-12 B) Student's t-test analysis was performed. For this study the group control was removed from the analysis. No significant effect of psychosis was found for both ratios TrkB-T1/β-actin ($t(36) = 1.150$, $p = 0.258$) and TrkB-T1/β-III-tubulin ($t(39) = 0.417$, $p = 0.679$).

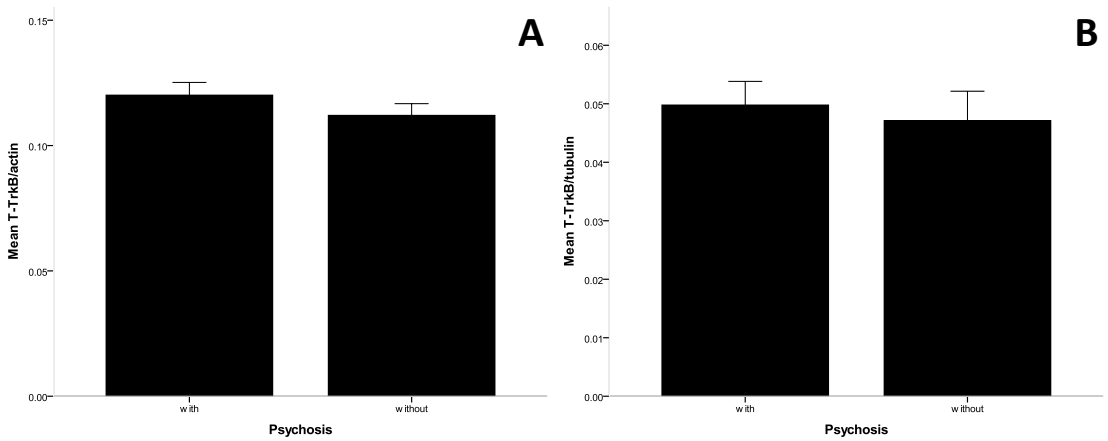

Figure 5-12: Mean (± SEM) ratios TrkB-T1/β-actin and TrkB-T1/β-III- in the PSD fraction and co-IP PSD depending on psychotic symptoms.

(A) Mean ratio TrkB-T1/β-actin after WB of the PSD fraction. (B) Mean ratio TrkB-T1/β-III-tubulin after co-IP of the PSD fraction.

The expression of TrkB-T1 was measured for both groups death by suicide or not with both WB and co-IP experiments (see Figure 5-13). Student's t-test analysis revealed a trend towards a significant decrease of the mean of the ratio TrkB-T1/β-actin ($t(48) = 1.701$, $p = 0.095$) in the group with death by suicide when the group control was included in the study (see Figure 5-13 A). A significant decrease of the mean of the ratio TrkB-T1/β-actin ($t(26.55) = 2.745$, $p = 0.011$) in the group with death by suicide when the group control was removed (see Figure 5-13 C). For the co-IP experiment a

significant increase of the expression of TrkB-T1 in the group with death by suicide was found for both TrkB-T1/β-III-tubulin (t(54) = 2.528, p = 0.014) and TrkB-T1/β-III-tubulin (t(39) = 3.289, p = 0.002) respectively with (see Figure 5-13 B) or without (see Figure 5-13 D) the group control.

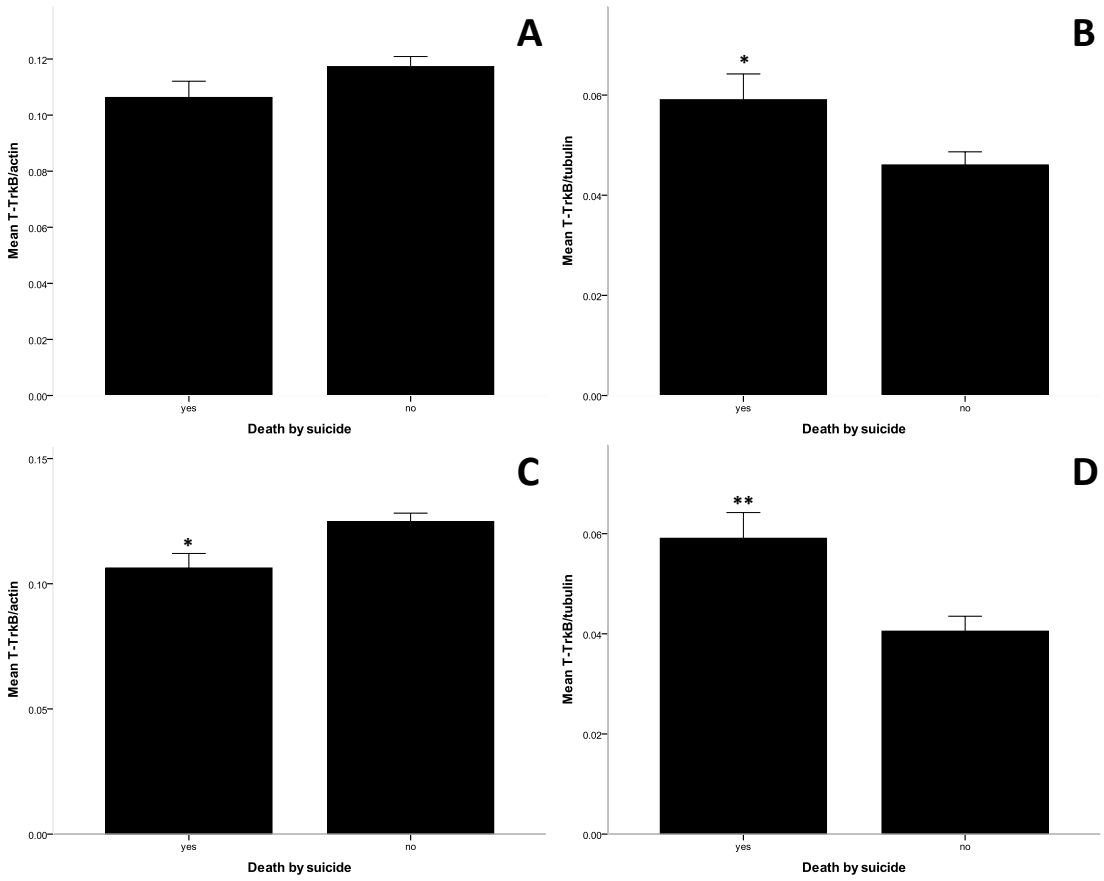

Figure 5-13: Mean (± SEM) ratios TrkB-T1/β-actin and TrkB-T1/β-III- in the PSD fraction and co-IP PSD depending on death by suicide.

(A) Mean ratio TrkB-T1/β-actin after WB of the PSD fraction. (B) Mean ratio TrkB-T1/β-III-tubulin after co-IP of the PSD fraction. (C) Mean ratio TrkB-T1/β-actin after WB of the PSD fraction (without controls). (D) Mean ratio TrkB-T1/β-III-tubulin after co-IP of the PSD fraction (without controls). Statistical Student's t test (* p<0.05; ** p<0.01).

The effects of the severity of substance and alcohol abuse on the expression of TrkB-T1 were assessed for both both WB (see Figure 5-14 A and C) and co-IP (see Figure 5-14 B and D) experiments with one-way ANOVA statistical test.

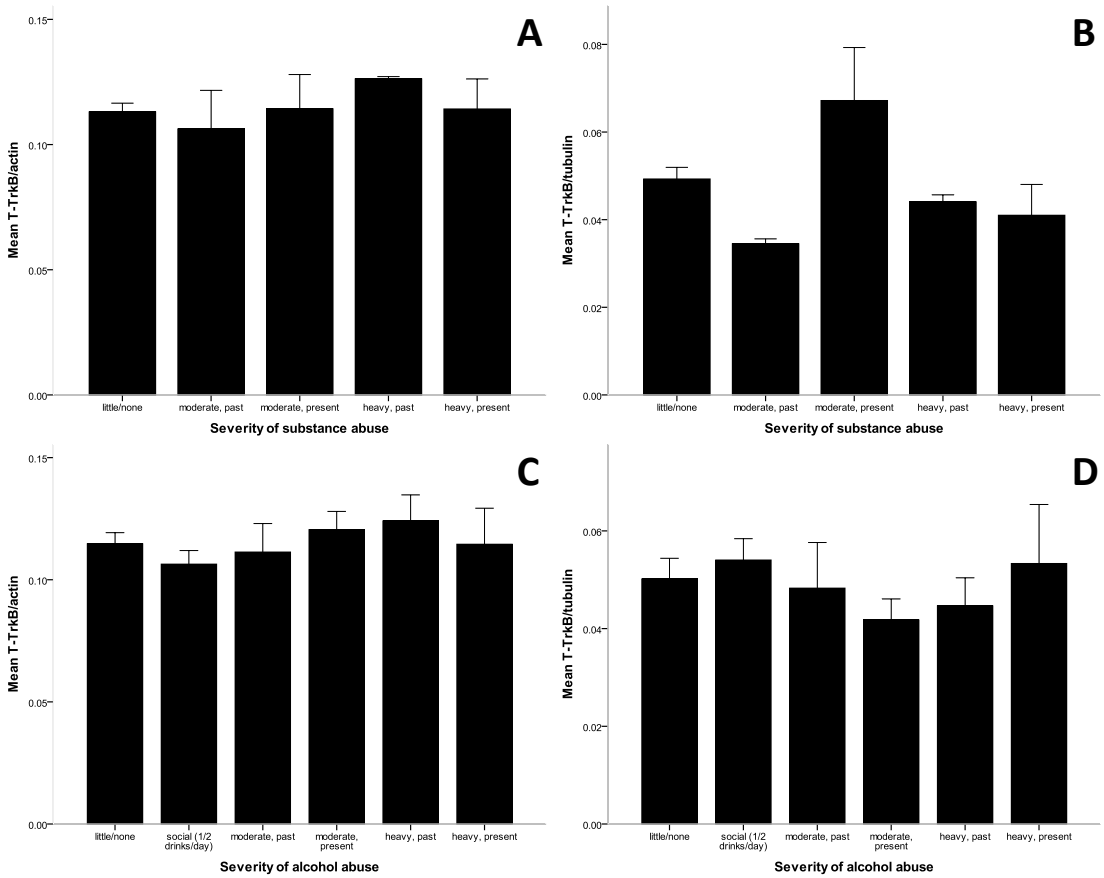

Figure 5-14: Mean (± SEM) ratios TrkB-T1/β-actin and TrkB-T1/β-III-tubulin in the PSD fraction and co-IP PSD depending on severity of substance and alcohol abuse.

(A) Mean ratio TrkB-T1/β-actin after WB of the PSD fraction. (B) Mean ratio TrkB-T1/β-III-tubulin after co-IP of the PSD fraction. (C) Mean ratio TrkB-T1/β-actin after WB of the PSD fraction. (D) Mean ratio TrkB-T1/β-III-tubulin after co-IP of the PSD fraction.

No significant difference was found for both TrkB-T1/β-actin (Substance abuse: $F(4, 45) = 0.212$, $p = 0.931$; Alcohol abuse: $F(5, 44) = 0.654$, $p = 0.660$) and TrkB-T1/β-III-tubulin

(Substance abuse: F(4, 50) = 2.199, p = 0.083; Alcohol abuse: F(5, 50) = 0.500, p = 0.775) neither for the effect of the severity of substance abuse (see Figure 5-14 A and B) nor the effect of the severity of alcohol abuse (see Figure 5-14 C and D).

To identify a correlation between the expression of TrkB-T1/β-actin and TrkB-T1/β-III-tubulin with the effect of the severity of substance and alcohol abuse a non-parametric correlation analysis of Spearman was performed. No significant correlation was observed between the severity of substance abuse and both ratios TrkB-T1/β-actin (ρ(50) = 0.018; p = 0.900) and TrkB-T1/β-III-tubulin (ρ(55) = -0.065; p = 0.639). Neither the ratio T-TrkB/β-actin (ρ(50) = 0.089; p = 0.538) nor the ratio TrkB-T1/β-III-tubulin (ρ(56) = -0.130; p = 0.340) were significantly correlated with an increase of the severity of alcohol abuse.

Table 5-5: Correlational effects of demographic and peri-mortem factors on the ratios TrkB-T1/β-actin and TrkB-T1/β-III-tubulin.

Spearman's correlation	Age at death	pH	Mass of the brain	PMI	Storage
TrkB-T1/β-actin (n=50)	0.072	**-0.394****	0.029	-0.109	0.121
TrkB-T1/β-III-tubulin (n=56)	**-0.305***	0.061	0.106	**-0.315***	-0.075

***p<0.05; **p<0.01**

The effects of age at death, pH of the brain, mass of the brain, PMI and duration of storage of the brain for both TrkB-T1/β-actin and TrkB-T1/β-III-tubulin were examined with non-parametric correlation analysis. A significant negative correlation was found between the pH of the brain and the ratio TrkB-T1/β-actin (ρ(50) = -0.394; p = 0.005) whereas age at death, mass of the brain, PMI and duration of storage of the brain

were found to have no effect. The pH of the brain, mass of the brain and duration of storage of the brain were found to have no effect on expression of TrkB-T1/β-III-tubulin whereas a decrease of the expression of TrkB-T1 was significantly correlated with an increase of the age at death ($\rho(56) = -0.305$; $p = 0.022$) and the post-mortem interval ($\rho(56) = -0.315$; $p = 0.018$) (see Table 5-5).

For the effects of age at death, age of onset of disease, duration of diseases and life time quantity of fluphenazine or equivalent on the expression of TrkB-T1 the group control was removed and were also examined with non-parametric correlation analysis. A significant negative correlation was found between age at death and the ratio TrkB-T1/β-III-tubulin ($\rho(41) = -0.420$; $p = 0.009$). Age of onset of disease, duration of diseases and life time quantity of fluphenazine or equivalent were found to have no effect on the ratio TrkB-T1/β-III-tubulin. Age at death, age of onset of disease, duration of diseases and life time quantity of fluphenazine or equivalent were found to have no effect on the the ratio TrkB-T1/β-actin (see Table 5-6).

Table 5-6: Correlational effects of demographic and peri-mortem factors on the ratios T-TrkB/β-actin and T-TrkB/β-III-tubulin (without controls).

Spearman's correlation	Age at death	Age of onset of disease	Duration of disease	Life time quantity of fluphenazine or equivalent
TrkB-T1/β-actin (n=38)	0.109	0.237	0.021	0.198
TrkB-T1/β-III-tubulin (n=41)	**-0.420****	-0.244	-0.082	0.015

****p<0.01**

To summarise the expression of TrkB-T1/β-III-tubulin was significantly affected by demographic and peri-mortem factors death by suicide, age at death and PMI for the co-IP experiments whereas for the expression of TrkB-T1/β-actin with the pH of the brain. Consequently an ANCOVA statistical analysis was performed to assess whether any significant difference of the mean of TrkB-T1/β-actin and TrkB-T1/β-III-tubulin for each diagnosis group would appear with the effect of demographic and peri-mortem factors as co-variables. No significant difference between diagnosis was found for TrkB-T1/β-actin ($F(3, 45) = 1.470$, $p = 0.235$) and for TrkB-T1/β-III-tubulin ($F(3, 49) = 2.209$, $p = 0.099$) with the effect of demographic and peri-mortem factors as co-variables.

5.4.4 Expression of p75 within the PSD

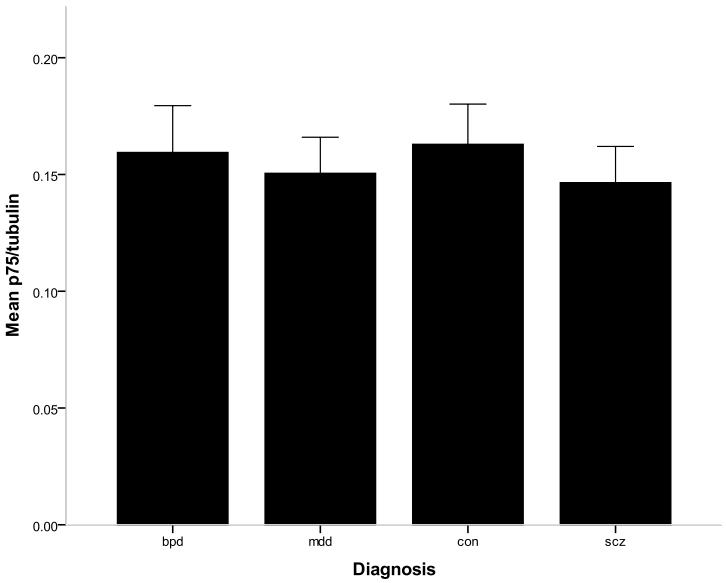

Figure 5-15: Mean (± SEM) ratio p75/β-III-tubulin co-IP PSD depending on diagnosis.

Mean ratio p75/β-III-tubulin after co-IP of the PSD fraction. (bpd) bipolar disorder ; (mdd) major depressive disorder ; (con) control ; (scz) schizophrenia.

For the WB experiments the signal from p75 was not ditinguishable from the background of the membranes, consequently the analysis of the expression of p75 was only carried out using co-IP experiments. The mean of the ratio p75/β-III-tubulin was compared between each diagnosis groups using one-way ANOVA statistical test (see Figure 5-15). For the ratio p75/β-III-tubulin ($F(3, 45) = 0.191$, $p = 0.902$) no significant changes between diagnosis were found.

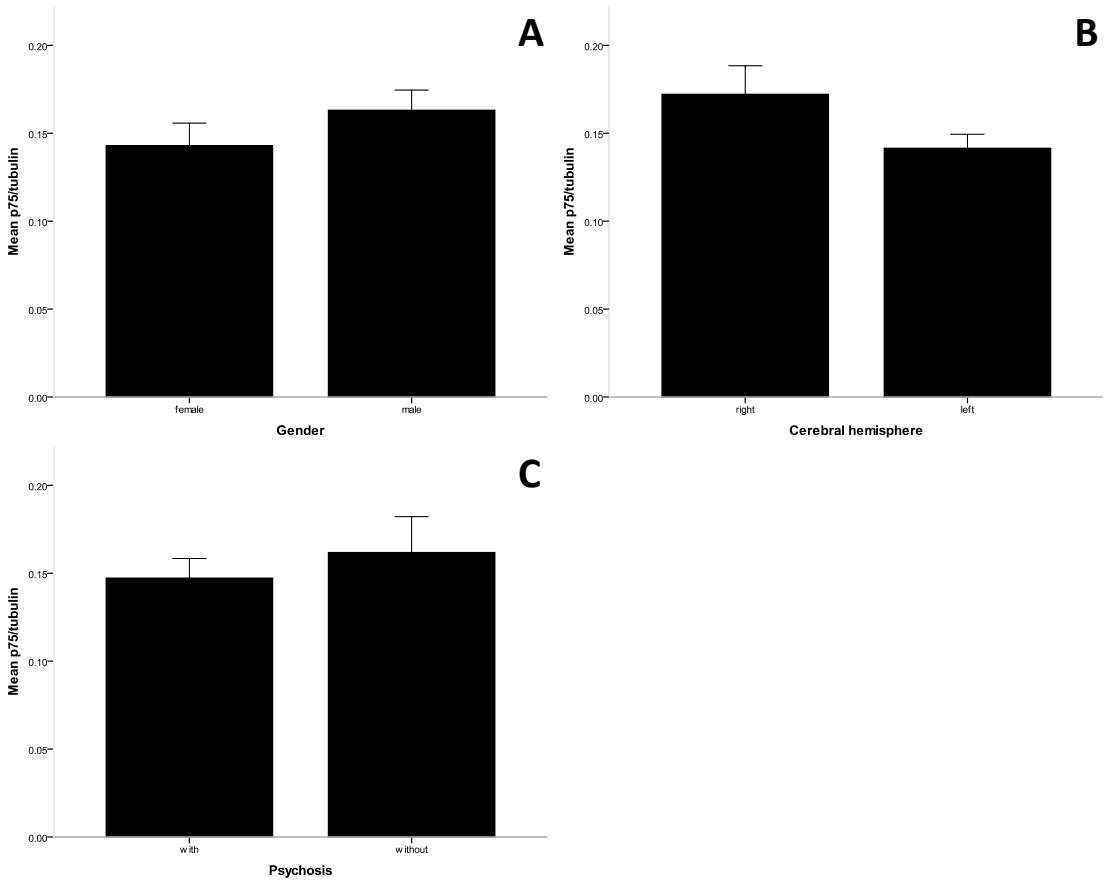

Figure 5-16: Mean (± SEM) ratio p75/β-III-tubulin co-IP PSD depending on gender, side of the cerebral hemisphere and psychotic symptoms.

(A) Mean of p75/β-III-tubulin after co-IP of the PSD fraction (gender). (B) Mean ratio p75/β-III-tubulin after co-IP of the PSD fraction (cerebral hemisphere) (C) Mean ratio p75/β-III-tubulin after co-IP of the PSD fraction (psychosis).

The effects of gender (see Figure 5-16 A), the side of the cerebral hemisphere (see Figure 5-16 B) on the ratio p75/β-III-tubulin were examined with Student's T-test analysis. No significant effect of gender was found for both p75/β-III-tubulin ($t(47) = 1.141$, $p = 0.260$). A trend towards a decrease of the ratio p75/β-III-tubulin ($t(30.88) = 1.707$, $p = 0.098$) was found in the left side of cerebral premotor cortex.

For the effect of psychotic symptoms the group control was removed from the analysis (see Figure 5-16 C). Student's t-test analysis did not show any significant effect of psychosis on the ratio p75/β-III-tubulin ($t(34) = 0.686$, $p = 0.497$).

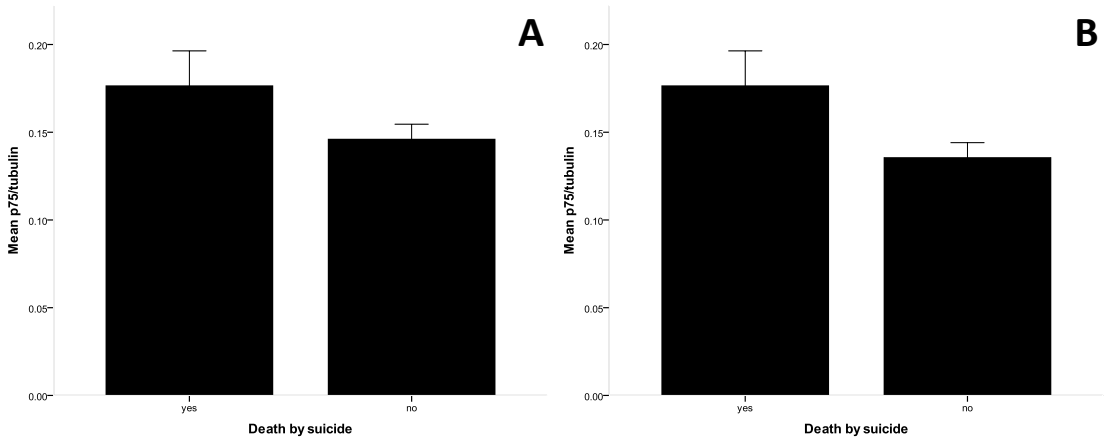

Figure 5-17: Mean (± SEM) ratio p75/β-III-tubulin co-IP PSD depending on death by suicide (co-IP).

(A) Mean ratio p75/β-III-tubulin after co-IP of the PSD fraction. (B) Mean ratio p75/β-III-tubulin after co-IP of the PSD fraction (without controls).

For the effect of death by suicide on the ratio p75/β-III-tubulin (see Figure 5-17 A and B), a Student's t-test analysis was carried out with and without the group control. No significant effect of death by suicide was found for the ratio p75/β-III-tubulin ($t(47) = 1.651$, $p = 0.105$) with the group control. Student's t-test for the ratio p75/β-III-tubulin

without the group control revealed a trend (t(19.18) = 1.888, p = 0.074) towards a significant decrease in the group without death by suicide.

One-way ANOVA statistical test was performed to compare the mean of the ratio p75/β-III-tubulin between each severity of substance (see Figure 5-18 A) and alcohol (see Figure 5-18 B) abuse. No significant difference between the means of the ratio p75/β-III-tubulin either for effect of the severity of substance abuse (F(4, 43) = 0.941, p = 0.450) or the effect of the severity of alcohol abuse (F(5, 43) = 0.812, p = 0.548) was observed.

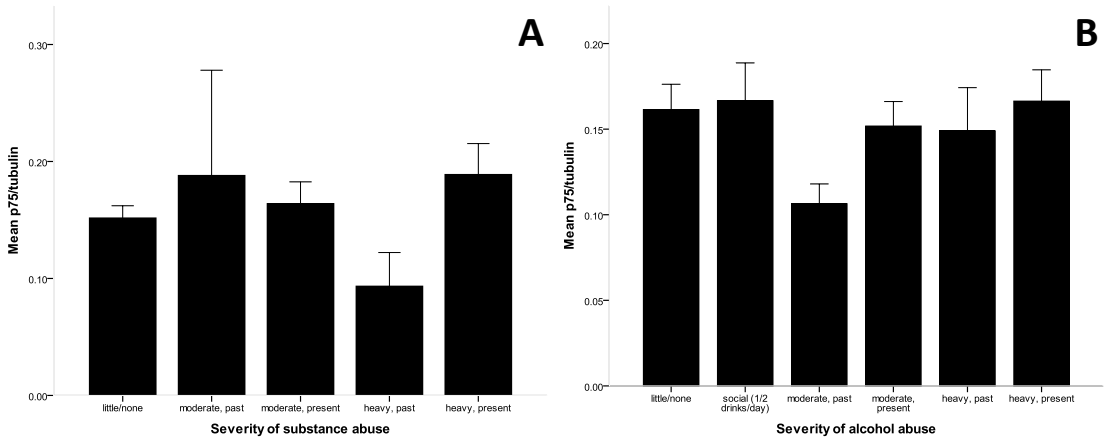

Figure 5-18: Mean (± SEM) ratio p75/β-III-tubulin co-IP PSD depending on severity of substance and alcohol abuse.

(A) Mean ratio p75/β-III-tubulin after co-IP of the PSD fraction (substance abuse). (B) Mean ratio p75/β-III-tubulin after co-IP of the PSD fraction (alcohol abuse).

To identify an eventual correlation between the expression of p75 with the effect of the severity of substance and alcohol abuse a non-parametric correlation analysis of Spearman was performed. No correlation was found between the mean of the ratio p75/β-III-tubulin either for the effect of the severity of substance abuse (ρ(48) = 0.094; p = 0.524) or the effect of the severity of alcohol abuse (ρ(49) = -0.050; p = 0.735).

Table 5-7: Correlational effects of demographic and peri-mortem factors on the ratio p75/β-III-tubulin.

Spearman's correlation	Age at death	pH	Mass of the brain	PMI	Storage
p75/β-III-tubulin (n=49)	-0.117	0.175	0.090	-.0173	-0.024

The effects of the age at death, the pH of the brain, the mass of the brain, the PMI and the duration of storage of the brain for the p75/β-III-tubulin were examined with non-parametric correlation analysis. No significant correlation was found between the ratio p75/β-III-tubulin and the demographic and peri-mortem factors (see Table 5-7).

The effects of age at death, age of onset of disease, duration of diseases and life time quantity of fluphenazine or equivalent for both β-actin and p75/β-III-tubulin were also examined with non-parametric correlation analysis. No significant correlation was found between the ratio p75/β-III-tubulin and the demographic and peri-mortem factors (see Table 5-8).

Table 5-8: Correlational effects of demographic and peri-mortem factors on the ratio p75/β-III-tubulin (without controls).

Spearman's correlation	Age at death	Age of onset of disease	Duration of disease	Life time quantity of fluphenazine or equivalent
p75/β-III-tubulin (n=36)	-0.253	-0.320	-0.063	-0.208

To summarise the expression of p75 was not significantly affected by any of the demographic and peri-mortem factors and subsequently no ANCOVA statistical analysis was performed.

5.5 Discussion and conclusions

This part of the thesis has established:

1. **That the expression of neurotrophic receptors involved in synaptic plasticity TrkB, T1-TrkB and p75 is not disturbed in any psychiatric disorder tested in this study compared to healthy control.**
2. **That intra-post-synaptic expression of the neurotrophic receptor T1-TrkB is decreased in bipolar disorder and schizophrenia when only compared to healthy control.**
3. **That extra-post-synaptic expression of the neurotrophic receptor T1-TrkB is increased schizophrenia when only compared to healthy control.**

Previous postmortem studies of TrkB have revealed a decrease in its expression in several regions of the brain in schizophrenia. One study assessed TrkB protein in the anterior cingulate cortex and hippocampus and found reduced expression in both regions (Takahashi et al., 2000). In another study, the distribution and localisation of TrkB in the hippocampal formation was assessed in schizophrenia. They immuno-labelled TrkB-positive neurons showed a signet-ring like shape in the hippocampus of healthy individual brains whereas no such findings were observed in neurons from schizophrenic patient brains (Iritani et al., 2003). These studies indicate that TrkB function may be disturbed in patients with schizophrenia. However, a study using immunohistochemistry and immunoblotting to quantify protein expression of TrkB in the cerebellum found reductions in TrkB expression in bipolar disorder, but not

schizophrenia (Soontornniyomkij et al., 2011). This study suggests that the expression of TrkB may be disturbed in a regionally specific manner in schizophrenia.

A study investigating TrkB mRNA expression suggested specific cell type disturbance in the DLPFC of patients with schizophrenia. The authors measured TrkB mRNA levels using *in situ* hybridisation. TrkB mRNAs were detected in large and small neurons in multiple cortical layers of the human DLPFC. They found significantly reduced expression of TrkB mRNA in large neurons in multiple cortical layers of patients with schizophrenia whereas the decrease of TrkB mRNA within the small neurons was not statistically significant (Weickert et al., 2005). Since neurons in the DLPFC integrate and communicate signals to various cortical and subcortical regions, these cell-type associated reductions in TrkB receptor may compromise the function and plasticity of the DLPFC and other areas of the brain in schizophrenia. A study reported a specific regional disturbance in the expression of TrkB mRNA within the hippocampus. Using *in situ* hybridisation in dentate gyrus, cornu ammonis subfields (CA1-4) subiculum and associated entorhinal cortex they found that the expression of TrkB mRNA was only reduced in CA4 in patients with schizophrenia compared with healthy subjects (Ray et al., 2011). Abnormal TrkB expression in specific region of the hippocampus of individuals with schizophrenia indicates that fundamental properties of hippocampal signalling transmission and plasticity may be affected in a specific neuronal network.

In the present study our measurement of TrkB protein levels within the PSD using co-IP and WB did not show any significant changes in the expression of TrkB in the premotor cortex of patients with any psychiatric disorders (see section 5.4.2). However, a trend increase in the expression of TrkB in the premotor cortex of patients with schizophrenia was found compared to bipolar disorder ($F(3, 49) = 3.411$, $p = 0.059$) and healthy individuals ($F(3, 49) = 3.411$, $p = 0.078$). The difference between the results obtained by co-IP and WB may be due the presence of glial contaminants in the PSD fraction, as glial cells express TrkB (Frisen et al., 1993). Also, the fact that we did not find any significant change in the expression of TrkB in the premotor cortex may be due to disease-associated regionally specific expression changes.

The heterozygous reeler mouse has been used as an animal model for schizophrenia based on several neuropathological and behavioural abnormalities homologous to schizophrenia. A study showed that in these mice both mRNA and protein levels of TrkB-T1 were significantly higher in the PFC (Pillai and Mahadik, 2008). For TrkB-T1, postmortem studies have reported variable results in schizophrenia depending on the area of the brain studied. A study using qPCR reported increased expression of TrkB-T1 mRNA in the DLPFC of patients with schizophrenia. In addition this study showed a significant decreases of the ratio TrkB/TrkB-T1 in schizophrenia for both mRNA and protein expression (Wong *et al.*, 2011). This study suggests that an imbalance of the neurotrophin receptors may be implicated in the pathophysiology of schizophrenia. However, a recent study using formalin-fixed paraffin-embedded hippocampal sections and immunoautoradiography revealed no changes in TrkB-T1 expression in schizophrenia (Dunham et al., 2009).

In the present study, neither co-IP nor WB of the PSD showed any significant change in the expression of TrkB-T1 for any of the psychiatric disorders (see section 5.4.3). However, using Student's t-test, co-IP of the PSD revealed that the expression of TrkB-T1 was significantly reduced in schizophrenia compared to healthy individuals ($t(26) = 2.384$, $p = 0.025$) and bipolar disorder ($t(20.60) = 2.101$, $p = 0.048$). By contrast for WB, a significant increase ($t(21) = 2.741$, $p = 0.012$) was revealed using Student's t-test for schizophrenia relative to healthy subjects. These results suggest that the expression of TrkB-T1 may be disturbed in schizophrenia and that the level of expression of TrkB-T1 may differ depending on the sub-cellular localisation.

No significant changes in expression levels for p75 were found in the heterozygous reeler mouse model of schizophrenia (Pillai and Mahadik, 2008). In addition, a postmortem study using immunoautoradiography showed no change of the expression of p75 in the hippocampus of patients with schizophrenia (Dunham et al., 2009). In the present study the expression of p75 was decreased in major depressive disorder and schizophrenia compared to healthy subjects (see section 5.4.4), however these did not

reach statistical significance. These results suggest that the expression of p75 is not altered in the premotor cortex of patients with schizophrenia.

Taken together, previous studies and findings from the present study suggest that neurotrophin receptors may be disturbed in schizophrenia in a regional and/or cellular specific manner. In the premotor cortex none of the neurotrophin receptors tested was altered in schizophrenia relative to major depressive disorder, bipolar disorder and healthy controls. However the expression of TrkB-T1 was altered when the schizophrenia group was assessed separately relative to controls. This contributes to previous evidence that an imbalance between the neurotrphin receptor subtypes may occur in schizophrenia.

6 General conclusions and future work

The aims of the studies presented in this thesis were to determine a possible change in the expression of proteins of the PSD involved in glutamatergic synaptic plasticity in premotor cortex in schizophrenia. Firstly, the method used to extract and purify the PSD was characterised using WB and TEM. Then protein expression studies were carried out using WB and co-IP. The ratio of NMDAR subunit NR2A, PSD-95, CaMKIIα, CaMKIIβ, NSF, TrkB, TrkB-T1 and p75 with β-actin and β-tubuin respectively for WB and co-IP was compared between schizophrenia, major depressive disorder, bipolar disorder and healthy controls.

6.1 Extraction and characterisation of the PSD fractions

6.1.1 Protocol of extraction of PSD

The method based on sucrose gradient separation developed in the present study to extract the PSD from human premotor cortex may be used to the parallel identification of compositional and post-transcriptional changes of proteins within the PSDs. Semi-quantitative analysis of protein levels as well as post-transcriptional modifications such as phosphorylation between different protein mixtures may become a powerful tool for human postmortem studies of the diturbances of the glutamatergic system associated with psychiatric disorders. Indeed, a typical PSD preparation uses brain tissue in gram quantities (Carlin et al., 1980; Hahn et al., 2009) whilst the present study only uses a few milligrams.

6.1.2 Characterisation of the PSD fractions

- **Transmission Electron Microscopy**

The presence of the PSDs from extracted PSD fractions was confirmed using TEM. The electron micrographs showed a heterogenic composition of the PSD. Indeed PSDs were detected, in addition to contaminants that resembled CaMKII clusters, mitochondria,

myelin and membrane vesicles. These results were in-line with previous studies using the same PSD isolation technique (Dosemeci et al., 2006).

- **Western Blotting**

The PSD-95, NR2A of the NMDAR, and subunits 2, 3 and 4 of AMPAR were all detected and enriched in the PSD fractions. Semi-quantitative analysis of the amount of PSD-95, NR2A and AMPAR subunits was carried out from six independent experiments of the isolation of the PSDs. The results showed a significant increase of the expression of PSD-95, NR2A and AMPAR in the PSD fractions compared to the total fractions. These results are in concordance with previous studies (Villasana et al., 2006; Hahn et al., 2009).

The presence of contaminants in the PSD fraction was also assessed. The pre-synaptic vesicle marker, synaptophysin, the cytoskeletal protein β-III-tubulin and a marker of astroglial cells, GFAP, were all immunodetected in the PSD fractions, similar to results obtained in previous studies (Dosemeci et al., 2006; Hahn et al., 2009), but contradictory with another study that used another type of PSD isolation (Villasana et al., 2006).

The present study demonstrated that:

1. **PSDs can be isolated from frozen blocks of human premotor cortex in reasonable purity using the protocol developed by Dosemeci *et al.* 2006.**
2. **The method used allowed us to use a minimal amount of human brain sample and obtain reasonable yield and purity of the PSD fraction.**
3. **The application of the same strategy for the purification of PSDs from hippocampal slices. While, as demonstrated, this highly purified preparation can be used in applications such as westerns for the quantification of selected proteins, the very low yields are, at the present, incompatible with quantitative proteomic applications.**

6.2 Expression of proteins of the PSD involved in synaptic plasticity

Sixty human premotor cortex (BA 6) provided from the Stanley Consortium postmortem brain collection were used for the present study. PSD extraction was carried out using premotor cortex tissue from 15 patients with schizophrenia, 15 patients with major depressive disorder, 15 patients with bipolar disorder and 15 non-psychiatrically ill subjects. The expression of NR2A, PSD-95, CaMKIIα, CaMKIIβ, NSF, TrkB, TrkB-T1 and p75 was semi-quantified using WB and co-IP. Differences between WB and co-IP methods were found. Possibly due to differences in the abundance of proteins docked at the synapse versus those at extra-synaptic or intracellular locations; or due to improved purity of the PSD after co-IP. The results obtained by co-IP were considered more appropriated to study the expression of NMDAR subunit NR2A, PSD-95, CaMKIIβ, NSF, TrkB, TrkB-T1 and p75 within the PSDs as discussed below.

- **Compared to healthy subjects the expression of NR2A, PSD-95, CaMKIIβ and TrkB-T1 were reduced in the premotor cortex of patients with schizophrenia using co-IP.**

6.2.1 Expression of NR2A

- **The expression of NR2A subunit is decreased in premotor cortex of patients with schizophrenia**

The NMDAR is a critical post-synaptic mediator of activity-dependent synaptic plasticity. Disturbance in the stochiometry of this ion channel may affect its Ca^{2+} permeability and the downstream signalling pathways. The NR1 subunit is associated with different intracellular signalling pathways (Bradley et al., 2006) and NR2A subunit confers different biophysical and pharmacologic properties to the channel (Lynch and Guttmann, 2001). NMDARs require postsynaptic depolarization to remove the Mg^{2+} ion that block the pore of the ionotropic receptor at resting membrane potential and

also require the binding of two agonists, glutamate (NR2 subunits), and either glycine or D-serine, at the glycine modulatory site (NR1 subunit) (Tsien, 2000).

Imbalance in the stochiometry of the NMDAR subunits may disturb intracellular signalling pathways involved in synaptic plasticity (Greer and Greenberg, 2008; Wayman et al., 2008). NR2A and NR2B subunits confer distinct properties to NMDA receptors; heteromers containing NR1 plus NR2B mediate a current that decays three to four times more slowly than receptors composed of NR1 plus NR2A (Paoletti and Neyton, 2007). A decreased expression of NR2A at the PSD may lead to to a hypoactivity of the NMDAR as well as of the synaptic activity.

6.2.2 Expression of PSD-95

- **The expression of PSD-95 is decreased in premotor cortex of patients with schizophrenia**

The MAGUK protein PSD-95, is a major scaffolding protein of the PSD (Cho et al., 1992b) which contains several PDZ and protein-protein interaction domains that stabilise interactions between neurotransmitter receptors, synaptic adhesion receptors, and actin-associated scaffolding molecules (Ethell and Pasquale, 2005). Studies have shown that the density and size of dendritic spines is reduced in cultured neurons with knockdown of PSD-95 (Ehrlich et al., 2007). In addition stimuli that normally promote LTP in hippocampal slices instead lead to spine destabilization in PSD-95 knockdown neurons (Ehrlich et al., 2007). These studies emphasise the important role of PSD-95 in activity-dependent synapse stabilisation. The reduction of PSD-95 in the PSD of premotor cortex neurons in patients with schizophrenia may lead to a dysfunction in synaptic plasticity mechanisms.

DISC1 has also been reported to be enriched in PSD fraction where it interacts with PSD-95 (Hayashi-Takagi et al., 2010). DISC1 also interacts with Kalirin-7, a GDP/GTP exchange factor for the small G protein Rac1, regulator of spine morphology and

plasticity (Hayashi-Takagi et al., 2010). Evidence suggests that DISC1 anchors Kal-7 to PSD-95, thereby sequestering Kal-7 to the PSD and preventing it from activating Rac1. This complex is modulated by neuronal activity, particularly NMDA receptor-dependent activity, which regulates Rac-1 mediated changes in spine morphology. Therefore disturbances of the expression of NR2A and PSD-95 observed in this study suggest that the function and morphology of the synapses may be affected in the premotor cortex of patients with schizophrenia.

6.2.3 Expression of CaMKIIα and CaMKIIβ

- **The expression of CaMKIIβ is decreased in premotor cortex of patients with schizophrenia**

CaMKII, a calcium-calmodulin protein kinase involved in synaptic plasticity (Colbran and Brown, 2004; Fink and Meyer, 2002; Hudmon and Schulman, 2002) consists mainly of CaMKIIα and CaMKIIβ isoforms in the CNS. CaMKIIβ is expressed during neurodevelopment and adulthood, whereas CaMKIIα is only expressed after birth (Fink et al., 2003; Lin and Redmond, 2008). The expression of CaMKIIα is correlated with the size of dendritic spines (Asrican et al., 2007) and the inhibition of CaMKIIα activity in mature neuronal cultures can reduce the activity-induced dendritic spine enlargement and stabilisation (Yamagata et al., 2009; Zha et al., 2009). In the present study we did not find any changes in the expression of CaMKIIα in the premotor cortex of patients with schizophrenia using WB. However this isoform could not be studied further using co-IP as the signal was indistinguishable from the heavy chain of the antibody used for the co-IP experiment. Cross-linking of the PSD-95 antibodies to the beads used to co-immunoprecipitate the PSD may solve this issue and may revealed disturbances in the expression of CaMKIIα that were not observed using WB.

The protein kinase CaMKIIβ contains a specific F-actin-binding domain that directly regulates F-actin and hence the stability of dendritic spines (Shen et al., 1998). A recent study revealed that knockdown of CaMKIIβ in hippocampal slices leads to a

significant loss of mature spines, transforming them into immature dendritic filopodia (Okamoto et al., 2007). Reduced expression of CaMKIIβ observed in our study suggests that dendritic spine stability may be affected in the premotor cortex of patients with schizophrenia.

6.3 Expression of neurotrophic receptors involved in synaptic plasticity

- **The expression of TrkB-T1 is decreased in premotor cortex of patients with schizophrenia**

Tropomyosin receptor kinase B (TrkB) is the receptor for the neurotrophin BDNF. In humans, three major isoforms of TrkBs, the full-length receptor (TrkB) and two C-terminal truncated receptors (TrkB-T1- and TrkB-Shc) are expressed in various tissues including in the CNS (Wong and Garner, 2012). These neurotrophin receptors activate different signalling pathways implicated in cell survival and cell differentiation mechanisms implicated in synaptic plasticity (Atwal et al., 2000). In the present study no changes in expression for the neurotrophin receptor TrkB, were found in the premotor cortex of patients with schizophrenia. TrkB is involved in BDNF -induced trafficking of AMPARs via interaction between NSF an ATPase and also stabilisation of surface AMPARs and the AMPAR subunit GluR2, important in different forms of synaptic plasticity (Narisawa-Saito et al., 2002). A recent study showed that disturbance of the interaction of NSF with the GluR2 subunit of AMPARs, promoted extensive loss of surface GluR2 in rat hippocampal neurons and decreased synaptic AMPAR current (Evers et al., 2010). Our study did not reveal any change of the expression of NSF in the premotor cortex of patients with schizophrenia. In summary, our results suggest that the NMDAR complex seems to be affected in the premotor cortex of patients with schizophrenia whereas the AMPAR complex may not.

The neurotrphin receptor p75 which binds pro-neurotrophin factors is implicated in neural cell death and activates death signalling pathway mediated via one or more of the intracellular receptor binding partners (Itself, TrkB or other synaptic receptors),

resulting in c-jun kinase (JNK) activation, and subsequent p53, Bax-like proteins and caspase activation (Roux and Barker, 2002; Coulson et al., 2004). In our study no significant changes in the expression of p75 were found in the premotor cortex of patients with schizophrenia.

In contrast with previous neurotrophin receptor studies, TrkB-T1 was downregulated in the premotor cortex of patients with schizophrenia in the present study. The role of the neurotrophin receptor TrkB-T1 is still unclear, however evidence is accumulating that it plays a role in synaptic plasticity. For example, knockdown of TrkB-T1 in mice was associated with increased anxiety and reduced length and complexity of neurites in the amygdala but not hippocampus. The authors also showed that TrkB-T1 regulates TrkB activity (Carim-Todd et al., 2009). Our findings suggest that the balance of neurotrophin receptors may be disturbed at the PSD of neurons and may affect neuronal synaptic plasticity in the premotor cortex of patients with schizophrenia.

6.4 Expression of proteins implicated in synactic plasticity in schizophrenia compared to other psychiatric disorders

- **The expression of NR2A is decreased in premotor cortex of patients with schizophrenia and major depressive disorder but not bipolar disorder**

The expression of NR2A, PSD-95, CaMKIIα, CaMKIIβ, NSF, TrkB, TrkB-T1 and p75 was also assessed in major depressive disorder and bipolar disorder.

Expression of the NR2A subunit of NMDAR was significantly decreased in major depressive disorder compared to healthy subject smilar to findings for schizophrenia. Furthermore, a significant decrease in the expression of NR2A was observed in schizophrenia compared to bipolar disorder.

Dysfunction of glutamatergic function in major depressive disorder and bipolar has been recently suggested (Hashimoto, 2009; Chen et al., 2010). The present findings report a lack of changes in the abundance of glutamate-related PSD proteins in bipolar

disorder in the premotor cortex. In contrast, it appears that major depressive disorder may share common disturbances in NR2A and NMDAR function with schizophrenia. However, the additional decreases in PSD-95, CaMKIIβ and TrkB-T1 in schizophrenia, but not major depressive disorder, suggests that dysfunction of the glutamatergic system in the premotor cortex in schizophrenia is more severe.

6.5 Conclusion

In the present thesis, the studies revealed that extraction and co-IP were suitable techniques for the study of proteins of the PSD from postmortem brains samples and that function of the proteins involved in synaptic plasticity may be disturbed in the premotor cortex of patients with schizophrenia. In addition, the number of PSD proteins that were affected in schizophrenia was much greater than for the affective disorders. This provides further evidence to suggestions that dysfunction of the glutamatergic system is a core feature of the pathophysiology of schizophrenia.

- **The present findings demonstrate a significant alteration of specific molecular mechanisms implicated in synaptic plasticity in the premotor cortex of patients with schizophrenia.**

Despite the contribution this study has made to the already large literature of NMDAR function in schizophrenia, the understanding of the possible causes and consequences NMDAR and associated proteins remains only speculative. Such findings must be accompanied by more detailed investigation in other brain areas such as PFC, temporal cortex and cerebellum. Furthermore investigation of the expression of other proteins of the PSD such as Homer, GKAP1 and Shank and of the phosphorylation status of these proteins may provide further insights into the pathophysiological mechanisms of schizophrenia.

APPENDICES

Appendix A : Pictures of the membranes obtained for the characterisation of the PSD fractions

A.1 Detection of PSD-95, tubulin and actin

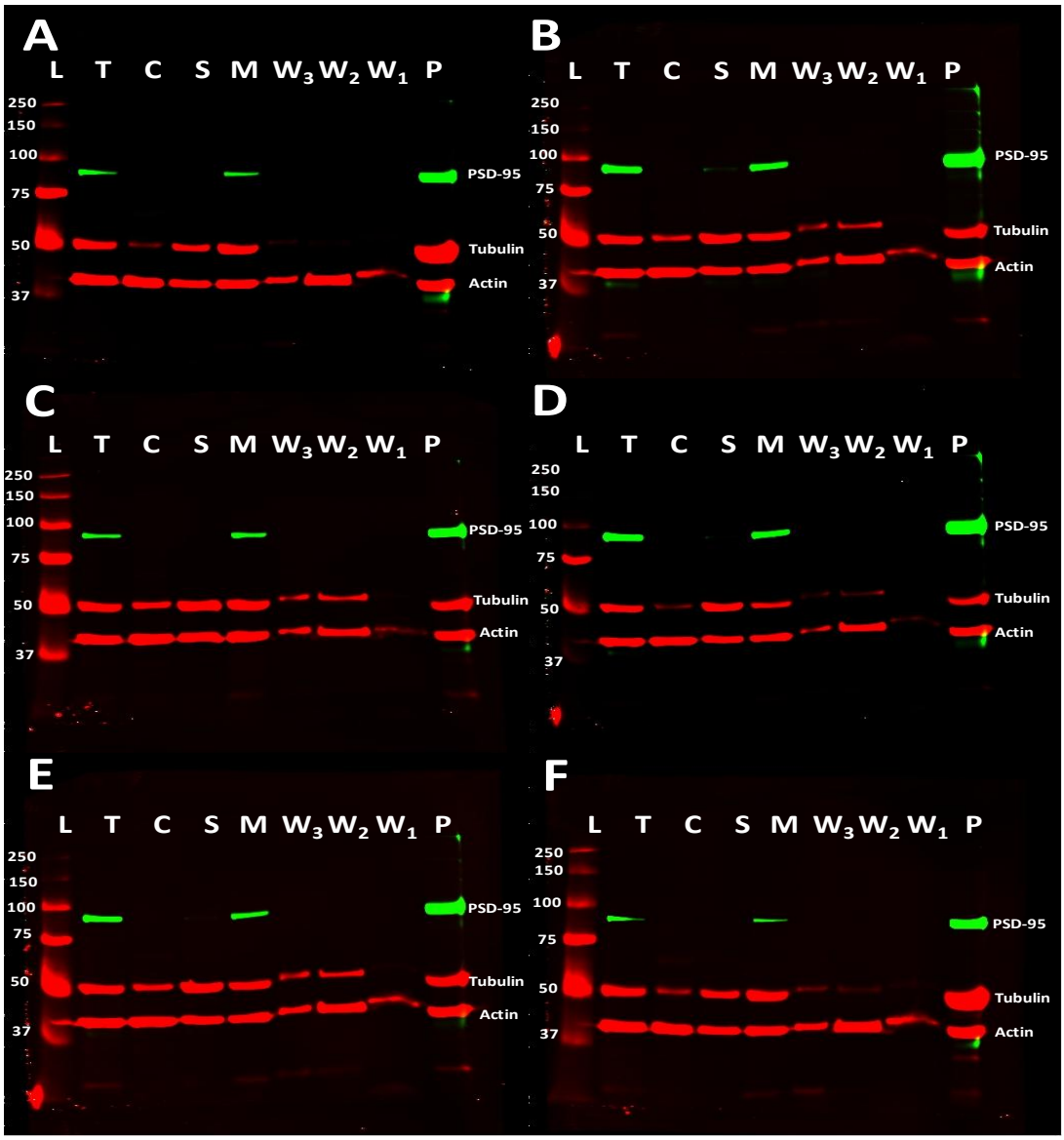

Figure A-1: Digital pictures of the membranes after detection of PSD-95, tubulin and actin.

(A-F) Experiment 1 (A) to experiment 6 (F). (L) ladder (KDa); (T) Total fraction; (C) Cytosolic fraction; (S) Sucrose 0.32 M fraction; (M) Myelin/light membranes fractions; (W_1) wash 1 fraction; (W_2) wash 2 fraction; (W_3) wash 3 fraction; (P) PSD fraction.

A.2 Detection of NR2A (control)

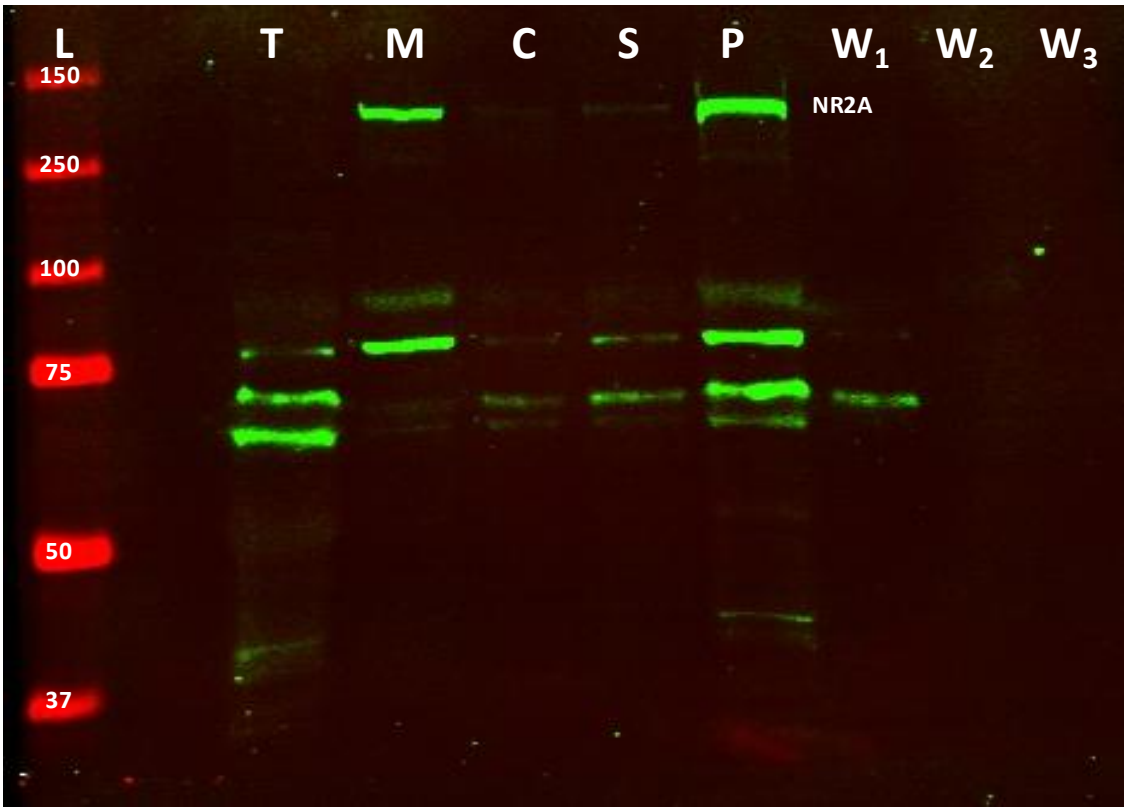

Figure A-2: Digital picture of the membrane after detection of NR2A (control).

(L) ladder (KDa); (T) Total fraction; (C) Cytosolic fraction; (S) Sucrose 0.32 M fraction; (M) Myelin/light membranes fractions; (W_1) wash 1 fraction; (W_2) wash 2 fraction; (W_3) wash 3 fraction; (P) PSD fraction.

A.3 Detection of NR2A

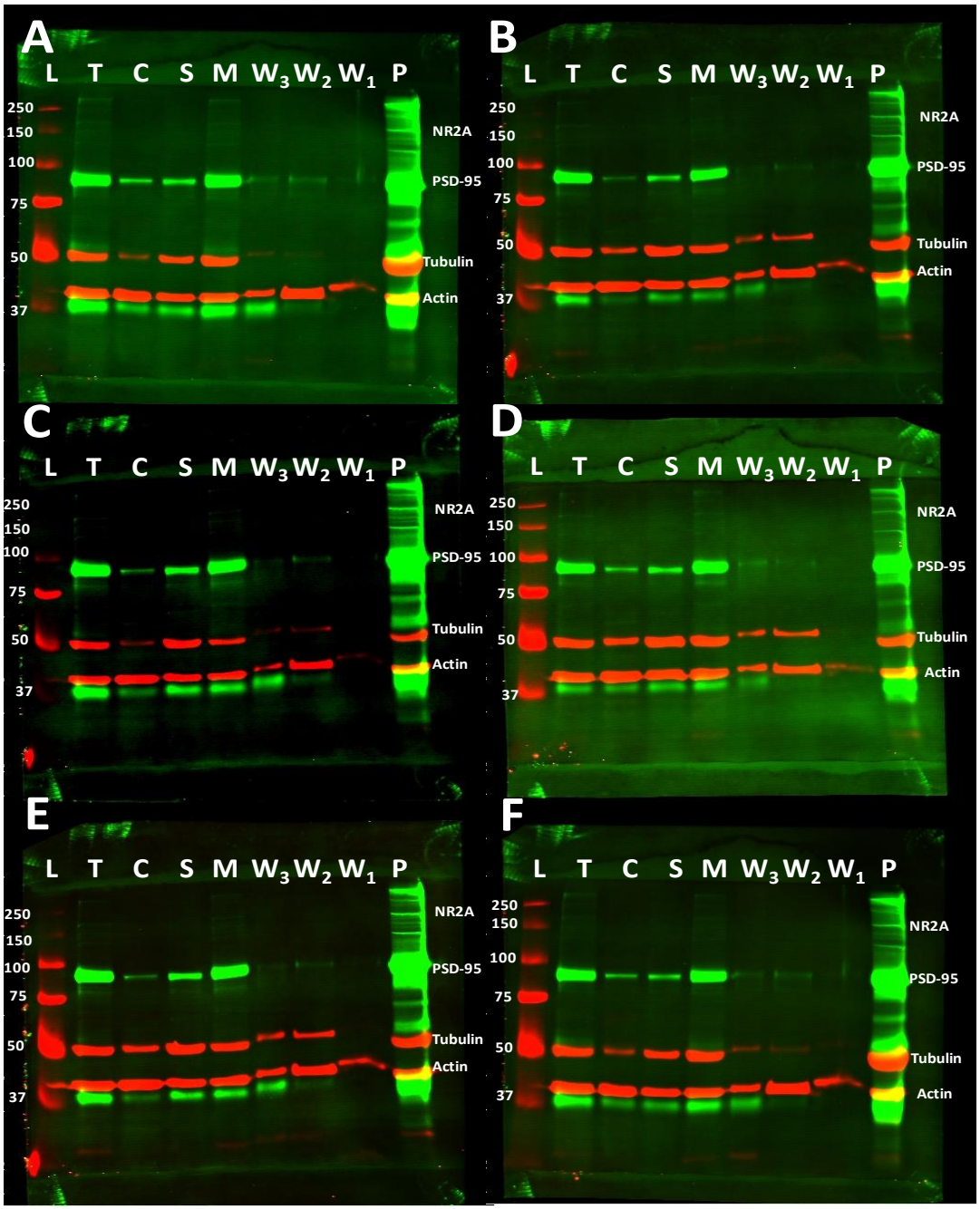

Figure A-3: Digital pictures of the membranes after detection of NR2A.

(A-F) Experiment 1 (A) to experiment 6 (F). (L) ladder (KDa); (T) Total fraction; (C) Cytosolic fraction; (S) Sucrose 0.32 M fraction; (M) Myelin/light membranes fractions; (W_1) wash 1 fraction; (W_2) wash 2 fraction; (W_3) wash 3 fraction; (P) PSD fraction.

A.4 Detection of synaptophysin

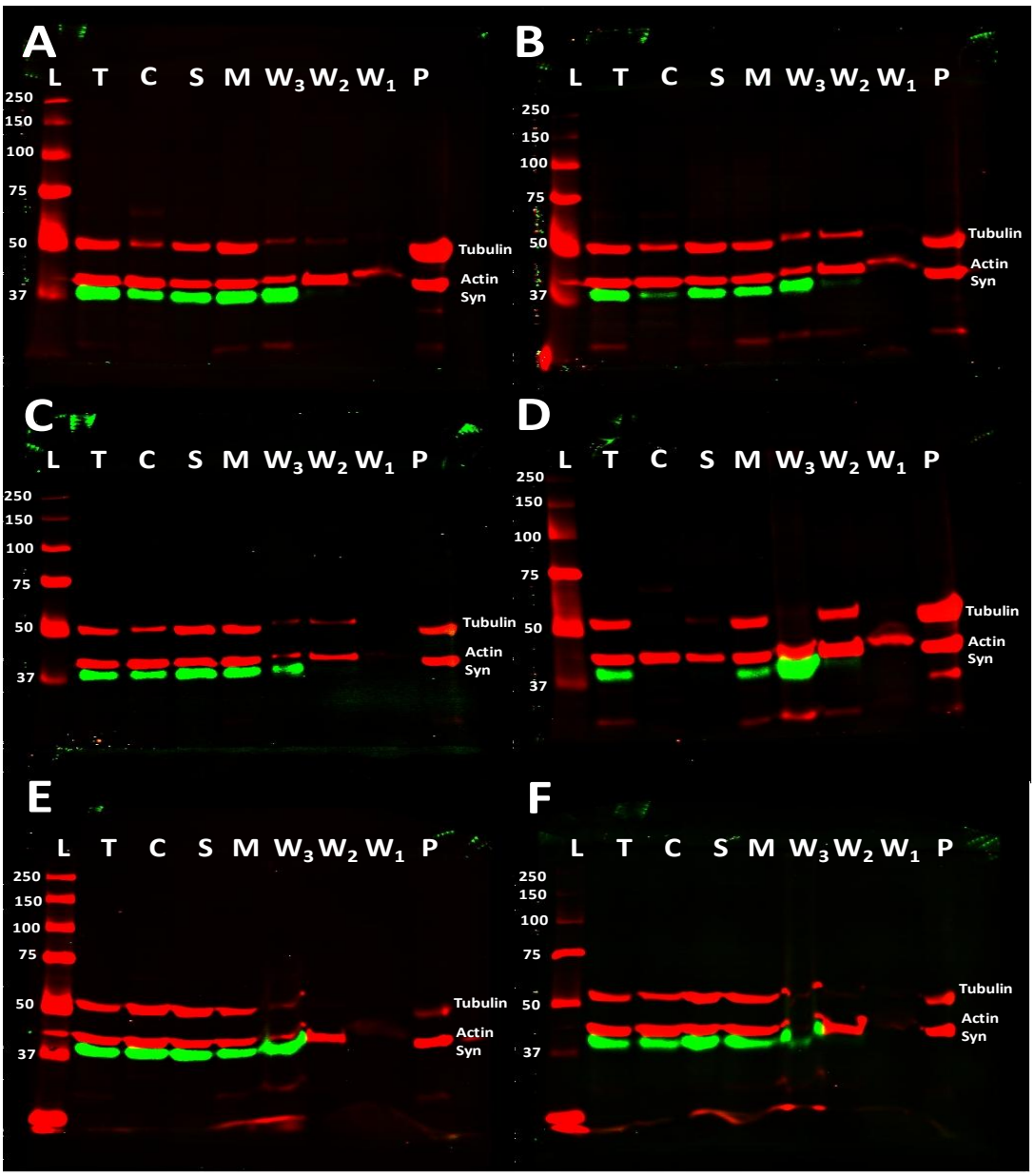

Figure A-4: Digital pictures of the membranes after detection of synaptophysin.

(A-F) Experiment 1 (A) to experiment 6 (F). (L) ladder (KDa); (T) Total fraction; (C) Cytosolic fraction; (S) Sucrose 0.32 M fraction; (M) Myelin/light membranes fractions; (W_1) wash 1 fraction; (W_2) wash 2 fraction; (W_3) wash 3 fraction; (P) PSD fraction. syn: synaptophysin

A.5 Detection of AMPAR and GFAP

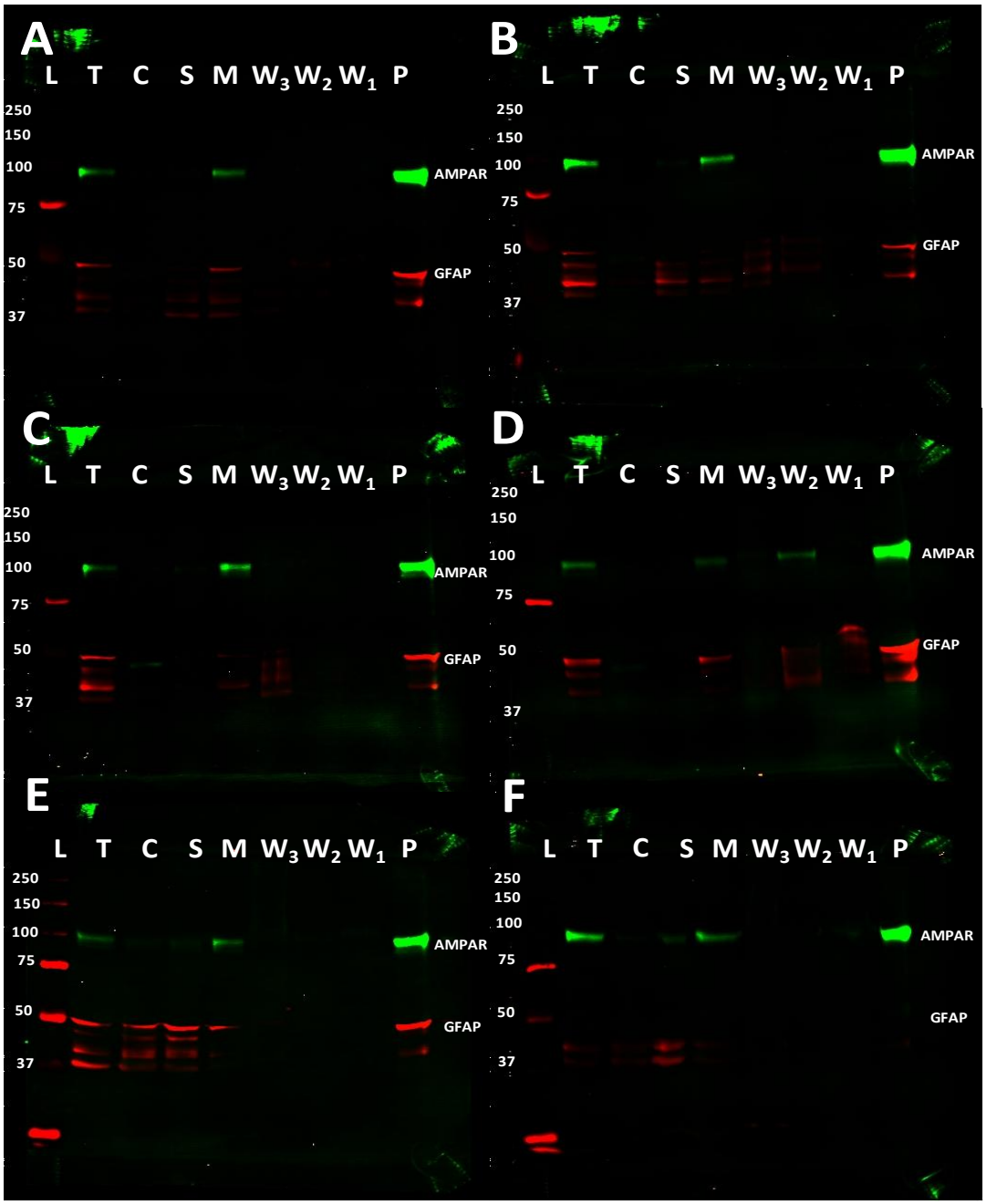

Figure A-5: Digital pictures of the membranes after detection AMPAR and GFAP.

(A-F) Experiment 1 (A) to experiment 6 (F). (L) ladder (KDa); (T) Total fraction; (C) Cytosolic fraction; (S) Sucrose 0.32 M fraction; (M) Myelin/light membranes fractions; (W_1) wash 1 fraction; (W_2) wash 2 fraction; (W_3) wash 3 fraction; (P) PSD fraction.

Appendix B : Pictures of the membranes obtained for the co-IP of the PSD fractions

B.1 Detection of PSD-95, NSF and actin

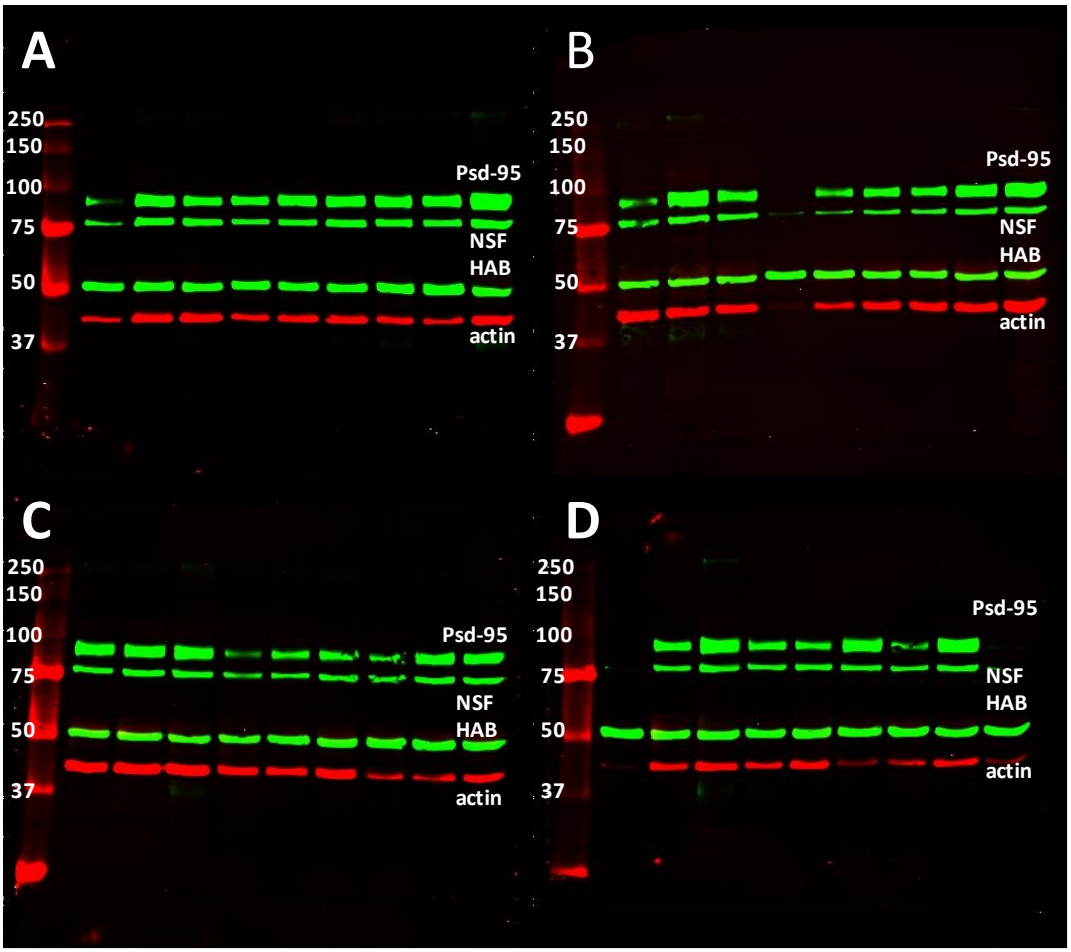

Figure B-1: Digital pictures of the membranes after detection of PSD-95, NSF and actin.

(A) Samples 1 to 9; (B) Samples 10 to 18; (C) Samples 19 to 27; (D) Samples 28 to 36.

HAB: Heavy chain of the antibody used for co-IP

Ladder in KDa

B.2 Detection of PSD-95, NSF and actin

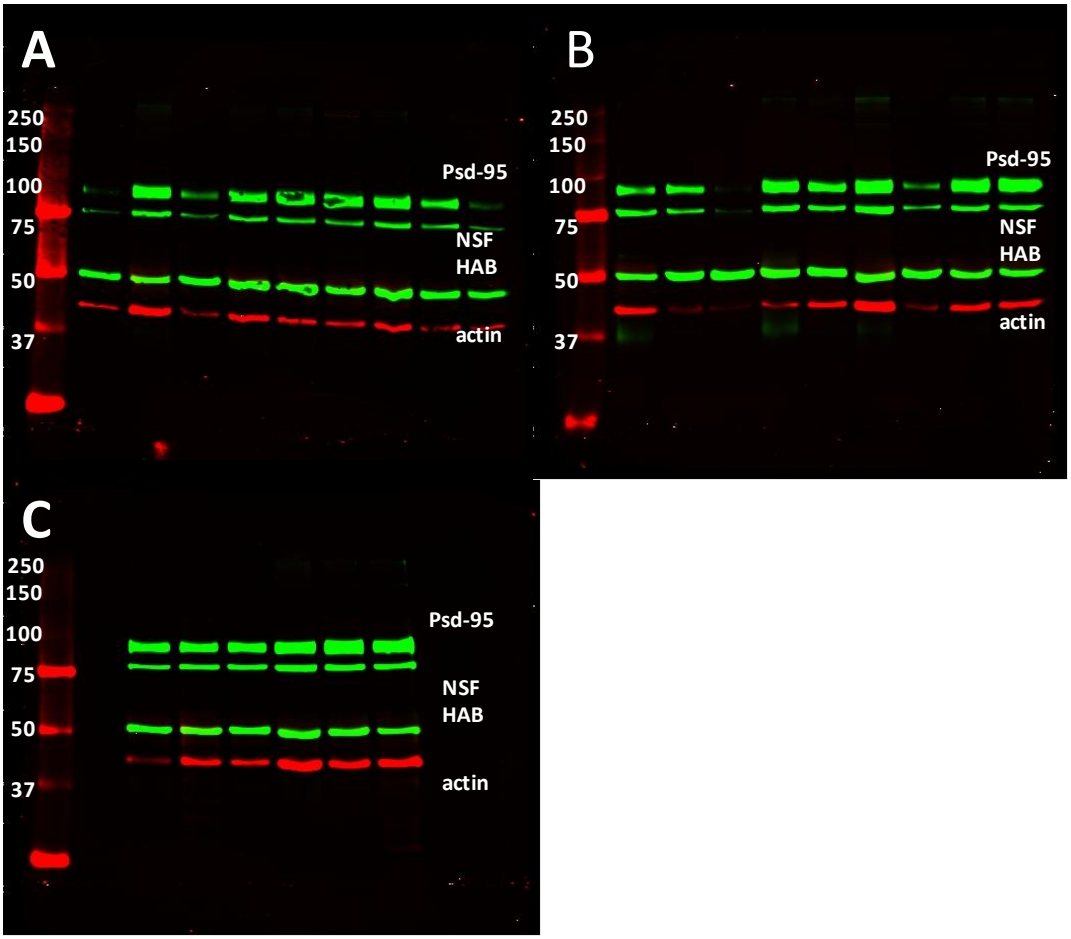

Figure B-2: Digital pictures of the membranes after detection PSD-95, NSF and actin.

(A) Samples 37 to 45; (B) Samples 46 to 54; (C) Samples 55 to 60

HAB: Heavy chain of the antibody used for co-IP

Ladder in KDa

B.3 Detection of tubulin

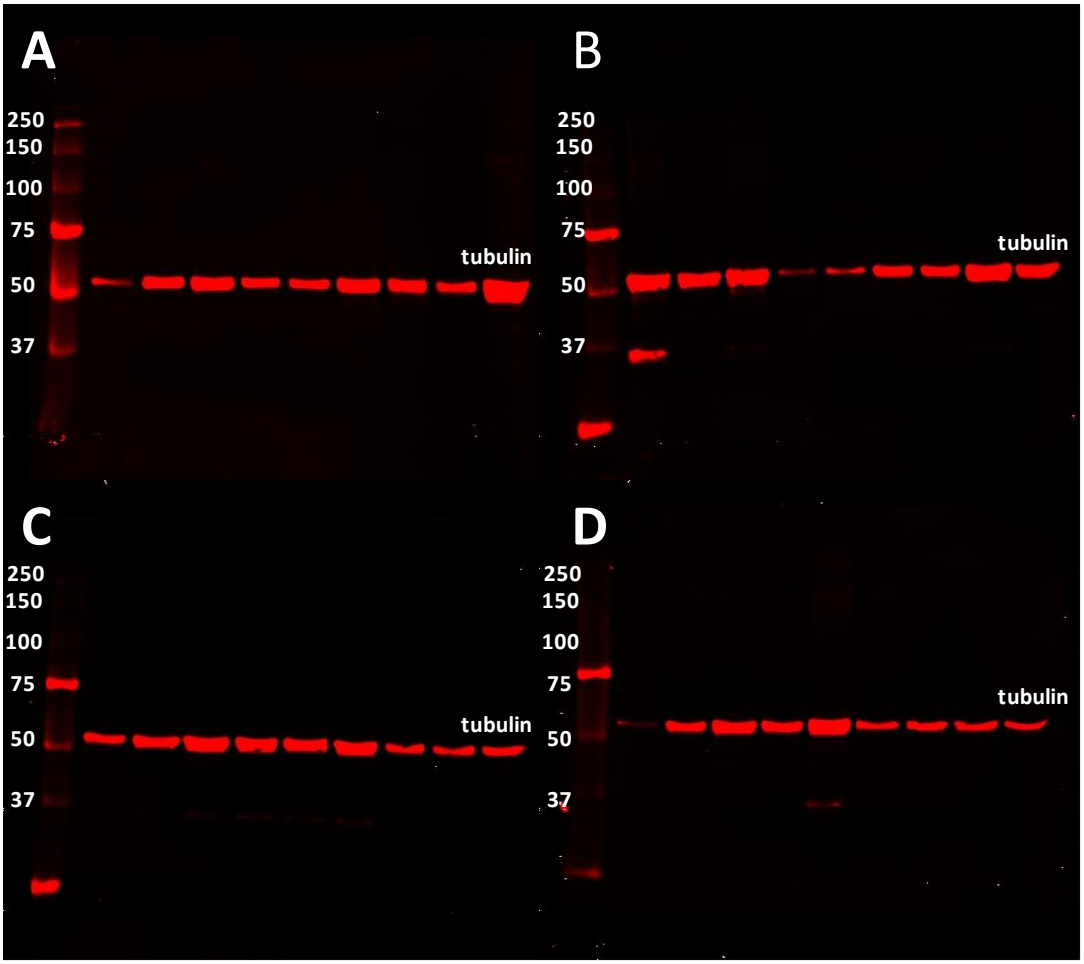

Figure B-3: Digital pictures of the membranes after detection tubulin.

(A) Samples 1 to 9; (B) Samples 10 to 18; (C) Samples 19 to 27; (D) Samples 28 to 36.

HAB: Heavy chain of the antibody used for co-IP

Ladder in KDa

B.4 Detection of tubulin

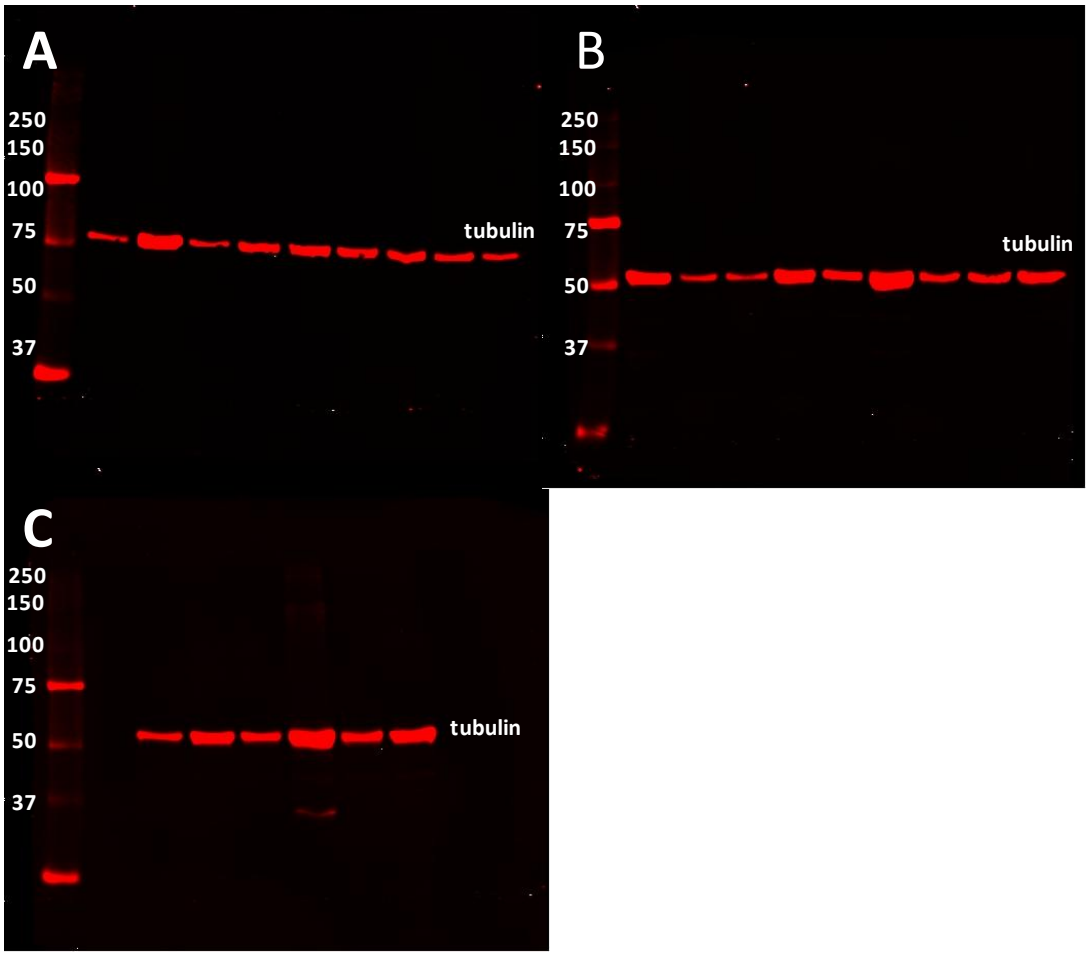

Figure B-4: Digital pictures of the membranes after detection tubulin.

(A) Samples 37 to 45; (B) Samples 46 to 54; (C) Samples 55 to 60

HAB: Heavy chain of the antibody used for co-IP

Ladder in KDa

B.5 Detection of NR2A

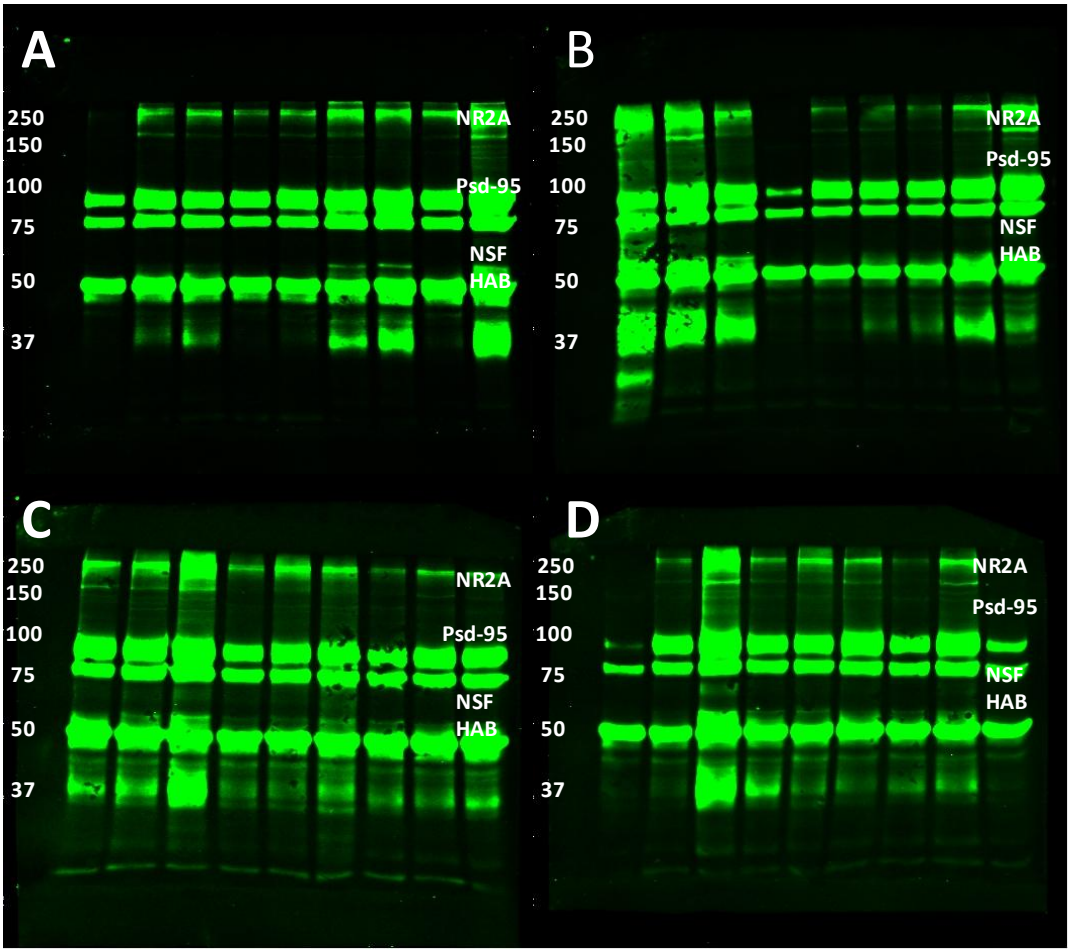

Figure B-5: Digital pictures of the membranes after detection of NR2A.

(A) Samples 1 to 9; (B) Samples 10 to 18; (C) Samples 19 to 27; (D) Samples 28 to 36.

HAB: Heavy chain of the antibody used for co-IP

Ladder in KDa

B.6 Detection of NR2A

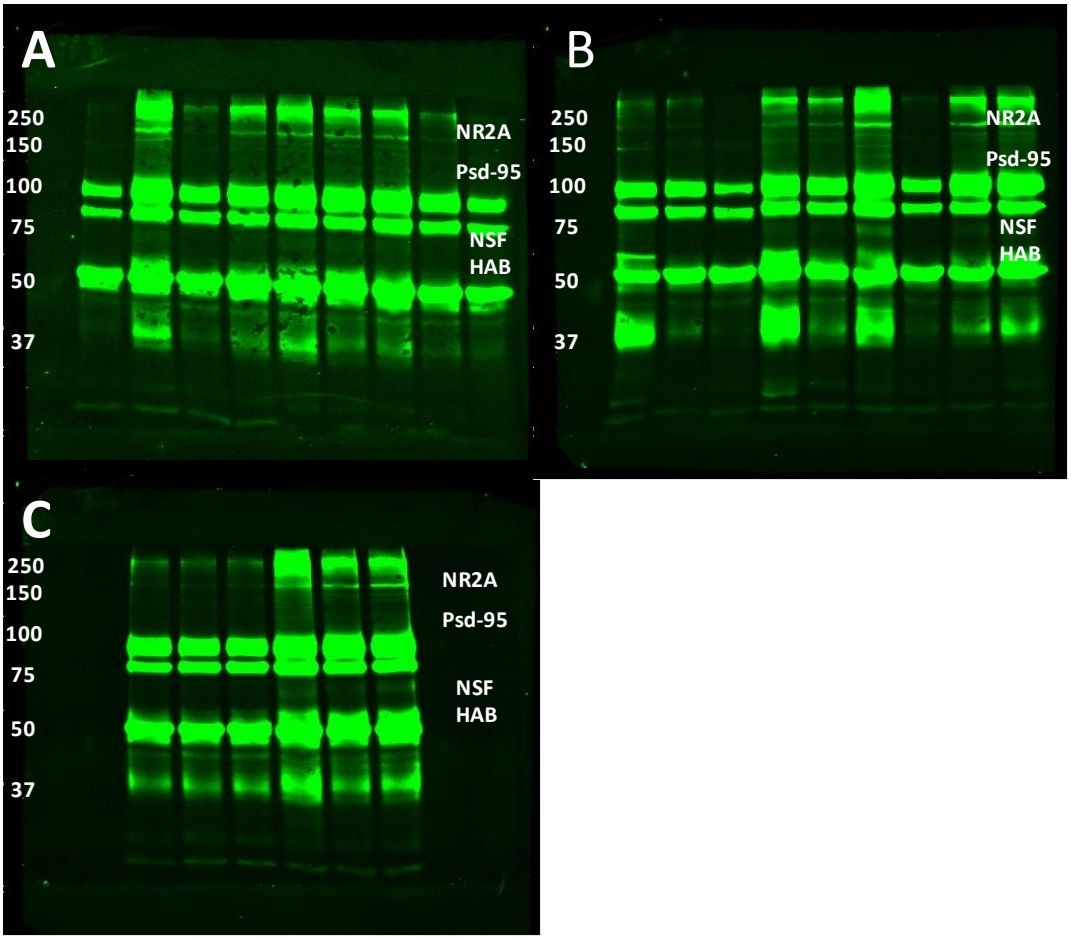

Figure B-6: Digital pictures of the membranes after detection of NR2A.

(A) Samples 37 to 45; (B) Samples 46 to 54; (C) Samples 55 to 60

HAB: Heavy chain of the antibody used for co-IP

Ladder in KDa

B.7 Detection of p75

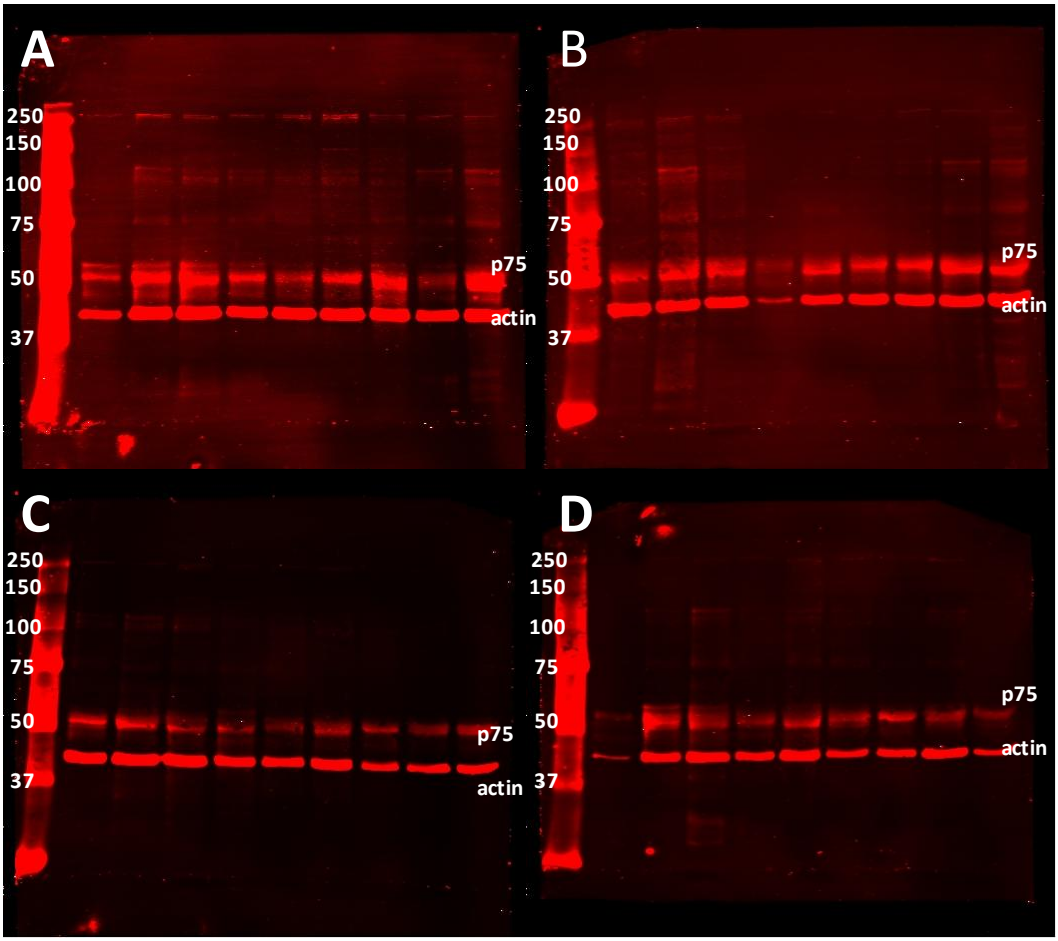

Figure B-7: Digital pictures of the membranes after detection of p75.

(A) Samples 1 to 9; (B) Samples 10 to 18; (C) Samples 19 to 27; (D) Samples 28 to 36.

Ladder in KDa

B.8 Detection of p75

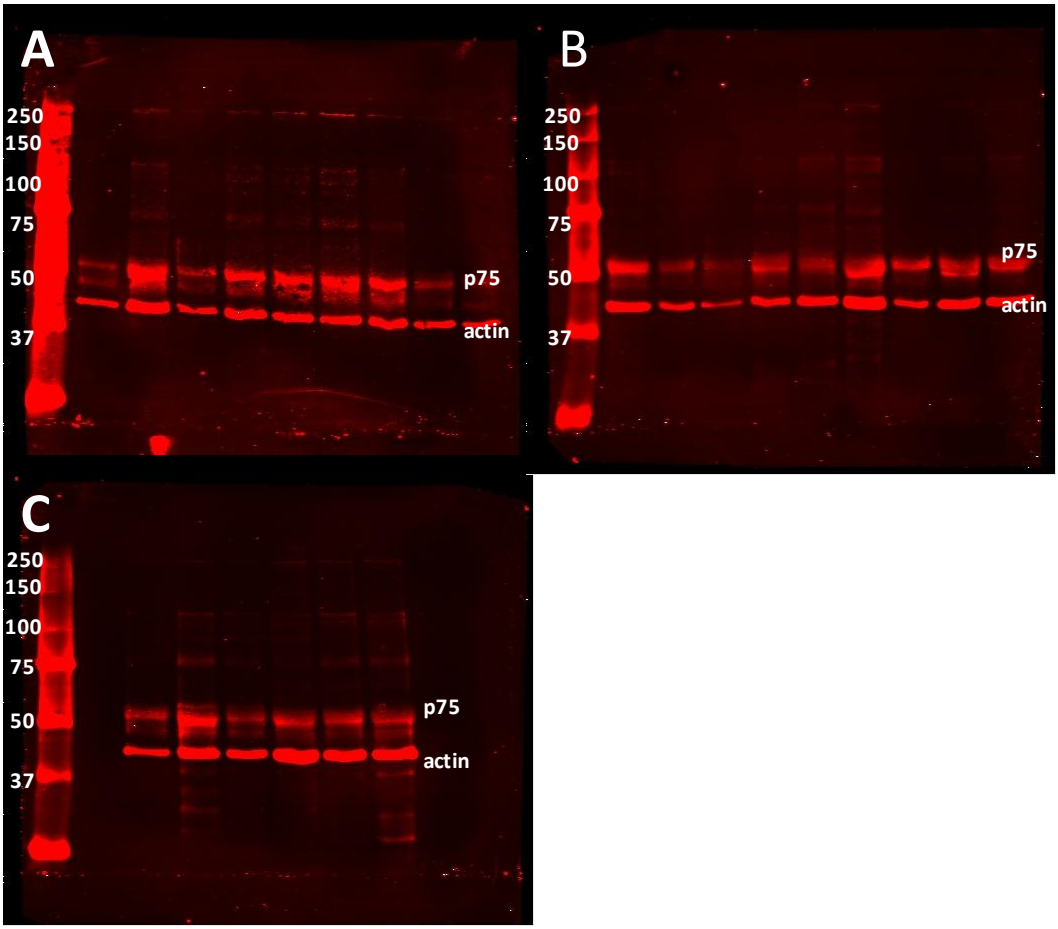

Figure B-8: Digital pictures of the membranes after detection of p75.

(A) Samples 37 to 45; (B) Samples 46 to 54; (C) Samples 55 to 60

Ladder in KDa

B.9 Detection of TrkB, TrkB-T1 and CaMKIIβ

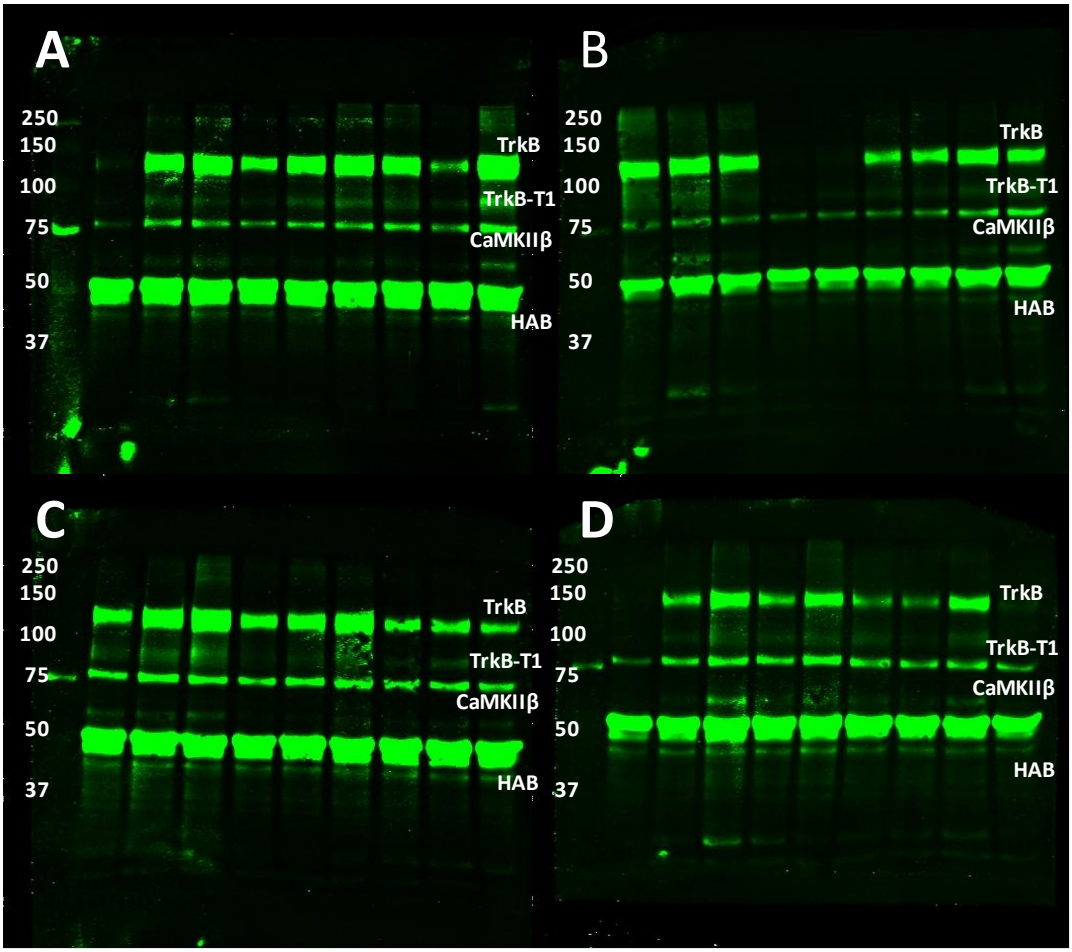

Figure B-9: Digital pictures of the membranes after detection of TrkB, TrkB-T1 and CaMKIIβ.

(A) Samples 1 to 9; (B) Samples 10 to 18; (C) Samples 19 to 27; (D) Samples 28 to 36.

HAB: Heavy chain of the antibody used for co-IP

Ladder in KDa

B.10 Detection of TrkB, TrkB-T1 and CaMKIIβ

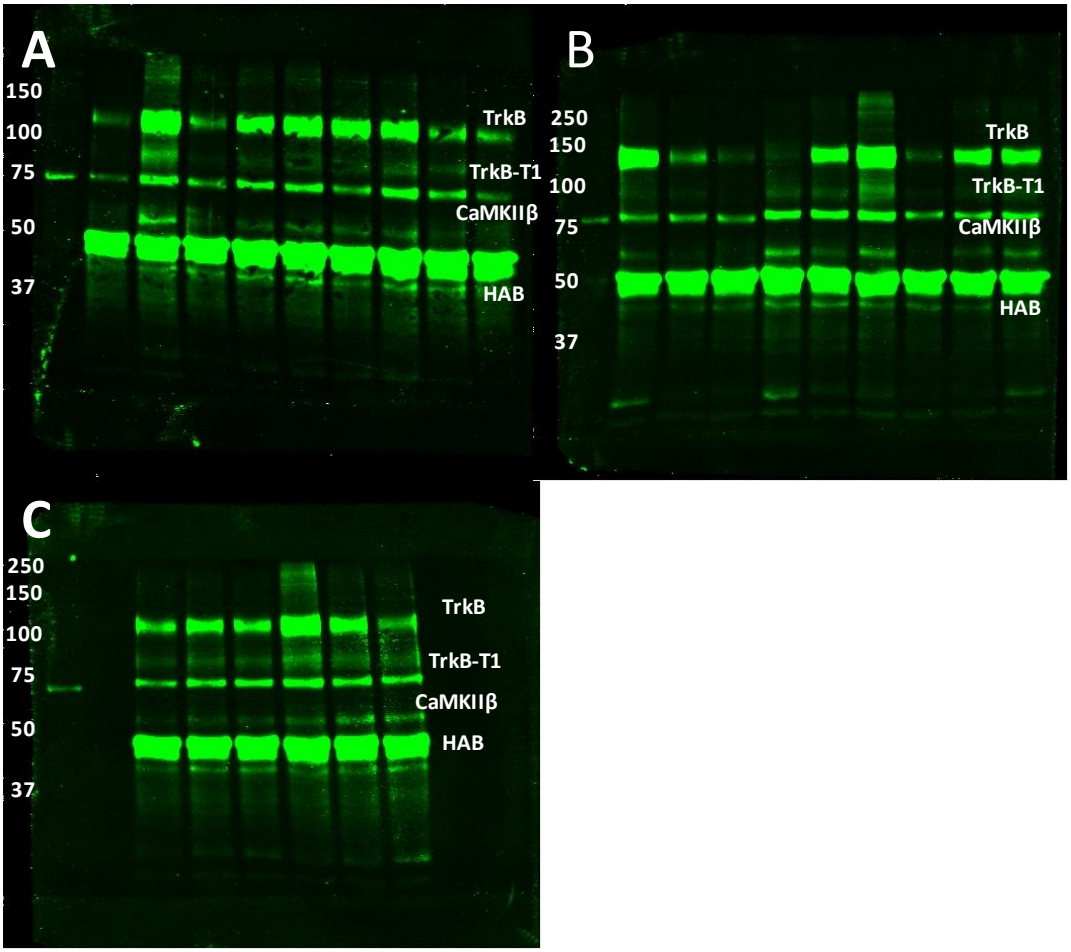

Figure B-10: Digital pictures of the membranes after detection of TrkB, TrkB-T1 and CaMKIIβ.

(A) Samples 37 to 45; (B) Samples 46 to 54; (C) Samples 55 to 60

HAB: Heavy chain of the antibody used for co-IP

Ladder in KDa

Appendix C Pictures of the membranes obtained for the WB of the PSD fractions

C.1 Detection of PSD-95, NSF, tubulin and actin

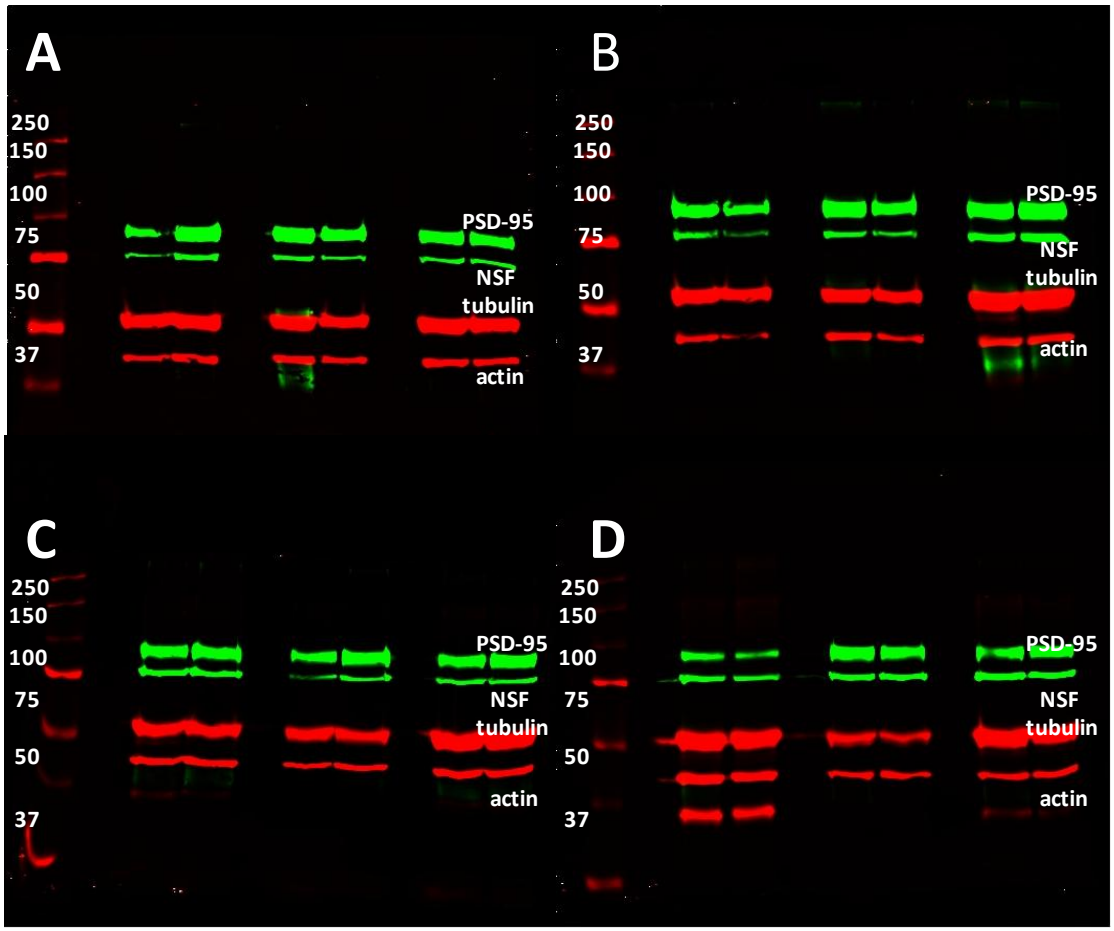

Figure C-1: Digital pictures of the membranes after detection of PSD-95, NSF, tubulin and actin.

(A) Samples 1 to 3 (Duplicate); (B) Samples 4 to 6 (Duplicate); (C) Samples 7 to 9 (Duplicate); (D) Samples 10 to 12 (Duplicate).

Ladder in KDa

C.2 Detection of PSD-95, tubulin and actin

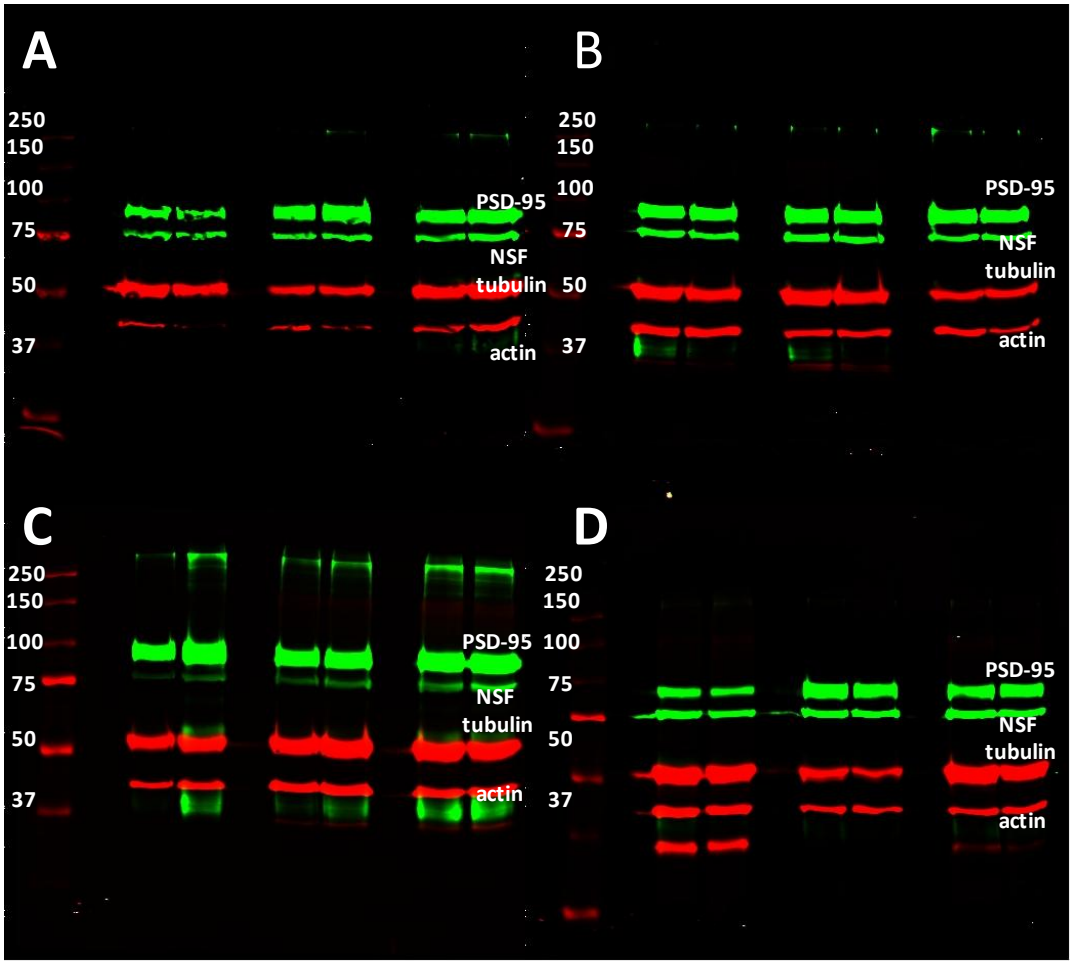

Figure C-2: Digital pictures of the membranes after detection of PSD-95, NSF, tubulin and actin.

(A) Samples 13 to 15 (Duplicate); (B) Samples 16 to 18 (Duplicate); (C) Samples 19 to 21 (Duplicate); (D) Samples 22 to 24 (Duplicate).

Ladder in KDa

C.3 Detection of PSD-95, tubulin and actin

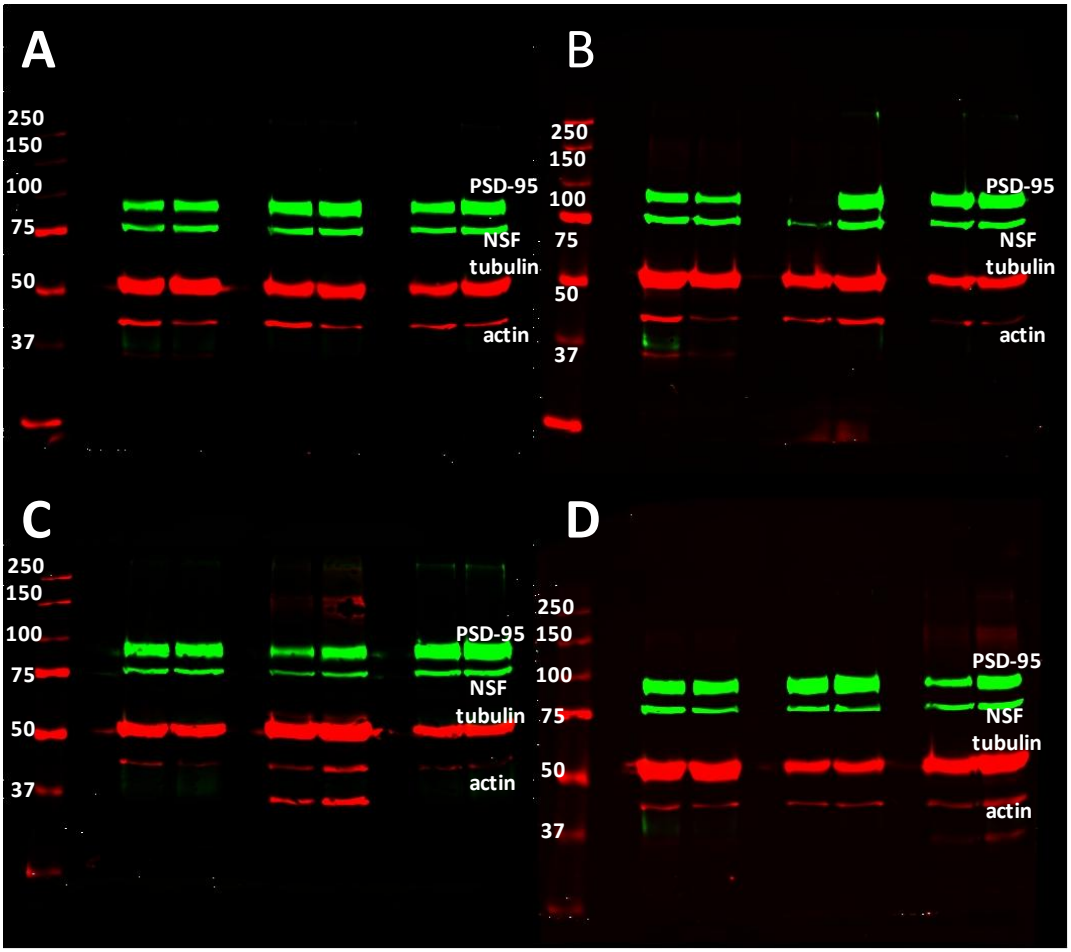

Figure C-3: Digital pictures of the membranes after detection of PSD-95, NSF, tubulin and actin.

(A) Samples 25 to 27 (Duplicate); (B) Samples 28 to 30 (Duplicate); (C) Samples 31 to 33 (Duplicate); (D) Samples 34 to 36 (Duplicate).

Ladder in KDa

C.4 Detection of PSD-95, tubulin and actin

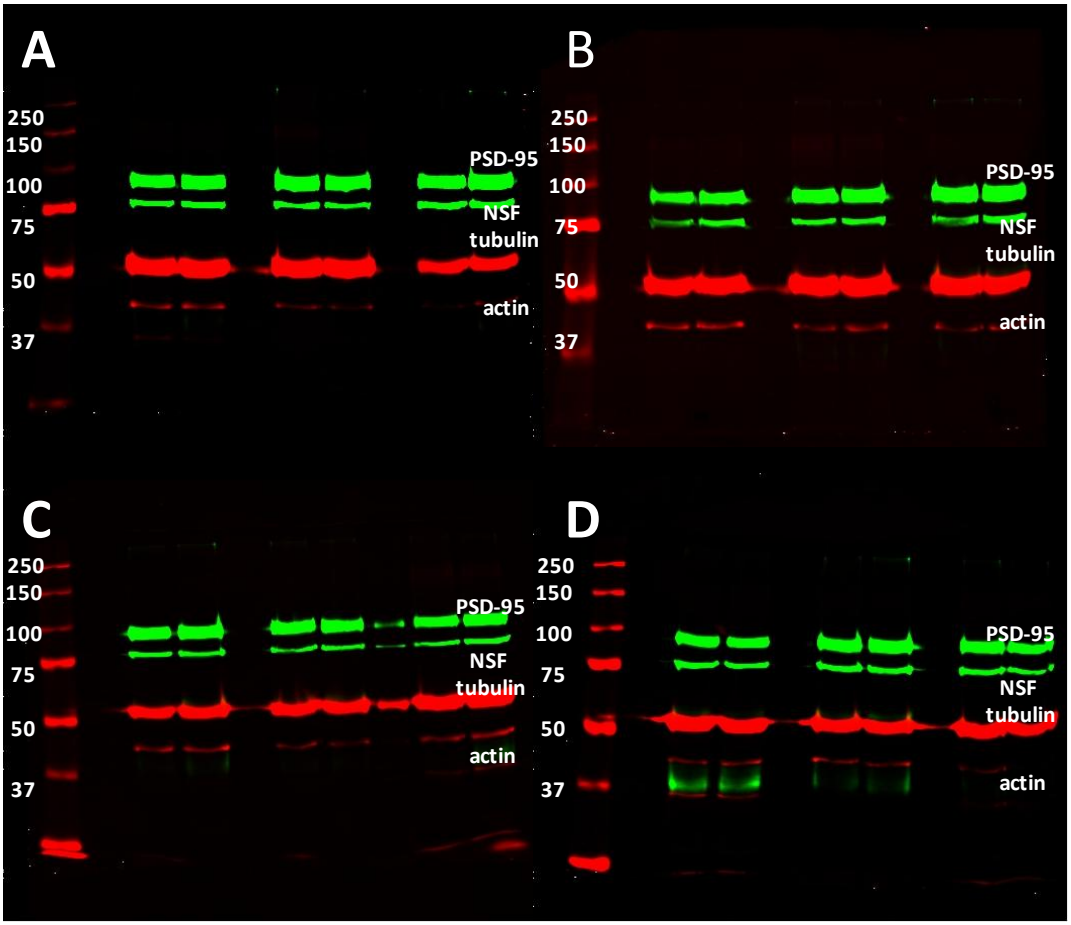

Figure C-4: Digital pictures of the membranes after detection of PSD-95, NSF, tubulin and actin.

(A) Samples 37 to 39 (Duplicate); (B) Samples 40 to 42 (Duplicate); (C) Samples 43 to 45 (Duplicate); (D) Samples 46 to 48 (Duplicate).

Ladder in KDa

C.5 Detection of PSD-95, tubulin and actin

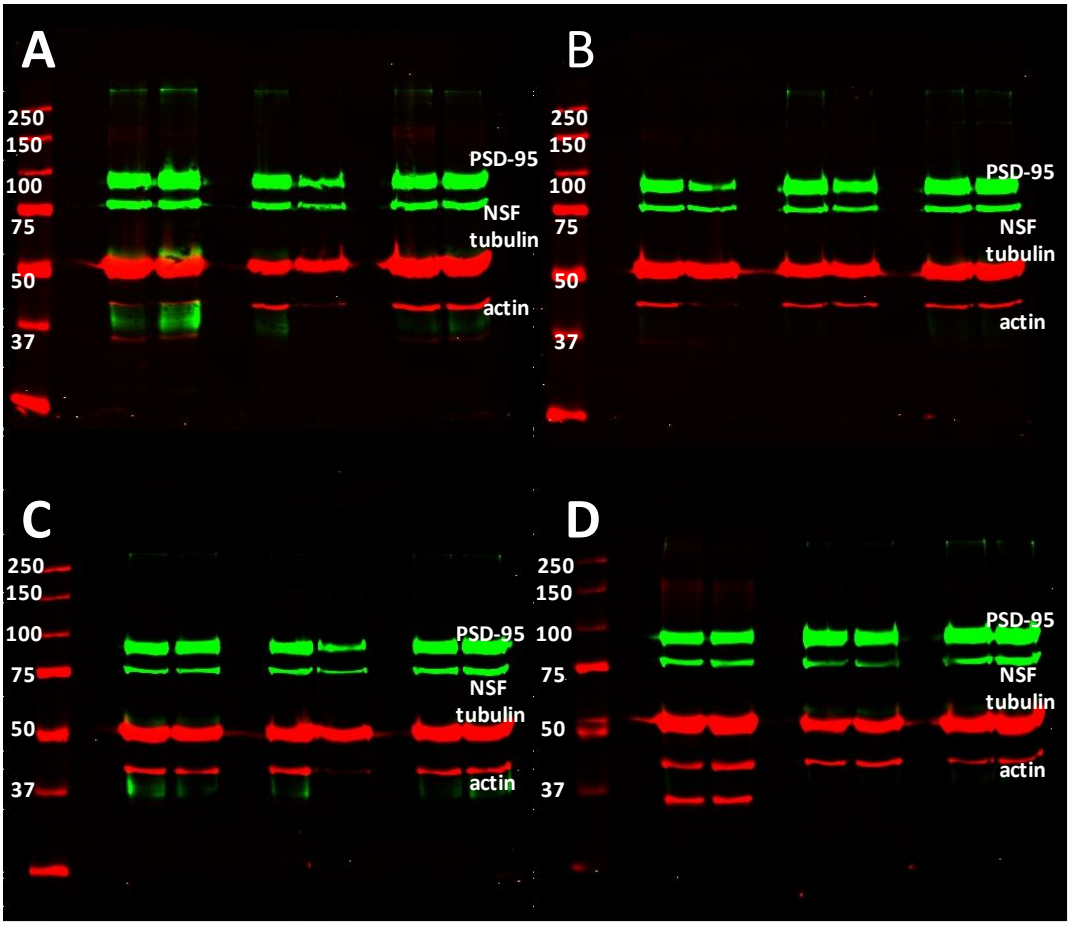

Figure C-5: Digital pictures of the membranes after detection of PSD-95, NSF, tubulin and actin.

(A) Samples 49 to 51 (Duplicate); (B) Samples 52 to 54 (Duplicate); (C) Samples 55 to 57 (Duplicate); (D) Samples 58 to 60 (Duplicate).

Ladder in KDa

C.6 Detection of PSD-95, tubulin and actin

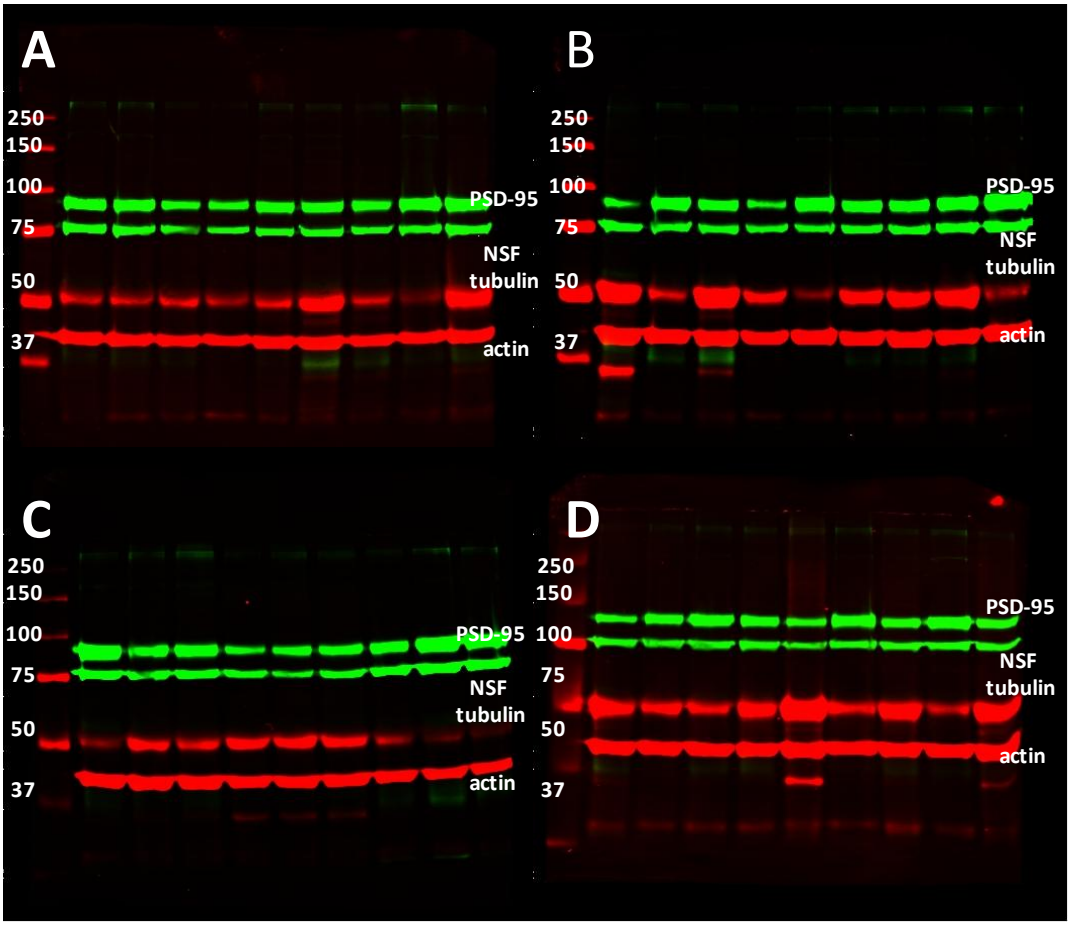

Figure C-6: Digital pictures of the membranes after detection of PSD-95, NSF, tubulin and actin.

(A) Samples 1 to 9; (B) Samples 10 to 18; (C) Samples 19 to 27; (D) Samples 28 to 36.

Ladder in KDa

C.7 Detection of PSD-95, tubulin and actin

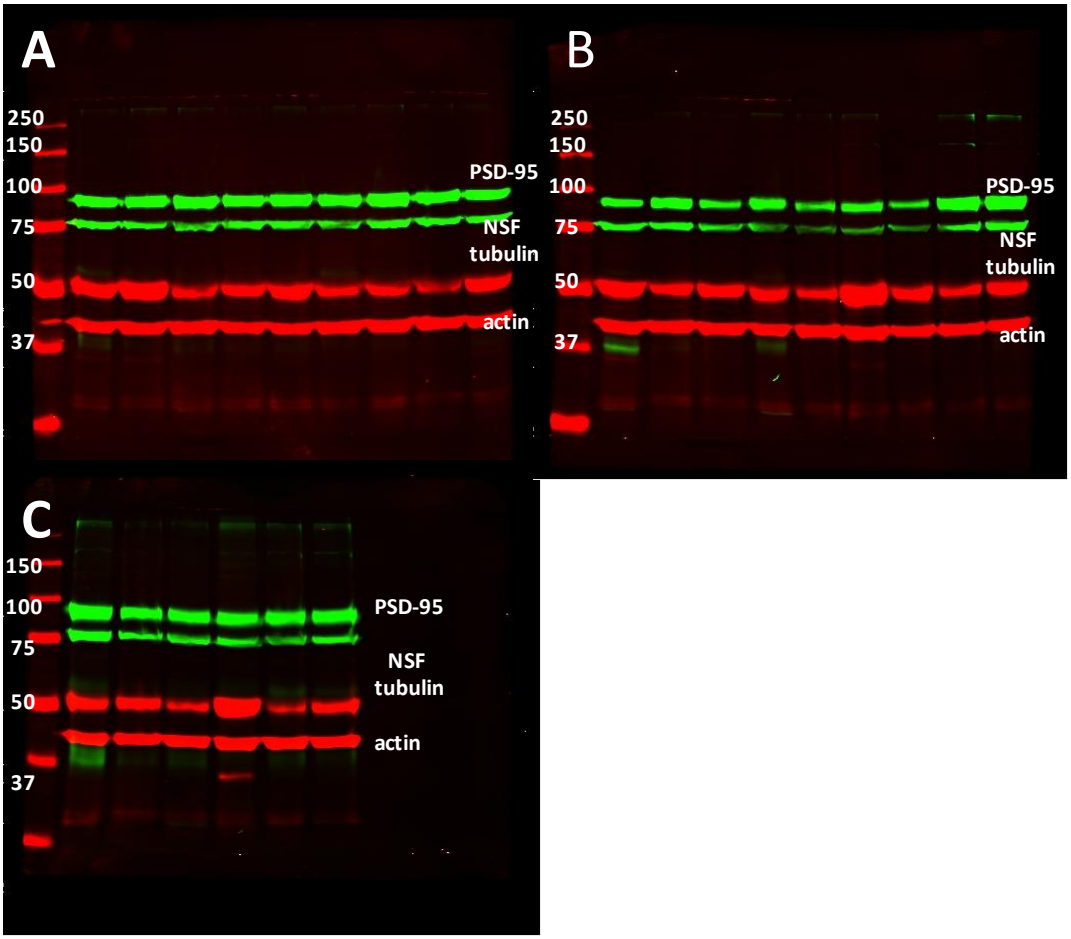

Figure C-7: Digital pictures of the membranes after detection of PSD-95, NSF, tubulin and actin.

(A) Samples 37 to 45; (B) Samples 46 to 54; (C) Samples 55 to 60.

Ladder in KDa

C.8 Detection of NR2A

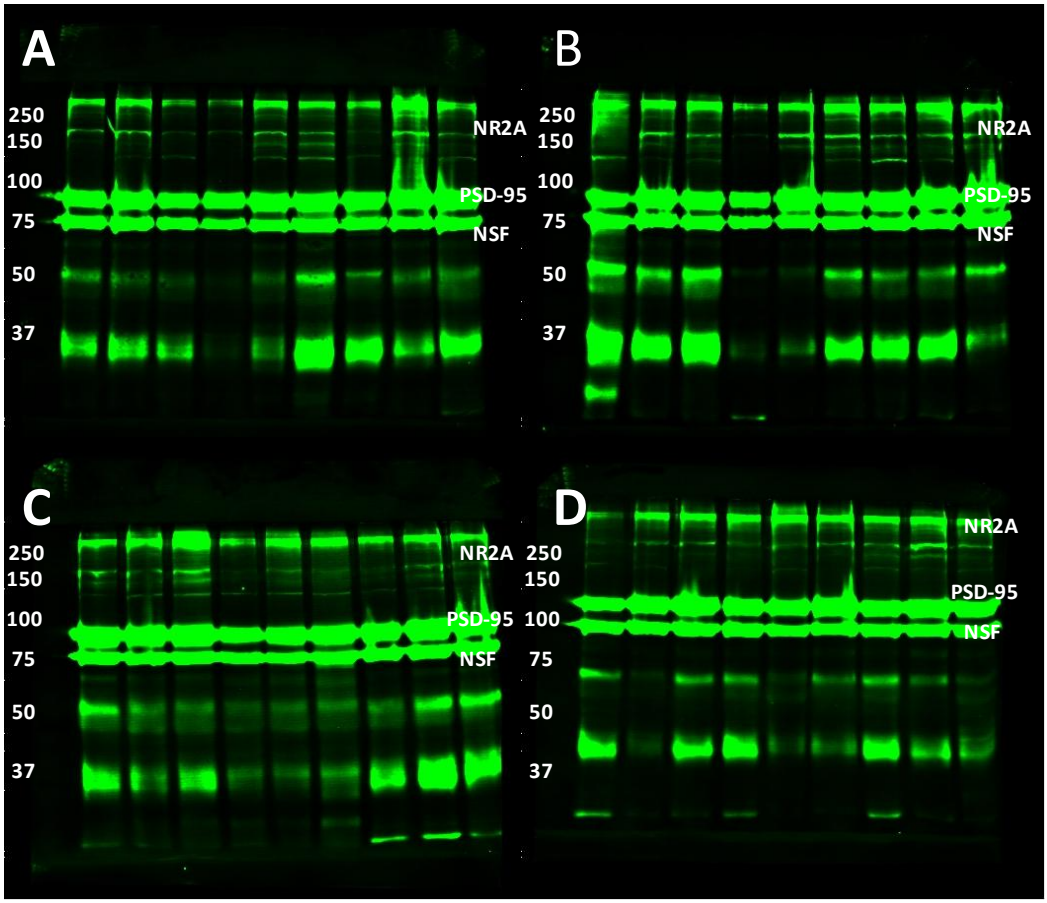

Figure C-8: Digital pictures of the membranes after detection of NR2A.

(A) Samples 1 to 9; (B) Samples 10 to 18; (C) Samples 19 to 27; (D) Samples 28 to 36.

Ladder in KDa

C.9 Detection of NR2A

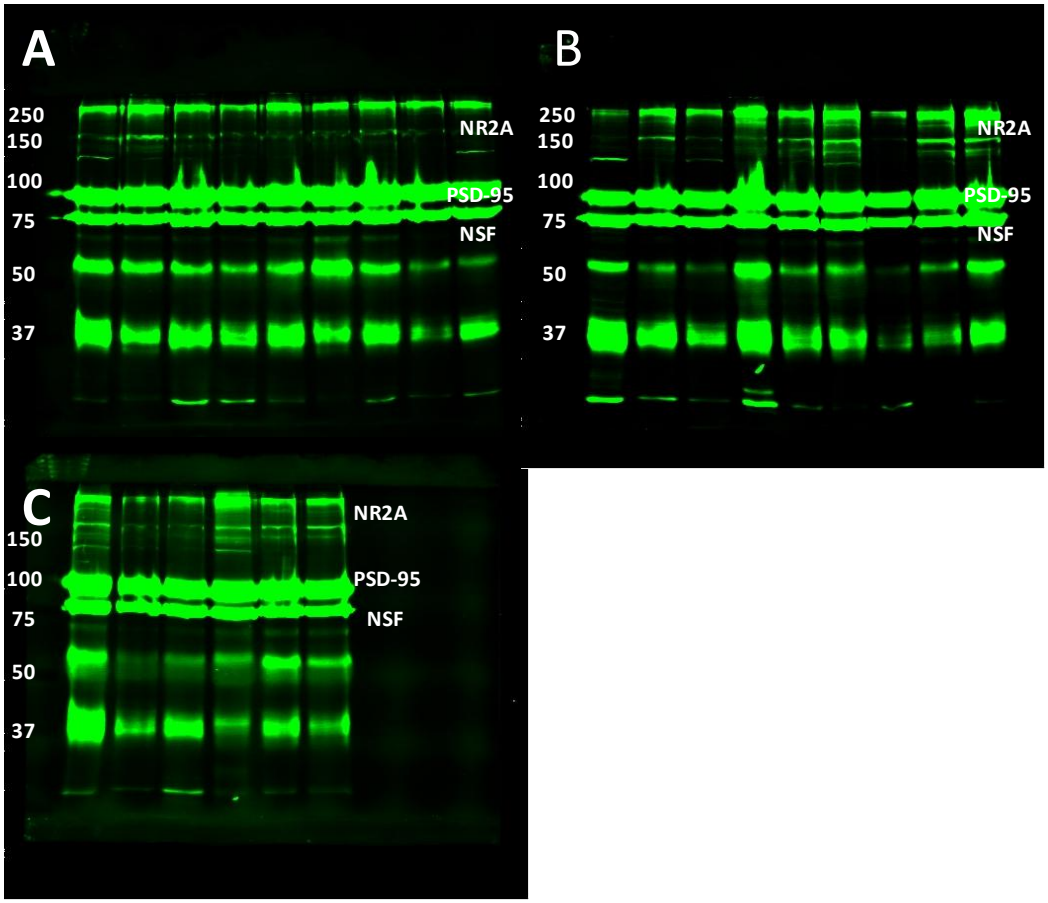

Figure C-9: Digital pictures of the membranes after detection of NR2A.

(A) Samples 37 to 45; (B) Samples 46 to 54; (C) Samples 55 to 60.

Ladder in KDa

C.10 Detection of TrkB, TrkB-T1, CaMKIIα and CaMKIIβ

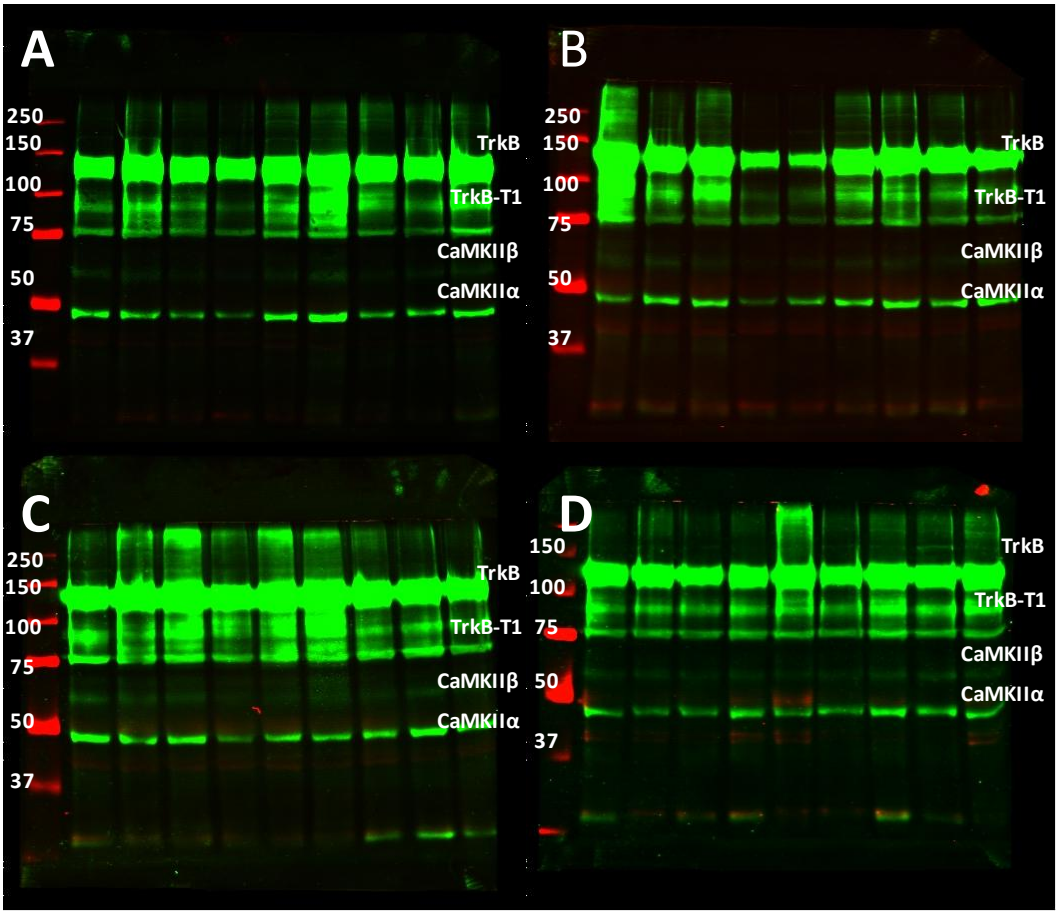

Figure C-10: Digital pictures of the membranes after detection of TrkB, TrkB-T1, CaMKIIα and CaMKIIβ.

(A) Samples 1 to 9; (B) Samples 10 to 18; (C) Samples 19 to 27; (D) Samples 28 to 36.

Ladder in KDa

C.11 Detection of TrkB, TrkB-T1, CaMKIIα and CaMKIIβ

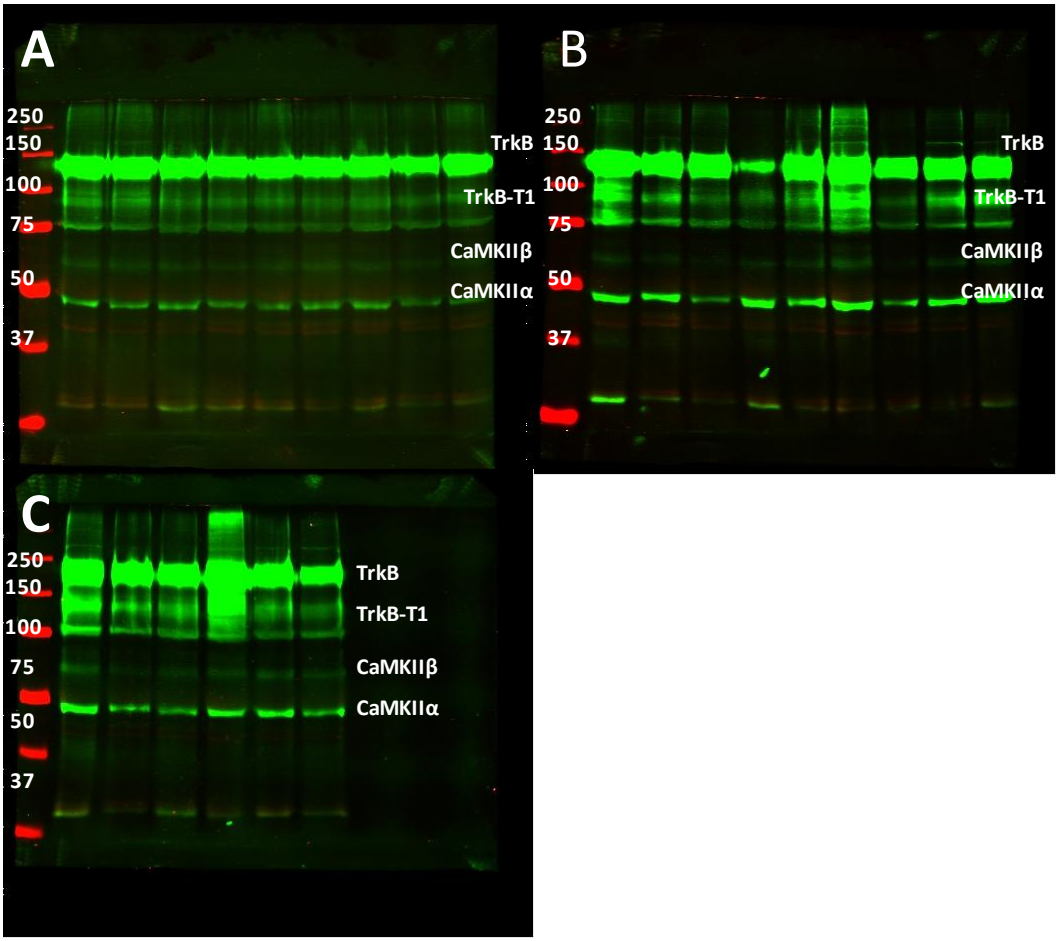

Figure C-11: Digital pictures of the membranes after detection of TrkB, TrkB-T1, CaMKIIα and CaMKIIβ.

(A) Samples 37 to 45; (B) Samples 46 to 54; (C) Samples 55 to 60.

Ladder in KDa

C.12 Detection of TrkB, TrkB-T1 and actin

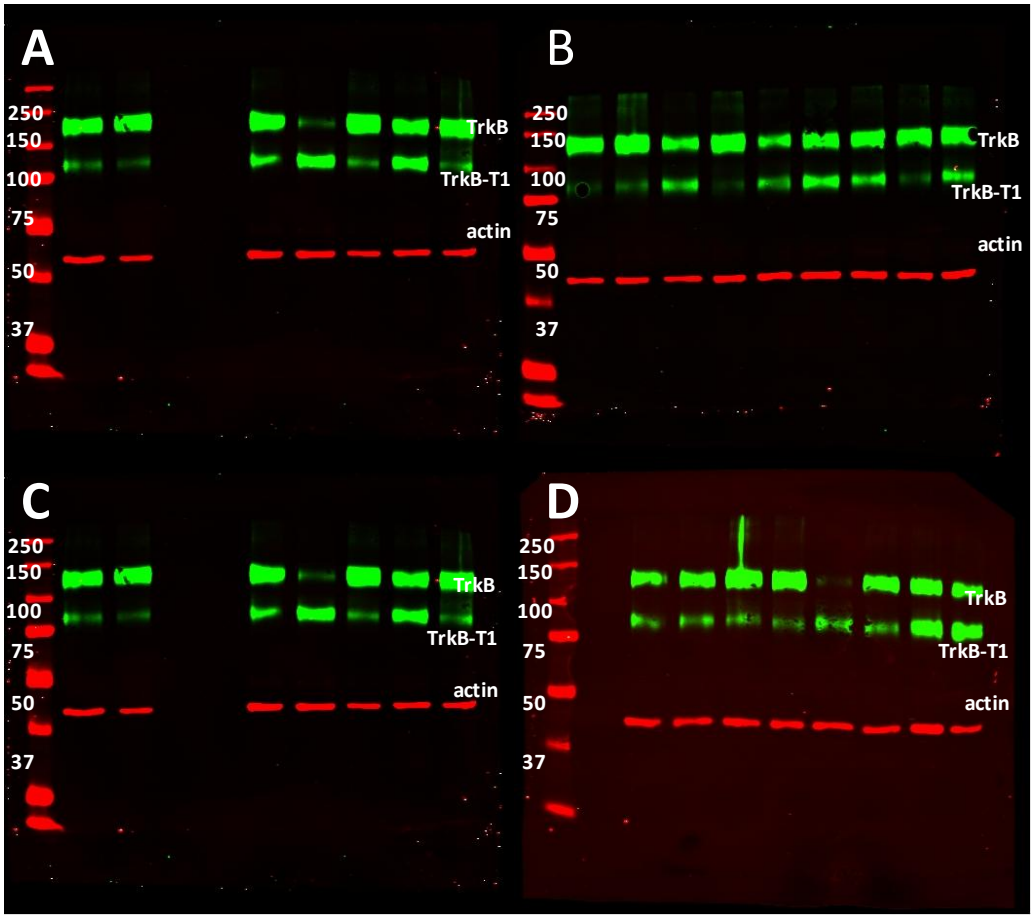

Figure C-12: Digital pictures of the membranes after detection of TrkB, TrkB-T1 and actin.

(A) Samples 3 to 9; (B) Samples 10 to 18; (C) Samples 19 to 25; (D) Samples 26 to 34.

Ladder in KDa

C.13 Detection of TrkB, TrkB-T1 and actin

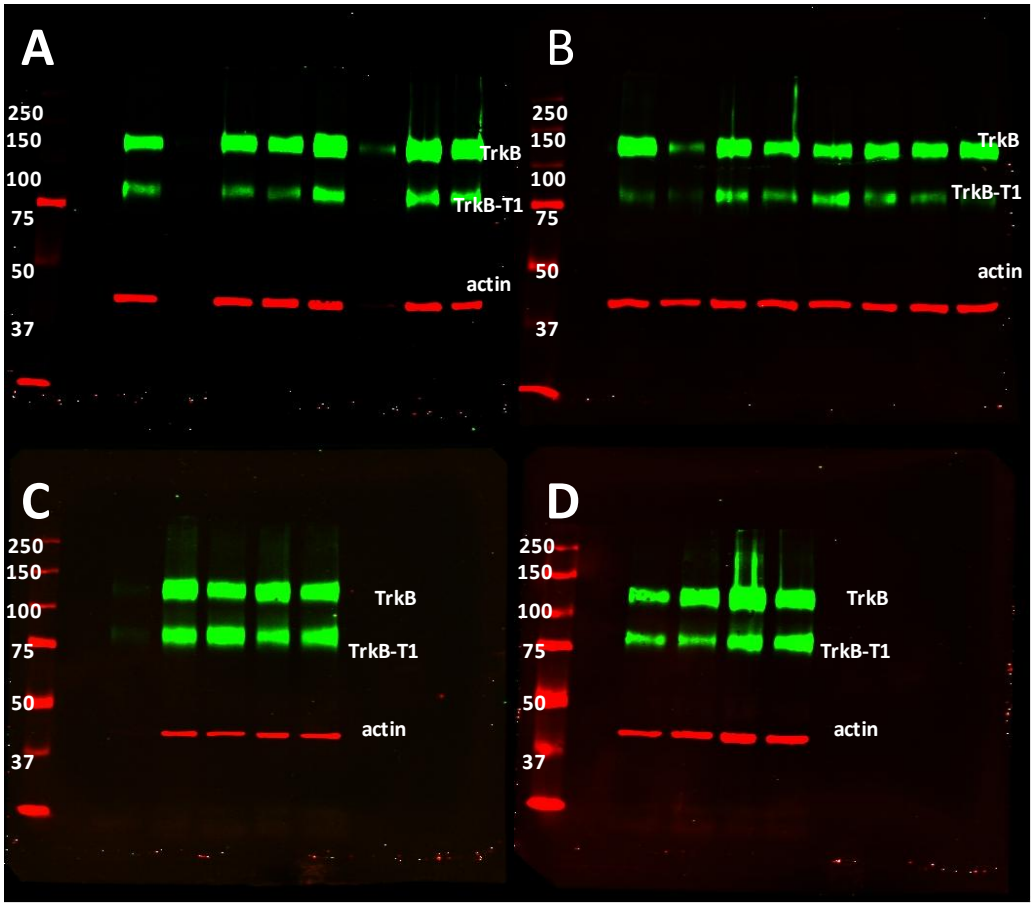

Figure C-13: Digital pictures of the membranes after detection of TrkB, TrkB-T1 and actin.

(A) Samples 35 to 43; (B) Samples 44 to 51; (C) Samples 52 to 56; (D) Samples 57 to 60.

Ladder in KDa

C.14 Detection of TrkB, TrkB-T1 and actin

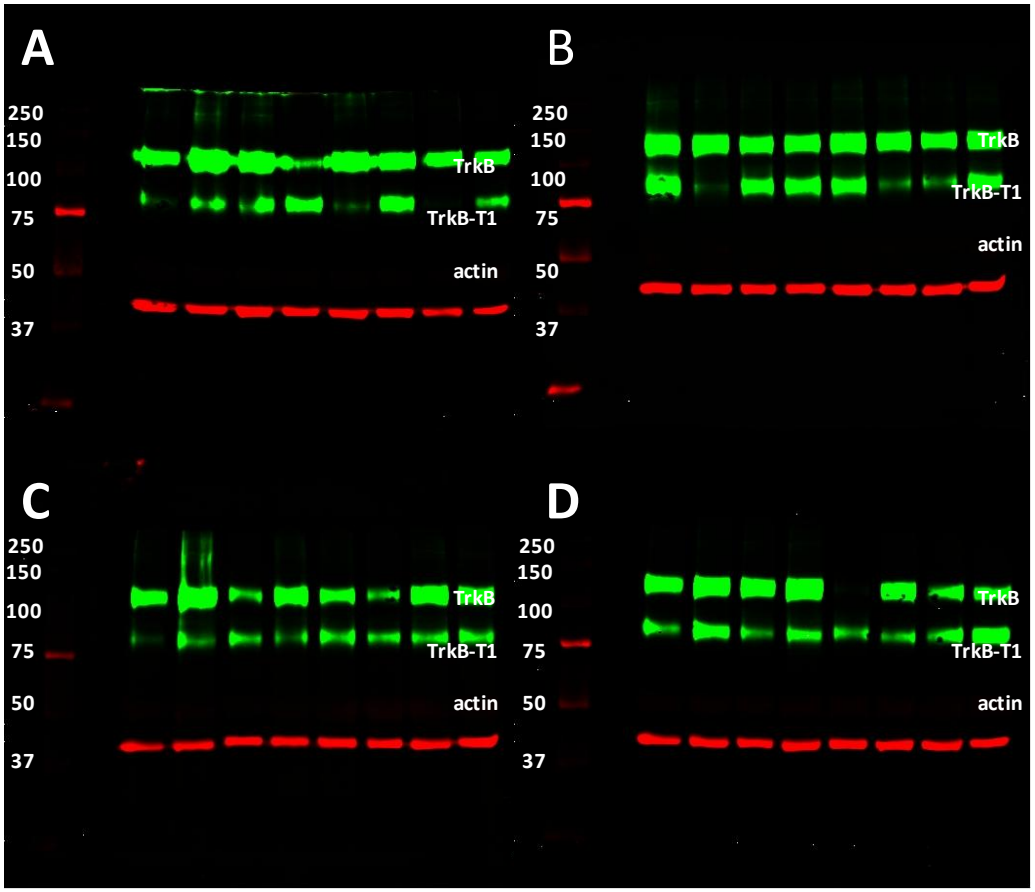

Figure C-14: Digital pictures of the membranes after detection of TrkB, TrkB-T1 and actin.

(A) Samples 3 to 11; (B) Samples 12 to 19; (C) Samples 20 to 27; (D) Samples 28 to 36.

Ladder in KDa

C.15 Detection of TrkB, TrkB-T1 and actin

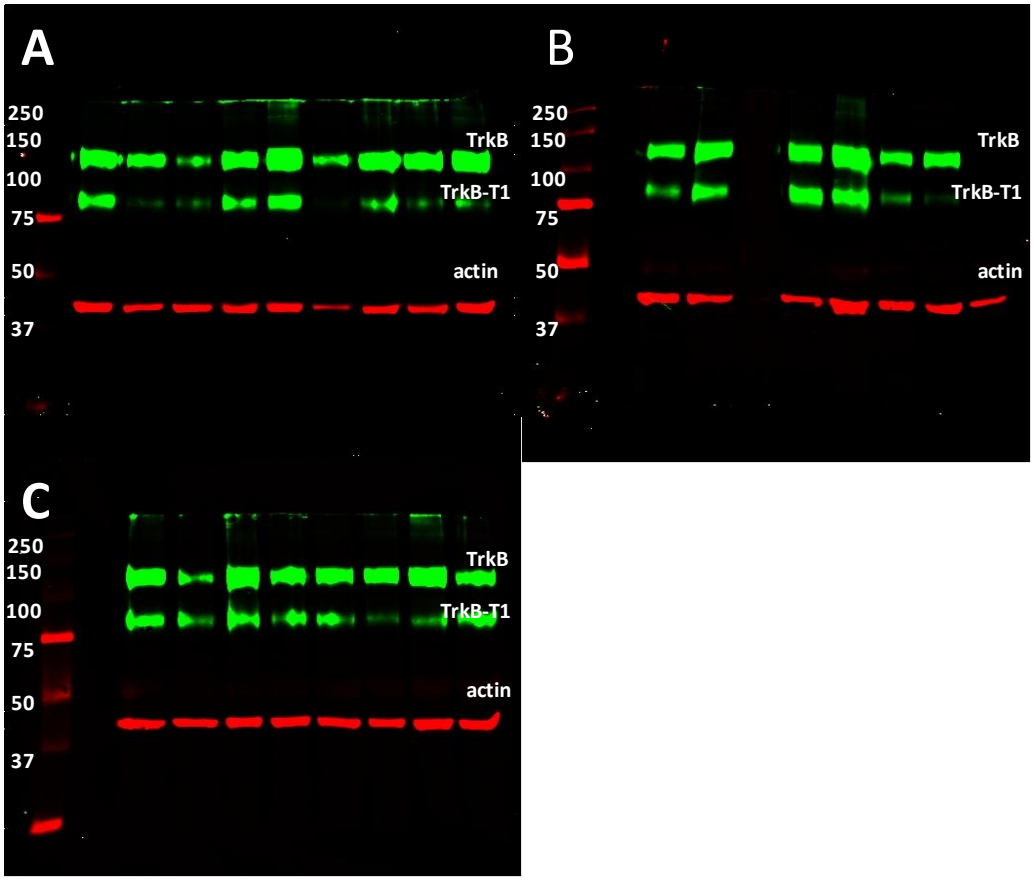

Figure C-15: Digital pictures of the membranes after detection of TrkB, TrkB-T1 and actin.

(A) Samples 37 to 45; (B) Samples 46 to 52; (C) Samples 53 to 60.

Ladder in KDa

C.16 Detection of CaMKIIα and CaMKIIβ

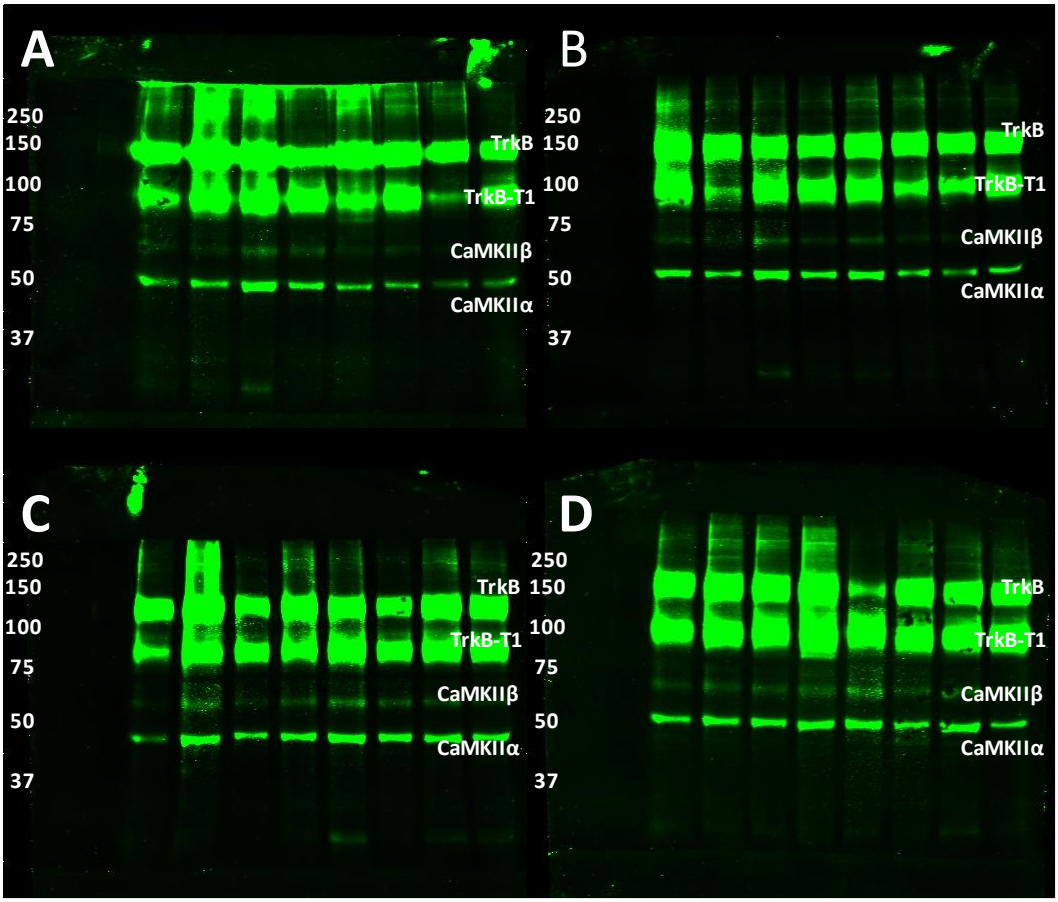

Figure C-16: Digital pictures of the membranes after detection of CaMKIIα and CaMKIIβ.

(A) Samples 3 to 11; (B) Samples 12 to 19; (C) Samples 20 to 27; (D) Samples 28 to 36.

Ladder in KDa

C.17 Detection of CaMKIIα and CaMKIIβ

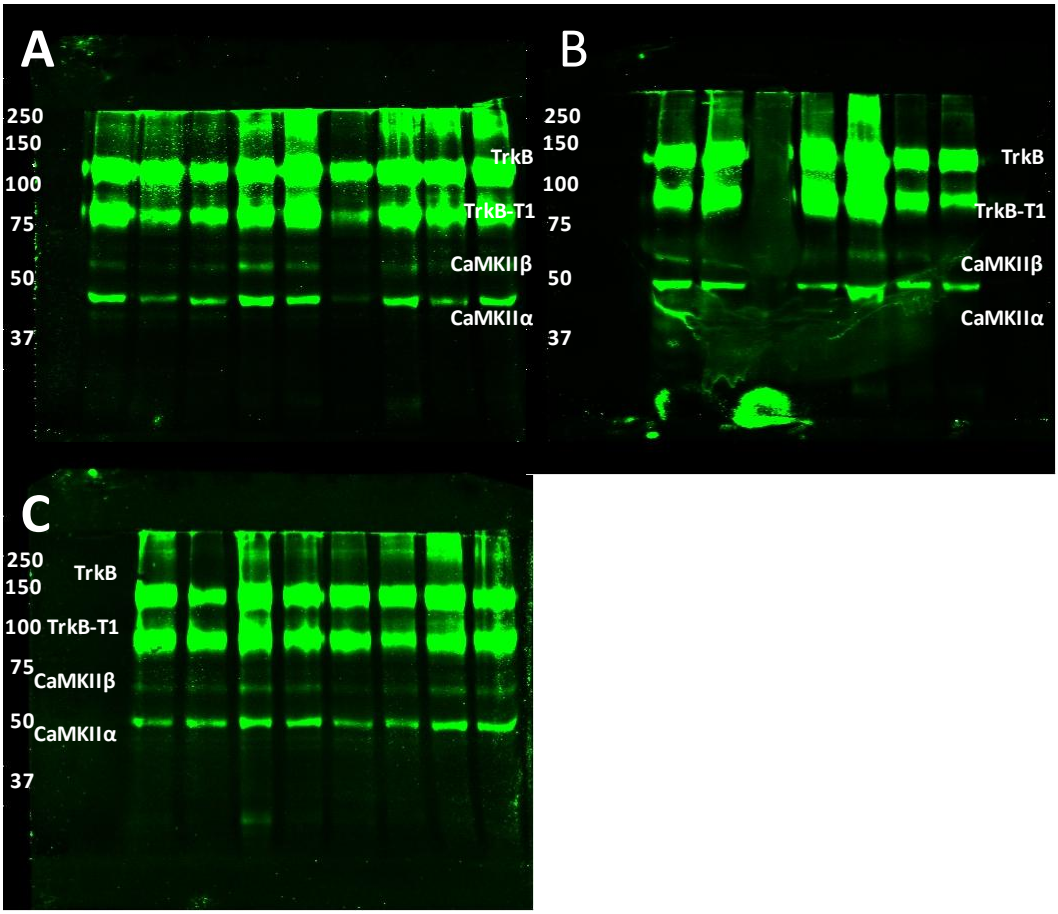

Figure C-17: Digital pictures of the membranes after detection of CaMKIIα and CaMKIIβ.

(A) Samples 37 to 45; (B) Samples 46 to 52; (C) Samples 53 to 60.

Ladder in KDa

C.18 Detection of CaMKIIα and CaMKIIβ

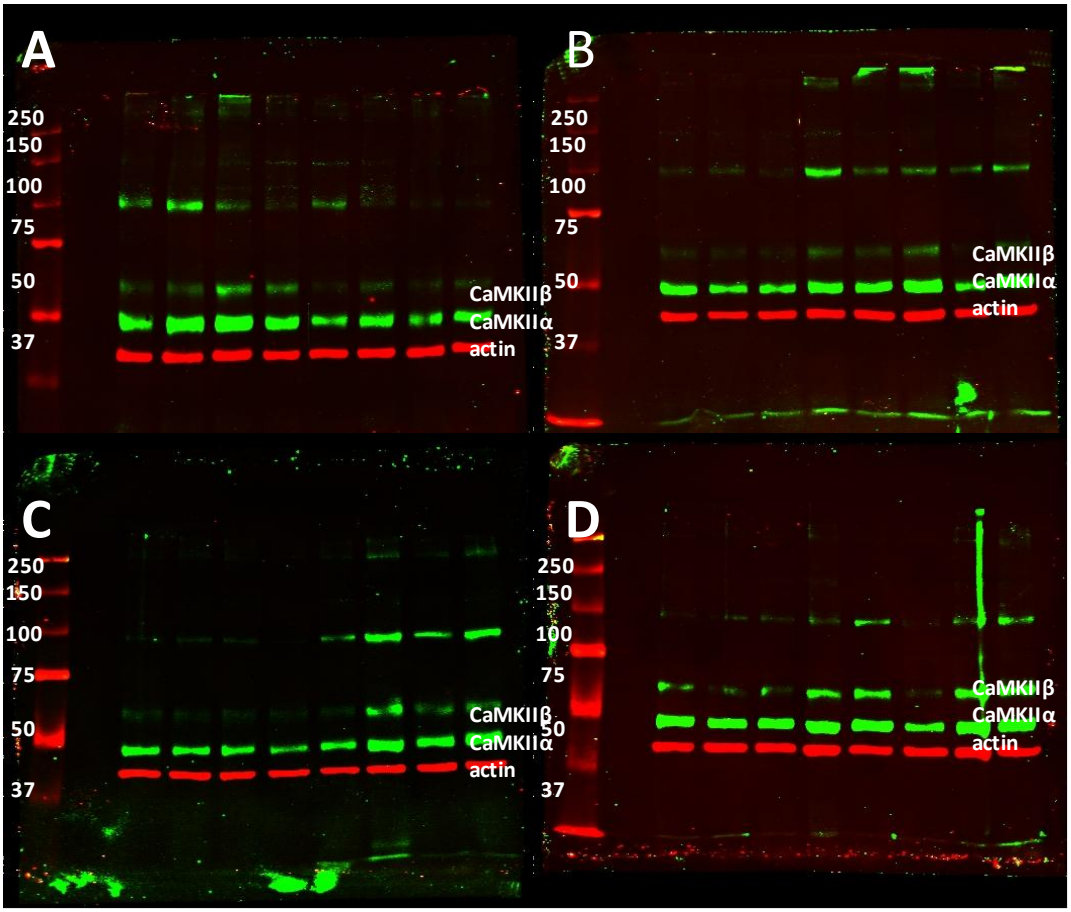

Figure C-18: Digital pictures of the membranes after detection of CaMKIIα and CaMKIIβ.

(A) Samples 3to 10; (B) Samples 11 to 18; (C) Samples 19 to 26; (D) Samples 27 to 35.

Ladder in KDa

C.19 Detection of CaMKIIα and CaMKIIβ

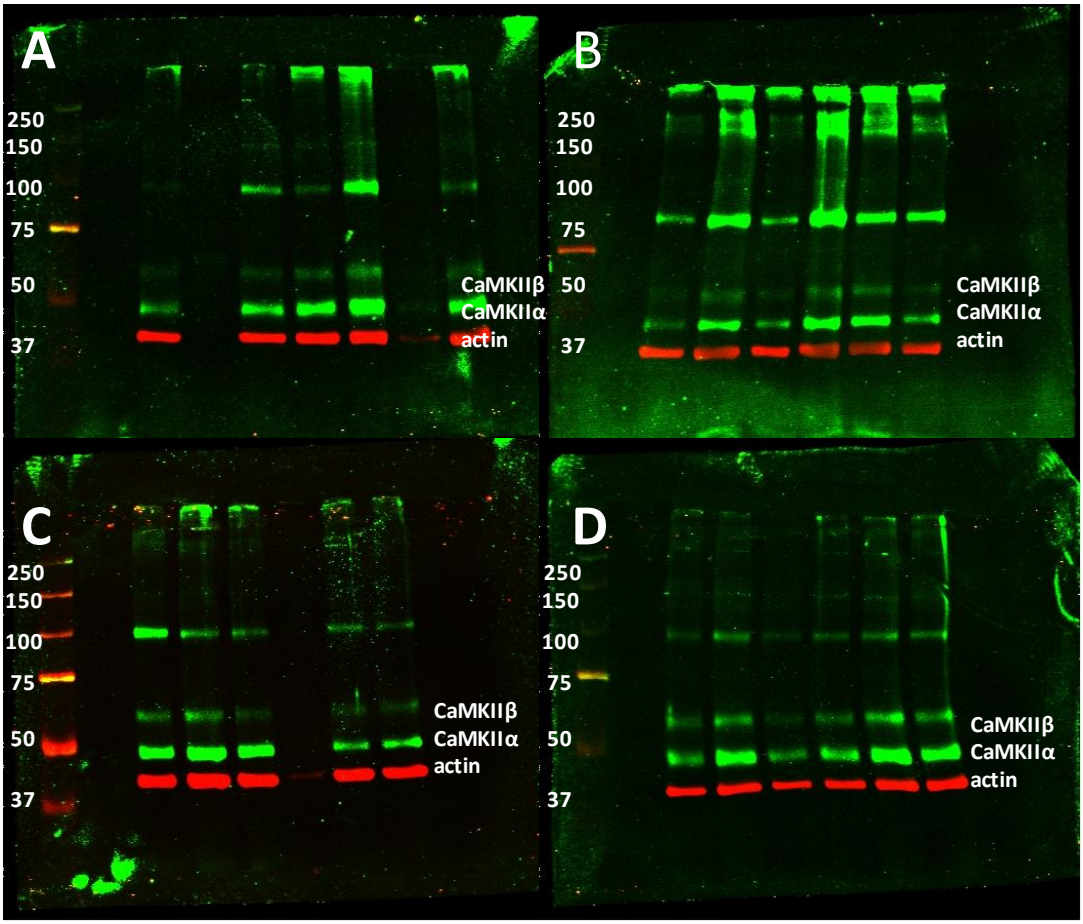

Figure C-19: Digital pictures of the membranes after detection of PSD-95, NSF, tubulin and actin.

(A) Samples 36 to 43 (B) Samples 44 to 49; (C) Samples 50 to 55; (D) Samples 56 to 60.

Ladder in KDa

REFERENCES

Akiyama, T. (1997), "DAP-1, a novel protein that interacts with the guanylate kinase-like domains of hDLG and PSD-95", *Genes to Cells,* vol. 2, no. 6, pp. 415-424.

Alié, A. and Manuël, M. (2010), "The backbone of the post-synaptic density originated in a unicellular ancestor of choanoflagellates and metazoans", *BMC Evolutionary Biology,* vol. 10, no. 1.

Amaral, M. D. and Pozzo-Miller, L. (2007), "TRPC3 channels are necessary for brain-derived neurotrophic factor to activate a nonselective cationic current and to induce dendritic spine formation", *Journal of Neuroscience,* vol. 27, no. 19, pp. 5179-5189.

Andreasen, N. C. (2000), "Schizophrenia: The fundamental questions", *Brain Research Reviews,* vol. 31, no. 2-3, pp. 106-112.

Ango, F., Prézeau, L., Muller, T., Tu, J. C., Xiao, B., Worley, P. F., Pin, J. P., Bockaert, J. and Fagni, L. (2001), "Agonist-independent activation of metabotropic glutamate receptors by the intracellular protein Homer", *Nature,* vol. 411, no. 6840, pp. 962-965.

Aoki, C., Miko, I., Oviedo, H., Mikeladze-Dvali, T., Alexandre, L., Sweeney, N. and Bredt, D. S. (2001), "Electron microscopic immunocytochemical detection of PSD-95, PSD-93, SAP-102, and SAP-97 at postsynaptic, presynaptic, and nonsynaptic sites of adult and neonatal rat visual cortex", *Synapse,* vol. 40, no. 4, pp. 239-257.

Asrican, B., Lisman, J. and Otmakhov, N. (2007), "Synaptic strength of individual spines correlates with bound Ca 2+-calmodulin-dependent kinase II", *Journal of Neuroscience,* vol. 27, no. 51, pp. 14007-14011.

Atwal, J. K., Massie, B., Miller, F. D. and Kaplan, D. R. (2000), "The TrkB-Shc site signals neuronal survival and local axon growth via MEK and PI3-Kinase", *Neuron,* vol. 27, no. 2, pp. 265-277.

Baciu, M. V., Rubin, C., Décorps, M. A. and Segebarth, C. M. (1999), "fMRI assessment of hemispheric language dominance using a simple inner speech paradigm", *NMR in biomedicine,* vol. 12, no. 5, pp. 293-298.

Badner, J. A. and Gershon, E. S. (2002), "Meta-analysis of whole-genome linkage scans of bipolar disorder and schizophrenia", *Molecular psychiatry,* vol. 7, no. 4, pp. 405-411.

Ballard, T. M., Pauly-Evers, M., Higgins, G. A., Ouagazzal, A. -., Mutel, V., Borroni, E., Kemp, J. A., Bluethmann, H. and Kew, J. N. C. (2002), "Severe impairment of NMDA receptor function in mice carrying targeted point mutations in the glycine

binding site results in drug-resistant nonhabituating hyperactivity", *Journal of Neuroscience,* vol. 22, no. 15, pp. 6713-6723.

Barakat, A., Dean, B., Scarr, E. and Evin, G. (2010), "Decreased Neuregulin 1 C-terminal fragment in Brodmann's area 6 of patients with schizophrenia", *Schizophrenia research,* vol. 124, no. 1-3, pp. 200-207.

Barbas, H. (2000), "Connections underlying the synthesis of cognition, memory, and emotion in primate prefrontal cortices", *Brain research bulletin,* vol. 52, no. 5, pp. 319-330.

Barbas, H. and Pandya, D. N. (1987), "Architecture and frontal cortical connections of the premotor cortex (area 6) in the rhesus monkey", *Journal of Comparative Neurology,* vol. 256, no. 2, pp. 211-228.

Basho, S., Palmer, E. D., Rubio, M. A., Wulfeck, B. and Müller, R. -. (2007), "Effects of generation mode in fMRI adaptations of semantic fluency: Paced production and overt speech", *Neuropsychologia,* vol. 45, no. 8, pp. 1697-1706.

Baudendistel, K., Schröder, J., Essig, M., Gerdssen, I., Jahn, T., Wenz, F., Linke, A., Knopp, M. V. and Schad, L. R. (1997), "Sensorimotor cortex and supplementary motor area activation changes in schizophrenia: Studies with functional magnetic resonance imaging", *NeuroImage,* vol. 5, no. 4 PART II.

Beneyto, M. and Meador-Woodruff, J. H. (2008), "Lamina-specific abnormalities of NMDA receptor-associated postsynaptic protein transcripts in the prefrontal cortex in schizophrenia and bipolar disorder", *Neuropsychopharmacology,* vol. 33, no. 9, pp. 2175-2186.

Bennett, A. O. M. R. (2008), "Dual constraints on synapse formation and regression in schizophrenia: neuregulin, neuroligin, dysbindin, DISC1, MuSK and agrin", *The Australian and New Zealand Journal of Psychiatry,* vol. 42, no. 8, pp. 662-677.

Berthoz, A. (1997), "Parietal and hippocampal contribution to topokinetic and topographic memory", *Philosophical Transactions of the Royal Society B: Biological Sciences,* vol. 352, no. 1360, pp. 1437-1448.

Bertolino, A., Esposito, G., Callicott, J. H., Mattay, V. S., Van Horn, J. D., Frank, J. A., Berman, K. F. and Weinberger, D. R. (2000), "Specific relationship between prefrontal neuronal N-acetylaspartate and activation of the working memory cortical network in schizophrenia", *American Journal of Psychiatry,* vol. 157, no. 1, pp. 26-33.

Biffo, S., Offenhauser, N., Carter, B. D. and Barde, Y. -. (1995), "Selective binding and internalisation by truncated receptors restrict the availability of BDNF during development", *Development,* vol. 121, no. 8, pp. 2461-2470.

Bitanihirwe, B. K. Y., Lim, M. P., Kelley, J. F., Kaneko, T. and Woo, T. U. W. (2009), "Glutamatergic deficits and parvalbumin-containing inhibitory neurons in the prefrontal cortex in schizophrenia", *BMC Psychiatry,* vol. 9.

Boeckers, T. M. (2006), "The postsynaptic density", *Cell and tissue research,* vol. 326, no. 2, pp. 409-422.

Bracken, B. K. and Tyrrigiano, G. G. (2009), "Experience-dependent regulation of TrkB isoforms in rodent visual cortex", *Developmental Neurobiology,* vol. 69, no. 5, pp. 267-278.

Bradley, J., Carter, S. R., Rao, V. R., Wang, J. and Finkbeiner, S. (2006), "Splice variants of the NR1 subunit differentially induce NMDA receptor-dependent gene expression", *Journal of Neuroscience,* vol. 26, no. 4, pp. 1065-1076.

Brakeman, P. R., Lanahan, A. A., O'Brien, R., Roche, K., Barnes, C. A., Huganir, R. L. and Worley, P. F. (1997), "Homer: A protein that selectively binds metabotropic glutamate receptors", *Nature,* vol. 386, no. 6622, pp. 284-288.

Brakke, M. K. (1951), "Density gradient centrifugation: A new separation technique", *Journal of the American Chemical Society,* vol. 73, no. 4, pp. 1847-1848.

Bublil, E. M. and Yarden, Y. (2007), "The EGF receptor family: spearheading a merger of signaling and therapeutics", *Current opinion in cell biology,* vol. 19, no. 2, pp. 124-134.

Buchanan, R. W. (2007), "Persistent negative symptoms in schizophrenia: An overview", *Schizophrenia bulletin,* vol. 33, no. 4, pp. 1013-1022.

Buchanan, R. W., Freedman, R., Javitt, D. C., Abi-Dargham, A. and Lieberman, J. A. (2007), "Recent advances in the development of novel pharmacological agents for the treatment of cognitive impairments in schizophrenia", *Schizophrenia bulletin,* vol. 33, no. 5, pp. 1120-1130.

Burnet, P. W. J., Anderson, P. N., Chen, L., Nikiforova, N., Harrison, P. J. and Wood, M. J. A. (2011), "D-Amino acid oxidase knockdown in the mouse cerebellum reduces NR2A mRNA", *Molecular and Cellular Neuroscience,* vol. 46, no. 1, pp. 167-175.

Burnet, P. W. J., Eastwood, S. L. and Harrison, P. J. (1996), "5-HT(1A) 5-HT(2A) receptor mRNAs and binding site densities are differentially altered in schizophrenia", *Neuropsychopharmacology,* vol. 15, no. 5, pp. 442-455.

Burton, M. W., Noll, D. C. and Small, S. L. (2001), "The anatomy of auditory word processing: Individual variability", *Brain and language,* vol. 77, no. 1, pp. 119-131.

Cannon, M. and Clarke, M. C. (2005), "Risk for schizophrenia - Broadening the concepts, pushing back the boundaries", *Schizophrenia research,* vol. 79, no. 1, pp. 5-13.

Cardno, A. G. and Gottesman, I. I. (2000), "Twin studies of schizophrenia: From bow-and-arrow concordances to star wars Mx and functional genomics", *American Journal of Medical Genetics - Seminars in Medical Genetics,* vol. 97, no. 1, pp. 12-17.

Carim-Todd, L., Bath, K. G., Fulgenzi, G., Yanpallewar, S., Jing, D., Barrick, C. A., Becker, J., Buckley, H., Dorsey, S. G., Lee, F. S. and Tessarollo, L. (2009), "Endogenous truncated TrkB.T1 receptor regulates neuronal complexity and TrkB kinase receptor function in vivo", *Journal of Neuroscience,* vol. 29, no. 3, pp. 678-685.

Carlin, R. K., Grab, D. J., Cohen, R. S. and Siekevitz, P. (1980), "Isolation and characterization of postsynaptic densities from various brain regions: enrichment of different types of postsynaptic densities", *Journal of Cell Biology,* vol. 86, no. 3, pp. 831-843.

Cascella, N. G., Fieldstone, S. C., Rao, V. A., Pearlson, G. D., Sawa, A. and Schretlen, D. J. (2010), "Gray-matter abnormalities in deficit schizophrenia", *Schizophrenia research,* vol. 120, no. 1-3, pp. 63-70.

Chan, R. C. K., Shum, D., Toulopoulou, T. and Chen, E. Y. H. (2008), "Assessment of executive functions: Review of instruments and identification of critical issues", *Archives of Clinical Neuropsychology,* vol. 23, no. 2, pp. 201-216.

Chao, M. V. (2003), "Neurotrophins and their receptors: A convergence point for many signalling pathways", *Nature Reviews Neuroscience,* vol. 4, no. 4, pp. 299-309.

Chen, G., Henter, I. D. and Manji, H. K. (2010), "Presynaptic Glutamatergic Dysfunction in Bipolar Disorder", *Biological psychiatry,* vol. 67, no. 11, pp. 1007-1009.

Chen, L., Chetkovich, D. M., Petralia, R. S., Sweeney, N. T., Kawasaki, Y., Wenthold, R. J., Bredt, D. S. and Nicoll, R. A. (2000), "Stargazin regulates synaptic targeting of AMPA receptors by two distinct mechanisms", *Nature,* vol. 408, no. 6815, pp. 936-943.

Chen, X., Vinade, L., Leapman, R. D., Petersen, J. D., Nakagawa, T., Phillips, T. M., Sheng, M. and Reese, T. S. (2005), "Mass of the postsynaptic density and

enumeration of three key molecules", *Proceedings of the National Academy of Sciences of the United States of America,* vol. 102, no. 32, pp. 11551-11556.

Cho, K. -., Hunt, C. A. and Kennedy, M. B. (1992a), "The rat brain postsynaptic density fraction contains a homolog of the Drosophila discs-large tumor suppressor protein", *Neuron,* vol. 9, no. 5, pp. 929-942.

Cho, K. -., Hunt, C. A. and Kennedy, M. B. (1992b), "The rat brain postsynaptic density fraction contains a homolog of the Drosophila discs-large tumor suppressor protein", *Neuron,* vol. 9, no. 5, pp. 929-942.

Clinton, S. M., Haroutunian, V., Davis, K. L. and Meador-Woodruff, J. H. (2003), "Altered transcript expression of NMDA receptor-associated postsynaptic proteins in the thalamus of subjects with schizophrenia", *American Journal of Psychiatry,* vol. 160, no. 6, pp. 1100-1109.

Clinton, S. M., Haroutunian, V. and Meador-Woodruff, J. H. (2006), "Up-regulation of NMDA receptor subunit and post-synaptic density protein expression in the thalamus of elderly patients with schizophrenia", *Journal of neurochemistry,* vol. 98, no. 4, pp. 1114-1125.

Clinton, S. M. and Meadow-Woodruff, J. H. (2004), "Abnormalities of the NMDA receptor and associated intracellular molecules in the thalamus in schizophrenia and bipolar disorder", *Neuropsychopharmacology,* vol. 29, no. 7, pp. 1353-1362.

Cohen, R. S., Blomberg, F., Berzins, K. and Siekevitz, P. (1977), "The structure of postsynaptic densities isolated from dog cerebral cortex. I. Overall morphology and protein composition", *Journal of Cell Biology,* vol. 74, no. 1, pp. 181-203.

Colbran, R. J. and Brown, A. M. (2004), "Calcium/calmodulin-dependent protein kinase II and synaptic plasticity", *Current opinion in neurobiology,* vol. 14, no. 3, pp. 318-327.

Colby, C. L. and Duhamel, J. -. (1991), "Heterogeneity of extrastriate visual areas and multiple parietal areas in the macaque monkey", *Neuropsychologia,* vol. 29, no. 6, pp. 517-537.

Collins, M. O., Husi, H., Yu, L., Brandon, J. M., Anderson, C. N., Blackstock, W. P., Choudhary, J. S. and Grant, S. G. (2006a), "Molecular characterization and comparison of the components and multiprotein complexes in the postsynaptic proteome.", *Journal of neurochemistry.,* vol. 97 Suppl 1, pp. 16-23.

Collins, M. O., Husi, H., Yu, L., Brandon, J. M., Anderson, C. N., Blackstock, W. P., Choudhary, J. S. and Grant, S. G. (2006b), "Molecular characterization and

comparison of the components and multiprotein complexes in the postsynaptic proteome.", *Journal of neurochemistry,* vol. 97 Suppl 1, pp. 16-23.

Corvin, A., McGhee, K. A., Murphy, K., Donohoe, G., Nangle, J. M., Schwaiger, S., Kenny, N., Clarke, S., Meagher, D., Quinn, J., Scully, P., Baldwin, P., Browne, D., Walsh, C., Waddington, J. L., Morris, D. W. and Gill, M. (2007), "Evidence for association and epistasis at the DAOA/G30 and D-amino acid oxidase loci in an Irish schizophrenia sample", *American Journal of Medical Genetics, Part B: Neuropsychiatric Genetics,* vol. 144, no. 7, pp. 949-953.

Cotman, C. W., Banker, G., Churchill, L. and Taylor, D. (1974), "Isolation of postsynaptic densities from rat brain", *Journal of Cell Biology,* vol. 63, no. 2.

Cotter, D., Kerwin, R., Al-Sarraji, S., Brion, J. P., Chadwich, A., Lovestone, S., Anderton, B. and Everall, I. (1998), "Abnormalities of Wnt signalling in schizophrenia - Evidence for neurodevelopmental abnormality", *Neuroreport,* vol. 9, no. 7, pp. 1379-1383.

Coulson, E.J., Reid, K., Shipham, K.M., Morley, S., Kilpatrick, T.J. and Bartlett, P.F., (2004), *The role of neurotransmission and the Chopper domain in p75 neurotrophin receptor death signaling*.

Craddock, N., O'Donovan, M. C. and Owen, M. J. (2005), "The genetics of schizophrenia and bipolar disorder: Dissecting psychosis", *Journal of medical genetics,* vol. 42, no. 3, pp. 193-204.

Crozier, S., Sirigu, A., Lehéricy, S., Van De Moortele, P. -., Pillon, B., Grafman, J., Agid, Y., Dubois, B. and Lebihan, D. (1999), "Distinct prefrontal activations in processing sequence at the sentence and script level: An fMRI study", *Neuropsychologia,* vol. 37, no. 13, pp. 1469-1476.

Dagher, A., Owen, A. M., Boecker, H. and Brooks, D. J. (1999), "Mapping the network for planning: A correlational PET activation study with the Tower of London task", *Brain,* vol. 122, no. 10, pp. 1973-1987.

Dale, T. C. (1998), "Signal transduction by the Wnt family of ligands", *Biochemical Journal,* vol. 329, no. 2, pp. 209-223.

Dalva, M. B., Takasu, M. A., Lin, M. Z., Shamah, S. M., Hu, L., Gale, N. W. and Greenberg, M. E. (2000), "EphB receptors interact with NMDA receptors and regulate excitatory synapse formation", *Cell,* vol. 103, no. 6, pp. 945-956.

Danckert, J., Rossetti, Y., D'Amato, T., Dalery, J. and Saoud, M. (2002), "Exploring imagined movements in patients with schizophrenia", *Neuroreport,* vol. 13, no. 5, pp. 605-609.

Dazzan, P. and Murray, R. M. (2002), "Neurological soft signs in first-episode psychosis: A systematic review", *British Journal of Psychiatry,* vol. 181, no. SUPPL. 43, pp. s50-s57.

De Carli, D., Garreffa, G., Colonnese, C., Giulietti, G., Labruna, L., Briselli, E., Ken, S., Macrì, M. A. and Maraviglia, B. (2007), "Identification of activated regions during a language task", *Magnetic resonance imaging,* vol. 25, no. 6, pp. 933-938.

Delint-Ramirez, I., Fernández, E., Bayés, A., Kicsi, E., Komiyama, N. H. and Grant, S. G. N. (2010), "In vivo composition of NMDA receptor signaling complexes differs between membrane subdomains and is modulated by PSD-95 and PSD-93", *Journal of Neuroscience,* vol. 30, no. 24, pp. 8162-8170.

Demily, C. and Thibaut, F. (2008), "Environmental Risk Factors and Schizophrenia", *Annales Medico-Psychologiques,* vol. 166, no. 8, pp. 606-611.

DeRosse, P., Funke, B., Burdick, K. E., Lencz, T., Ekholm, J. M., Kane, J. M., Kucherlapati, R. and Malhotra, A. K. (2006), "Dysbindin genotype and negative symptoms in schizophrenia", *American Journal of Psychiatry,* vol. 163, no. 3, pp. 532-534.

Dietz, N. A. E., Jones, K. M., Gareau, L., Zeffiro, T. A. and Eden, G. F. (2005), "Phonological decoding involves left posterior fusiform gyrus", *Human brain mapping,* vol. 26, no. 2, pp. 81-93.

Ding, L. and Hegde, A. N. (2009), "Expression of RGS4 Splice Variants in Dorsolateral Prefrontal Cortex of Schizophrenic and Bipolar Disorder Patients", *Biological psychiatry,* vol. 65, no. 6, pp. 541-545.

Dong, H., O'Brien, R. J., Fung, E. T., Lanahan, A. A., Worley, P. F. and Huganir, R. L. (1997), "GRIP: A synaptic PDZ domain-containing protein that interacts with AMPA receptors", *Nature,* vol. 386, no. 6622, pp. 279-284.

Dosemeci, A., Makusky, A. J., Jankowska-Stephens, E., Yang, X., Slotta, D. J. and Markey, S. P. (2007), "Composition of the synaptic PSD-95 complex", *Molecular and Cellular Proteomics,* vol. 6, no. 10, pp. 1749-1760.

Dosemeci, A., Reese, T. S., Petersen, J. and Tao-Cheng, J. -. (2000), "A novel particulate form of Ca2+/CaMKII-dependent protein kinase II in neurons", *Journal of Neuroscience,* vol. 20, no. 9, pp. 3076-3084.

Dosemeci, A., Tao-Cheng, J. -., Vinade, L. and Jaffe, H. (2006), "Preparation of postsynaptic density fraction from hippocampal slices and proteomic analysis", *Biochemical and biophysical research communications,* vol. 339, no. 2, pp. 687-694.

Dosemeci, A., Tao-Cheng, J. -., Vinade, L., Winters, C. A., Pozzo-Miller, L. and Reese, T. S. (2001), "Glutamate-induced transient modification of the postsynaptic density", *Proceedings of the National Academy of Sciences of the United States of America,* vol. 98, no. 18, pp. 10428-10432.

Dracheva, S., Marras, S. A. E., Elhakem, S. L., Kramer, F. R., Davis, K. L. and Haroutunian, V. (2001), "N-methyl-D-aspartic acid receptor expression in the dorsolateral prefrontal cortex of elderly patients with schizophrenia", *American Journal of Psychiatry,* vol. 158, no. 9, pp. 1400-1410.

Dum, R. P. and Strick, P. L. (1991), "The origin of corticospinal projections from the premotor areas in the frontal lobe", *Journal of Neuroscience,* vol. 11, no. 3, pp. 667-689.

Dum, R. P. and Strick, P. L. (2005), "Frontal lobe inputs to the digit representations of the motor areas on the lateral surface of the hemisphere", *Journal of Neuroscience,* vol. 25, no. 6, pp. 1375-1386.

Dunham, J. S., Deakin, J. F. W., Miyajima, F., Payton, A. and Toro, C. T. (2009), "Expression of hippocampal brain-derived neurotrophic factor and its receptors in Stanley consortium brains", *Journal of psychiatric research,* vol. 43, no. 14, pp. 1175-1184.

Eastwood, S.L., (2003), *The synaptic pathology of schizophrenia: Is aberrant neurodevelopment and plasticity to blame?*.

Eastwood, S. L. and Harrison, P. J. (1995), "Decreased synaptophysin in the medial temporal lobe in schizophrenia demonstrated using immunoautoradiography", *Neuroscience,* vol. 69, no. 2, pp. 339-343.

Ehrlich, I., Klein, M., Rumpel, S. and Malinow, R. (2007), "PSD-95 is required for activity-driven synapse stabilization", *Proceedings of the National Academy of Sciences of the United States of America,* vol. 104, no. 10, pp. 4176-4181.

Eide, F. F., Vining, E. R., Eide, B. L., Zang, K., Wang, X. -. and Reichardt, L. F. (1996), "Naturally occurring truncated trkB receptors have dominant inhibitory effects on brain-derived neurotrophic factor signaling", *Journal of Neuroscience,* vol. 16, no. 10, pp. 3123-3129.

El-Husseini, A. E. -., Schnell, E., Chetkovich, D. M., Nicoll, R. A. and Bredt, D. S. (2000), "PSD-95 involvement in maturation of excitatory synapses", *Science,* vol. 290, no. 5495, pp. 1364-1368.

El-Husseini, A. E. -., Schnell, E., Dakoji, S., Sweeney, N., Zhou, Q., Prange, O., Gauthier-Campbell, C., Aguilera-Moreno, A., Nicoll, R. A. and Bredt, D. S. (2002), "Synaptic strength regulated by palmitate cycling on PSD-95", *Cell,* vol. 108, no. 6, pp. 849-863.

Elias, G. M. and Nicoll, R. A. (2007), "Synaptic trafficking of glutamate receptors by MAGUK scaffolding proteins", *Trends in cell biology,* vol. 17, no. 7, pp. 343-352.

Emes, R. D., Pocklington, A. J., Anderson, C. N. G., Bayes, A., Collins, M. O., Vickers, C. A., Croning, M. D. R., Malik, B. R., Choudhary, J. S., Armstrong, J. D. and Grant, S. G. N. (2008), "Evolutionary expansion and anatomical specialization of synapse proteome complexity", *Nature neuroscience,* vol. 11, no. 7, pp. 799-806.

Emilien, G., Maloteaux, J. -., Geurts, M., Hoogenberg, K. and Cragg, S. (1999), "Dopamine receptors - Physiological understanding to therapeutic intervention potential", *Pharmacology and Therapeutics,* vol. 84, no. 2, pp. 133-156.

Escamilla, M. A. (2001), "Diagnosis and treatment of mood disorders that co-occur with schizophrenia", *Psychiatric Services,* vol. 52, no. 7, pp. 911-919.

Ethell, I. M. and Pasquale, E. B. (2005), "Molecular mechanisms of dendritic spine development and remodeling", *Progress in neurobiology,* vol. 75, no. 3, pp. 161-205.

Etienne-Manneville, S. and Hall, A. (2002), "Rho GTPases in cell biology", *Nature,* vol. 420, no. 6916, pp. 629-635.

Evers, D. M., Matta, J. A., Hoe, H. -., Zarkowsky, D., Lee, S. H., Isaac, J. T. and Pak, D. T. S. (2010), "Plk2 attachment to NSF induces homeostatic removal of GluA2 during chronic overexcitation", *Nature neuroscience,* vol. 13, no. 10, pp. 1199-1207.

Exner, C., Weniger, G., Schmidt-Samoa, C. and Irle, E. (2006), "Reduced size of the pre-supplementary motor cortex and impaired motor sequence learning in first-episode schizophrenia", *Schizophrenia research,* vol. 84, no. 2-3, pp. 386-396.

Fallon, J. H., Opole, I. O. and Potkin, S. G. (2003), "The neuroanatomy of schizophrenia: Circuitry and neurotransmitter systems", *Clinical Neuroscience Research,* vol. 3, no. 1-2, pp. 77-107.

Farr, C. D., Gafken, P. R., Norbeck, A. D., Doneanu, C. E., Stapels, M. D., Barofsky, D. F., Minami, M. and Saugstad, J. A. (2004), "Proteomic analysis of native metabotropic

glutamate receptor 5 protein complexes reveals novel molecular constituents", *Journal of neurochemistry,* vol. 91, no. 2, pp. 438-450.

Féron, F., Perry, C., Hirning, M. H., McGrath, J. and Mackay-Sim, A. (1999), "Altered adhesion, proliferation and death in neural cultures from adults with schizophrenia", *Schizophrenia research,* vol. 40, no. 3, pp. 211-218.

Fincham, J. M., Carter, C. S., Van Veen, V., Stenger, V. A. and Anderson, J. R. (2002), "Neural mechanisms of planning: A computational analysis using event-related fMRI", *Proceedings of the National Academy of Sciences of the United States of America,* vol. 99, no. 5, pp. 3346-3351.

Fink, C. C., Bayer, K. -., Myers, J. W., Ferrell Jr., J. E., Schulman, H. and Meyer, T. (2003), "Selective regulation of neurite extension and synapse formation by the β but not the α isoform of CaMKII", *Neuron,* vol. 39, no. 2, pp. 283-297.

Fink, C. C. and Meyer, T. (2002), "Molecular mechanisms of CaMKII activation in neuronal plasticity", *Current opinion in neurobiology,* vol. 12, no. 3, pp. 293-299.

Fiorentini, C., Gardoni, F., Spano, P., Di Luca, M. and Missale, C. (2003), "Regulation of dopamine D1 receptor trafficking and desensitization by oligomerization with glutamate N-methyl-D-aspartate receptors", *Journal of Biological Chemistry,* vol. 278, no. 22, pp. 20196-20202.

Forrest, D., Yuzaki, M., Soares, H. D., Ng, L., Luk, D. C., Sheng, M., Stewart, C. L., Morgan, J. I., Connor, J. A. and Curran, T. (1994), "Targeted disruption of NMDA receptor 1 gene abolishes NMDA response and results in neonatal death", *Neuron,* vol. 13, no. 2, pp. 325-338.

Fox, P. T., Ingham, R. J., Ingham, J. C., Zamarripa, F., Xiong, J. -. and Lancaster, J. L. (2000), "Brain correlates of stuttering and syllable production: A PET performance-correlation analysis", *Brain,* vol. 123, no. 10, pp. 1985-2004.

Franck, N., Farrer, C., Georgieff, N., Marie-Cardine, M., Daléry, J., D'Amato, T. and Jeannerod, M. (2001), "Defective recognition of one's own actions in patients with schizophrenia", *American Journal of Psychiatry,* vol. 158, no. 3, pp. 454-459.

Frankle, W. G., Lerma, J. and Laruelle, M. (2003), "The synaptic hypothesis of Schizophrenia", *Neuron,* vol. 39, no. 2, pp. 205-216.

Friederici, A. D. (2006), "Broca's area and the ventral premotor cortex in language: Functional differentiation and specificity", *Cortex,* vol. 42, no. 4, pp. 472-475.

Friedman, J. I., Vrijenhoek, T., Markx, S., Janssen, I. M., Van Der Vliet, W. A., Faas, B. H. W., Knoers, N. V., Cahn, W., Kahn, R. S., Edelmann, L., Davis, K. L., Silverman, J. M.,

Brunner, H. G., Van Kessel, A. G., Wijmenga, C., Ophoff, R. A. and Veltman, J. A. (2008), "CNTNAP2 gene dosage variation is associated with schizophrenia and epilepsy", *Molecular psychiatry,* vol. 13, no. 3, pp. 261-266.

Frisen, J., Verge, V. M. K., Fried, K., Risling, M., Persson, H., Trotter, J., Hokfelt, T. and Lindholm, D. (1993), "Characterization of glial trkB receptors: Differential response to injury in the central and peripheral nervous systems", *Proceedings of the National Academy of Sciences of the United States of America,* vol. 90, no. 11, pp. 4971-4975.

Fryer, R. H., Kaplan, D. R. and Kromer, L. F. (1997), "Truncated trkB receptors on nonneuronal cells inhibit BDNF-induced neurite outgrowth in vitro", *Experimental neurology,* vol. 148, no. 2, pp. 616-627.

Fujii, T. and Kunugi, H. (2009), "p75NTR as a therapeutic target for neuropsychiatric diseases", *Current Molecular Pharmacology,* vol. 2, no. 1, pp. 70-76.

Fujii, Y., Shibata, H., Kikuta, R., Makino, C., Tani, A., Hirata, N., Shibata, A., Ninomiya, H., Tashiro, N. and Fukumaki, Y. (2003), "Positive associations of polymorphisms in the metabotropic glutamate receptor type 3 gene (GRM3) with schizophrenia", *Psychiatric genetics,* vol. 13, no. 2, pp. 71-76.

Fukaya, M., Kato, A., Lovett, C., Tonegawa, S. and Watanabe, M. (2003), "Retention of NMDA receptor NR2 subunits in the lumen of endoplasmic reticulum in targeted NR1 knockout mice", *Proceedings of the National Academy of Sciences of the United States of America,* vol. 100, no. 8, pp. 4855-4860.

Funk, A. J., Rumbaugh, G., Harotunian, V., McCullumsmith, R. E. and Meador-Woodruff, J. H. (2009), "Decreased expression of NMDA receptor-associated proteins in frontal cortex of elderly patients with schizophrenia", *Neuroreport,* vol. 20, no. 11, pp. 1019-1022.

Fuster, J. M. (2002), "Frontal lobe and cognitive development", *Brain Cell Biology,* vol. 31, no. 3-5, pp. 373-385.

Galderisi, S., Quarantelli, M., Volpe, U., Mucci, A., Cassano, G. B., Invernizzi, G., Rossi, A., Vita, A., Pini, S., Cassano, P., Daneluzzo, E., De Peri, L., Stratta, P., Brunetti, A. and Maj, M. (2008), "Patterns of structural MRI abnormalities in deficit and nondeficit schizophrenia", *Schizophrenia bulletin,* vol. 34, no. 2, pp. 393-401.

Galletti, C. (1996), "Functional demarcation of a border between areas V6 and V6A in the superior parietal gyrus of the macaque monkey", *European Journal of Neuroscience,* vol. 8, no. 1, pp. 30-52.

Garcia, R. A. G., Vasudevan, K. and Buonanno, A. (2000), "The neuregulin receptor ErbB-4 interacts with PDZ-containing proteins at neuronal synapses", *Proceedings of the National Academy of Sciences of the United States of America,* vol. 97, no. 7, pp. 3596-3601.

Gardoni, F., Mauceri, D., Fiorentini, C., Bellone, C., Missale, C., Cattabeni, F. and Di Luca, M. (2003), "CaMKII-dependent Phosphorylation Regulates SAP97/NR2A Interaction", *Journal of Biological Chemistry,* vol. 278, no. 45, pp. 44745-44752.

Gardoni, F., Polli, F., Cattabeni, F. and Di Luca, M. (2006), "Calcium-calmodulin-dependent protein kinase II phosphorylation modulates PSD-95 binding to NMDA receptors", *European Journal of Neuroscience,* vol. 24, no. 10, pp. 2694-2704.

Garey, L. J., Ong, W. Y., Patel, T. S., Kanani, M., Davis, A., Mortimer, A. M., Barnes, T. R. E. and Hirsch, S. R. (1998), "Reduced dendritic spine density on cerebral cortical pyramidal neurons in schizophrenia", *Journal of Neurology Neurosurgery and Psychiatry,* vol. 65, no. 4, pp. 446-453.

Gervasoni, N., Aubry, J. -., Bondolfi, G., Osiek, C., Schwald, M., Bertschy, G. and Karege, F. (2005), "Partial normalization of serum brain-derived neurotrophic factor in remitted patients after a major depressive episode", *Neuropsychobiology,* vol. 51, no. 4, pp. 234-238.

Geyer, S., Matelli, M., Luppino, G. and Zilles, K. (2000), "Functional neuroanatomy of the primate isocortical motor system", *Anatomy and Embryology,* vol. 202, no. 6, pp. 443-474.

Glantz, L. A. and Lewis, D. A. (2000), "Decreased dendritic spine density on prefrontal cortical pyramidal neurons in schizophrenia", *Archives of General Psychiatry,* vol. 57, no. 1, pp. 65-73.

Glazer, W. M. and Dickson, R. A. (1998), "Clozapine reduces violence and persistent aggression in schizophrenia", *Journal of Clinical Psychiatry,* vol. 59, no. SUPPL. 3, pp. 8-14.

Godschalk, M., Lemon, R. N., Kuypers, H. G. J. M. and Ronday, H. K. (1984), "Cortical afferents and efferents of monkey postarcuate area: An anatomical and electrophysiological study", *Experimental Brain Research,* vol. 56, no. 3, pp. 410-424.

Gogtay, N., Giedd, J. N., Lusk, L., Hayashi, K. M., Greenstein, D., Vaituzis, A. C., Nugent III, T. F., Herman, D. H., Clasen, L. S., Toga, A. W., Rapoport, J. L. and Thompson, P. M. (2004), "Dynamic mapping of human cortical development during childhood

through early adulthood", *Proceedings of the National Academy of Sciences of the United States of America,* vol. 101, no. 21, pp. 8174-8179.

Goldberg, E. and Bougakov, D. (2005), "Neuropsychologic assessment of frontal lobe dysfunction", *Psychiatric Clinics of North America,* vol. 28, no. 3 SPEC. ISS., pp. 567-580.

Goldberg, T. E., Berman, K. F., Randolph, C., Gold, J. M. and Weinberger, D. R. (1996), "Isolating the mnemonic component in spatial delayed response: A controlled PET 15O-labeled water regional cerebral blood flow study in normal humans", *NeuroImage,* vol. 3, no. 1, pp. 69-78.

Gomes, R. A., Hampton, C., El-Sabeawy, F., Sabo, S. L. and McAllister, A. K. (2006), "The dynamic distribution of TrkB receptors before, during, and after synapse formation between cortical neurons", *Journal of Neuroscience,* vol. 26, no. 44, pp. 11487-11500.

Granger, B. and Albu, S. (2005), "The haloperidol story", *Annals of Clinical Psychiatry,* vol. 17, no. 3, pp. 137-140.

Gray, L., Scarr, E. and Dean, B. (2006), "N-Ethylmaleimide sensitive factor in the cortex of subjects with schizophrenia and bipolar I disorder", *Neuroscience letters,* vol. 391, no. 3, pp. 112-115.

Greer, P. L. and Greenberg, M. E. (2008), "From Synapse to Nucleus: Calcium-Dependent Gene Transcription in the Control of Synapse Development and Function", *Neuron,* vol. 59, no. 6, pp. 846-860.

Grosbras, M. -., Lobel, E., Van de Moortele, P. -., LeBihan, D. and Berthoz, A. (1999), "An anatomical landmark for the supplementary eye fields in human revealed with functional magnetic resonance imaging", *Cerebral Cortex,* vol. 9, no. 7, pp. 705-711.

Gu, W. -., Yang, S., Shi, W. -., Jin, G. -. and Zhen, X. -. (2007), "Requirement of PSD-95 for dopamine D1 receptor modulating glutamate NR1a/NR2B receptor function", *Acta Pharmacologica Sinica,* vol. 28, no. 6, pp. 756-762.

Haapasalo, A., Koponen, E., Hoppe, E., Wong, G. and Castrén, E. (2001), "Truncated trkB.T1 is dominant negative inhibitor of trkB.TK+-mediated cell survival", *Biochemical and biophysical research communications,* vol. 280, no. 5, pp. 1352-1358.

Haapasalo, A., Saarelainen, T., Moshnyakov, M., Arumäe, U., Kiema, T. -., Saarma, M., Wong, G. and Castrén, E. (1999), "Expression of the naturally occurring truncated

trkB neurotrophin receptor induces outgrowth of filopodia and processes in neuroblastoma cells", *Oncogene,* vol. 18, no. 6, pp. 1285-1296.

Haggard, P. (2008), "Human volition: Towards a neuroscience of will", *Nature Reviews Neuroscience,* vol. 9, no. 12, pp. 934-946.

Hahn, C. -., Banerjee, A., MacDonald, M. L., Cho, D. -., Kamins, J., Nie, Z., Borgmann-Winter, K. E., Grosser, T., Pizarro, A., Ciccimaro, E., Arnold, S. E., Wang, H. -. and Blair, I. A. (2009), "The post-synaptic density of human postmortem brain tissues: An experimental study paradigm for neuropsychiatric illnesses", *PLoS ONE,* vol. 4, no. 4.

Hahn, C. -., Wang, H. -., Cho, D. -., Talbot, K., Gur, R. E., Berrettini, W. H., Bakshi, K., Kamins, J., Borgmann-Winter, K. E., Siegel, S. J., Gallop, R. J. and Arnold, S. E. (2006), "Altered neuregulin 1-erbB4 signaling contributes to NMDA receptor hypofunction in schizophrenia", *Nature medicine,* vol. 12, no. 7, pp. 824-828.

Halsband, U. and Lange, R. K. (2006), "Motor learning in man: A review of functional and clinical studies", *Journal of Physiology Paris,* vol. 99, no. 4-6, pp. 414-424.

Harrison, P. J. (1999), "The neuropathology of schizophrenia. A critical review of the data and their interpretation", *Brain,* vol. 122, no. 4, pp. 593-624.

Harrison, P. J. (2004), "The hippocampus in schizophrenia: A review of the neuropathological evidence and its pathophysiological implications", *Psychopharmacology,* vol. 174, no. 1, pp. 151-162.

Hashimoto, K. (2009), "Emerging role of glutamate in the pathophysiology of major depressive disorder", *Brain Research Reviews,* vol. 61, no. 2, pp. 105-123.

Hashimoto, T., Nishino, N., Nakai, H. and Tanaka, C. (1991), "Increase in serotonin 5-HT(1A) receptors in prefrontal and temporal cortices of brains from patients with chronic schizophrenia", *Life Sciences,* vol. 48, no. 4, pp. 355-363.

Hayashi-Takagi, A., Takaki, M., Graziane, N., Seshadri, S., Murdoch, H., Dunlop, A. J., Makino, Y., Seshadri, A. J., Ishizuka, K., Srivastava, D. P., Xie, Z., Baraban, J. M., Houslay, M. D., Tomoda, T., Brandon, N. J., Kamiya, A., Yan, Z., Penzes, P. and Sawa, A. (2010), "Disrupted-in-Schizophrenia 1 (DISC1) regulates spines of the glutamate synapse via Rac1", *Nature neuroscience,* vol. 13, no. 3, pp. 327-332.

He, S. -., Dum, R. P. and Strick, P. L. (1995), "Topographic organization of corticospinal projections from the frontal lobe: Motor areas on the medial surface of the hemisphere", *Journal of Neuroscience,* vol. 15, no. 5 I, pp. 3284-3306.

Henrik Ehrsson, H., Naito, E., Geyer, S., Amunts, K., Zilles, K., Forssberg, H. and Roland, P. E. (2000), "Simultaneous movements of upper and lower limbs are coordinated by motor representations that are shared by both limbs: A PET study", *European Journal of Neuroscience,* vol. 12, no. 9, pp. 3385-3398.

Hirao, K., Hata, Y., Deguchi, M., Yao, I., Ogura, M., Rokukawa, C., Kawabe, H., Mizoguchi, A. and Takai, Y. (2000), "Association of synapse-associated protein 90/Postsynaptic density-95- associated protein (SAPAP) with neurofilaments", *Genes to Cells,* vol. 5, no. 3, pp. 203-210.

Hirao, K., Hata, Y., Ide, N., Takeuchi, M., Irie, M., Yao, I., Deguchi, M., Toyoda, A., Sudhof, T. C. and Takai, Y. (1998), "A novel multiple PDZ domain-containing molecule interacting with N- methyl-D-aspartate receptors and neuronal cell adhesion proteins", *Journal of Biological Chemistry,* vol. 273, no. 33, pp. 21105-21110.

Ho, V. M., Lee, J. -. and Martin, K. C. (2011), "The cell biology of synaptic plasticity", *Science,* vol. 334, no. 6056, pp. 623-628.

Horváth, S. and Mirnics, K. (2009), "Breaking the gene barrier in schizophrenia", *Nature medicine,* vol. 15, no. 5, pp. 488-490.

Hoshi, E. (2006), "Functional specialization within the dorsolateral prefrontal cortex: A review of anatomical and physiological studies of non-human primates", *Neuroscience research,* vol. 54, no. 2, pp. 73-84.

Huang, E.J. and Reichardt, L.F., (2003), *Trk receptors: Roles in neuronal signal transduction*.

Huang, Y. Z., Wang, Q., Xiong, W. C. and Mei, L. (2001), "Erbin is a Protein Concentrated at Postsynaptic Membranes that Interacts with PSD-95", *Journal of Biological Chemistry,* vol. 276, no. 22, pp. 19318-19326.

Huang, Y. Z., Won, S., Ali, D. W., Wang, Q., Tanowitz, M., Du, Q. S., Pelkey, K. A., Yang, D. J., Xiong, W. C., Salter, M. W. and Mei, L. (2000), "Regulation of neuregulin signaling by PSD-95 interacting with ErbB4 at CNS synapses", *Neuron,* vol. 26, no. 2, pp. 443-455.

Hudmon, A. and Schulman, H., (2002), *Neuronal Ca2+/calmodulin-dependent protein kinase II: The role of structure and autoregulation in cellular function*.

Hunsucker, S. W., Solomon, B., Gawryluk, J., Geiger, J. D., Vacano, G. N., Duncan, M. W. and Patterson, D. (2008), "Assessment of post-mortem-induced changes to the mouse brain proteome", *Journal of neurochemistry,* vol. 105, no. 3, pp. 725-737.

Imai, C., Sugai, T., Iritani, S., Niizato, K., Nakamura, R., Makifuchi, T., Kakita, A., Takahashi, H. and Nawa, H. (2001), "A quantitative study on the expression of synapsin II and N-ethylmaleimide-sensitive fusion protein in schizophrenic patients", *Neuroscience letters,* vol. 305, no. 3, pp. 185-188.

Innocenti, G. M., Ansermet, F. and Parnas, J. (2003), "Schizophrenia, neurodevelopment and corpus callosum", *Molecular psychiatry,* vol. 8, no. 3, pp. 261-274.

Insel, T. R. (2010), "Rethinking schizophrenia", *Nature,* vol. 468, no. 7321, pp. 187-193.

Irie, M., Hata, Y., Takeuchi, M., Ichtchenko, K., Toyoda, A., Hirao, K., Takai, Y., Rosahl, T. W. and Südhof, T. C. (1997), "Binding of neuroligins to PSD-95", *Science,* vol. 277, no. 5331, pp. 1511-1515.

Iritani, S., Niizato, K., Nawa, H., Ikeda, K. and Emson, P. C. (2003), "Immunohistochemical study of brain-derived neurotrophic factor and its receptor, TrkB, in the hippocampal formation of schizophrenic brains", *Progress in Neuro-Psychopharmacology and Biological Psychiatry,* vol. 27, no. 5, pp. 801-807.

Iversen, S. D. and Iversen, L. L. (2007), "Dopamine: 50 years in perspective", *Trends in neurosciences,* vol. 30, no. 5, pp. 188-193.

Javitt, D. C. (2012), "Twenty-five years of glutamate in schizophrenia: Are we there yet?", *Schizophrenia bulletin,* vol. 38, no. 5, pp. 911-913.

Javitt, D. C. and Zukin, S. R. (1991), "Recent advances in the phencyclidine model of schizophrenia", *American Journal of Psychiatry,* vol. 148, no. 10, pp. 1301-1308.

Jenkins, I. H., Jahanshahi, M., Jueptner, M., Passingham, R. E. and Brooks, D. J. (2000), "Self-initiated versus externally triggered movements. II. The effect of movement predictability on regional cerebral blood flow", *Brain,* vol. 123, no. 6, pp. 1216-1228.

Ji, Y., Pang, P. T., Feng, L. and Lu, B. (2005), "Cyclic AMP controls BDNF-induced TrkB phosphorylation and dendritic spine formation in mature hippocampal neurons", *Nature neuroscience,* vol. 8, no. 2, pp. 164-172.

Johnson, P. B., Ferraina, S., Bianchi, L. and Caminiti, R. (1996), "Cortical networks for visual reaching: Physiological and anatomical organization of frontal and parietal lobe arm regions", *Cerebral Cortex,* vol. 6, no. 2, pp. 102-119.

Kajimoto, Y., Shirakawa, O., Lin, X. -., Hashimoto, T., Kitamura, N., Murakami, N., Takumi, T. and Maeda, K. (2003), "Synapse-associated protein 90/postsynaptic density-95-associated protein (SAPAP) is expressed differentially in phencyclidine-

treated rats and is increased in the nucleus accumbens of patients with schizophrenia", *Neuropsychopharmacology,* vol. 28, no. 10, pp. 1831-1839.

Kapur, S. and Mamo, D. (2003), "Half a century of antipsychotics and still a central role for dopamine D2 receptors", *Progress in Neuro-Psychopharmacology and Biological Psychiatry,* vol. 27, no. 7, pp. 1081-1090.

Kapur, S., Tulving, E., Cabeza, R., McIntosh, A. R., Houle, S. and Craik, F. I. M. (1996), "The neural correlates of intentional learning of verbal materials: A PET study in humans", *Cognitive Brain Research,* vol. 4, no. 4, pp. 243-249.

Karege, F., Vaudan, G., Schwald, M., Perroud, N. and La Harpe, R. (2005), "Neurotrophin levels in postmortem brains of suicide victims and the effects of antemortem diagnosis and psychotropic drugs", *Molecular Brain Research,* vol. 136, no. 1-2, pp. 29-37.

Kawabe, H., Hata, Y., Takeuchi, M., Ide, N., Mizoguchi, A. and Takai, Y. (1999), "nArgBP2, a novel neural member of ponsin/ArgBP2/vinexin family that interacts with synapse-associated protein 90/postsynaptic density-95- associated protein (SAPAP)", *Journal of Biological Chemistry,* vol. 274, no. 43, pp. 30914-30918.

Kawada, R., Yoshizumi, M., Hirao, K., Fujiwara, H., Miyata, J., Shimizu, M., Namiki, C., Sawamoto, N., Fukuyama, H., Hayashi, T. and Murai, T. (2009), "Brain volume and dysexecutive behavior in schizophrenia", *Progress in Neuro-Psychopharmacology and Biological Psychiatry,* vol. 33, no. 7, pp. 1255-1260.

Kelleher III, R. J., Govindarajan, A., Jung, H. -., Kang, H. and Tonegawa, S. (2004), "Translational control by MAPK signaling in long-term synaptic plasticity and memory", *Cell,* vol. 116, no. 3, pp. 467-479.

Kennedy, M. B. (2000), "Signal-processing machines at the postsynaptic density", *Science,* vol. 290, no. 5492, pp. 750-754.

Kennedy, M. B., Bennett, M. K. and Erondu, N. E. (1983), "Biochemical and immunochemical evidence that the 'major postsynaptic density protein' is a subunit of a calmodulin-dependent protein kinase", *Proceedings of the National Academy of Sciences of the United States of America,* vol. 80, no. 23 I, pp. 7357-7361.

Kim, E., Naisbitt, S., Hsueh, Y. -., Rao, A., Rothschild, A., Craig, A. M. and Sheng, M. (1997), "GKAP, a novel synaptic protein that interacts with the guanylate kinase-like domain of the PSD-95/SAP90 family of channel clustering molecules", *Journal of Cell Biology,* vol. 136, no. 3, pp. 669-678.

Kim, E. and Sheng, M. (2004), "PDZ domain proteins of synapses", *Nature Reviews Neuroscience,* vol. 5, no. 10, pp. 771-781.

Kim, S., Burette, A., Chung, H. S., Kwon, S. -., Woo, J., Lee, H. W., Kim, K., Kim, H., Weinberg, R. J. and Kim, E. (2006), "NGL family PSD-95-interacting adhesion molecules regulate excitatory synapse formation", *Nature neuroscience,* vol. 9, no. 10, pp. 1294-1301.

Kindler, S., Rehbein, M., Classen, B., Richter, D. and Böckers, T. M. (2004), "Distinct spatiotemporal expression of SAPAP transcripts in the developing rat brain: A novel dendritically localized mRNA", *Molecular Brain Research,* vol. 126, no. 1, pp. 14-21.

Kistner, U., Wenzel, B. M., Veh, R. W., Cases-Langhoff, C., Garner, A. M., Appeltauer, U., Voss, B., Gundelfinger, E. D. and Garner, C. C. (1993), "SAP90, a rat presynaptic protein related to the product of the Drosophila tumor suppressor gene dlg-A", *Journal of Biological Chemistry,* vol. 268, no. 7, pp. 4580-4583.

Klann, E. and Dever, T. E. (2004), "Biochemical mechanisms for translational regulation in synaptic plasticity", *Nature Reviews Neuroscience,* vol. 5, no. 12, pp. 931-942.

Klein, R. (2004), "Eph/ephrin signaling in morphogenesis, neural development and plasticity", *Current opinion in cell biology,* vol. 16, no. 5, pp. 580-589.

Knable, M. B., Barci, B. M., Webster, M. J., Meador-Woodruff, J. and Torrey, E. F. (2004), "Molecular abnormalities of the hippocampus in severe psychiatric illness: Postmortem findings from the Stanley Neuropathology Consortium", *Molecular psychiatry,* vol. 9, no. 6, pp. 609-620.

Knauff, M., Mulack, T., Kassubek, J., Salih, H. R. and Greenlee, M. W. (2002), "Spatial imagery in deductive reasoning: A functional MRI study", *Cognitive Brain Research,* vol. 13, no. 2, pp. 203-212.

Knüsel, B., Rabin, S. J., Hefti, F. and Kaplan, D. R. (1994), "Regulated neurotrophin receptor responsiveness during neuronal migration and early differentiation", *Journal of Neuroscience,* vol. 14, no. 3 II, pp. 1542-1554.

Kodama, S., Fukuzako, H., Fukuzako, T., Kiura, T., Nozoe, S., Hashiguchi, T., Yamada, K., Takenouchi, K., Takigawa, M., Nakabeppu, Y. and Nakajo, M. (2001), "Aberrant brain activation following motor skill learning in schizophrenic patients as shown by functional magnetic resonance imaging", *Psychological medicine,* vol. 31, no. 6, pp. 1079-1088.

Kornack, D. R. and Rakic, P. (2001), "The generation, migration, and differentiation of olfactory neurons in the adult primate brain", *Proceedings of the National Academy of Sciences of the United States of America,* vol. 98, no. 8, pp. 4752-4757.

Korostishevsky, M., Kremer, I., Kaganovich, M., Cholostoy, A., Murad, I., Muhaheed, M., Bannoura, I., Rietschel, M., Dobrusin, M., Bening-Abu-Shach, U., Belmaker, R. H., Maier, W., Ebstein, R. P. and Navon, R. (2006), "Transmission disequilibrium and haplotype analyses of the G72/G30 locus: Suggestive linkage to schizophrenia in Palestinian Arabs living in the North of Israel", *American Journal of Medical Genetics - Neuropsychiatric Genetics,* vol. 141 B, no. 1, pp. 91-95.

Koshimizu, H., Kiyosue, K., Hara, T., Hazama, S., Suzuki, S., Uegaki, K., Nagappan, G., Zaitsev, E., Hirokawa, T., Tatsu, Y., Ogura, A., Lu, B. and Kojima, M. (2009), "Multiple functions of precursor BDNF to CNS neurons: Negative regulation of neurite growth, spine formation and cell survival", *Molecular Brain,* vol. 2, no. 1.

Kristiansen, L. V., Beneyto, M., Haroutunian, V. and Meador-Woodruff, J. H. (2006), "Changes in NMDA receptor subunits and interacting PSD proteins in dorsolateral prefrontal and anterior cingulate cortex indicate abnormal regional expression in schizophrenia", *Molecular psychiatry,* vol. 11, no. 8, pp. 737-747.

Kristiansen, L. V., Huerta, I., Beneyto, M. and Meador-Woodruff, J. H. (2007a), "NMDA receptors and schizophrenia", *Current Opinion in Pharmacology,* vol. 7, no. 1, pp. 48-55.

Kristiansen, L. V., Huerta, I., Beneyto, M. and Meador-Woodruff, J. H. (2007b), "NMDA receptors and schizophrenia", *Current Opinion in Pharmacology,* vol. 7, no. 1, pp. 48-55.

Kruusmägi, M., Kumar, S., Zelenin, S., Brismar, H., Aperia, A. and Scott, L. (2009), "Functional differences between D1 and D5 revealed by high resolution imaging on live neurons", *Neuroscience,* vol. 164, no. 2, pp. 463-469.

Krystal, J. H., Karper, L. P., Seibyl, J. P., Freeman, G. K., Delaney, R., Bremner, J. D., Heninger, G. R., Bowers Jr., M. B. and Charney, D. S. (1994), "Subanesthetic effects of the noncompetitive NMDA antagonist, ketamine, in humans: Psychotomimetic, perceptual, cognitive, and neuroendocrine responses", *Archives of General Psychiatry,* vol. 51, no. 3, pp. 199-214.

Kullander, K. and Klein, R. (2002), "Mechanisms and functions of Eph and ephrin signalling", *Nature Reviews Molecular Cell Biology,* vol. 3, no. 7, pp. 475-486.

Kuperberg, G., Kerwin, R. and Murray, R. (2002), "Developments in the pharmacological treatment of schizophrenia", *Expert opinion on investigational drugs,* vol. 11, no. 10, pp. 1335-1341.

Kurachi, M. (2003), "Pathogenesis of schizophrenia: Part I. Symptomatology, cognitive characteristics and brain morphology", *Psychiatry and clinical neurosciences,* vol. 57, no. 1, pp. 3-8.

Kurata, K. (1991), "Corticocortical inputs to the dorsal and ventral aspects of the premotor cortex of macaque monkeys", *Neuroscience research,* vol. 12, no. 1, pp. 263-280.

Lahti, A. C., Koffel, B., LaPorte, D. and Tamminga, C. A. (1995), "Subanesthetic doses of ketamine stimulate psychosis in schizophrenia", *Neuropsychopharmacology,* vol. 13, no. 1, pp. 9-19.

Lambert, T. J. R. and Castle, D. J. (2003), "Pharmacological approaches to the management of schizophrenia", *Medical Journal of Australia,* vol. 178, no. 9 SUPPL., pp. S57-S61.

Lamm, C., Windischberger, C., Leodolter, U., Moser, E. and Bauer, H. (2001), "Evidence for premotor cortex activity during dynamic visuospatial imagery from single-trial functional magnetic resonance imaging and event-related slow cortical potentials", *NeuroImage,* vol. 14, no. 2, pp. 268-283.

Lang, S. B., Stein, V., Bonhoeffer, T. and Lohmann, C. (2007), "Endogenous brain-derived neurotrophic factor triggers fast calcium transients at synapses in developing dendrites", *Journal of Neuroscience,* vol. 27, no. 5, pp. 1097-1105.

Lau, C. G. and Zukin, R. S. (2007), "NMDA receptor trafficking in synaptic plasticity and neuropsychiatric disorders", *Nature Reviews Neuroscience,* vol. 8, no. 6, pp. 413-426.

Lee, R., Kermani, P., Teng, K. K. and Hempstead, B. L. (2001), "Regulation of cell survival by secreted proneurotrophins", *Science,* vol. 294, no. 5548, pp. 1945-1948.

Lei, S. and McBain, C. J. (2002), "Distinct NMDA receptors provide differential modes of transmission at mossy fiber-interneuron synapses", *Neuron,* vol. 33, no. 6, pp. 921-933.

Leonard, A. S., Davare, M. A., Horne, M. C., Garner, C. C. and Hell, J. W. (1998), "SAP97 is associated with the α-amino-3-hydroxy-5-methylisoxazole-4- propionic acid receptor GluR1 subunit", *Journal of Biological Chemistry,* vol. 273, no. 31, pp. 19518-19524.

Levinson, D. F., Umapathy, C. and Musthaq, M. (1999), "Treatment of schizoaffective disorder and schizophrenia with mood symptoms", *American Journal of Psychiatry,* vol. 156, no. 8, pp. 1138-1148.

Lewis, D. A. and Moghaddam, B. (2006), "Cognitive dysfunction in schizophrenia: Convergence of γ-aminobutyric acid and glutamate alterations", *Archives of Neurology,* vol. 63, no. 10, pp. 1372-1376.

Li, Y., Jin, Y. -., Cul, K., Li, N., Zheng, Z. -., Wang, Y. -. and Yuan, X. -. (2005), "Essential role of TRPC channels in the guidance of nerve growth cones by brain-derived neurotrophic factor", *Nature,* vol. 434, no. 7035, pp. 894-898.

Liang, M., Zhou, Y., Jiang, T., Liu, Z., Tian, L., Liu, H. and Hao, Y. (2006), "Widespread functional disconnectivity in schizophrenia with resting-state functional magnetic resonance imaging", *Neuroreport,* vol. 17, no. 2, pp. 209-213.

Liddle, P. F. (1996), "Functional imaging - schizophrenia", *British medical bulletin,* vol. 52, no. 3, pp. 486-494.

Liddle, P. F. (2001), "Is disordered cerebral connectivity the core problem in schizophrenia?", *Neuroscience News,* vol. 4, no. 1, pp. 62-73.

Lim, S., Naisbitt, S., Yoon, J., Hwang, J. -., Suh, P. -., Sheng, M. and Eunjoon, K. (1999), "Characterization of the Shank family of synaptic proteins. Multiple genes, alternative splicing, and differential expression in brain and development", *Journal of Biological Chemistry,* vol. 274, no. 41, pp. 29510-29518.

Lim, S., Sala, C., Yoon, J., Park, S., Kuroda, S., Sheng, M. and Kim, E. (2001), "Sharpin, a novel postsynaptic density protein that directly interacts with the shank family of proteins", *Molecular and Cellular Neuroscience,* vol. 17, no. 2, pp. 385-397.

Lin, Y. -. and Redmond, L. (2008), "CaMKIIβ binding to stable F-actin in vivo regulates F-actin filament stability", *Proceedings of the National Academy of Sciences of the United States of America,* vol. 105, no. 41, pp. 15791-15796.

Liu, L., Wong, T. P., Pozza, M. F., Lingenhoehl, K., Wang, Y., Sheng, M., Auberson, Y. P. and Wang, Y. T. (2004), "Role of NMDA Receptor Subtypes in Governing the Direction of Hippocampal Synaptic Plasticity", *Science,* vol. 304, no. 5673, pp. 1021-1024.

Liu, X. -., Chu, X. -., Mao, L. -., Wang, M., Lan, H. -., Li, M. -., Zhang, G. -., Parelkar, N., Fibuch, E., Haines, M., Neve, K. A., Liu, F., Xiong, Z. -. and Wang, J. Q. (2006), "Modulation of D2R-NR2B Interactions in Response to Cocaine", *Neuron,* vol. 52, no. 5, pp. 897-909.

Longcamp, M., Anton, J. -., Roth, M. and Velay, J. -. (2003), "Visual presentation of single letters activates a premotor area involved in writing", *NeuroImage,* vol. 19, no. 4, pp. 1492-1500.

Longcamp, M., Anton, J. -., Roth, M. and Velay, J. -. (2005), "Premotor activations in response to visually presented single letters depend on the hand used to write: A study on left-handers", *Neuropsychologia,* vol. 43, no. 12, pp. 1801-1809.

López-Muñoz, F., Alamo, C., Cuenca, E., Shen, W. W., Clervoy, P. and Rubio, G. (2005), "History of the discovery and clinical introduction of chlorpromazine", *Annals of Clinical Psychiatry,* vol. 17, no. 3, pp. 113-135.

Lu, B., Pang, P. T. and Woo, N. H. (2005), "The yin and yang of neurotrophin action", *Nature Reviews Neuroscience,* vol. 6, no. 8, pp. 603-614.

Lu, J., Helton, T. D., Blanpied, T. A., Rácz, B., Newpher, T. M., Weinberg, R. J. and Ehlers, M. D. (2007), "Postsynaptic Positioning of Endocytic Zones and AMPA Receptor Cycling by Physical Coupling of Dynamin-3 to Homer", *Neuron,* vol. 55, no. 6, pp. 874-889.

Lu, M. -., Preston, J. B. and Strick, P. L. (1994), "Interconnections between the prefrontal cortex and the premotor areas in the frontal lobe", *Journal of Comparative Neurology,* vol. 341, no. 3, pp. 375-392.

Luppino, G., Matelli, M., Camarda, R. and Rizzolatti, G. (1993), "Corticocortical connections of area F3 (SMA-proper) and area F6 (pre-SMA) in the Macaque monkey", *Journal of Comparative Neurology,* vol. 338, no. 1, pp. 114-140.

Luppino, G., Matelli, M., Camarda, R. and Rizzolatti, G. (1994), "Corticospinal projections from mesial frontal and cingulate areas in the monkey", *Neuroreport,* vol. 5, no. 18, pp. 2545-2548.

Luppino, G., Murata, A., Govoni, P. and Matelli, M. (1999), "Largely segregated parietofrontal connections linking rostral intraparietal cortex (areas AIP and VIP) and the ventral premotor cortex (areas F5 and F4)", *Experimental Brain Research,* vol. 128, no. 1-2, pp. 181-187.

Lynch, D. R. and Guttmann, R. P. (2001), "NMDA receptor pharmacology: Perspectives from molecular biology", *Current Drug Targets,* vol. 2, no. 3, pp. 215-231.

Mao, Y., Ge, X., Frank, C. L., Madison, J. M., Koehler, A. N., Doud, M. K., Tassa, C., Berry, E. M., Soda, T., Singh, K. K., Biechele, T., Petryshen, T. L., Moon, R. T., Haggarty, S. J. and Tsai, L. -. (2009), "Disrupted in Schizophrenia 1 Regulates Neuronal

Progenitor Proliferation via Modulation of GSK3β/β-Catenin Signaling", *Cell,* vol. 136, no. 6, pp. 1017-1031.

Maruff, P., Wilson, P. and Currie, J. (2003), "Abnormalities of motor imagery associated with somatic passivity phenomena in schizophrenia", *Schizophrenia research,* vol. 60, no. 2-3, pp. 229-238.

Massey, P. V., Johnson, B. E., Moult, P. R., Auberson, Y. P., Brown, M. W., Molnar, E., Collingridge, G. L. and Bashir, Z. I. (2004), "Differential roles of NR2A and NR2B-containing NMDA receptors in cortical long-term potentiation and long-term depression", *Journal of Neuroscience,* vol. 24, no. 36, pp. 7821-7828.

Matelli, M., Govoni, P., Galletti, C., Kutz, D. F. and Luppino, G. (1998), "Superior area 6 afferents from the superior parietal lobule in the macaque monkey", *Journal of Comparative Neurology,* vol. 402, no. 3, pp. 327-352.

Matsumoto, T., Rauskolb, S., Polack, M., Klose, J., Kolbeck, R., Korte, M. and Barde, Y. -. (2008), "Biosynthesis and processing of endogenous BDNF: CNS neurons store and secrete BDNF, not pro-BDNF", *Nature neuroscience,* vol. 11, no. 2, pp. 131-133.

Mauceri, D., Gardoni, F., Marcello, E. and Di Luca, M. (2007), "Dual role of CaMKII-dependent SAP97 phosphorylation in mediating trafficking and insertion of NMDA receptor subunit NR2A", *Journal of neurochemistry,* vol. 100, no. 4, pp. 1032-1046.

Mayer, M.L. and Armstrong, N., (2004), *Structure and function of glutamate receptor ion channels*.

McDermott, K. B., Petersen, S. E., Watson, J. M. and Ojemann, J. G. (2003), "A procedure for identifying regions preferentially activated by attention to semantic and phonological relations using functional magnetic resonance imaging", *Neuropsychologia,* vol. 41, no. 3, pp. 293-303.

McDonald, C., Grech, A., Toulopoulou, T., Schulze, K., Chapple, B., Sham, P., Walshe, M., Sharma, T., Sigmundsson, T., Chitnis, X. and Murray, R. M. (2002), "Brain volumes in familial and non-familial schizophrenic probands and their unaffected relatives", *American Journal of Medical Genetics - Neuropsychiatric Genetics,* vol. 114, no. 6, pp. 616-625.

McGrath, J. J. (2006), "Variations in the incidence of schizophrenia: Data versus dogma", *Schizophrenia bulletin,* vol. 32, no. 1, pp. 195-197.

Mednick, S. A., Machon, R. A., Huttunen, M. O. and Bonett, D. (1988), "Adult schizophrenia following prenatal exposure to an influenza epidemic", *Archives of General Psychiatry,* vol. 45, no. 2, pp. 189-192.

Meltzer, H. Y. and Okayli, G. (1995), "Reduction of suicidality during clozapine treatment of neuroleptic- resistant schizophrenia: Impact on risk-benefit assessment", *American Journal of Psychiatry,* vol. 152, no. 2, pp. 183-190.

Meyer-Lindenberg, A., Polin, J. -., Kohn, P. D., Holt, J. L., Egan, M. F., Weinberger, D. R. and Berman, K. F. (2001), "Evidence for abnormal cortical functional connectivity during working memory in schizophrenia", *American Journal of Psychiatry,* vol. 158, no. 11, pp. 1809-1817.

Meyer-Lindenberg, A. S., Olsen, R. K., Kohn, P. D., Brown, T., Egan, M. F., Weinberger, D. R. and Berman, K. F. (2005), "Regionally specific disturbance of dorsolateral prefrontal-hippocampal functional connectivity in schizophrenia", *Archives of General Psychiatry,* vol. 62, no. 4, pp. 379-386.

Mirnics, K., Middleton, F. A., Marquez, A., Lewis, D. A. and Levitt, P. (2000), "Molecular characterization of schizophrenia viewed by microarray analysis of gene expression in prefrontal cortex", *Neuron,* vol. 28, no. 1, pp. 53-67.

Miyai, I., Suzuki, T., Kang, J., Kubota, K. and Volpe, B. T. (1999), "Middle cerebral artery stroke that includes the premotor cortex reduces mobility outcome", *Stroke,* vol. 30, no. 7, pp. 1380-1383.

Miyamoto, Y., Yamada, K., Noda, Y., Mori, H., Mishina, M. and Nabeshima, T. (2001), "Hyperfunction of dopaminergic and serotonergic neuronal systems in mice lacking the NMDA receptor ε1 subunit", *Journal of Neuroscience,* vol. 21, no. 2, pp. 750-757.

Mlakar, J., Jensterle, J. and Frith, C. D. (1994), "Central monitoring deficiency and schizophrenic symptoms", *Psychological medicine,* vol. 24, no. 3, pp. 557-564.

Moghaddam, B., Adams, B., Verma, A. and Daly, D. (1997), "Activation of glutamatergic neurotransmission by ketamine: A novel step in the pathway from NMDA receptor blockade to dopaminergic and cognitive disruptions associated with the prefrontal cortex", *Journal of Neuroscience,* vol. 17, no. 8, pp. 2921-2927.

Mohn, A. R., Gainetdinov, R. R., Caron, M. G. and Koller, B. H. (1999), "Mice with reduced NMDA receptor expression display behaviors related to schizophrenia", *Cell,* vol. 98, no. 4, pp. 427-436.

Morita, Y., Ujike, H., Tanaka, Y., Otani, K., Kishimoto, M., Morio, A., Kotaka, T., Okahisa, Y., Matsushita, M., Morikawa, A., Hamase, K., Zaitsu, K. and Kuroda, S. (2007), "A Genetic Variant of the Serine Racemase Gene Is Associated with Schizophrenia", *Biological psychiatry,* vol. 61, no. 10, pp. 1200-1203.

Morris, D. W., Rodgers, A., McGhee, K. A., Schwaiger, S., Scully, P., Quinn, J., Meagher, D., Waddington, J. L., Gill, M. and Corvin, A. P. (2004), "Confirming RGS4 as a Susceptibility Gene for Schizophrenia", *American Journal of Medical Genetics - Neuropsychiatric Genetics,* vol. 125 B, no. 1, pp. 50-53.

Muakkassa, K. F. and Strick, P. L. (1979), "Frontal lobe inputs to primate motor cortex: Evidence for four somatotopically organized 'premotor' areas", *Brain research,* vol. 177, no. 1, pp. 176-182.

Murata, A., Fadiga, L., Fogassi, L., Gallese, V., Raos, V. and Rizzolatti, G. (1997), "Object representation in the ventral premotor cortex (Area F5) of the monkey", *Journal of neurophysiology,* vol. 78, no. 4, pp. 2226-2230.

Nabeshima, T., Mouri, A., Murai, R. and Noda, Y., (2006), *Animal model of schizophrenia: Dysfunction of NMDA receptor-signaling in mice following withdrawal from repeated administration of phencyclidine*.

Nachev, P., Kennard, C. and Husain, M. (2008), "Functional role of the supplementary and pre-supplementary motor areas", *Nature Reviews Neuroscience,* vol. 9, no. 11, pp. 856-869.

Nadri, C., Dean, B., Scarr, E. and Agam, G. (2004), "GSK-3 parameters in postmortem frontal cortex and hippocampus of schizophrenic patients", *Schizophrenia research,* vol. 71, no. 2-3, pp. 377-382.

Naisbitt, S., Eunjoon, K., Tu, J. C., Xiao, B., Sala, C., Valtschanoff, J., Weinberg, R. J., Worley, P. F. and Sheng, M. (1999), "Shank, a novel family of postsynaptic density proteins that binds to the NMDA receptor/PSD-95/GKAP complex and cortactin", *Neuron,* vol. 23, no. 3, pp. 569-582.

Naisbitt, S., Valtschanoff, J., Allison, D. W., Sala, C., Kim, E., Craig, A. M., Weinberg, R. J. and Sheng, M. (2000), "Interaction of the postsynaptic density-95/guanylate kinase domain- associated protein complex with a light chain of myosin-V and dynein", *Journal of Neuroscience,* vol. 20, no. 12, pp. 4524-4534.

Nakai, T., Kato, C. and Matsuo, K. (2005), "An FMRI study to investigate auditory attention: a model of the cocktail party phenomenon.", *Magnetic resonance in medical sciences : MRMS : an official journal of Japan Society of Magnetic Resonance in Medicine.,* vol. 4, no. 2, pp. 75-82.

Nakano, K., Kayahara, T., Tsutsumi, T. and Ushiro, H. (2000), "Neural circuits and functional organization of the striatum", *Journal of Neurology, Supplement,* vol. 247, no. 5, pp. V1-V15.

Nambu, A., Takada, M., Inase, M. and Tokuno, H. (1996), "Dual somatotopical representations in the primate subthalamic nucleus: Evidence for ordered but reversed body-map transformations from the primary motor cortex and the supplementary motor area", *Journal of Neuroscience,* vol. 16, no. 8, pp. 2671-2683.

Narisawa-Saito, M., Iwakura, Y., Kawamura, M., Araki, K., Kozaki, S., Takei, N. and Nawa, H. (2002), "Brain-derived neurotrophic factor regulates surface expression of α-amino-3-hydroxy-5-methyl-4-isoxazolepropionic acid receptors by enhancing the N-ethylmaleimide-sensitive factor/GLuR2 interaction in developing neocortical neurons", *Journal of Biological Chemistry,* vol. 277, no. 43, pp. 40901-40910.

Nguyen, P. V., Abel, T. and Kandel, E. R. (1994), "Requirement of a critical period of transcription for induction of a late phase of LTP", *Science,* vol. 265, no. 5175, pp. 1104-1107.

Nichols, D. E. (2004), "Hallucinogens", *Pharmacology and Therapeutics,* vol. 101, no. 2, pp. 131-181.

Niethammer, M., Kim, E. and Sheng, M. (1996), "Interaction between the C terminus of NMDA receptor subunits and multiple members of the PSD-95 family of membrane-associated guanylate kinases", *Journal of Neuroscience,* vol. 16, no. 7, pp. 2157-2163.

Nishimune, A., Isaac, J. T. R., Molnar, E., Noel, J., Nash, S. R., Tagaya, M., Collingridge, G. L., Nakanishi, S. and Henley, J. M. (1998), "NSF binding to GluR2 regulates synaptic transmission", *Neuron,* vol. 21, no. 1, pp. 87-97.

Nobre, A. C., Sebestyen, G. N., Gitelman, D. R., Mesulam, M. M., Frackowiak, R. S. J. and Frith, C. D. (1997), "Functional localization of the system for visuospatial attention using positron emission tomography", *Brain,* vol. 120, no. 3, pp. 515-533.

Novak, G., Seeman, P. and Tallerico, T. (2000), "Schizophrenia: Elevated mRNA for calcium-calmodulin-dependent protein kinase IIβ in frontal cortex", *Molecular Brain Research,* vol. 82, no. 1-2, pp. 95-100.

Novak, G., Seeman, P. and Tallerico, T. (2006), "Increased expression of calcium/calmodulin-dependent protein kinase IIβ in frontal cortex in schizophrenia and depression", *Synapse,* vol. 59, no. 1, pp. 61-68.

Numakawa, T., Yagasaki, Y., Ishimoto, T., Okada, T., Suzuki, T., Iwata, N., Ozaki, N., Taguchi, T., Tatsumi, M., Kamijima, K., Straub, R. E., Weinberger, D. R., Kunugi, H. and Hashimoto, R. (2004), "Evidence of novel neuronal functions of dysbindin, a

susceptibility gene for schizophrenia", *Human molecular genetics,* vol. 13, no. 21, pp. 2699-2708.

Ohira, K., Funatsu, N., Homma, K. J., Sahara, Y., Hayashi, M., Kaneko, T. and Nakamura, S. (2007), "Truncated TrkB-T1 regulates the morphology of neocortical layer I astrocytes in adult rat brain slices", *European Journal of Neuroscience,* vol. 25, no. 2, pp. 406-416.

Ohira, K., Homma, K. J., Hirai, H., Nakamura, S. and Hayashi, M. (2006), "TrkB-T1 regulates the RhoA signaling and actin cytoskeleton in glioma cells", *Biochemical and biophysical research communications,* vol. 342, no. 3, pp. 867-874.

Ohira, K., Shimizu, K. and Hayashi, M. (1999), "Change of expression of full-length and truncated TrkBs in the developing monkey central nervous system", *Developmental Brain Research,* vol. 112, no. 1, pp. 21-29.

Ohira, K., Shimizu, K. and Hayashi, M. (2001), "TrkB dimerization during development of the prefrontal cortex of the macaque", *Journal of neuroscience research,* vol. 65, no. 5, pp. 463-469.

Ohira, K., Shimizu, K., Yamashita, A. and Hayashi, M. (2005), "Differential expression of the truncated TrkB receptor, T1, in the primary motor and prefrontal cortices of the adult macaque monkey", *Neuroscience letters,* vol. 385, no. 2, pp. 105-109.

Okamoto, K. -., Narayanan, R., Lee, S. H., Murata, K. and Hayashi, Y. (2007), "The role of CaMKII as an F-actin-bundling protein crucial for maintenance of dendritic spine structure", *Proceedings of the National Academy of Sciences of the United States of America,* vol. 104, no. 15, pp. 6418-6423.

Owen, M. J., Williams, N. M. and O'Donovan, M. C. (2004), "The molecular genetics of schizophrenia: New findings promise new insights", *Molecular psychiatry,* vol. 9, no. 1, pp. 14-27.

Oxley, T., Fitzgerald, P. B., Brown, T. L., De Castella, A., Jeff Daskalakis, Z. and Kulkarni, J. (2004), "Repetitive transcranial magnetic stimulation reveals abnormal plastic response to premotor cortex stimulation in schizophrenia", *Biological psychiatry,* vol. 56, no. 9, pp. 628-633.

Pantelis, C., Velakoulis, D., McGorry, P. D., Wood, S. J., Suckling, J., Phillips, L. J., Yung, A. R., Bullmore, E. T., Brewer, W., Soulsby, B., Desmond, P. and McGuire, P. K. (2003), "Neuroanatomical abnormalities before and after onset of psychosis: A cross-sectional and longitudinal MRI comparison", *Lancet,* vol. 361, no. 9354, pp. 281-288.

Paoletti, P. and Neyton, J. (2007), "NMDA receptor subunits: function and pharmacology", *Current Opinion in Pharmacology,* vol. 7, no. 1, pp. 39-47.

Parwani, A., Weiler, M. A., Blaxton, T. A., Warfel, D., Hardin, M., Frey, K. and Lahti, A. C. (2005), "The effects of a subanesthetic dose of ketamine on verbal memory in normal volunteers", *Psychopharmacology,* vol. 183, no. 3, pp. 265-274.

Paulesu, E., Perani, D., Blasi, V., Silani, G., Borghese, N. A., De Giovanni, U., Sensolo, S. and Fazio, F. (2003), "A functional-anatomical model for lipreading", *Journal of neurophysiology,* vol. 90, no. 3, pp. 2005-2013.

Payoux, P., Boulanouar, K., Sarramon, C., Fabre, N., Descombes, S., Galitsky, M., Thalamas, C., Brefel-Courbon, C., Sabatini, U., Manelfe, C., Chollet, F., Schmitt, L. and Rascol, O. (2004), "Cortical motor activation in akinetic schizoophrenic patients: A pilot functional MRI study", *Movement Disorders,* vol. 19, no. 1, pp. 83-90.

Peters, A., Sethares, C. and Luebke, J. I. (2008), "Synapses are lost during aging in the primate prefrontal cortex", *Neuroscience,* vol. 152, no. 4, pp. 970-981.

Peterson, D. A., Dickinson-Anson, H. A., Leppert, J. T., Lee, K. -. and Gage, F. H. (1999), "Central neuronal loss and behavioral impairment in mice lacking neurotrophin receptor p75", *Journal of Comparative Neurology,* vol. 404, no. 1, pp. 1-20.

Petrie, R. X. A., Reid, I. C. and Stewart, C. A. (2000), "The N-methyl-D-aspartate receptor, synaptic plasticity, and depressive disorder: A critical review", *Pharmacology and Therapeutics,* vol. 87, no. 1, pp. 11-25.

Petryshen, T. L., Middleton, F. A., Kirby, A., Aldinger, K. A., Purcell, S., Tahl, A. R., Morley, C. P., McGann, L., Gentile, K. L., Rockwell, G. N., Medeiros, H. M., Carvalho, C., Macedo, A., Dourado, A., Valente, J., Ferreira, C. P., Patterson, N. J., Azevedo, M. H., Daly, M. J., Pato, C. N., Pato, M. T. and Sklar, P. (2005), "Support for involvement of neuregulin 1 in schizophrenia pathophysiology", *Molecular psychiatry,* vol. 10, no. 4, pp. 366-374.

Picard, N. and Strick, P. L. (2001), "Imaging the premotor areas", *Current opinion in neurobiology,* vol. 11, no. 6, pp. 663-672.

Pickard, B. S., Malloy, M. P., Clark, L., LeHellard, S., Ewald, H. L., Mors, O., Porteous, D. J., Blackwood, D. H. R. and Muir, W. J. (2005), "Candidate psychiatric illness genes identified in patients with pericentric inversions of chromosome 18", *Psychiatric genetics,* vol. 15, no. 1, pp. 37-44.

Pillai, A. (2008), "Brain-derived neurotropic factor/TrkB signaling in the pathogenesis and novel pharmacotherapy of schizophrenia", *NeuroSignals,* vol. 16, no. 2-3, pp. 183-193.

Pillai, A. and Mahadik, S. P. (2008), "Increased truncated TrkB receptor expression and decreased BDNF/TrkB signaling in the frontal cortex of reeler mouse model of schizophrenia", *Schizophrenia research,* vol. 100, no. 1-3, pp. 325-333.

Platel, H., Price, C., Baron, J. -., Wise, R., Lambert, J., Frackowiak, R. S. J., Lechevalier, B. and Eustache, F. (1997), "The structural components of music perception. A functional anatomical study", *Brain,* vol. 120, no. 2, pp. 229-243.

Price, C. J., Green, D. W. and Von Studnitz, R. (1999), "A functional imaging study of translation and language switching", *Brain,* vol. 122, no. 12, pp. 2221-2235.

Price, C. J., Wise, R. J. S., Watson, J. D. G., Patterson, K., Howard, D. and Frackowiak, R. S. J. (1994), "Brain activity during reading. The effects of exposure duration and task", *Brain,* vol. 117, no. 6, pp. 1255-1269.

Qualmann, B., Boeckers, T. M., Jeromin, M., Gundelfinger, E. D. and Kessels, M. M. (2004), "Linkage of the Actin Cytoskeleton to the Postsynaptic Density via Direct Interactions of Abp1 with the ProSAP/Shank Family", *Journal of Neuroscience,* vol. 24, no. 10, pp. 2481-2495.

Ragland, J. D., Laird, A. R., Ranganath, C., Blumenfeld, R. S., Gonzales, S. M. and Glahn, D. C. (2009), "Prefrontal activation deficits during episodic memory in schizophrenia", *American Journal of Psychiatry,* vol. 166, no. 8, pp. 863-874.

Raij, T. T., Valkonen-Korhonen, M., Holi, M., Therman, S., Lehtonen, J. and Hari, R. (2009), "Reality of auditory verbal hallucinations", *Brain,* vol. 132, no. 11, pp. 2994-3001.

Rämä, P., Martinkauppi, S., Linnankoski, I., Koivisto, J., Aronen, H. J. and Carlson, S. (2001), "Working memory of identification of emotional vocal expressions: An fMRI study", *NeuroImage,* vol. 13, no. 6, pp. 1090-1101.

Ranganath, C., Johnson, M. K. and D'Esposito, M. (2003), "Prefrontal activity associated with working memory and episodic long-term memory", *Neuropsychologia,* vol. 41, no. 3, pp. 378-389.

Ray, M. T., Weickert, C. S., Wyatt, E. and Webster, M. J. (2011), "Decreased BDNF, trkB-TK+ and GAD 67 mRNA expression in the hippocampus of individuals with schizophrenia and mood disorders", *Journal of Psychiatry and Neuroscience,* vol. 36, no. 3, pp. 195-203.

Regalado, M. P., Terry-Lorenzo, R. T., Waites, C. L., Garner, C. C. and Malenka, R. C. (2006), "Transsynaptic signaling by postsynaptic synapse-associated protein 97", *Journal of Neuroscience,* vol. 26, no. 8, pp. 2343-2357.

Reichardt, L. F. (2006a), "Neurotrophin-regulated signalling pathways", *Philosophical Transactions of the Royal Society B: Biological Sciences,* vol. 361, no. 1473, pp. 1545-1564.

Reichardt, L. F. (2006b), "Neurotrophin-regulated signalling pathways", *Philosophical Transactions of the Royal Society B: Biological Sciences,* vol. 361, no. 1473, pp. 1545-1564.

Renn, C. L., Leitch, C. C. and Dorsey, S. G. (2009), "In vivo evidence that truncated trkB.T1 participates in nociception", *Molecular Pain,* vol. 5.

Reverberi, C., Cherubini, P., Rapisarda, A., Rigamonti, E., Caltagirone, C., Frackowiak, R. S. J., Macaluso, E. and Paulesu, E. (2007), "Neural basis of generation of conclusions in elementary deduction", *NeuroImage,* vol. 38, no. 4, pp. 752-762.

Rizzolatti, G., Camarda, R., Fogassi, L., Gentilucci, M., Luppino, G. and Matelli, M. (1988), "Functional organization of inferior area 6 in the macaque monkey. II. Area F5 and the control of distal movements", *Experimental Brain Research,* vol. 71, no. 3, pp. 491-507.

Rizzolatti, G. and Matelli, M. (2003), "Two different streams form the dorsal visual system: Anatomy and functions", *Experimental Brain Research,* vol. 153, no. 2, pp. 146-157.

Rösch, H., Schweigreiter, R., Bonhoeffer, T., Barde, Y. -. and Korte, M. (2005), "The neurotrophin receptor p75NTR modulates long-term depression and regulates the expression of AMPA receptor subunits in the hippocampus", *Proceedings of the National Academy of Sciences of the United States of America,* vol. 102, no. 20, pp. 7362-7367.

Roussignol, G., Ango, F., Romorini, S., Tu, J. C., Sala, C., Worley, P. F., Bockaert, J. and Fagni, L. (2005), "Shank expression is sufficient to induce functional dendritic spine synapses in aspiny neurons", *Journal of Neuroscience,* vol. 25, no. 14, pp. 3560-3570.

Roux, P. P. and Barker, P. A. (2002), "Neurotrophin signaling through the p75 neurotrophin receptor", *Progress in neurobiology,* vol. 67, no. 3, pp. 203-233.

Rowland, L. M., Shadmehr, R., Kravitz, D. and Holcomb, H. H. (2008), "Sequential neural changes during motor learning in schizophrenia", *Psychiatry Research - Neuroimaging,* vol. 163, no. 1, pp. 1-12.

Rozzi, S., Calzavara, R., Belmalih, A., Borra, E., Gregoriou, G. G., Matelli, M. and Luppino, G. (2006), "Cortical connections of the inferior parietal cortical convexity of the macaque monkey", *Cerebral Cortex,* vol. 16, no. 10, pp. 1389-1417.

Rumbaugh, G., Sia, G. -., Garner, C. C. and Huganir, R. L. (2003), "Synapse-associated protein-97 isoform-specific regulation of surface AMPA receptors and synaptic function in cultured neurons", *Journal of Neuroscience,* vol. 23, no. 11, pp. 4567-4576.

Rupp, C. I., Fleischhacker, W. W., Kemmler, G., Oberbauer, H., Scholtz, A. W., Wanko, C. and Hinterhuber, H. (2005), "Various bilateral olfactory deficits in male patients with schizophrenia", *Schizophrenia bulletin,* vol. 31, no. 1, pp. 155-165.

Sandoval, M., Sandoval, R., Thomas, U., Spilker, C., Smalla, K. -., Falcon, R., Marengo, J. J., Calderón, R., Saavedra, V., Heumann, R., Bronfman, F., Garner, C. C., Gundelfinger, E. D. and Wyneken, U. (2007), "Antagonistic effects of TrkB and p75NTR on NMDA receptor currents in post-synaptic densities transplanted into Xenopus oocytes", *Journal of neurochemistry,* vol. 101, no. 6, pp. 1672-1684.

Sans, N., Prybylowski, K., Petralia, R. S., Chang, K., Wang, Y. -., Racca, C., Vicini, S. and Wenthold, R. J. (2003), "NMDA receptor trafficking through an interaction between PDZ proteins and the exocyst complex", *Nature cell biology,* vol. 5, no. 6, pp. 520-530.

Sarbassov, D. D., Ali, S. M. and Sabatini, D. M. (2005), "Growing roles for the mTOR pathway", *Current opinion in cell biology,* vol. 17, no. 6, pp. 596-603.

Scheuerecker, J., Ufer, S., Käpernick, M., Wiesmann, M., Brückmann, H., Kraft, E., Seifert, D., Koutsouleris, N., Möller, H. J. and Meisenzahl, E. M. (2009), "Cerebral network deficits in post-acute catatonic schizophrenic patients measured by fMRI", *Journal of psychiatric research,* vol. 43, no. 6, pp. 607-614.

Schnell, E., Sizemore, M., Karimzadegan, S., Chen, L., Bredt, D. S. and Nicoll, R. A. (2002), "Direct interactions between PSD-95 and stargazin control synaptic AMPA receptor number", *Proceedings of the National Academy of Sciences of the United States of America,* vol. 99, no. 21, pp. 13902-13907.

Schubotz, R. I. and Von Cramon, D. Y. (2002), "A blueprint for target motion: fMRI reveals perceived sequential complexity to modulate premotor cortex", *NeuroImage,* vol. 16, no. 4, pp. 920-935.

Shaywitz, A.J. and Greenberg, M.E., (1999), *CREB: A stimulus-induced transcription factor activated by a diverse array of extracellular signals*.

Shen, K., Teruel, M. N., Subramanian, K. and Meyer, T. (1998), "CaMKIIβ functions as an F-actin targeting module that localizes CaMKIIα/β heterooligomers to dendritic spines", *Neuron,* vol. 21, no. 3, pp. 593-606.

Shen, W. W. (1999), "A history of antipsychotic drug development", *Comprehensive psychiatry,* vol. 40, no. 6, pp. 407-414.

Sheng, M. and Hoogenraad, C.C., (2007), *The postsynaptic architecture of excitatory synapses: A more quantitative view*.

Sheng, M. and Sala, C., (2001), *PDZ domains and the organization of supramolecular complexes*.

Shuster, L. I. and Lemieux, S. K. (2005), "An fMRI investigation of covertly and overtly produced mono- and multisyllabic words", *Brain and language,* vol. 93, no. 1, pp. 20-31.

Song, J. -., Ichtchenko, K., Südhof, T. C. and Brose, N. (1999), "Neuroligin 1 is a postsynaptic cell-adhesion molecule of excitatory synapses", *Proceedings of the National Academy of Sciences of the United States of America,* vol. 96, no. 3, pp. 1100-1105.

Soontornniyomkij, B., Everall, I. P., Chana, G., Tsuang, M. T., Achim, C. L. and Soontornniyomkij, V. (2011), "Tyrosine kinase B protein expression is reduced in the cerebellum of patients with bipolar disorder", *Journal of affective disorders,* vol. 133, no. 3, pp. 646-654.

Stahl, S. M. (2007), "Beyond the dopamine hypothesis to the NMDA glutamate receptor hypofunction hypothesis of schizophrenia", *CNS Spectrums,* vol. 12, no. 4, pp. 265-268.

Stefansson, H., Sigurdsson, E., Steinthorsdottir, V., Bjornsdottir, S., Sigmundsson, T., Ghosh, S., Brynjolfsson, J., Gunnarsdottir, S., Ivarsson, O., Chou, T. T., Hjaltason, O., Birgisdottir, B., Jonsson, H., Gudnadottir, V. G., Gudmundsdottir, E., Bjornsson, A., Ingvarsson, B., Ingason, A., Sigfusson, S., Hardardottir, H., Harvey, R. P., Lai, D., Zhou, M., Brunner, D., Mutel, V., Gonzalo, A., Lemke, G., Sainz, J., Johannesson, G., Andresson, T., Gudbjartsson, D., Manolescu, A., Frigge, M. L., Gurney, M. E., Kong, A., Gulcher, J. R., Petursson, H. and Stefansson, K. (2002), "Neuregulin 1 and Susceptibility to Schizophrenia", *American Journal of Human Genetics,* vol. 71, no. 4, pp. 877-892.

Stephan, K. E., Baldeweg, T. and Friston, K. J. (2006), "Synaptic Plasticity and Dysconnection in Schizophrenia", *Biological psychiatry,* vol. 59, no. 10, pp. 929-939.

Stephan, K. M., Fink, G. R., Passingham, R. E., Silbersweig, D., Ceballos-Baumann, A. O., Frith, C. D. and Frackowiak, R. S. J. (1995), "Functional anatomy of the mental representation of upper extremity movements in healthy subjects", *Journal of neurophysiology,* vol. 73, no. 1, pp. 373-386.

Stepniewska, I., Preuss, T. M. and Kaas, J. H. (2006), "Ipsilateral cortical connections of dorsal and ventral premotor areas in New World owl monkeys", *Journal of Comparative Neurology,* vol. 495, no. 6, pp. 691-708.

Stip, E. (2002), "Happy birthday neuroleptics! 50 years later: La folie du doute", *European Psychiatry,* vol. 17, no. 3, pp. 115-119.

Stotz-Ingenlath, G. (2000), "Epistemological aspects of Eugen Bleuler's conception of schizophrenia in 1911.", *Medicine, health care, and philosophy,* vol. 3, no. 2, pp. 153-159.

Straub, R. E., Jiang, Y., MacLean, C. J., Ma, Y., Webb, B. T., Myakishev, M. V., Harris-Kerr, C., Wormley, B., Sadek, H., Kadambi, B., Cesare, A. J., Gibberman, A., Wang, X., O'Neill, F. A., Walsh, D. and Kendler, K. S. (2002), "Genetic variation in the 6p22.3 Gene DTNBP1, the human ortholog of the mouse dysbindin gene, is associated with schizophrenia", *American Journal of Human Genetics,* vol. 71, no. 2, pp. 337-348.

Sullivan, P. F., Kendler, K. S. and Neale, M. C. (2003), "Schizophrenia as a Complex Trait: Evidence from a Meta-analysis of Twin Studies", *Archives of General Psychiatry,* vol. 60, no. 12, pp. 1187-1192.

Sun, P., Wang, J., Gu, W., Cheng, W., Jin, G. -., Friedman, E., Zheng, J. and Zhen, X. (2009), "PSD-95 regulates D1 dopamine receptor resensitization,but not receptor-mediated Gs-protein activation", *Cell research,* vol. 19, no. 5, pp. 612-624.

Swayze, R. D., Lisé, M. -., Levinson, J. N., Phillips, A. and El-Husseini, A. (2004), "Modulation of dopamine mediated phosphorylation of AMPA receptors by PSD-95 and AKAP79/150", *Neuropharmacology,* vol. 47, no. 5, pp. 764-778.

Takahashi, M., Shirakawa, O., Toyooka, K., Kitamura, N., Hashimoto, T., Maeda, K., Koizumi, S., Wakabayashi, K., Takahashi, H., Someya, T. and Nawa, H. (2000), "Abnormal expression of brain-derived neurotrophic factor and its receptor in the corticolimbic system of schizophrenic patients", *Molecular psychiatry,* vol. 5, no. 3, pp. 293-300.

Takeuchi, M., Hata, Y., Hirao, K., Toyoda, A., Irie, M. and Takai, Y. (1997), "SAPAPs. A family of PSD-95/SAP90-associated proteins localized at postsynaptic density", *Journal of Biological Chemistry,* vol. 272, no. 18, pp. 11943-11951.

Talbot, K., Eidem, W. L., Tinsley, C. L., Benson, M. A., Thompson, E. W., Smith, R. J., Hahn, C. -., Siegel, S. J., Trojanowski, J. Q., Gur, R. E., Blake, D. J. and Arnold, S. E. (2004), "Dysbindin-1 is reduced in intrinsic, glutamatergic terminals of the hippocampal formation in schizophrenia", *Journal of Clinical Investigation,* vol. 113, no. 9, pp. 1353-1363.

Tanaka, M. and Kunimatsu, J. (2011), "Contribution of the central thalamus to the generation of volitional saccades", *European Journal of Neuroscience,* vol. 33, no. 11, pp. 2046-2057.

Tanaka, S., Honda, M. and Sadato, N. (2005), "Modality-specific cognitive function of medial and lateral human Brodmann area 6", *Journal of Neuroscience,* vol. 25, no. 2, pp. 496-501.

Tandon, R., Nasrallah, H. A. and Keshavan, M. S. (2009), "Schizophrenia, "just the facts" 4. Clinical features and conceptualization", *Schizophrenia research,* vol. 110, no. 1-3, pp. 1-23.

Tanné-Gariépy, J., Rouiller, E. M. and Boussaoud, D. (2002), "Parietal inputs to dorsal versus ventral premotor areas in the macaque monkey: Evidence for largely segregated visuomotor pathways", *Experimental Brain Research,* vol. 145, no. 1, pp. 91-103.

Toro, C. and Deakin, J. F. W. (2005), "NMDA receptor subunit NRI and postsynaptic protein PSD-95 in hippocampus and orbitofrontal cortex in schizophrenia and mood disorder", *Schizophrenia research,* vol. 80, no. 2-3, pp. 323-330.

Toro, C. T. and Deakin, J. F. (2007), "Adult neurogenesis and schizophrenia: a window on abnormal early brain development?", *Schizophrenia research,* vol. 90, no. 1-3, pp. 1-14.

Torrey, E. F., Miller, J., Rawlings, R. and Yolken, R. H. (1997), "Seasonality of births in schizophrenia and bipolar disorder: A review of the literature", *Schizophrenia research,* vol. 28, no. 1, pp. 1-38.

Trichard, C., Paillère-Martinot, M. -., Attar-Levy, D., Blin, J., Feline, A. and Martinot, J. -. (1998), "No serotonin 5-HT(2A) receptor density abnormality in the cortex of schizophrenic patients studied with PET", *Schizophrenia research,* vol. 31, no. 1, pp. 13-17.

Tsai, S. -., Hong, C. -., Cheng, C. -., Liao, D. -. and Liou, Y. -. (2007), "Association study of polymorphisms in post-synaptic density protein 95 (PSD-95) with schizophrenia", *Journal of neural transmission,* vol. 114, no. 4, pp. 423-426.

Tsien, J. Z. (2000), "Linking Hebb's coincidence-detection to memory formation", *Current opinion in neurobiology,* vol. 10, no. 2, pp. 266-273.

Tu, J. C., Xiao, B., Naisbitt, S., Yuan, J. P., Petralia, R. S., Brakeman, P., Doan, A., Aakalu, V. K., Lanahan, A. A., Sheng, M. and Worley, P. F. (1999), "Coupling of mGluR/Homer and PSD-95 complexes by the Shank family of postsynaptic density proteins", *Neuron,* vol. 23, no. 3, pp. 583-592.

Tu, J. C., Xiao, B., Yuan, J. P., Lanahan, A. A., Leoffert, K., Li, M., Linden, D. J. and Worley, P. F. (1998), "Homer binds a novel proline-rich motif and links group I metabotropic glutamate receptors with IP3 receptors", *Neuron,* vol. 21, no. 4, pp. 717-726.

Tulving, E., Kapur, S., Markowitsch, H. J., Craik, F. I. M., Habib, R. and Houle, S. (1994), "Neuroanatomical correlates of retrieval in episodic memory: Auditory sentence recognition", *Proceedings of the National Academy of Sciences of the United States of America,* vol. 91, no. 6, pp. 2012-2015.

Uchino, S., Wada, H., Honda, S., Nakamura, Y., Ondo, Y., Uchiyama, T., Tsutsumi, M., Suzuki, E., Hirasawa, T. and Kohsaka, S. (2006), "Direct interaction of post-synaptic density-95/Dlg/ZO-1 domain-containing synaptic molecule Shank3 with GluR1 α-amino-3-hydroxy-5-methyl-4-isoxazole propionic acid receptor", *Journal of neurochemistry,* vol. 97, no. 4, pp. 1203-1214.

van Os, J. and Kapur, S. (2009), "Schizophrenia", *The Lancet,* vol. 374, no. 9690, pp. 635-645.

Velakoulis, D., Wood, S. J., Wong, M. T. H., McGorry, P. D., Yung, A., Phillips, L., Smith, D., Brewer, W., Proffitt, T., Desmond, P. and Pantelis, C. (2006), "Hippocampal and amygdala volumes according to psychosis stage and diagnosis: A magnetic resonance imaging study of chronic schizophrenia, first-episode psychosis, and ultra-high-risk individuals", *Archives of General Psychiatry,* vol. 63, no. 2, pp. 139-149.

Villasana, L. E., Klann, E. and Tejada-Simon, M. V. (2006), "Rapid isolation of synaptoneurosomes and postsynaptic densities from adult mouse hippocampus", *Journal of neuroscience methods,* vol. 158, no. 1, pp. 30-36.

Waldo, M. C., Cawthra, E., Adler, L. E., Dubester, S., Staunton, M., Nagamoto, H., Baker, N., Madison, A., Simon, J., Scherzinger, A., Drebing, C., Gerhardt, G. and

Freedman, R. (1994), "Auditory sensory gating, hippocampal volume, and catecholamine metabolism in schizophrenics and their siblings", *Schizophrenia research,* vol. 12, no. 2, pp. 93-106.

Wang, Y., Isoda, M., Matsuzaka, Y., Shima, K. and Tanji, J. (2005), "Prefrontal cortical cells projecting to the supplementary eye field and presupplementary motor area in the monkey", *Neuroscience research,* vol. 53, no. 1, pp. 1-7.

Wang, Y., Shima, K., Isoda, M., Sawamura, H. and Tanji, J. (2002), "Spatial distribution and density of prefrontal cortical cells projecting to three sectors of the premotor cortex", *Neuroreport,* vol. 13, no. 10, pp. 1341-1344.

Warburton, E., Wise, R. J. S., Price, C. J., Weiller, C., Hadar, U., Ramsay, S. and Frackowiak, R. S. J. (1996), "Noun and verb retrieval by normal subjects: Studies with PET", *Brain,* vol. 119, no. 1, pp. 159-179.

Wayman, G. A., Lee, Y. -., Tokumitsu, H., Silva, A. and Soderling, T. R. (2008), "Calmodulin-Kinases: Modulators of Neuronal Development and Plasticity", *Neuron,* vol. 59, no. 6, pp. 914-931.

Weickert, C. S., Ligons, D. L., Romanczyk, T., Ungaro, G., Hyde, T. M., Herman, M. M., Weinberger, D. R. and Kleinman, J. E. (2005), "Reductions in neurotrophin receptor mRNAs in the prefrontal cortex of patients with schizophrenia", *Molecular psychiatry,* vol. 10, no. 7, pp. 637-650.

Weickert, C. S., Straub, R. E., McClintock, B. W., Matsumoto, M., Hashimoto, R., Hyde, T. M., Herman, M. M., Weinberger, D. R. and Kleinman, J. E. (2004), "Human dysbindin (DTNBP1) gene expression in normal brain and in schizophrenic prefrontal cortex and midbrain", *Archives of General Psychiatry,* vol. 61, no. 6, pp. 544-555.

Wise, S. P. (1996), "Corticospinal efferents of the supplementary sensorimotor area in relation to the primary motor area.", *Advances in Neurology,* vol. 70, pp. 57-69.

Wong, J. and Garner, B. (2012), "Evidence that truncated TrkB isoform, TrkB-Shc can regulate phosphorylated TrkB protein levels", *Biochemical and biophysical research communications,* vol. 420, no. 2, pp. 331-335.

Woo, J., Kwon, S. -., Choi, S., Kim, S., Lee, J. -., Dunah, A. W., Sheng, M. and Kim, E. (2009), "Trans-synaptic adhesion between NGL-3 and LAR regulates the formation of excitatory synapses", *Nature neuroscience,* vol. 12, no. 4, pp. 428-437.

Woo, N. H., Teng, H. K., Siao, C. -., Chiaruttini, C., Pang, P. T., Milner, T. A., Hempstead, B. L. and Lu, B. (2005), "Activation of p75NTR by proBDNF facilitates hippocampal long-term depression", *Nature neuroscience,* vol. 8, no. 8, pp. 1069-1077.

Woo, T. -. W., Walsh, J. P. and Benes, F. M. (2004), "Density of glutamic acid decarboxylase 67 messenger RNA-containing neurons that express the N-methyl-D-aspartate receptor subunit NR2A in the anterior cingulate cortex in schizophrenia and bipolar disorder", *Archives of General Psychiatry,* vol. 61, no. 7, pp. 649-657.

Wright, J. W., Alt, J. A., Turner, G. D. and Krueger, J. M. (2004), "Differences in spatial learning comparing transgenic p75 knockout, New Zealand Black, C57BL/6, and Swiss Webster mice", *Behavioural brain research,* vol. 153, no. 2, pp. 453-458.

Wu, K., Xu, Suen, Levine, E., Huang, Mount, H. T. J., Lin and Black, I. B. (1996), "Functional trkB neurotrophin receptors are intrinsic components of the adult brain postsynaptic density", *Molecular Brain Research,* vol. 43, no. 1-2, pp. 286-290.

Xia, J., Zhang, X., Staudinger, J. and Huganir, R. L. (1999), "Clustering of AMPA receptors by the synaptic PD domain-containing protein PICK1", *Neuron,* vol. 22, no. 1, pp. 179-187.

Xiao, B., Tu, J. C., Petralia, R. S., Yuan, J. P., Doan, A., Breder, C. D., Ruggiero, A., Lanahan, A. A., Wenthold, R. J. and Worley, P. F. (1998), "Homer regulates the association of group 1 metabotropic glutamate receptors with multivalent complexes of Homer-related, synaptic proteins", *Neuron,* vol. 21, no. 4, pp. 707-716.

Xing, G., Russell, S., Hough, C., O'Grady, J., Zhang, L., Yang, S., Zhang, L. -. and Post, R. (2002), "Decreased prefrontal CaMKII α mRNA in bipolar illness", *Neuroreport,* vol. 13, no. 4, pp. 501-505.

Yacoubian, T. A. and Lo, D. C. (2000), "Truncated and full-length TrkB receptors regulate distinct modes of dendritic growth", *Nature neuroscience,* vol. 3, no. 4, pp. 342-349.

Yamada, Y., Chochi, Y., Ko, J. -., Sobue, K. and Inui, M. (1999), "Activation of channel activity of the NMDA receptor-PSD-95 complex by guanylate kinase-associated protein (GKAP)", *FEBS letters,* vol. 458, no. 3, pp. 295-298.

Yamagata, Y., Kobayashi, S., Umeda, T., Inoue, A., Sakagami, H., Fukaya, M., Watanabe, M., Hatanaka, N., Totsuka, M., Yagi, T., Obata, K., Imoto, K., Yanagawa, Y., Manabe, T. and Okabe, S. (2009), "Kinase-dead knock-in mouse reveals an

essential role of kinase activity of Ca 2+/calmodulin-dependent protein kinase IIα in dendritic spine enlargement, long-term potentiation, and learning", *Journal of Neuroscience,* vol. 29, no. 23, pp. 7607-7618.

Yang, J., Siao, C. -., Nagappan, G., Marinic, T., Jing, D., McGrath, K., Chen, Z. -., Mark, W., Tessarollo, L., Lee, F. S., Lu, B. and Hempstead, B. L. (2009), "Neuronal release of proBDNF", *Nature neuroscience,* vol. 12, no. 2, pp. 113-115.

Yao, W. -., Spealman, R. D. and Zhang, J. (2008), "Dopaminergic signaling in dendritic spines", *Biochemical pharmacology,* vol. 75, no. 11, pp. 2055-2069.

Yoshii, A. and Constantine-Paton, M. (2007a), "BDNF induces transport of PSD-95 to dendrites through PI3K-AKT signaling after NMDA receptor activation", *Nature neuroscience,* vol. 10, no. 6, pp. 702-711.

Yoshii, A. and Constantine-Paton, M. (2007b), "BDNF induces transport of PSD-95 to dendrites through PI3K-AKT signaling after NMDA receptor activation", *Nature neuroscience,* vol. 10, no. 6, pp. 702-711.

Yoshimura, Y., Yamauchi, Y., Shinkawa, T., Taoka, M., Donai, H., Takahashi, N., Isobe, T. and Yamauchi, T. (2004a), "Molecular constituents of the postsynaptic density fraction revealed by proteomic analysis using multidimensional liquid chromatography-tandem mass spectrometry", *Journal of neurochemistry,* vol. 88, no. 3, pp. 759-768.

Yoshimura, Y., Yamauchi, Y., Shinkawa, T., Taoka, M., Donai, H., Takahashi, N., Isobe, T. and Yamauchi, T. (2004b), "Molecular constituents of the postsynaptic density fraction revealed by proteomic analysis using multidimensional liquid chromatography-tandem mass spectrometry", *Journal of neurochemistry,* vol. 88, no. 3, pp. 759-768.

Zagrebelsky, M., Holz, A., Dechant, G., Barde, Y. -., Bonhoeffer, T. and Korte, M. (2005), "The p75 neurotrophin receptor negatively modulates dendrite complexity and spine density in hippocampal neurons", *Journal of Neuroscience,* vol. 25, no. 43, pp. 9989-9999.

Zha, X. -., Dailey, M. E. and Green, S. H. (2009), "Role of Ca2+/calmodulin-dependent protein kinase II in dendritic spine remodeling during epileptiform activity in vitro", *Journal of neuroscience research,* vol. 87, no. 9, pp. 1969-1979.

Zhang, J., Vinuela, A., Neely, M. H., Hallett, P. J., Grant, S. G. N., Miller, G. M., Isacson, O., Caron, M. G. and Yao, W. -. (2007), "Inhibition of the dopamine D1 receptor signaling by PSD-95", *Journal of Biological Chemistry,* vol. 282, no. 21, pp. 15778-15789.

Zhang, J., Xu, T. -., Hallett, P. J., Watanabe, M., Grant, S. G. N., Isacson, O. and Yao, W. -. (2009), "PSD-95 uncouples dopamine-glutamate interaction in the D 1/PSD-95/NMDA receptor complex", *Journal of Neuroscience,* vol. 29, no. 9, pp. 2948-2960.

Ziff, E. B. (1997), "Enlightening the postsynaptic density", *Neuron,* vol. 19, no. 6, pp. 1163-1174.